MOLECULAR PHYSIOLOGY AND BIOPHYSICS

OBESITY DYSLIPIDEMIA: THE EFFECT OF CENTRAL NERVOUS SYSTEM NEUROPEPTIDE Y ON HEPATIC LIPOPROTEIN METABOLISM

JENNIFER MARIE ROJAS

Dissertation under the direction of Associate Professor Kevin Dean Niswender

Elevated very low-density lipoprotein (VLDL)-triglyceride (TG) secretion from liver contributes to atherogenic dyslipidemia that is associated with obesity, diabetes, and the metabolic syndrome. Numerous models of obesity are characterized by increased central nervous system (CNS) neuropeptide Y (NPY) tone which contributes to positive energy balance and obesity. In fact, an acute, single intracerebroventricular (ICV) administration of NPY in lean fasted rats elevates hepatic VLDL-TG secretion. *Thus, our overarching hypothesis is that elevated CNS NPY action contributes to dyslipidemia by activating central circuits that modulate liver lipid metabolism.* Our studies focused on identifying molecular determinants in the hypothalamus and the liver by which increased CNS NPY signaling modulates hepatic lipoprotein metabolism.

First, we sought to determine if the effects of NPY on feeding and/or obesity are dissociable from effects on hepatic VLDL-TG secretion. ICV NPY-treated chow-fed rats pair-fed to vehicle-treated controls develop hypertriglyceridemia in the absence of increased food intake and body fat accumulation. Acute ICV injection of selective Y1, Y2, Y4, and Y5 receptor agonists all induced hyperphagia in lean *ad-libitum* fed rats with the Y2 receptor agonist having the most pronounced effect. The NPY Y1 receptor agonist robustly stimulated hepatic VLDL-TG secretion, while a Y2 receptor agonist had a modest effect on VLDL-TGs, and no effect was observed for Y4 and Y5 receptor agonists in lean fasted rats. These findings raise the possibility

that NPY regulates feeding and lipoprotein metabolism partially via separate NPY receptor systems and/or mechanisms.

Lastly, we sought to identify novel regulatory mechanisms in the liver engaged by CNS NPY signaling. We observed, in ICV NPY- and Y1 agonist-treated lean fasted rats, that oleic and linoleic acid were enriched in the liver phospholipid (PL) pool and secreted into plasma TGs. Furthermore, CNS NPY signaling via the Y1 receptor robustly activated key hepatic regulatory enzymes, ADP-ribosylation factor-1 and lipin-1, involved in remodeling liver PL into TG for VLDL maturation and secretion. Altogether, this body of work has overarching implications in further understanding how obesity-related CNS dysfunction contributes to the pathophysiology of atherogenic dyslipidemia associated with obesity, diabetes, and the metabolic syndrome.

Approved: Associate Professor Kevin D. Niswender M.D., Ph.D.

OBESITY DYSLIPIDEMIA: THE EFFECT OF CENTRAL NERVOUS SYSTEM NEUROPEPTIDE Y ON HEPATIC LIPOPROTEIN METABOLISM

By

Jennifer Marie Rojas

Dissertation

Submitted to the Faculty of the

Graduate School of Vanderbilt University

in partial fulfillment of the requirements

for the degree of

DOCTOR OF PHILOSOPHY

in

Molecular Physiology and Biophysics

May, 2013

Nashville, Tennessee

Approved:

Associate Professor Alyssa H. Hasty Ph.D.

Professor Owen P. McGuinness Ph.D.

Professor Richard M. O'Brien Ph.D.

Assistant Professor John M. Stafford M.D., Ph.D.

In memory of my past advisor, Professor Richard Fehn, an extraordinary and inspirational teacher and a dedicated mentor who inspired my life-long passion for research.

To my family, Mom, Dad, Darlynn, Nicole, and Michael

for their loving support and positive encouragement throughout this long journey.

ACKNOWLEDGEMENTS

It is with immense gratitude that I acknowledge the support and help of so many people who have made this dissertation possible.

First and foremost, I cannot find words to express my gratitude to my mentor, Dr. Kevin Niswender for providing me with the opportunity to train in his laboratory. Over the years, he has played an invaluable role in shaping me into the scientist I am today and equipping me with the required skills to succeed as an accomplished scientist in the near future. He is a truly brilliant and charismatic scientist with a positive enthusiasm and passion for research. Thank you for always believing in me and empowering me with the confidence to succeed. For your generosity, patience, positive encouragement, and inexhaustible dedication to training me as a scientist, thank you.

I am incredibly thankful to my dissertation committee, Dr. Alyssa Hasty, Dr. Owen McGuinness, Dr. John Stafford, and Dr. Richard O'Brien. They have really challenged me to think outside the box on key concepts and technical aspects of my dissertation which has had a major impact on the development and success of this body of work. I am truly thankful for their invaluable feedback, extensive guidance, and support on my project over the years in addition to their generous time, dedication, and scientific contributions to this dissertation. I am thankful for Alyssa for being such an amazing committee chairperson and for her inexhaustible dedication to helping me succeed in graduate school. Her door is always open and I am truly grateful for her cheerful personality and positive enthusiasm which brightens my day. I especially like to thank John for mentoring me throughout the years. His door is always open (and nearby) and I greatly appreciate his invaluable advice and helpfulness in answering my endless questions.

I would also like to thank the past and present members of the Niswender lab. They have impacted my life throughout the years as supportive colleagues and friends. My success as a graduate student was made possible by the expert technical support provided by Sanaz Saadat,

Leena George, and Maxine Turney. Thank you Sanaz and Leena for helping make my projects run smoothly. I truly appreciate your friendship and support over the years. I especially would like to thank Maxine for her excellent technical expertise and for her many significant contributions she has made to my project.

Next, it is with immense gratitude that I acknowledge the support and help of Dr. Richard Printz, who has served as my mentor and colleague throughout the years in the Niswender lab. He is truly a brilliant scientist. Richard has always been patient and kind, never showing any mild annoyance to my endless questions and requests for his help on my project. He has helped shape me into the scientist today and I am forever grateful.

I would like to especially thank the Department of Molecular Physiology and Biophysics for providing an excellent and very supportive training environment that has helped me succeed as a graduate student. Thank you Alyssa for serving as an excellent Director of Graduate Studies in addition to Chuck Cobb, Danny Winder, and Angie Pernell whom have all been an invaluable resource, helping me successfully navigate through graduate school. I would also like to thank the Charles R. Park and the Jackie D. Corbin/Sharron H. Francis Student Travel Award for funding my traveling expenses to scientific conferences.

Finally, many thanks to my family, especially my parents, Linda and Tony and my sisters, Darlynn and Nicole and my brother Michael for their loving support, positive encouragement, and for giving me the strength to succeed in this long journey.

Funding for this research has been provided to Dr. Niswender through the Veterans Affairs Merit Review Award and the National Institutes of Health (NIH) grant, DK085712. I have been supported by the Molecular Endocrinology Training Grant, 5T32DK07563 and the National Research Service Award, 5F31DK089906 from the NIH. This work was partially supported by resources of Vanderbilt Diabetes Center Hormone Assay & Analytical Services Core (DK020593), the DRTC Mouse Metabolic Phenotyping Center (MMPC; DK59637), and the Vanderbilt Translational Pathology Shared Resource Core (DK059637).

TABLE OF CONTENTS

Page

LIST OF TABLES

LIST OF FIGURES

LIST OF ABBREVIATIONS/LIPOPROTEIN NOMENCLATURE

ABBREVIATIONS

ACC	Acetyl-CoA carboxylase
ACOX1	Acyl-CoA oxidase-1
AGPAT	Acylglycerol-3-phosphate acyltransferase
ARF-1	ADP-ribosylation factor-1
AgRP	Agouti related peptide
ApoB	Apolipoprotein B
ARC	Arcuate nucleus
ACL	ATP citrate lyase
DMN	Dorsomedial hypothalamic nucleus
CVD	Cardiovascular disease
CRE	cAMP-dependent regulatory elements
CREB	cAMP response element-binding protein
CPT-1	Carnitine palmitoyltransferase-1
CNS	Central nervous system
CE	Cholesteryl ester
CETP	Cholesteryl ester transfer protein
CD36	Cluster of Differentiation 36
cAMP	Cyclic adenosine monophosphate
DAG	Diacylglycerol
DNL	*De novo* lipogenesis
DGAT	Diacylglycerol acyltransferase
DIO	Diet-induced obesity
4E-BP	Eukaryotic initiation factor 4E-binding protein
FDPS	Farnesyl diphosphate synthase
FAS	Fatty acid synthase
fld	Fatty liver dystrophy
FFA	Free fatty acid
FoxO1	Forkhead box protein O1
G6PC	Glucose-6-phosphatase
GAPDH	Glyceraldehyde 3-phosphate dehydrogenase
GC	Glucocorticoid
GRE	Glucocorticoid response element
GR	Glucocorticoid receptor
GTT	Glucose tolerance test
GSK3β	Glycogen synthase kinase 3β
GPAT	Glycerol-3-phosphate acyltransferase
GIRK	G-protein-coupled inwardly rectifying potassium channels
GPCR	G-protein coupled receptor
HSP70	Heat shock protein 70
HGP	Hepatic glucose production
HRicKO	Hepatocyte-specific *Rictor* knockout
HFD	High-fat diet
HDAC1	Histone deacetylase 1
HMGR	HMG-CoA reductase
HMGS-1	HMG-CoA synthase-1

HPA	Hypothalamic-pituitary-adrenal
ITT	Insulin tolerance test
Insig	Insulin-induced gene
IR	Insulin receptor
IRS	Insulin receptor substrate
ICV	Intracerebroventricular
IP	Intraperitoneal
LHA	Lateral hypothalamic area
LDLR	LDL receptor
LPL	Lipoprotein lipase
LXRα	Liver X receptor-α
LCFA	Long chain fatty acid
LFD	Low-fat diet
LPA	Lysophosphatidate
mTOR	Mammalian target of rapamycin
mTORC1	mTOR complex 1
mTORC2	mTOR complex 2
MCR	Melanocortin receptor
MTP	Microsomal triglyceride transfer protein
MUFA	Monounsaturated fatty acid
NPY	Neuropeptide Y
NAFLD	Nonalcoholic fatty liver disease
NE	Norepinephrine
PF	Pair-fed
PP	Pancreatic polypeptide
PVN	Paraventricular nucleus
PYY	Peptide YY
PPARα	Peroxisome proliferator activated receptor-α
PGC-1α	Peroxisome proliferator activated receptor -ɣ-coactivator-1α
PEPCK	Phosphoenolpyruvate carboxykinase
PTEN	Phosphatase and tensin homolog
PA	Phosphatidic acid
PAP	Phosphatidic acid phosphatase
PC	Phosphatidylcholine
PDK-1	Phosphoinositide-dependent kinase-1
PE	Phosphatidylethanolamine
PI3K	Phosphatidylinositol 3-kinase
PL	Phospholipid
PLD	Phospholipase D
PUFA	Polyunsaturated fatty acid
POMC	Proopiomelanocortin
AKT/PKB	Protein kinase B
PKCα	Protein kinase Cα
PTT	Pyruvate tolerance test
RQ	Respiratory quotient
RPL13A	Ribosomal protein L13a
S6K	p70 ribosomal S6 kinase
SGK	Serum- and glucocorticoid-induced protein kinase
SS	Squalene synthase
SREBP	Sterol regulatory element binding protein
SCAP	SREBP cleavage activating protein

SCD-1	Stearoyl-CoA desaturase-1
SRE	Sterol response element
SNS	Sympathetic nervous system
Sx	sympathetic denervation
TG	Triglyceride
TNF-α	Tumor necrosis factor-α
Veh	Vehicle
VMN	Ventromedial hypothalamic nucleus
ZF	*fa/fa* Zucker fatty rat

LIPOPROTEIN PARTICE

HDL	High-density lipoprotein
LDL	Low-density lipoprotein
VLDL	Very low-density lipoprotein

TOTAL LIPOPROTEIN CONCENTRATION

HDL-C	High-density lipoprotein cholesterol
LDL-C	Low-density lipoprotein cholesterol
VLDL-TG	Very low-density lipoprotein-triglyceride

CHAPTER I

INTRODUCTION

Cardiovascular risk factors

Classical cardiovascular risk factors

With the advent of antibiotics in 1940s and the implementation of public health measures to control infectious disease outbreaks, infectious disease mortality declined and human life expectancy increased (1, 2). However, as a consequence of these changes, cardiovascular disease (CVD) emerged as the main cause of mortality (1). Because very little was known about the origin and causes of CVD, the Framingham heart study was founded in 1948 by the United States Public Health Service to study the epidemiology and risk factors for CVD (3). The first cohort included 5,029 healthy residents between 30 and 60 years of age from the town of Framingham, Massachusetts. This study population has been examined biennially to identify common patterns related to CVD development (1). Careful analysis of the Framingham study population has led to the identification of the following classical cardiovascular risk factors: male sex, family history of CVD, hypertension, high cholesterol, and smoking. Clinicians have become increasingly adept at treating these classical cardiovascular risk factors, particularly cholesterol, hypertension, and smoking (4). For example, the therapeutic effect of statin therapy to lower low-density lipoprotein cholesterol (LDL-C) levels has clearly reduced CVD risk and is a public health success. In the Heart Protection Study, high risk patients received either statin therapy or placebo to compare the relative reduction in CVD events. Lowering LDL-C with a statin produced a substantial 25% reduction in major CVD events irrespective of their initial cholesterol concentrations (5). Yet, closer inspection reveals that 75% of the CVD risk remained despite statin therapy. *One*

hypothesis to explain this unaddressed risk is that obesity generates additional novel factors for CVD beyond those in the Framingham model and beyond absolute LDL-C levels.

Cardiometabolic burden of obesity and diabetes

Although deaths from CVD plateaued between 1990 and 2000 and dropped considerably between 2000 and 2008 (6), death rates for diabetes increased by 45% from 1987 to 2002 (7) and declined by about 12% from 2002 to 2010 (2). The alarming rise in diabetes-related deaths is primarily due to CVD (6). Thus, CVD remains one of the leading causes of death in the US and worldwide (6, 8). Clearly, the landscape for CVD risk has changed. This is thought to be largely due to the alarming increase in the prevalence of obesity and diabetes that has reached epidemic proportions in the US and worldwide (9). In the US alone, more than 35.7% of adults and approximately 17% of children and adolescents aged 2-19 years are obese (10). Obesity confers not only an elevated risk of diabetes but also of CVD and other associated co-morbidities (9, 11). CVD has a tremendous economic impact on the US, as related healthcare expenditures were estimated to be $444 billion in 2011 accounting for 17% of national health care expenditures (12). As the population ages, these costs are expected to increase substantially (12).

Metabolic syndrome: Dyslipidemia associated with obesity and diabetes

Metabolic syndrome, a constellation of cardiovascular risk factors, was first described in the 1920s by Kylin, a Swedish physician, as a clustering of hypertension, hyperglycemia, and gout (13). Twenty years later in 1947, central obesity associated with diabetes and CVD was included in the defining criteria of the metabolic syndrome, at the time known as Syndrome X (13). Today, in accordance with the clinical definition by the National Cholesterol Education Program Adult Treatment Panel III (NCEP:ATP III), individuals with three or more of the following criteria are diagnosed with the metabolic syndrome as shown in Table 1.1: central obesity, hypertriglyceridemia, low high-density lipoprotein cholesterol (HDL-C), hypertension,

and impaired fasting glucose (14). These factors are all well-documented risk factors for CVD (13, 14). The dyslipidemia associated with obesity and diabetes, and a key component of the metabolic syndrome, consists of elevated very low-density lipoprotein-triglyceride (VLDL-TG) together with small-dense LDL-C and reduced HDL-C levels (14-16). This form of dyslipidemia is an increasingly recognized cardiovascular risk factor (16).

Table 1.1. Clinical identification of the metabolic syndrome

Risk factor	Defining level
Abdominal obesity—	
waist circumference	
Men	>102 cm (>40 in)
Women	>88 cm (>35 in)
TG	≥150 mg/dl
HDL-C	
Men	< 40 mg/dl
Women	< 50 mg/dl
Blood pressure	≥130/≥85 mm Hg
Fasting glucose	≥110 mg/dl

Adapted from Ginsberg et al. (14). Abbreviations: high-density lipoprotein cholesterol (HDL-C); Triglyceride (TG).

Adipose tissue as an energy storage organ

The primary and classical role of the adipose tissue beyond insulating and cushioning the body includes long term energy storage as reviewed in Hajer et al. (17). During the postprandial state, free fatty acids (FFA) are taken up by the adipose tissue from the hydrolysis of triglyceride (TG)-rich lipoproteins (VLDL-TGs, chylomicrons, and their remnants) by lipoprotein lipase (LPL). These FFAs are either oxidized for energy or re-esterified into TG for storage as a lipid droplet. During a state of fasting and starvation, mobilization of FFA occurs by the hydrolysis of adipocyte TG via hormone sensitive lipase (HSL). HSL is activated by lipolytic hormones (i.e. glucagon, catecholamines, cortisol) while insulin is a potent inhibitor of this enzyme. Insulin is

also an important activator of LPL, thereby enhancing FFA uptake and TG synthesis in adipocytes (17).

Adipose tissue as an endocrine organ: Relevance to the metabolic syndrome

The classical view that adipose tissue is a passive storage depot for fatty acids is now obsolete. It has been replaced over the past 20 years by the notion that adipose tissue is a complex and highly active metabolic and endocrine organ (18). Adipocytes and adipose tissue produce a variety of hormones and cytokines involved in glucose metabolism (i.e. adiponectin, resistin), lipid metabolism (i.e. FFA, cholesteryl ester transfer protein; CETP), inflammation (i.e. tumor necrosis factor-α; TNFα, interleukin-6; IL-6), coagulation (plasminogen activator inhibitor-1; PAI-1), blood pressure (angiotensinogen, angiotensin II), and feeding behavior (leptin), as illustrated in Figure 1.1 (19). Thus, adipose tissue secreted products affect metabolism and function of many organs including muscle, liver, vasculature, and brain (17). It is widely accepted that increased adiposity, particularly visceral fat, is associated with marked changes in the secretory function of adipocytes and macrophages, which become pro-inflammatory (13, 20). It is thought that in obesity, elevated levels of adipocyte-derived proinflammatory cytokines such as TNF-α (21, 22), FFAs (23-25), and reductions in the insulin sensitizing adipokine, adiponectin (26, 27) can modulate lipoprotein metabolism by virtue of their ability to alter insulin sensitivity. Furthermore, visceral adipose tissue volume is inversely correlated with insulin-mediated glucose disposal indicating a clear relationship between the degree of adiposity and insulin resistance (28). Altogether, central obesity leads to the development of chronic low grade inflammation, as well as an increased risk to develop insulin resistance, diabetes, and CVD, all manifestations of the metabolic syndrome (17).

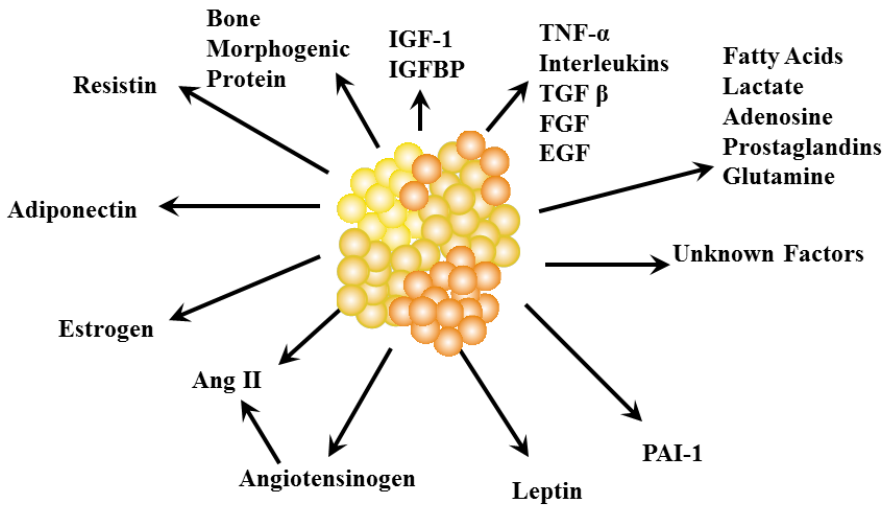

Figure 1.1. Why obesity is bad: The active adipose tissue. Increased visceral adiposity raises cardiometabolic risk, including diabetes and cardiovascular disease (adapted from Roth et al. (19)).

Current model of dyslipidemia associated with obesity and diabetes

A current model of dyslipidemia in the context of obesity and diabetes suggests that the VLDL-TG secretion rate is largely determined by the rate of substrate (FFA) delivery to the liver and hepatic insulin sensitivity (23-25). In a stable isotope study, Riches et al. (23) showed that hepatic secretion of VLDL-TG directly correlates with the degree of visceral adiposity and insulin resistance. A key component of the model is that as visceral fat mass expands, insulin resistance at the adipose and liver tissue develops. Adipocyte insulin resistance results in elevated adipocyte lipolysis, which is normally potently suppressed by insulin. Lipolysis leads to the release of FFA into the circulation, and visceral adipose lipolysis increases the portal FFA concentration. These FFAs are efficiently cleared by the liver and re-esterified to generate TG. This TG is loaded onto a nascent apolipoprotein B (apoB) particle, ultimately resulting in VLDL maturation and secretion (23-25). This process is ordinarily suppressed by integrated hepatic insulin action either via the inhibition of apoB translation and/or increased degradation (29, 30).

As reviewed by Ginsberg (15), with a rise in VLDL-TG in the circulation, interactions between very low-density lipoprotein **(**VLDL) and high-density lipoprotein (HDL) particles in the presence of CETP stimulates the exchange of HDL-cholesteryl esters (CE) with TGs from VLDL. The resulting TG-rich HDL particle then becomes a good substrate for hepatic lipase (and possibly LPL), and the TG is hydrolyzed. This in turn generates a smaller HDL particle leading to the dissociation of apoA-I from HDL and thus, facilitates increased clearance of apoA-I by the kidney, ultimately lowering HDL-C levels. Functionally, HDL plays an important role in reverse cholesterol transport (RCT); whereas in obesity and diabetes, this function is impaired by the mechanism just discussed and is posited to contribute to increased risk of CVD.

Similarly, interactions between VLDL and low-density lipoprotein (LDL) particle allows for CETP-mediated exchange of VLDL-TG for LDL CEs. The subsequent hydrolysis generates the accumulation of atherogenic, LDL-C particles (reviewed in (15, 31)). Consequently, this atherogenic dyslipidemia predisposes insulin resistant individuals to CVD. Elevated levels of cholesteryl-enriched VLDL and LDL particles are able to deliver more cholesterol per particle to the vessel wall and accumulate in atherosclerotic plaques. Fewer HDL particles translate to reduced efflux of excess cholesterol from the peripheral tissues, which is a step in RCT (15). Thus, the single effect of delivering FFA to the liver (in the context of insulin resistance) and increasing VLDL-TG translates into abnormalities in both HDL-C and LDL-C as illustrated in Figure 1.2. *While peripheral factors (visceral adiposity and insulin resistance) clearly contribute to this disorder, we hypothesized that regulation of lipid homeostasis is normally subject to additional central nervous system (CNS) regulatory forces, which we sought to investigate in Chapters III and IV.*

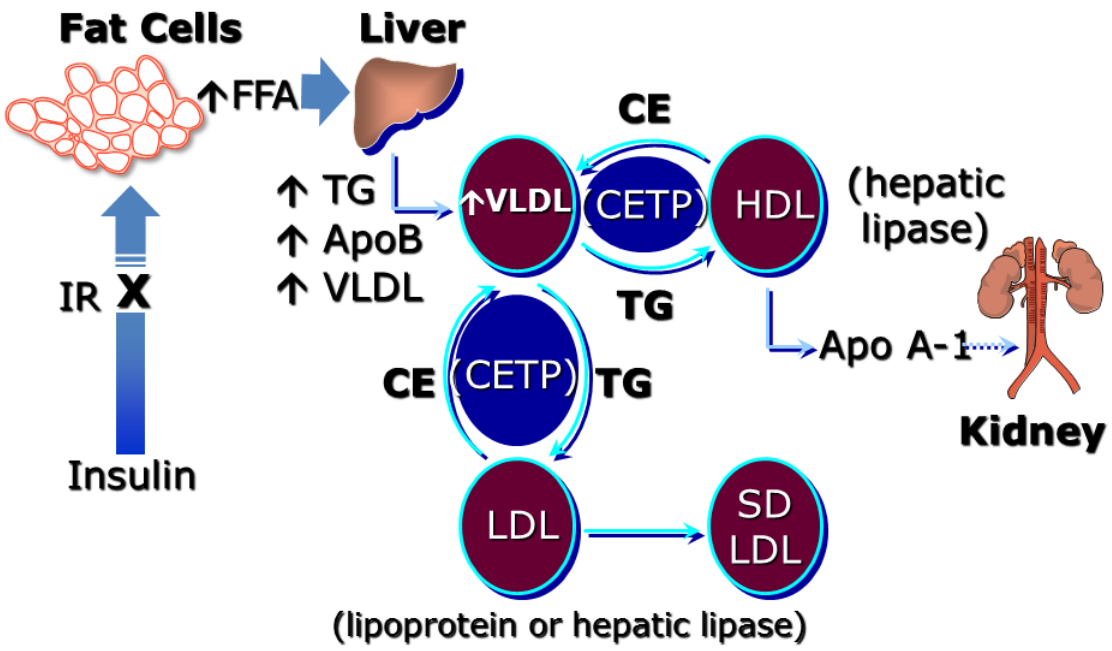

Figure 1.2. Current model of dyslipidemia associated with obesity and diabetes. This model suggests that increased visceral fat mass and insulin resistance leads to elevated adipocyte lipolysis. In turn, visceral adipose lipolysis increases free fatty acid (FFA) delivery to the liver, where it is efficiently cleared, re-esterified to triglyceride (TG) and loaded onto a nascent apolipoprotein B (apoB) particle, ultimately resulting in very low-density lipoprotein (VLDL) maturation and secretion. Increasing VLDL-TG translates into abnormalities in both high-density lipoprotein-cholesterol (HDL-C) and low-density lipoprotein cholesterol (LDL-C). Cholesteryl ester transfer protein (CETP). Figure from Ginsberg (15).

Elevated VLDL-TGs and CVD risk

Historically, elevated plasma TGs in the form of VLDL-TG have not been directly associated with CVD risk. Currently, the extent to which plasma TGs directly contribute to CVD risk remains controversial (32). Increasing evidence by a number of case-control and prospective studies show a role for hypertriglyceridemia in CVD risk (as reviewed in (33)). A meta-analysis of population-based prospective studies in 1996 (34), in addition to current studies (35), show evidence that plasma TGs are a risk factor for CVD for both men and women in the general population, independent of HDL-C. One example of how insulin resistance and elevated TGs affect the risk of CVD events is the Quebec cardiovascular study (36). This study found that with

increasing concentration of fasting insulin levels reflecting insulin resistance, the risk for CVD increased. However, the increased risk was even more dramatic in the context of elevated VLDL-apoB levels. In a VA-HIT study, treatment with the fibrate gemfibrozil reduced TG levels up to 30% and increased HDL-C levels up to 8%, concomitantly decreasing the incidence of CVD events by 20 to 30% (37). Nonetheless, even in this case, 70 to 80% CVD event risk remains. Thus, a better understanding of the biology behind the regulation of lipoprotein metabolism, particularly in novel areas investigating the dyslipidemia associated with obesity and diabetes, may lead to fundamentally novel therapeutic treatments aimed at lowering some or all of the remaining CVD risk. At this intersection of energy homeostasis and lipid homeostasis biology, it is hypothesized future studies will yield additional novel insight.

Energy homeostasis

Key principles of body weight regulation

The alarming increase in the obesity epidemic in the US and worldwide raises a fundamental question: Is body weight physiologically regulated? Indeed, extensive experimental evidence indicates that body adiposity is tightly regulated and constrained to a physiological range. For example, Sims (38) elegantly demonstrated in "Experimental Obesity in Man" studies, key principles of body weight regulation. In these studies, subjects were motivated by a monetary incentive to consume excess calories for 25 weeks. At baseline, these subjects were weight stable, in which energy intake (1,500 kcal/m^2/day) closely matched energy expenditure. Motivated by the monetary incentive, these subjects became hyperphagic, doubling their basal food intake to ~2,500-3,000 kcal/m^2/day leading to positive energy balance and a 20% body weight gain. Intriguingly, the subject's higher body weight stabilized between 12 and 22 weeks and thus, it can be inferred that energy expenditure nearly doubled from1,500 kcal/m^2/day to 2,500-3,000 kcal/m^2/day to maintain weight stability. Once the monetary incentive was discontinued (by 25

weeks) and the subjects were allowed to eat freely, they became profoundly hypophagic in which their total caloric intake approached zero. This reduction in spontaneous food intake, which lasted for 8 or more weeks led to negative energy balance and a rapid loss of body weight. This complex human study demonstrates the existence of a body weight regulatory system involving the regulation of energy intake and energy expenditure and similar observations are documented in rats (39, 40).

Energy homeostasis can be defined as the physiological process whereby energy intake is precisely matched to energy expenditure over time to promote the stability of body adiposity. A relatively small mismatch between energy intake to expenditure over time, estimated to be less than 0.5% will lead to weight gain or loss (41). Therefore, this regulatory system defends body weight, and specifically, body fat against perturbations (42). The concept that body adiposity is regulated by a feedback loop in which the status of the body fat is sensed, and a signal is sent to the hypothalamus to regulate energy intake and fat storage was first proposed nearly 60 years ago by Gordon Kennedy (43). The regulation of body adipose mass, according to currently accepted models (Figure 1.3) is by a neuroendocrine feedback loop. This involves the "adiposity negative feedback signals," the pancreatic β-cell-derived hormone insulin and the adipocyte-derived hormone leptin, which are long-term regulators of feeding and body weight (reviewed in (44, 45)).

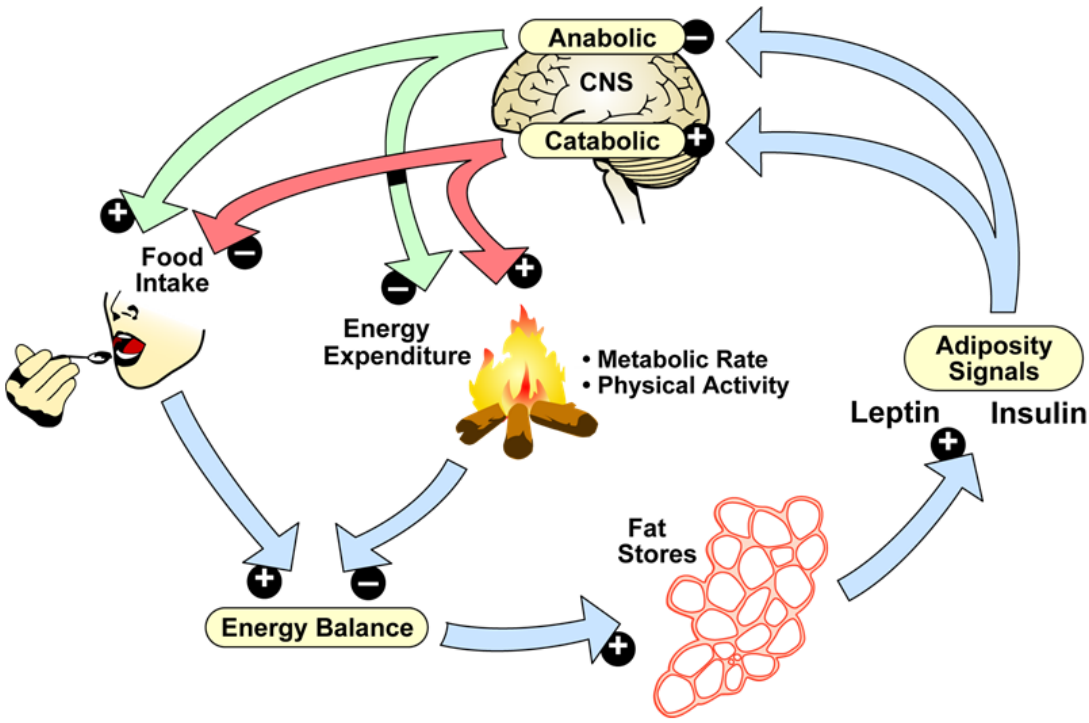

Figure 1.3. Endocrine feedback loop model of body adiposity regulation. The adiposity negative feedback signals insulin and leptin are secreted in proportion to body fat stores and interact with key regulatory neurons found in the hypothalamus. These primary neurons then regulate a series of neural circuits that function *in toto* to control food intake and energy expenditure, ultimately normalizing body fat mass. Figure from Schwartz et al. (45).

Adiposity negative feedback signals

In 1953, Kennedy postulated the existence of a circulating "adiposity signal" that communicates to the CNS about the status of body fat stores (43). Conceptually, a circulating humoral signal must meet several criteria in order to function as an adiposity signal as reviewed in (41). First, the signal(s) should circulate in the bloodstream in proportion to body fat stores. Second, the signal must enter and be sensed by the CNS by acting on and regulating the function of key homeostatic neuronal subsets (i.e. anabolic and catabolic neurons found in the mediobasal hypothalamus (46) and elsewhere (47)). Finally, the acute administration of the putative signal should reduce food intake and/or increase energy expenditure in a neuroendocrine feedback loop

while deficiency of this signal should promote hyperphagia, positive energy balance and obesity. The hormones insulin and leptin, satisfy all of the criteria as adiposity negative feedback signals (48).

Insulin

The concept that insulin functions as an adiposity negative feedback signal to the CNS and controls food intake and weight gain was first proposed by Porte and Woods in the late 1970s (49, 50). Insulin is secreted in direct proportion to body adiposity in the basal state (51) as well as in response to elevated blood glucose levels during and after meals (52). Insulin entry into the brain parenchyma and cerebrospinal fluid occurs primarily across the blood-brain barrier (BBB) endothelium by a receptor mediated saturable transport process (53, 54). The alternative route for insulin access to the brain is via diffusion across the median eminence in the mediobasal hypothalamus, a relatively leaky BBB. This facilitates the entry of circulating insulin into the arcuate nucleus (ARC), a neuronal region rich in insulin receptors (55). While a prototypical anabolic and glucoregulatory hormone in the peripheral tissues, insulin action in the CNS is catabolic in the sense that it reduces food intake, weight gain, and adiposity. A number of elegant basic science approaches have clarified the role of insulin in energy homeostasis. Insulin administered directly into the brain of animals ranging from baboons (56) to rodents (57) lowers food intake and body weight. Genetic modifications that reduce insulin signaling in mice, such as the disruption of the insulin receptor (IR) or insulin receptor substrate-2 (IRS-2) (58-60), as well as mutations in insulin signaling homologues in even more primitive organisms, such as flies and nematodes (46), lead to increased fat mass in these organisms. Administration of Wortmannin and LY29002, inhibitors of the insulin-phosphatidylinositol 3-kinase (PI3K) signaling pathway directly into the third ventricle of the brain inhibits insulin's ability to suppress food intake (61). Thus, insulin signaling through IRS-PI3K pathway in the hypothalamus is a key mediator of appetite and weight regulation (61).

Leptin

Positional cloning and sequencing of the *ob* gene, which encodes leptin, was completed by Jeffrey Friedman's group (62). Similar to insulin, leptin is secreted in direct proportion to the amount of fat stored in adipocytes (63). The importance of leptin as an adiposity signal to the brain is revealed by animals that have impaired synthesis of leptin due to mutations in the *ob* gene (*ob/ob* mice (62)) or that have a genetic mutation in the functional leptin receptor (*db/db* mice (64) and *fa/fa* Zucker fatty rats (65)). These animals are characterized by hyperphagia and extreme obesity (66, 67), and the central administration of microgram amounts of leptin in the brain of *ob/ob* mice but not in *db/db* mice reverses this syndrome (68).

Similarly, rare clinical cases have been reported in children with congenital leptin deficiency (69). These children are massively hyperphagic, have excessive weight gain in early life, and are morbidly obese (70). Treatment with recombinant leptin replacement therapy in these children leads to a suppressive effect on food intake with no alteration in energy expenditure resulting in negative energy balance and sustained weight loss (70). Clearly, leptin is a key regulator of appetite and body weight in humans and rodents.

Obesity pathogenesis: CNS insulin and leptin resistance

Despite the existence of a central homeostatic system that precisely regulates energy homeostasis, there is an alarming increase in the prevalence of obesity in the US and worldwide. Although there is clearly a heritable component that increases an individual susceptibility to obesity such as monogenic and polygenic human obesity (reviewed in (71), it is thought that the adoption of the "Western lifestyle" has been the major predisposing factor to the rapid development of obesity in human populations (44). The Western lifestyle typically consists of the excessive consumption of calorically dense, high-fat, high-carbohydrate foods coupled with an inactive life (72, 73). Indeed, the overconsumption of a diet containing a high proportion of calories as fat leads to the development of obesity (72). As body fat mass increases, there is a

corresponding increase in circulating insulin and leptin levels, which circulate at extremely high levels in severely obese humans (41). Yet, food intake and energy expenditure are relatively normal, or dramatically abnormal if normalized to the degree of hyperleptinemia and hyperinsulinemia (41). This suggests that insulin and leptin are no longer regulating the central homeostatic circuits involved in the regulation of feeding and energy expenditure. This indicates that these obese individuals have acquired functional CNS insulin and leptin resistance, which in turn, contributes to the pathological weight gain (74). Indeed, experimental evidence from our laboratory (74) as well as others (75) show that obesity is characterized by both behavioral and biochemical CNS insulin and leptin resistance. For example, the injection of insulin or leptin directly in the brain via the intracerebroventricular (ICV) route in lean, low-fat fed rats potently reduces food intake and robustly activates hypothalamic insulin or leptin signaling pathways (74). Conversely, these behavioral and biochemical effects are completely blunted in a high-fat fed obese animal (74). Therefore, it is likely that the acquired insulin and leptin resistance in the brain characterizes human obesity and drives the defense of a higher body adiposity, which undermines the ability to lose weight over time (41).

Hypothalamic arcuate nucleus

Situated adjacent to the floor of the third ventricle and the median eminence in the mediobasal hypothalamus, is the ARC, which is an elongate collection of neuronal cell bodies (reviewed in (76)). The median eminence is a circumventricular organ (CVO), lacking endothelial tight junctions and is considered a leaky BBB (77). This allows the ARC access to the third ventricle and the hypophysial portal system, which is the vascular link between the median eminence and the pituitary gland (76). The CVO allows the diffusional exchange of solutes from the blood to the CSF which flows retrograde to the adjacent brain parenchyma, such as the ARC (77). Thus, the ARC is uniquely positioned to sample and respond to a wide variety of hormones and nutrients in both the blood and cerebrospinal fluid (76).

As illustrated in Figure 1.4, neurons found in the ARC are identified by the neuropeptides they express and consist primarily of the opposing anabolic Neuropeptide Y (NPY)/Agouti Related Peptide (AgRP) neurons and the catabolic Proopiomelanocortin (POMC)/Cocaine- and amphetamine regulated transcript (CART) neurons (as reviewed in (78)). These neuronal subsets are known as first-order neurons that express a high concentration of leptin and insulin receptors and respond directly to fluctuations in the levels of these hormones (55, 79, 80). The first-order neurons in the ARC integrate information about body fat stores and then relay this information via projections to other brain regions, containing second-order neurons (78). These brain regions, which also express leptin (79, 81, 82) and insulin receptors (83), include the paraventricular nucleus (PVN), lateral hypothalamic area (LHA), dorsomedial hypothalamic nucleus (DMN), ventromedial hypothalamic nucleus (VMN), hindbrain, and others, and are involved in feeding, energy expenditure, and autonomic regulation (84).

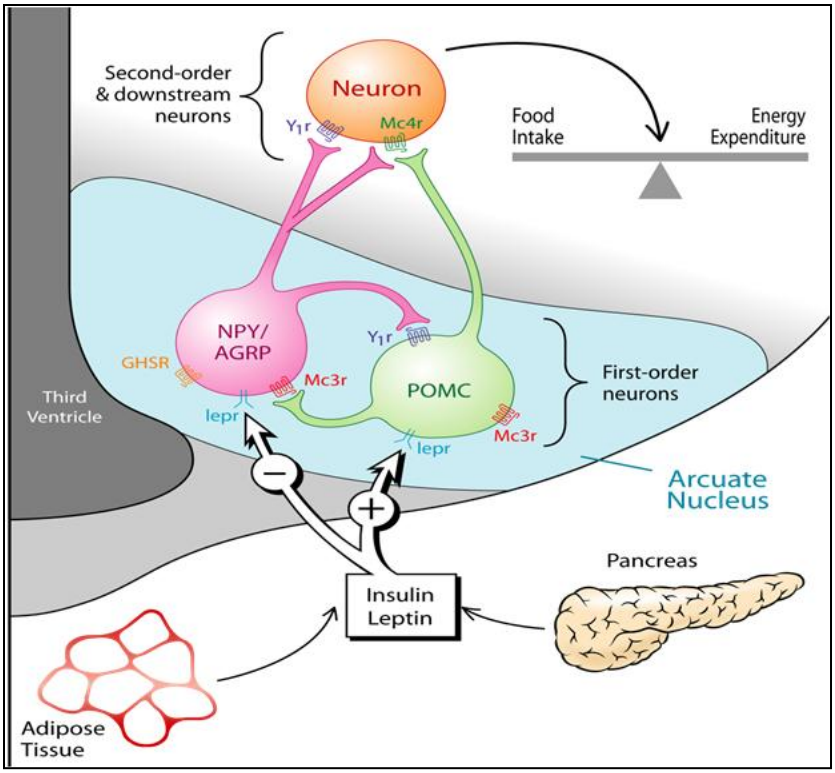

Figure 1.4. Schematic of the arcuate nucleus (ARC) structure located in the mediobasal hypothalamus. The neurons found in the ARC consist of the opposing anabolic neuropeptide Y (NPY)/agouti related peptide (AgRP) neurons that are suppressed by insulin and leptin, and the catabolic proopiomelanocortin (POMC)/Cocaine- and amphetamine regulated transcript (CART) neurons that are activated by insulin and leptin. The net activity of circuits regulated by these neurons determines food intake, energy expenditure, and ultimately body adiposity. Figure from Niswender et al. (44).

Catabolic/anorexigenic POMC/CART neurons

Concentrated in the dorsolateral ARC are the catabolic POMC expressing neurons that are activated by leptin and insulin and suppressed in states of negative energy balance (fasting, starvation) or defective leptin and insulin signaling (obesity, diabetes) (reviewed in (78)). The post-translational modification of the POMC polypeptide precursor generates melanocortins such as α-melanocyte stimulating hormone (α-MSH) (reviewed in (85)). In response to elevated insulin and leptin levels, α-MSH is released from the POMC expressing neurons which exert anorexigenic effects via binding to the melanocortin receptor (MCR), MC3R and MC4R found in

second order neurons (86). In turn, activation of the melanocortin pathway, inhibits feeding and increases energy expenditure, ultimately resulting in decreased adipose stores (87, 88). Thus, central administration of the potent MCR agonist, MTII inhibits food intake in mouse models of hyperphagia (i.e. fasted C57BL/6J and *ob/ob* mice) whereas co-administration of the MCR antagonist, SHU9119 completely blocks this inhibition (86). Mutations in MC4R produces profound obesity in rodents (88) and humans (89), indicating that this pathway is crucial for the regulation of energy homeostasis.

Anabolic/orexigenic NPY/AgRP neurons

Found within the ventromedial ARC and adjacent to POMC neurons are the anabolic NPY neurons that co-express AgRP. NPY/AgRP are suppressed by insulin and leptin, and activated by negative energy balance (fasting, starvation) or states of defective leptin and insulin signaling (obesity, diabetes) (reviewed in (78)). In response to falling insulin and leptin levels, these neurons release NPY which activates downstream anabolic circuits to promote positive energy balance by increasing food intake and reducing energy expenditure (90). Subsequently, these neurons reduce melancortin signaling via the release of AgRP, which competitively antagonizes MC3R and MC4R (91).

Neuropeptide Y biology

The NPY family of peptides: Discovery, function, and tissue distribution

NPY was first isolated and sequenced in 1982 from porcine brain (92). NPY is a member of the NPY family that includes peptide YY (PYY) and pancreatic polypeptide (PP) (93). PYY and PP share 70 and 50% sequence homology with NPY (Figure 1.5). These peptides are 36 amino acids long, characterized by a large number of tyrosine residues and are amidated at their C-terminal ends. They share a common hairpin like tertiary structure known as a PP fold

characterized by a polyproline like helix (residues 1-8 form) and an amphipathic α-helix (residues 15-30) (94) as illustrated in Figure 1.5. NPY is one of the most conserved peptides known among species (95). By contrast, PYY shows greater variability, and PP is the most rapidly evolving member of the NPY peptide family with only 50% identity within mammals (95).

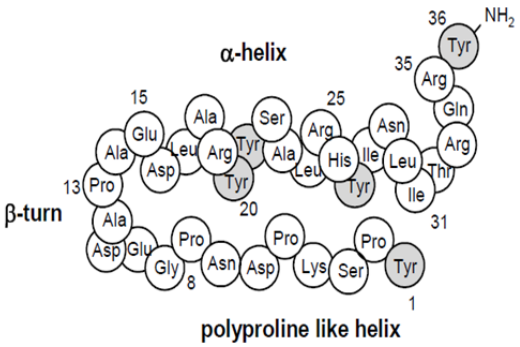

hNPY	YPSKPDNPGEDAPAEDMARYYSALRHYINLITRQRY-NH_2
hPYY	**YP**I**KP**EA**PGEDA**SP**E**ELN**RYY**AS**LRHY**L**NL**V**TRQRY**-NH_2
hPP	A**P**LE**P**VY**PG**DN**A**TP**E**Q**MA**QY**AADLRR**Y**I**N**ML**TR**P**RY**-NH_2

Figure 1.5. The NPY family of peptides. On top: the schematic structure of the characteristic PP-fold family shown for porcine NPY. Residues 1-8 form a polyproline helix followed by a β-turn and a α-helix comprised of the residues 15-30. On bottom: Amino acid sequences of human (h) neuropeptide Y (NPY), hpeptide YY (hPYY), and hpancreatic polypeptide (hPP). Amino acids which are homologous to hNPY are shown in bold. The constant positions among all species are underlined for each peptide. Adapted from Cabrele et al. (94).

NPY is widely distributed within the peripheral and central nervous system and is one of the most abundant neuropeptides in the brain of rodents (96) and humans (97, 98). It is widely distributed in the CNS, including the hypothalamic ARC that projects to the DMN, PVN, LHA, VMN, and the brainstem; key regions involved in feeding, energy expenditure, and autonomic regulation (84). In the periphery, the sympathetic neurons represent the main source of the neurotransmitter NPY, where it is co-localized and co-released with norepinephrine (NE) (99). Additionally, the adrenal medulla is the primary source of circulating NPY, although it is expressed in other peripheral regions, including the liver, heart, spleen, bone marrow, adipocytes,

and peripheral blood cells (100). Conversely, PYY is predominately synthesized in the digestive tract while PP is found in pancreatic endocrine cells, which are released in response to meals to regulate feeding behavior, energy homeostasis, gastric, and pancreatic secretion (reviewed in (101, 102)).

NPY has a significant role in the regulation of a number of biological functions. The relative abundance of NPY combined with its widespread distribution, suggests that NPY is involved in diverse physiological roles beyond the regulation of food intake. In general, NPY participates in the control of neuroendocrine coordination (i.e. hypothalamic-pituitary-adrenal axis (HPA)), learning and memory, locomotion, body temperature regulation, sexual behavior, emotional behavior, neuronal excitability, cardiovascular function, circadian rhythms, blood pressure, and hormone secretion (i.e. pancreatic insulin secretion) and others (reviewed in (99, 103)).

NPY synthesis and processing

The biologically active NPY is derived from a 97-amino acid precursor, pre-pro-NPY following at least four post-translational events as shown in Figure 1.6. The translational product, pre-pro-NPY, is directed into the endoplasmic reticulum (ER) where the signal peptide is cleaved. Then, pro-NPY undergoes cleavage by the proconverting enzymes PC1/3 and/or PC2 at a dibasic site, which generates NPY 1-39 and the C-flanking peptide of NPY (CPON). Two further sequential truncations at the C-terminal end by a carboxypeptidase and the peptidylglycine α-amidating monooxygenase produce the biologically active amidated NPY 1-36. The mature NPY can be further processed by two enzymes, the amino peptidase P and dipeptidyl peptidase IV (DPPIV) producing NPY 2-36 and NPY 3-36, respectively (99, 104).

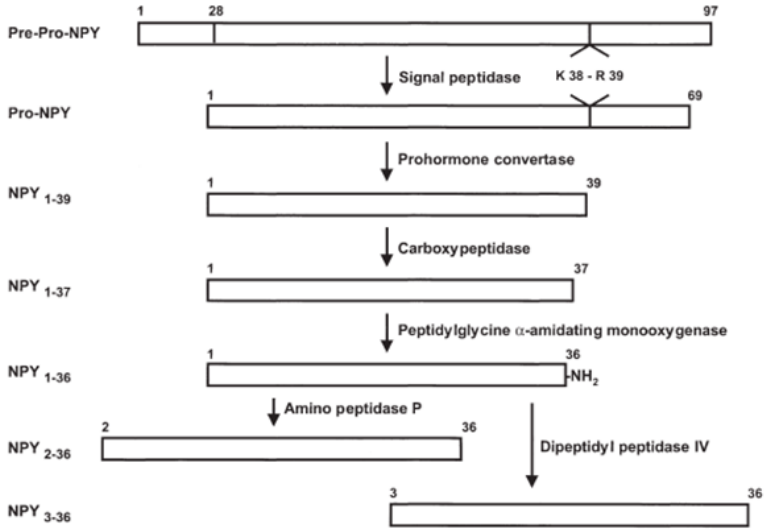

Figure 1.6. NPY synthesis and processing. Figure from Pedrazzini et al. (99).

NPY Y receptor biology

Neuropeptide Y receptors: Preferred ligands, distribution, and physiological functions

The NPY-family peptides elicit numerous physiological responses by the activation of a family of five NPY receptor subtypes, Y1, Y2, Y4, Y5 and y6, which have all been cloned from mammals (reviewed in (93, 105)). However, the y6 receptor has been established as a mouse and rabbit receptor subtype, as it is absent in rats and non-functional in humans (105). The receptors all belong to the rhodopsin-like superfamily of G-protein coupled receptors (GPCRs) characterized by a seven transmembrane (7-TM) helix structure (105). All NPY Y receptors modulate a variety of pathways through the coupling to pertussis toxin-sensitive inhibitory heterotrimeric GTP-binding protein (Gi/Go) (94). One of the typical signaling responses of the NPY receptor activation is the inhibition of adenylyl-cyclase, thus, mediating the inhibition of cyclic adenosine monophosphate (cAMP) accumulation (106-108). The other signal transduction pathway that may be triggered is the stimulation of Ca^{2+} release from intracellular stores by the activation of the phospholipase C pathway (inositol phosphate accumulation) (107-109). NPY can

also directly hyperpolarize neurons by activating the Y1 receptor subtype coupled to the Gi protein signaling pathway and subsequent activation of the G-protein-coupled inwardly rectifying potassium channels (GIRK) (110, 111). For example, a study by Chee et al. (110) reports that NPY inhibits the excitatory (anorexigenic) outflow between the VMN and ARC POMC neural circuitry via the activation of the NPY Y1 receptor subtype in the VMN that couples to the activation of GIRK channels and thus, hyperpolarizes VMN neurons.

The most important properties of the four intensely investigated NPY Y receptor subtypes, Y1, Y2, Y4, and Y5, are summarized in Table 1.2. These NPY Y receptor subtypes have individual ligand binding profiles for members of the NPY family (Table 1.2). Thus, Y1, Y2, and Y5 receptors preferentially bind NPY and PYY whereas the Y4 receptor shows a higher binding affinity for PP (105, 109). Both NPY and PYY can be further processed by DPPIV resulting in the removal of the first 2 amino acids from the N-terminus producing a shorter peptide fragment (i.e. NPY 3-36 and PYY 3-36) which leads to preferential binding affinities to the NPY Y2 receptor (112).

All NPY Y receptors are expressed in the brain and are particularly highly concentrated in the hypothalamus (113, 114); the region involved in the regulation of energy homeostasis. Additionally, all NPY Y receptors are expressed in the peripheral tissues except for the brain specific Y5 receptor (Table 1.2). In the brain, Y2 receptors are found more often pre-synaptically expressed and their activation suppresses neurotransmitter release (115). However, Y2 receptors have also been found to be post-synaptically expressed on neurons (116). Conversely, the NPY Y1, Y4, and Y5 receptors are post-synaptically expressed (117, 118).

NPY receptors play a role in a plethora of physiological processes in both the central and peripheral tissues as shown in Table 1.2. The most predominant effect of NPY is involvement in the regulation of feeding and energy homeostasis. For example, ICV administration of Y1 and Y5 receptor agonists increases food intake in rats (119-122). Conversely, intra-arcuate administration of NPY Y2 receptor agonist inhibits food intake (123), although these findings remain

controversial (124). Thus, as obesity and CVD is a serious public health threat to the US and worldwide, there is special interest in the NPY receptor ligands as a therapeutic treatment for human obesity (93). In Chapter III, we will determine whether NPY receptor(s) are an important target for treating the dyslipidemia associated with obesity, diabetes, and the metabolic syndrome independently of effects on feeding and increased visceral adiposity.

Table 1.2. Neuropeptide Y family of receptors, their preferred ligands, receptor distribution, and physiological functions

Receptor subtype	**Y1**	**Y2**	**Y4**	**Y5**
Ligand binding profile (agonists)	NPY ≈ PYY ≈ [Leu^{31},Pro^{34}] NPY > NPY_{2-36} ≈ NPY_{3-36} ≥ PP ≈ NPY_{13-36}	PYY > PYY^{3-36} ≈ NPY_{3-36} ≈ NPY_{2-36} ≈ NPY_{13-36} >> [Leu^{31},Pro^{34}]NPY	PP ≥ GW1229 > PYY ≥ NPY > NPY_{2-36}	NPY ≈ PYY ≈ NPY_{2-36} ≈ [Leu^{31},Pro^{34}] NPY > hPP >[D-Trp^{32}]NPY > NPY_{13-36} > rPP
Signal transduction	Gi/o → cAMP↓; [Ca2+]↑	Gi/o → cAMP↓; [Ca2+]↑	Gi/o → cAMP↓; [Ca2+]↑	Gi/o → cAMP↓; [Ca2+]↑
Receptor expression (central vs. peripheral)	**Central:** Hypothalamus, cerebral cortex, hippocampus, amygdala, brain stem, thalamus **Peripheral:** Liver, muscle, adipose tissue, vascular smooth muscle cells, immune cells, osteoblasts	**Central:** Hypothalamus, hippocampus, brainstem **Peripheral:** Autonomic nerves, gastrointestinal tract, endothelial cells, adipocytes	**Central:** Hypothalamus, hippocampus **Peripheral:** Colon, small intestine, prostate, heart	**Central:** Hypothalamus, cerebral cortex, hippocampus, amygdala, brain stem, plexiform cortex of the olfactory bulb, suprachiasmatic nucleus
Pre-synaptic vs. post-synaptic expression	Post-synaptic	Pre- and post-synaptic	Post-synaptic	Post-synaptic
Physiological function (central vs. peripheral)	**Central:** Regulation of energy homeostasis, anxiolysis **Peripheral:** Oxidative fuel selection, physical activity, adipogenesis, vasoconstriction, regulation of neurotransmitter release	**Central:** Regulation of food intake, inhibition of neurotransmitter release, learning and memory, circadian rhythm **Peripheral:** Inhibition of norepinephrine release, angiogenesis, adipogenesis	**Central:** Regulation of food intake **Peripheral:** Motility of the gastrointestinal tract, pancreatic secretion	**Central:** Regulation of energy homeostasis, anti-epileptic

Data presented were collected from recent reviews (Hirsch et al. (117), Lindner et al. (105), Shi et al. (125), and Chambers et al. (126)) as well as findings from Zhang et al. (127). Abbreviations: Cyclic adenosine monophosphate (cAMP); neuropeptide Y (NPY), pancreatic polypeptide (PP); peptide YY (PYY).

Physiological functions of NPY

NPY in the regulation of food intake and energy homeostasis

The seminal observation in 1984 that direct injection of NPY into the brain of rats elicited an increase in food intake (128-130) was the first demonstration that an endogenous peptide is synthesized in the brain and has potent orexigenic effects. This observation precedes the discovery of other potent orexigenic neuropeptides (galanin, ghrelin, the orexins, AgRP, and melanin-concentrating hormone) (126).

NPY is a potent orexigenic peptide and when delivered by chronic infusion directly into the brain of rats and mice, has been observed to promote hyperphagia, obesity, obesity dyslipidemia, and the metabolic syndrome (131, 132), similar to that of the leptin deficient *ob/ob* mouse (62, 67, 133) and the genetically leptin resistant *fa/fa* Zucker fatty (ZF) rat (65, 66). These genetic models of obesity are characterized by high NPY mRNA and peptide levels in the hypothalamus, secondary to the absence of negative feed-back regulation by leptin (134-137). In Chapter IV, we will utilize the *fa/fa* ZF rat to investigate the effects of elevated CNS NPY tone on liver lipid metabolism independently of hyperphagia and obesity.

Chronic peripheral administration of leptin to *ob/ob* (leptin-deficient) but not *db/db* (leptin-resistant) mice reduces food intake, obesity, hyperglycemia, and hypothalamic NPY mRNA levels (136, 138). Rodent models of diet-induced obesity (DIO; made obese by feeding a highly palatable diet) and streptozotocin (STZ)-induced diabetes (insulin-deficient), which are more typical of human diabetes, are also characterized by elevated CNS NPY tone (139, 140). ICV administration of insulin in STZ-induced diabetic rats attenuates elevated NPY levels and hyperphagia (139). Paradoxically, germline deletion of NPY does not affect food intake and body weight in mice (141). However, NPY deficiency does impair the re-feeding response to fasting and attenuates DIO and genetic obesity (*ob/ob*) in mice (141, 142).

Similar to rodent models (139, 140), it has been documented in humans (98, 143, 144) that obesity and diabetes are associated with elevated hypothalamic NPY tone with a concomitant reduction of POMC tone. For example, in obese non-diabetic Mexican-American families, a significant linkage was found between obesity and the *NPY* gene (145). However, a study by Roche et al. (146), found no evidence for a linkage between *NPY, NPY1R,* and *NPY5R* loci and obesity in French Caucasian morbidly obese families. Nor did a genome-wide scan for obesity genes in Pima Indians detect a linkage between obesity and the *NPY* gene (147, 148). Although, a study by Goldstone et al. (149) found that NPY expression was reduced in the postmortem hypothalami of obese human subjects, other studies report that plasma NPY levels are found to be the highest in obese hypertensive and diabetic patients (143, 144). Furthermore, a key recent study by Saderi et al. (98) found an increase in NPY immunoreactivity in the ARC of diabetic human subjects. It is thought that elevated hypothalamic NPY tone results from defects in inhibitory feedback signaling to the CNS, including neuronal insulin and leptin resistance, and impaired nutrient sensing, leading to impaired ability of these neuronal subsets to sense energy excess (74, 75).

NPY Y receptor subtypes in the regulation of food intake and energy homeostasis

The key brain region where NPY regulates food intake and energy homeostasis is the hypothalamus, which expresses all four NPY Y receptor subtypes, Y1, Y2, Y4, and Y5 (113, 114, 150). The most studied circuits which are NPY-regulated sites are diagrammed in Figure 1.7. The ARC and the DMN contain NPY neurons and have axon projections to the PVN, VMN, and the LHA areas (126). Of particular interest, the PVN and the VMN are highly sensitive to the orexigenic actions of NPY. Bilateral electrolytic lesions of these hypothalamic sites in rats which recapitulates a state of elevated NPY tone, leads to hyperphagia and obesity (151, 152). Furthermore, direct microinjection of NPY into these hypothalamic sites can stimulate food intake and reduce energy expenditure (153-155).

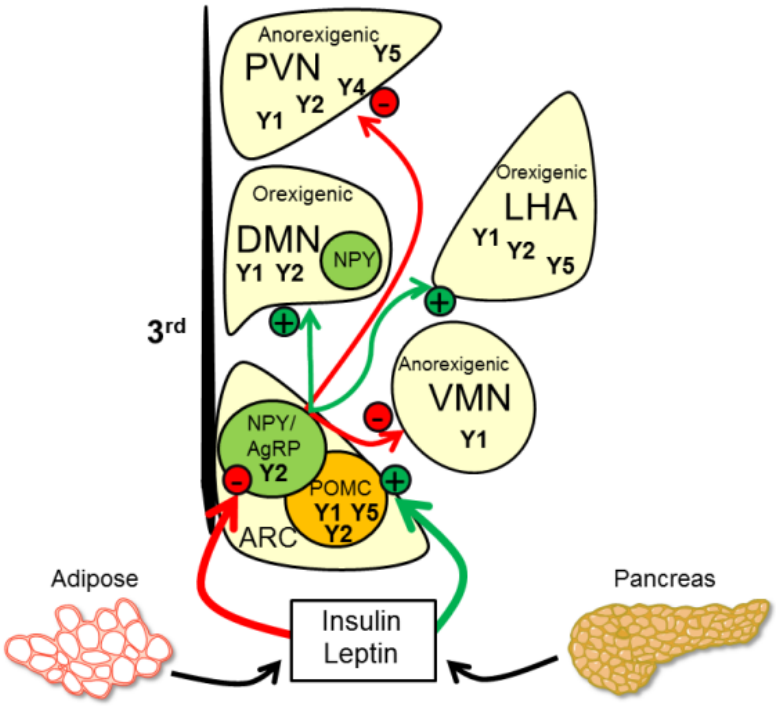

Figure 1.7. A unilateral view of the hypothalamus at the level of the ARC. The key brain region where neuropeptide Y (NPY) regulates food intake and energy homeostasis is the hypothalamus, which expresses all four NPY Y receptor subtypes, Y1, Y2, Y4, and Y5. The arcuate nucleus (ARC) and the dorsomedial hypothalamic nucleus (DMN) contain NPY neurons and have axon projections to the paraventricular nucleus (PVN), lateral hypothalamic area (LHA), and the ventromedial hypothalamic nucleus (VMN). Abbreviations: agouti related peptide (AgRP); proopiomelanocortin (POMC). Adapted from Chambers et al. (126).

Many studies have focused on identifying the NPY receptor subtype(s) involved in mediating the NPY effect on feeding and energy homeostasis. The utilization of highly selective receptor subtype agonists and antagonists have revealed that Y1 and Y5 receptor subtypes may be the predominant receptors involved in NPY regulation of feeding behavior (93). Both receptors have been found to be co-localized and highly expressed within the cortex, hippocampus, hypothalamus, amygdala, and brainstem corresponding to major actions of NPY (118). There is a reported close physical localization and apparent functional relationship between NPY Y1 and Y2 receptors in neurons found within the ARC, LHA, DMN, and PVN in contrast to the VMN which

contains only Y1 receptor positive neurons (114). This provides compelling evidence that NPY may also act through the Y2 receptor to modulate feeding behavior.

ICV administration of Y1 and Y5 receptor agonists increases food intake in rats (119-122), whereas the administration of Y1 and Y5 antagonists (156-162) or antisense oligonucleotides (163-166) decreases food intake. However, studies investigating the effect of NPY, Y1, and Y5 receptor deficiency on energy homeostasis are quite surprising. Germline deletion of Y1 or Y5 receptor in mice does not produce a lean phenotype. In fact, Y1 and Y5 receptor deletion in mice paradoxically leads to the development of late-onset obesity (167, 168). Thus, these contrary observations with genetic manipulation suggest that in the absence of Y1 or Y5 receptors, compensation may occur during development. However, impaired fasting-induced re-feeding is observed in Y1 receptor deficient mice and the NPY-induced hyperphagia is abolished in Y5 receptor deficient mice which implicates these receptors as important mediators in feeding regulation (167, 169). Previous studies report that Y1 and Y5 receptor deletion attenuates DIO or genetic obesity (*ob/ob*) in mice consistent with findings reported for NPY deficiency (141, 142, 170, 171). Although, there has been special interest in the Y1 and Y5 receptor as a potential therapeutic treatment for human obesity (93), a Y5 receptor antagonist failed to induce clinically significant weight loss in overweight and obese humans (172).

Conversely, the gut-derived PYY 3-36, a Y2 receptor agonist, and the pancreatic-derived, PP, a Y4 receptor agonist, dose-dependently inhibits food intake in fasted rodents when peripherally injected (123, 173). Notably, this reduction in food intake is entirely mediated via the Y2 or Y4 receptor since this effect is completely abolished in Y2 and Y4 receptor null mice, respectively (123, 174). Similarly, NPY Y2 receptor null mice are hyperphagic and obese (175) whereas, surprisingly, Y4 receptor null mice are lean (176).

Both Y2 and Y4 receptors are implicated as potential targets for the treatment of obesity (176). Crossing the Y2 receptor null mouse onto the *ob/ob* background attenuated obesity whereas the Y4 receptor deficiency on this genetically obese background conferred no beneficial

effects (176, 177). Chronic administration of PYY 3-36 or PP in obese rodents significantly reduces food intake and body weight (178-180). In humans, peripheral administration of either PYY 3-36 or PP to lean (123, 181, 182) or obese (183, 184) subjects significantly reduces appetite and food intake. The mechanism involved in the Y2 and Y4 receptor anorexigenic effects are thought to be mediated in part, by decreasing hypothalamic NPY and elevating POMC tone (123, 180, 185).

Paradoxically, central (ICV) administration of PYY 3-36 or PP increases food intake in *ad-libitum* fed rodents (124, 173) and intra-arcuate administration of PYY 3-36 inhibits food intake in fasted rats (123). Because the inhibitory Y2 receptor is found on both the ARC NPY and POMC neurons, this adds an additional layer of complexity to the regulation of the NPY/POMC neural circuit, further suggesting that the effect of endogenous and exogenous Y2 ligands on the ARC neuronal subsets is context dependent as elegantly described in Ghamari-Langroudi et al. (116). For example, in the study by Batterham et al. (123), PYY 3-36 was injected directly into the ARC of 24-hour fasted rats characterized by high endogenous NPY tone, and thus the action of the exogenously added NPY Y2 ligand on the ARC neurons may result in an anorexigenic response to inhibit food intake (suppression of NPY neurons). In contrast, injection of the NPY Y2 receptor agonist directly into the third ventricle of *ad-libitum* fed rats characterized by low endogenous NPY tone, may result in an orexigenic response from the action of the NPY Y2 ligand, resulting in the stimulation of food intake (suppression of POMC neurons) (124). An additional consideration is that ICV administration of an Y2 or Y4 receptor agonist may result in its dispersion to other hypothalamic and non-hypothalamic regions. Finally, the potential activation of the Y5 receptor by PYY 3-36 or PP could also explain the increase in food intake.

NPY in the regulation of glucose metabolism

It has been shown previously that hypothalamic leptin and insulin signaling are required for the inhibition of hepatic glucose production (HGP). Indeed, ICV infusion of insulin or leptin

in rodents can potently suppress glucose production whereas antagonism of insulin or leptin signaling in the hypothalamus can impair the ability of peripheral insulin to suppress HGP (136, 186-188). Evidence suggests that NPY neurons are involved in this process (136) and that ICV infusion of NPY can induce hepatic insulin resistance impairing the ability of insulin to suppress HGP in rats (189-192). These data clearly suggest the existence of a hypothalamic-hepatic circuit, potentially mediated by the sympathetic nervous system (SNS) that is involved in the regulation of HGP (189, 192). Thus, under conditions characterized by increased hypothalamic NPY tone (fasting, obesity, and diabetes), NPY activates sympathetic outflow to the liver. This, in turn induces hepatic insulin resistance to maximize HGP (189, 192) contributing to the dysglycemia associated with obesity, diabetes, and the metabolic syndrome (13).

NPY in the regulation of the HPA axis

The activity of the HPA axis is reportedly increased in obesity and diabetes in humans (193-196) and in rodent models of genetic obesity (177, 197), DIO (198), and STZ-induced diabetes (199). In normal animals, NPY activates the HPA axis in response to stress resulting in the release of corticotropin-releasing hormone (CRH) from the PVN (117). In rats, administration of NPY into the ventricles immediately produced an increase in adrenocorticotropic hormone (ACTH) and the glucocorticoid (GC), corticosterone (200, 201). GC infusion in rats increases hypothalamic NPY expression and upregulates NPY Y1 receptor expression through the type II glucocorticoid receptor (GR) whereas this effect can be blocked by the type II selective antagonist, RU486 (99). Additionally, Yi et al. (202) demonstrates that local administration of the GC, dexamethasone in the ARC but not the PVN under hyperinsulinemic-euglycemic clamp conditions in rats induced severe hepatic insulin resistance which was completely prevented by either ICV co-administration of Y1 receptor antagonist BIBP3226 or by hepatic sympathetic denervation (Sx). Moreover, blockade of the central melanocortin system (which can be antagonized by the NPY/AgRP neural circuit) has been shown to regulate hepatic TG synthesis

via the upregulation of *de novo* lipogenic target genes, fatty acid synthase (*FASN*) and stearoyl-CoA desaturase-1 (*SCD*), an effect that requires a fully functional HPA axis (203). Therefore, some of the hormonal and metabolic effects of chronic CNS NPY signaling in normal rats depends on circulating corticosterone, since adrenalectomy prevented these NPY-induced effects, including hyperphagia, obesity, hyperinsulinemia, and hypertriglyceridemia (201). Altogether, these studies suggest that the effect of CNS NPY on hepatic liver lipid metabolism may be dependent on the activation of the HPA axis, which will be further investigated in Chapter IV.

NPY in the regulation of lipid metabolism

Although NPY is an important regulator of feeding and energy homeostasis, it is increasingly recognized as having a role in lipid homeostasis. Elevated hypothalamic NPY tone induces hyperphagia and elicits a series of obesogenic changes that ultimately promotes energy storage. These hormonal and metabolic changes of obesity elicited by increased central NPY signaling include the following: 1) hyperinsulinemia and hypercorticosteronemia (200, 201, 204-207); 2) reduction in body temperature (208) and brown fat thermogenesis (209), indicating decreased energy expenditure; 3) greater glucose utilization for lipid synthesis in adipose tissue (201, 207); 4) increased *de novo* lipogenic activity in liver and adipose tissues, and increased clearance of circulating TG mediated by elevated LPL activity (207); 5) increase in respiratory exchange ratio, indicative of a higher preference for oxidizing carbohydrate over lipids as a fuel source (210). Additionally, Zhang et al. (127) found that Y1 receptor null mice had greater utilization of lipid as an oxidative fuel source. This most likely involved increases in liver and muscle carnitine palmitoyltransferase-1 (CPT-1) protein levels as well as increases in the activity of enzymes involved in β-oxidation, suggesting that Y1-receptor-signaling controls mitochondrial capacity for FFA transport and oxidation.

NPY in the regulation of lipoprotein metabolism: Dyslipidemia associated with obesity and diabetes

Although the current model of dyslipidemia in the context of obesity and diabetes suggests that hepatic VLDL-TG secretion rate is largely determined by the rate of substrate (FFA) delivery to the liver and hepatic insulin sensitivity (23-25), we (211) and others (191, 192) clearly show that CNS NPY signaling is an important regulator of lipoprotein metabolism. Indeed, Van Den Hoek et al. (191) is the first study to show that ICV NPY administration in the context of hyperinsulinemia, which would suppress CNS NPY signaling, resulted in impaired suppression of hepatic VLDL-TG secretion by insulin. We previously demonstrated that ICV administration of NPY directly into the third ventricle of lean, fasted, wild-type rats increases hepatic VLDL-TG secretion independently of increased food intake and visceral adiposity (211). Peripherally administered NPY had no such effect and taken together, these findings suggest that NPY-regulated neural circuits may be involved in the regulation of TG metabolism in the liver (211).

Furthermore, studies in VMN-lesioned rats, which recapitulates a state of elevated NPY tone, have elevated plasma TGs (212). Even under pair-feeding conditions to prevent hyperphagia, VMN-lesioned rats develop hypertriglyceridemia as early as 10 days postoperatively, together with decreased plasma FFA and glucose levels (213). Finally, perfused livers from VMN-lesioned rats secrete more TGs than controls (213). Intriguingly, chronic ICV infusion of NPY and not the MC4R antagonist HS014 in rats pair-fed to the vehicle-treated controls mimicked the effect of VMN-lesions by increasing plasma TGs concomitant with a reduction in FFAs (214). These studies suggest that CNS NPY may be a key regulator of liver lipid metabolism.

In the same hypothalamic feeding circuits engaged by NPY, hypothalamic glucose (215) and glycine (216) metabolism suppresses VLDL-TG production. Conversely, increased CNS resistin (217) and glucocorticoid signaling (202) induces hepatic insulin resistance via hypothalamic NPY. The CNS NPY effect on hepatic insulin resistance and VLDL-TG secretion

can be effectively blocked by liver Sx in rats (189, 192, 202). In the context of the findings from the aforementioned studies, coupled with our findings (211), provides a compelling argument that CNS NPY plays a critical role in the regulation of lipoprotein metabolism. Furthermore, in human population studies, screening of the entire coding region of the *NPY* gene revealed a frequent polymorphism (T1128C) that was strongly associated with high serum total cholesterol and LDL-C levels in obese subjects (218). This single nucleotide polymorphism (SNP), resulting in the substitution in the 7th amino acid from leucine to a proline in the signal peptide of pre-pro-NPY, leads to an increase in NPY peptide secretion (219).

The receptor subtype(s) involved in the central NPY regulation of lipoprotein metabolism are not well understood. Previous studies show that chronic infusion of an NPY Y5 receptor agonist in mice dose-dependently increases adiposity, plasma TGs, and cholesterol levels and this effect remained even under pair-feeding conditions (220). Our studies show that an acute ICV injection of a selective Y5 receptor agonist can double hepatic VLDL-TG secretion in lean fasted rats whereas an antagonist for the Y1 receptor can suppress VLDL-TG secretion (211). Therefore, in Chapter III, we sought to determine which of the various NPY receptor subtypes (Y1, Y2, Y4, and Y5) are involved in feeding versus VLDL-TG secretion.

Several studies have investigated the effect of global deletion of the NPY Y1, Y2, Y4, and Y5 receptors on the background of the *ob/ob* mouse model characterized by elevated CNS NPY tone and severe hypertriglyceridemia. Unfortunately, these studies only report on the effect of this genetic manipulation on energy homeostasis and not on whether deletion of the various NPY receptors attenuate hypertriglyceridemia, except for the Y2 receptor which was noted to have no effect (167, 170, 176, 177). Intriguingly, a genetic association study conducted in severely obese human subjects matched for body mass index (BMI) revealed that those individuals with the CC haplotype (relative to the TT/CT polymorphism) of the un-translated region of the *NPY1R* gene had elevated fasting serum TGs and significantly lower HDL-C concentrations (221). It is not yet clear if this haplotype correlates with a relative gain of NPY Y1

receptor function, but we would hypothesize based upon our findings (211, 222), that the CC haplotype is a relatively hyperfunctional allele and thus, would confer increased TGs in the setting of obesity. Altogether, further understanding of the biology of individual NPY receptor subtypes may lend novel insight into how CNS NPY regulates lipoprotein metabolism.

Lipoprotein metabolism

VLDL assembly and secretion

In the context of integrated energy homeostasis, short term energy stores are provided by glucose and glycogen, while long term needs are met by adipose- and liver-derived lipids. Physiologically, TGs are more energy dense (9 kcal/g) than other fuels, such as carbohydrates (4 kcal/g) and either are stored (adipose tissue) or utilized as an energy source in the peripheral tissues, particularly the muscle (223). Since lipids are hydrophobic, one major function of the liver and the intestine is to package insoluble lipids (i.e. TGs, cholesterol) into the soluble lipoprotein form that can be efficiently transported and delivered to various organs and tissues by the circulatory system (224, 225). This function is achieved by the assembly and secretion of hepatic-derived VLDL or intestinal-derived chylomicrons consisting of a neutral TG and CE core surrounded by a monolayer of amphipathic phospholipids (PL), cholesterol, and apoB (223, 225). In humans, apoB-100 is virtually the only form of apoB expressed in the liver, whereas apoB-48, which is the truncated form of apoB-100 is synthesized in the intestines and packaged in chylomicrons (226). In contrast to humans, the rat produces predominately apoB-48 instead of apoB-100 in the liver (227).

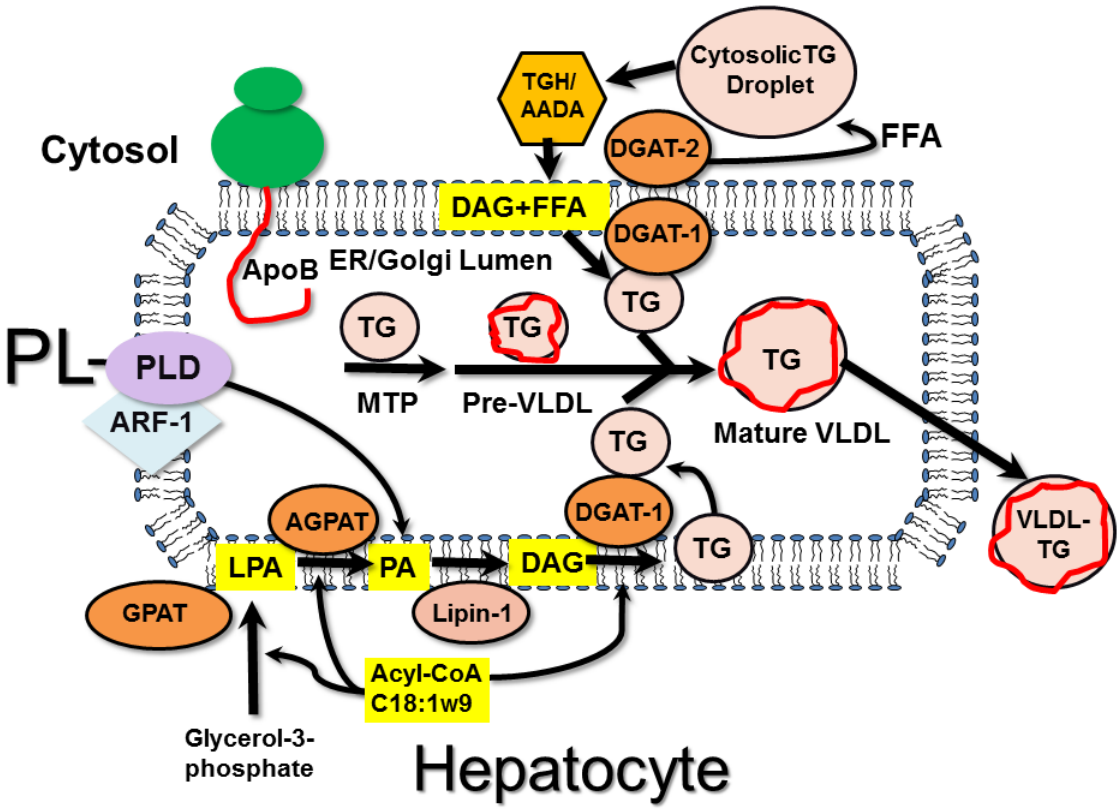

Figure 1.8. VLDL assembly and secretion. Very low-density lipoprotein (VLDL) is the major TG-rich lipoprotein and is assembled in hepatocytes in a complex, two-step process. In the first step, lipid is loaded onto apoB as it is translated into the ER lumen by MTP to produce HDL-sized pre-VLDL lipoprotein. Next, a larger lipid droplet is added to the apoB-containing pre-VLDL to form the mature VLDL particle in the ER/Golgi lumen. PA, a key substrate that provides the TG precursor, DAG for VLDL assembly and secretion can be generated from PL remodeling (catalyzed by ARF-1 and PLD) or via the glycerolipid biosynthetic pathway (catalyzed by GPAT, AGPAT, and lipin-1). The lipases TGH and AADA are involved in the lipolytic mobilization of cytosolic TG stores that are re-esterified by DGATs, which are then channeled into the VLDL maturation pathway or recycled back into the cytosolic TG pool. Abbreviations: acylglycerol-3-phosphate acyltransferase (AGPAT); ADP-ribosylation factor-1 (ARF-1); apolipoprotein B (apoB); arylacetamide deacetylase (AADA); diacylglycerol (DAG); diacylglycerol acyltransferase (DGAT), glycerol-3-phosphate acyltransferase (GPAT); lysophosphatidate (LPA); microsomal triglyceride transfer protein (MTP); phosphatidic acid (PA); phospholipid (PL); phospholipase D (PLD); triglyceride (TG); triglyceride hydrolase (TGH). Adapted from Gibbons et al. (228) and Sundaram et al. (225).

The assembly and secretion of TG-rich VLDL represents a key component of hepatic TG homeostasis, which is a tightly regulated and complex two-step process as illustrated in Figure 1.8 (reviewed in (225, 228)). In the first step, a small quantity of TG is assembled onto the

structural protein, apoB-100 during its co-translational translocation through a protein channel in the membrane of the rough ER lumen. This process is accompanied by the acquisition of a PL monolayer encasing the TG core. The resulting formation of the HDL-sized pre-VLDL lipoprotein is dependent on microsomal triglyceride transfer protein (MTP) (228). Mutations leading to the loss of MTP activity which is linked to familial abetalipoproteinemia leads to impaired VLDL assembly and secretion (229). In the absence of lipid or MTP, apoB translocation is halted, and becomes a target for proteasomal degradation (230).

The second step, which is less well-characterized, involves the fusion of a larger droplet of TG with the apoB-containing pre-VLDL to form the mature VLDL particle before exiting from the ER (228, 231). This process can be blocked by integrated hepatic insulin action leading to enhanced degradation of apoB and suppression of VLDL-TG secretion (29, 30). A number of studies suggest that the assembly of VLDL is not completed within the ER but continues en route to the Golgi apparatus (232-234). As much as 50% TG and 30% PL may be added to the VLDL particle in the Golgi compartment (232). The VLDL maturation process is dependent on the activity of ADP-ribosylation factor-1 (ARF-1), a member of the RAS superfamily of GTP binding proteins which activates phospholipase D (PLD) (233, 234). Indeed, overexpression of ARF-1 or PLD in cultured rat hepatocytes can increase VLDL-TG secretion whereas hepatic overexpression of a dominant negative ARF-1 results in a suppressive effect (234). Brefeldin A can inhibit the maturation phase of VLDL assembly by blocking the guanine nucleotide exchange (GDP to GTP) on ARF-1 without affecting formation of the VLDL precursor (235). Unlike the first step of VLDL assembly which is dependent on MTP, there are a plethora of other factors involved in the second step of VLDL maturation, which includes diacylglycerol acyltransferase (DGAT)-1 and -2, triglyceride hydrolase (TGH), arylacetamide deacetylase (AADA), ARF-1, PLD, and lipin-1 as summarized in Figure 1.8.

Sources of lipid for VLDL secretion

VLDL is the chief carrier of TG in the postabsorptive state (236). The TG utilized for VLDL assembly and secretion can be derived either from fatty acids produced by hepatic *de novo* lipogenesis (*DNL*), by the uptake and re-esterification of plasma FFAs, or by the uptake of chylomicron and VLDL lipoprotein remnants by the liver (236). Using a combination of stable isotope-labeled tracer and indirect calorimetry, Diraison et al. (236) estimated in normal human subjects in the postabsorptive state that hepatic re-esterification of plasma FFA accounted for 50-55% of TG secretion, whereas *DNL* was a minor contributor. The remaining lipids were presumed to be provided by stored lipids (cytosolic TG and PL) or lipoprotein remnants taken up by the liver. However, the method by Diraison et al. (236) is semi-quantitative as it does not allow for the determination of the overall contribution of these potential lipid sources to TG secretion.

Growing evidence suggest that TG utilized for VLDL assembly and secretion can originate from sources other than that arising from hepatic fatty acid synthesized *de novo* and from extracellular FFAs (224). It has been reported that up to 70% of secreted VLDL-TG by the liver is attributable to the hydrolysis and re-esterification of pre-existing PL and cytosolic TG (224). Clearly, some of the TG which ends up as VLDL is derived from a pool of intracellular PL, a novel source of lipid given the current assumption that intracellular membrane PL merely plays a structural role in VLDL assembly (224).

Key regulators of hepatic VLDL assembly and secretion

ARF-1, PLD, and lipin-1: Key regulators of PL remodeling

As summarized in Figure 1.8, key regulatory enzymes involved in the transfer of PL fatty acids into TG, otherwise known as PL remodeling, involve PLD which is activated by ARF-1. This leads to the production of phosphatidic acid (PA) from the PL, phosphatidylcholine (PC)

(228, 233). PA can be additionally generated from the glycerolipid biosynthetic pathway. This involves glycerol-3-phosphate acyltransferase (GPAT) which catalyzes the esterification of glycerol-3-phosphate with a fatty acyl-CoA (preferably oleic acid; C18:1w9) to produce lysophosphatidate (LPA). In turn, LPA is converted by acylglycerol-3-phosphate acyltransferase (AGPAT) to the PA substrate (225, 237). PA is then dephosphorylated by the key rate-limiting enzyme, lipin-1, a phosphatidic acid phosphatase (PAP) producing the TG precursor, diacylglycerol (DAG). The resulting DAG serves as a substrate for the synthesis of TG and the PLs, PC and phosphatidylethanolamine (PE) that is required for lipidation of the nascent VLDL particle resulting in maturation and secretion as TG-rich VLDL particles by the liver (238). In Chapter IV, we will investigate whether CNS NPY utilizes liver PL as the TG precursor for VLDL maturation and secretion by robustly activating the key hepatic regulatory enzymes involved in PL remodeling, ARF-1 and lipin-1.

DGATs, which are membrane bound enzymes, complete the final step of TG synthesis (239). The ER-localized DGAT-1 converts DAG into TG for VLDL maturation whereas the cytosolic-localized DGAT-2 enzyme generates TG destined for lipid storage in cytoplasmic droplets (239). The lipases TGH and AADA are involved in the lipolytic mobilization of cytosolic TG stores that are re-esterified by DGATs, which are then channeled into the VLDL maturation pathway or recycled back into the cytosolic TG pool (228).

The lipin (PAP) protein family: Discovery, structure, function, and tissue distribution

The molecular identity of mammalian PAP was unknown until it was discovered in *Saccharomyces cerevisiae* in 2006 to be encoded by lipin (240). The *Lpin1* gene was first isolated through positional cloning in 2001 from the fatty liver dystrophy (*fld*) mutant mouse strain where this null mutation in the *Lpin1* gene results in lipodystrophy, insulin resistance, neonatal fatty liver, hypertriglyceridemia, and peripheral neuropathy (241-243). The *Lpin2* and *Lpin3* were identified based on their sequence similarities to *Lpin1* (243). Although human lipin-1 deficiency

is not associated with lipodystrophy, it does lead to recurrent rhabdomyolysis in childhood (244) and genetic variants within the *Lpin1* and *Lpin2* genes are associated with traits of the metabolic syndrome (reviewed in (245)). The *Lpin1* gene encodes two alternatively spliced isoforms, lipin-1α and lipin-1β, which although they phenotypically exhibit nuclear and cytoplasmic localization, respectively, both proteins show extensive association with microsomal membranes (238, 246).

All mammalian lipin proteins possess PAP activity that is dependent on Mg^{2+} and on PA as a substrate and exhibit unique but overlapping tissue distributions (247). Lipin-1 is expressed at highest levels in brown and white adipose tissue, skeletal muscle, and testis and at lower levels in other tissues, including kidney, lung, brain, heart, and liver (243, 247). Lipin-2 is predominately expressed in liver whereas lipin-3 is also expressed in this tissue but at low levels (247). Lipins are complex, bifunctional proteins and in all species, share two highly conserved regions termed the N-terminal lipin (N-LIP) and the C-terminal lipin (C-LIP) domains as illustrated in Figure 1.9. The C-LIP domain contains two functional motifs: A DIDGT motif which constitutes the catalytic site for PAP-1 enzyme activity (240) and an LXXIL motif that is required for the transcriptional co-activator activity to modulate gene transcription (248). Near the N-LIP domain, lipin proteins in most species contain a nuclear localization sequence (245).

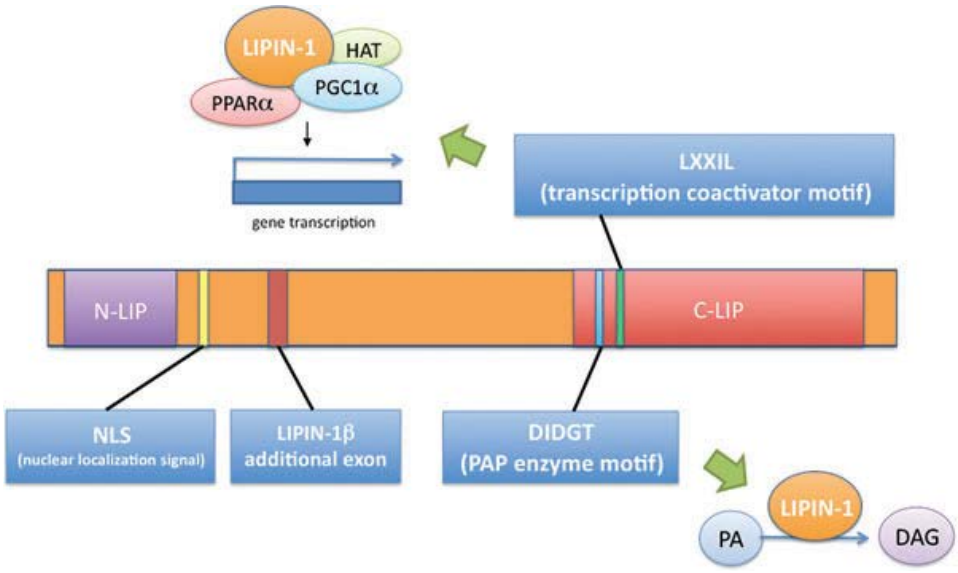

Figure 1.9. Lipin protein structure and functional domains. N-terminal lipin (N-LIP) and C-terminal lipin (C-LIP) domains are highly conserved evolutionarily across yeast and mammals. The alternative splicing of *Lpin1* gene generates the lipin-1β region. A DIDGT motif is required for PAP-1 enzyme activity to convert phosphatidic acid (PA) to diacylglycerol (DAG) for triglyceride (TG) synthesis. An LXXIL motif is required for transcriptional co-activator activity to interact with peroxisome proliferator activated receptor -ɣ-coactivator-1α (PGC-1α) and peroxisome proliferator activated receptor-α (PPARα) to modulate gene transcription. A nuclear localization signal is found in the lipin protein in most species. Figure from Csaki et al. (245).

Lipin-1 dual molecular function impacts VLDL assembly and secretion

Abundant evidence indicates that lipin-1 is the major isoform involved in hepatic VLDL assembly and secretion. The subcellular localization and compartmentalization of lipin-1 determines its dual molecular function as either a glycerolipid biosynthetic enzyme or a transcriptional co-activator as shown in Figure 1.10 (reviewed in (249)). Insulin stimulates the phosphorylation of lipin-1 at Serine (Ser) 106 which is dependent on PI3K activity and mammalian target of rapamycin (mTOR) pathway (250) sequestering it into the cytosol, which affects its intrinsic PAP-1 activity (251). Dephosphorylation of lipin-1 occurs in response to fatty acids (i.e. oleic acid) and epinephrine leading to its translocation from the cytosol to the ER membrane where it performs its PAP-1 activity (252). In turn, this generates the lipid substrates (TG, PC, and PE) required for the lipidation of the apoB carrying pre-VLDL precursor required

for its maturation and secretion as TG-rich VLDL lipoprotein by the liver (238, 253). Conversely, sumoylation of lipin-1 leads to its translocation to the nucleus where it acts as a transcriptional co-activator with peroxisome proliferator activated receptor -ɣ-coactivator-1α (PGC-1α) and peroxisome proliferator activated receptor-α (PPARα) leading to the induction of genes involved in fatty acid oxidation, including *PPARA*, *CPT1A*, and acyl-CoA oxidase-1 (*ACOX1*) (248, 254) which would oppose its function as a glycerolipid biosynthetic enzyme.

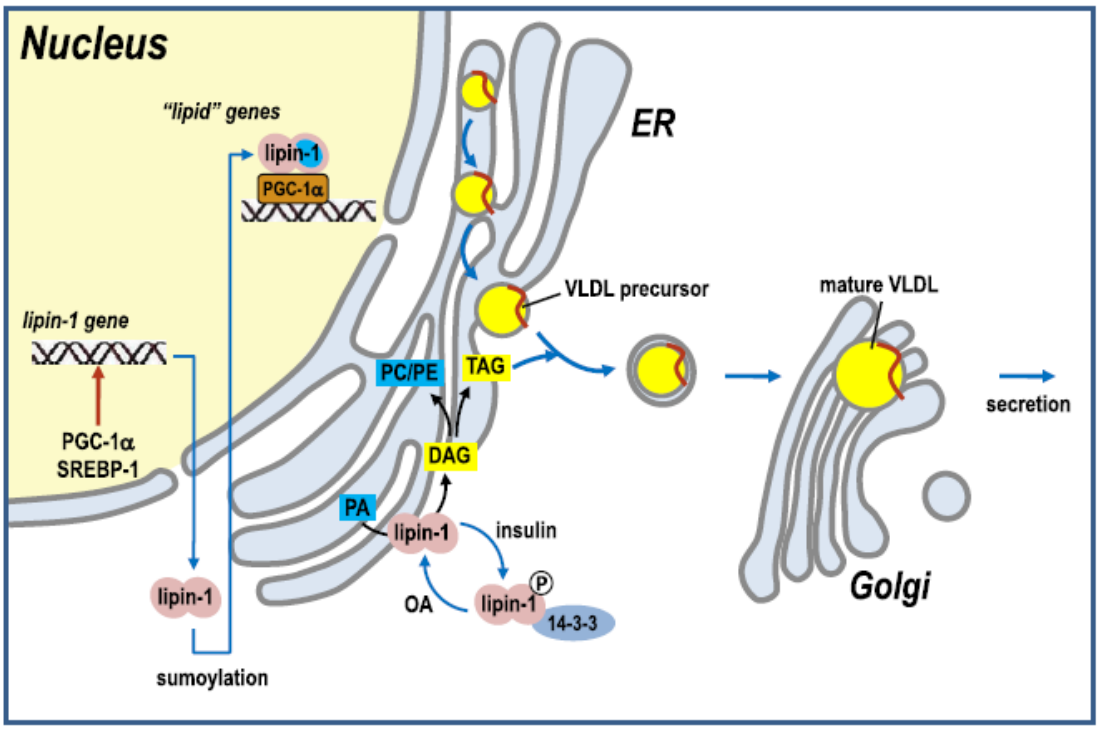

Figure 1.10. Regulation of lipin-1 expression and subcellular localization. Model depicting how lipin-1 gene expression, post-translational modification (phosphorylation) and subcellular localization determines its dual molecular function as either a glycerolipid biosynthetic enzyme or a transcriptional co-activator. Figure from Khalil et al. (249).

Recent studies have revealed that lipin-1 is a critical regulator of hepatic lipoprotein metabolism. Transient transfection experiments in rat cultured hepatocytes have shown that the overexpression of either lipin-1α or lipin-1β isoform in the presence of oleic acid markedly increases glycerolipid synthesis and secretion of VLDL-TG (238). Conversely siRNA mediated

knockdown of lipin-1 decreases VLDL assembly and secretion even though total cellular PAP activity is not altered, presumably due to compensation by lipin-2 and -3 (238). These results are inconsistent with findings in primary hepatocytes isolated from 14 day old lipin-1 deficient *fld* mice which have an elevated rate of TG synthesis and secretion (255), concomitant with normal PAP activity despite the lack of lipin-1 expression (256). These findings suggest that lipin-2 may contribute to a complex regulatory mechanism in the liver (256). Furthermore, the adenoviral overexpression of lipin-1β in adult *fld* hepatocytes markedly suppressed VLDL-TG secretion (255). Intriguingly, it was determined that the overexpression of the lipin-1 mutant (D712E), which lacks intrinsic PAP-1 activity, resulted in the suppression of TG secretion in wild-type mice (255). In contrast, the overexpression of the lipin-1 mutant (LXXFF) which lacked both PAP-1 and transcriptional co-activator activity failed to suppress TG secretion (255). This suggests that the transcriptional co-activator regulatory function of lipin-1 may oppose its PAP-1 activity involved in regulating lipoprotein metabolism.

Similar to the findings in rodents, the ability of lipin-1 to function as a regulator of VLDL assembly and secretion is also controversial in humans. For example, it was found that lipin-1β but not lipin-1α in liver and adipose tissue were inversely related to BMI, plasma insulin concentration, and insulin resistance in extremely obese human subjects (257). Surprisingly, the dramatic weight loss and decrease in hepatic VLDL-TG secretion as an outcome of gastric bypass surgery in obese subjects (258) was associated with a marked increase in lipin-1β expression (257). Therefore, in the context of these conflicting observations in both rodent and human studies, the interplay of various factors that regulate lipin-1 subcellular localization and substrate availability may influence the outcome of lipin-1 as a modulator of VLDL secretion.

Regulation of lipin-1 expression and activity

As illustrated in Figure 1.11, lipin-1 expression and activity is regulated by a variety of physiologic and pathological stimuli that are known to influence lipoprotein metabolism. Only

lipin-1, but not lipin-2 or -3 expression and activity is upregulated by GCs (259), which act through the GR that is bound to the functional glucocorticoid response element (GRE) upstream of the *Lpin1* promoter region (260). Glucagon through cAMP, synergistically enhances the effect of GC on lipin-1 expression and activity and this effect is antagonized by insulin in mouse and rat hepatocytes (259). In both un-treated and insulin-treated hepatocytes, the half-life of PAP-1 activity is 5-7 hours which is increased to 12 hours by glucagon (through cAMP formation) (261). Thus, the increase in the half-life of PAP-1 activity is thought to be the underlying cause for the synergistic effect of GC and cAMP treatment on lipin-1 expression and activity in hepatocytes (259). cAMP may additionally regulate *Lpin1* gene transcription via the activation of cAMP response element-binding protein (CREB) which in turn, induces *Lpin1* expression by binding to the cAMP-dependent regulatory elements (CRE) upstream of the *Lpin1* promoter (262, 263).

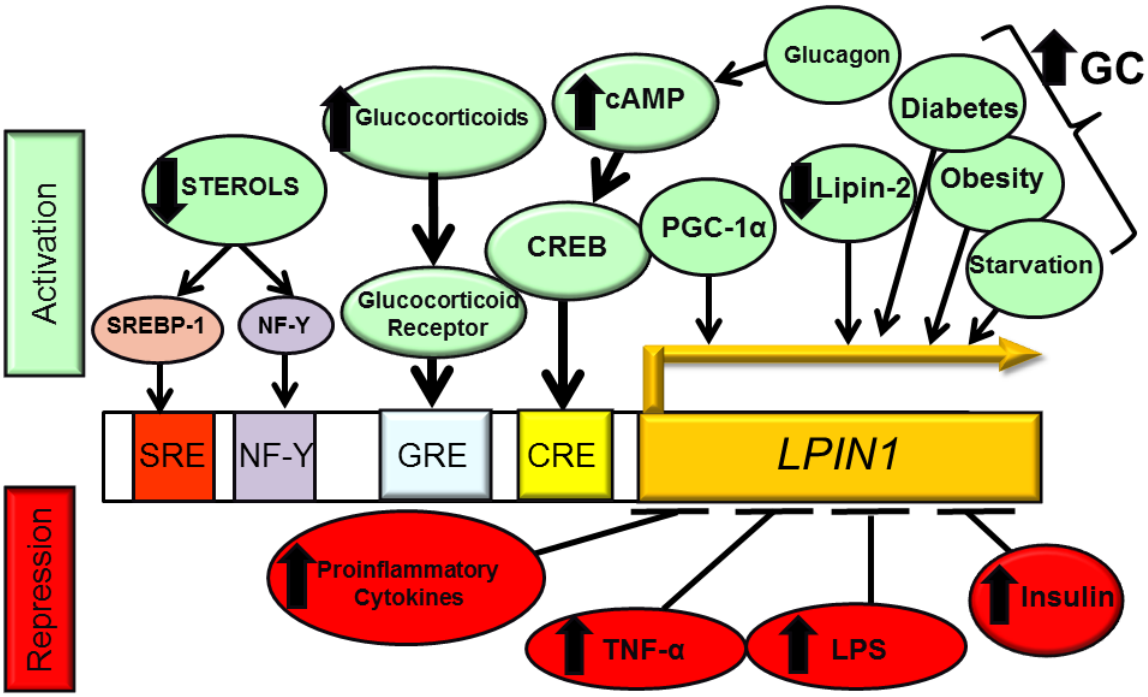

Figure 1.11. Transcriptional regulation of the *Lpin1* gene. A schematic of *Lpin1* gene promoter region and the regulatory elements are shown. Conditions known to activate *Lpin1* gene expression are shown in the upper panel. Negative regulators of *Lpin1* gene expression are shown in the bottom panel. Abbreviations: cyclic adenosine monophosphate (cAMP); cAMP-dependent regulatory elements (CRE); cAMP response element-binding protein (CREB); glucocorticoid (GC); glucocorticoid response element (GRE); lipopolysaccharide (LPS); nuclear factor Y (NF-Y); peroxisome proliferator activated receptor -ɣ-coactivator-1α (PGC-1α)**;** sterol regulatory element binding protein (SREBP)-1; sterol response element (SRE); tumor necrosis-α (TNF-α). Adapted from Csaki et al. (245).

Previous studies (238, 259) report that lipin-1 is responsible for the increase in VLDL secretion in response to GC treatment in cultured rat hepatocytes (264-266). *Thus, it is hypothesized that under conditions that lead to elevated activity of the HPA axis (i.e. starvation, diabetes, and obesity) resulting in an increase in circulating GC, the subsequent GC-induced increase in lipin-1 activity augments the capacity for the liver to sequester excess FFA as TG for VLDL secretion when FFAs are not immediately required for β-oxidation* (238, 259). Consistent with this hypothesis, there is an elevation in hepatic PAP-1 activity under stress conditions, such as partial hepatectomy (267), starvation (268), diabetes (248, 269), obesity (248), and in response to dietary fat/carbohydrate or ethanol challenge (270-272).

The expression of hepatic lipin-1 is induced by PGC-1α (248), a transcriptional coactivator that is markedly upregulated under conditions of fasting and diabetes and is involved in the activation of genes that modulate gluconeogenesis and fatty acid oxidation (248, 273-275). Conditions that dictate an increase in mitochondrial fatty acid oxidation, such as fasting and diabetes, leads to the upregulation of PGC-1α, which in turn, induces lipin-1 expression (248). Thus, lipin-1 becomes an inducible amplifier of the PPARα/PGC-1α pathway to increase hepatic capacity for β-oxidation in response to an increase in the influx of FFAs to the liver (248).

Lpin1 gene expression is also controlled by sterol regulatory element binding protein (SREBP)-1, which regulates many genes involved in fatty acid and triglyceride biosynthesis (276). In response to sterol depletion, SREBP-1 and nuclear factor-Y (NF-Y) acts through an NF-Y and sterol response element (SRE) binding site in the human *Lpin1* promoter to induce *Lpin1* gene expression in human hepatoblastoma cells (277). Conversely, inflammation and sepsis appear to suppress *Lpin1* gene expression in adipocytes through pro-inflammatory cytokines, including TNF-α and lipopolysaccharide (LPS) (278, 279). Finally, *in vitro* studies in HeLa M and 3T3-L1 cells indicate that lipin-1 and -2 may negatively regulate one another (280).

Hepatic insulin signaling

AKT and Rictor/mTORC2: Key mediators of insulin action

Insulin is a key metabolic regulator of liver glucose and lipid metabolism. Insulin regulation of metabolic processes often involves PI3K signaling that is coupled to phosphoinositide-dependent kinase-1 (PDK-1) and the Ser/Threonine (Thr) kinase AKT (also known as protein kinase B; PKB) (281). AKT is activated via phosphorylation at Ser473 by the rictor containing mTOR complex 2 (mTORC2) in addition to PDK1-directed phosphorylation at Thr308 (282, 283). AKT2 is the major isoform expressed in liver and mediates many of the metabolic actions of insulin (284, 285). Hepatic overexpression of constitutively active AKT in

mice results in the development of nonalcoholic fatty liver disease (NAFLD), hypertriglyceridemia, and hypoglycemia (286). These effects are phenocopied by the loss of hepatic phosphatase and tensin homolog (PTEN), a negative regulator of PI3K-dependent protein kinase activity, including AKT (287). The loss of AKT2 effectively negates the effect of PTEN deficiency on fatty liver and improved systemic glucose tolerance (288), and similarly, reverses hepatic steatosis in obese, insulin resistant mouse models (285). The lipo-regulatory effects of hepatic AKT are largely due to the regulation of SREBP-1c and SREBP-2, which modulate many genes involved in fatty acid, triglyceride, and cholesterol biosynthesis (276). The effects on glycemia are due, in part, to AKT-directed phosphorylation and inhibition of the transcription factor Forkhead box protein O1 (FoxO1), leading to its nuclear exclusion and termination of transcription of rate controlling enzymes of gluconeogenesis, phosphoenolpyruvate carboxykinase (PEPCK) and glucose-6-phosphatase (G6PC), thereby limiting HGP (289).

mTOR is a Ser/Thr kinase and a key regulator of cell growth and metabolism, activated in response to insulin, nutrients, and growth factors (Figure 1.12) (290). mTOR is found in two distinct multiprotein complexes that are defined by their subunit composition, rapamycin sensitivity, and substrate selectivity (290). The rapamycin sensitive mTOR complex 1 (mTORC1) consists of raptor, mLST8, PRAS40 (291) and mTOR, whereas the rapamycin insensitive complex, mTORC2, consists of rictor, mSIN1, mLST8, protor, and mTOR (290, 292). The best characterized substrates of mTORC1 are p70 ribosomal S6 kinase (S6K) and eukaryotic initiation factor 4E-binding protein (4E-BP), which are important in the regulation of protein synthesis (292). mTORC2 phosphorylates members of the AGC kinase family, including AKT (282), serum- and glucocorticoid-induced protein kinase (SGK) (293), and protein kinase Cα (PKCα) (294), and thus, controls cell survival, actin cytoskeleton organization, and other metabolic processes.

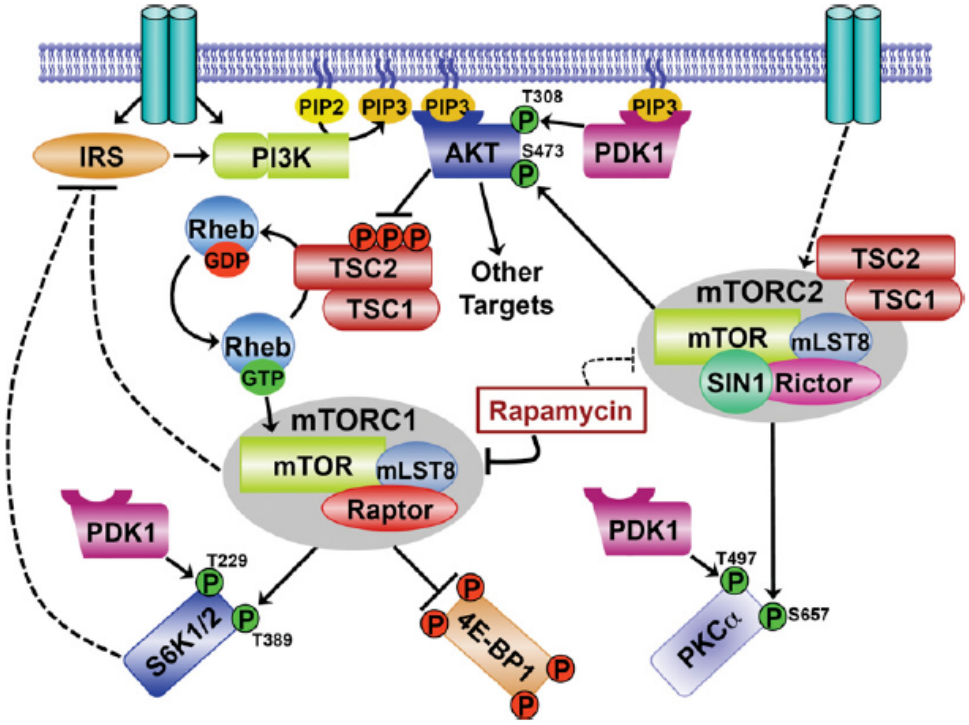

Figure 1.12. AKT and Rictor/mTORC2: Key mediators of insulin action. AKT2 is the major isoform expressed in liver and mediates many of the metabolic actions of insulin. In the canonical insulin signaling pathway, insulin binding to the insulin receptor (IR) tyrosine kinase is coupled to the tyrosine phosphorylation and activation of the scaffolding proteins, such as insulin receptor substrate (IRS)-1. In turn, IRS activates phosphatidylinositol 3-kinase (PI3-Kinase) which phosphorylates phosphatidylinositol-4,5-bisphosphate (PIP2) to generate phosphatidylinositol-3,4,5-trisphosphate (PIP3), a reaction that can be reversed by phosphatase and tensin homolog (PTEN). Accumulation of PIP3 recruits AKT and PDK-1 to the plasma membrane, where PDK-1 phosphorylates the activation loop of AKT at Threonine 308. Through an unknown mechanism, the IR signaling also activates the rictor containing mammalian target of rapamycin (mTOR) complex 2 (mTORC2). Rictor, is the key regulatory protein that directs mTORC2 to phosphorylate the hydrophobic motif of AKT at Serine 473 leading to the full activation of this serine/threonine kinase. mTORC2 also phosphorylates other AGC family protein kinases, serum- and glucocorticoid-induced protein kinase (SGK) and protein kinase Cα (PKCα) and thus is poised to regulate multiple metabolic processes. AKT activates mTORC1 through multisite phosphorylation of TSC2 within the TSC1-TSC2 complex. The best characterized downstream targets of mTORC1 are p70 ribosomal S6 kinase (S6K) and eukaryotic initiation factor 4E-binding protein (4E-BP), which are important in the regulation of protein synthesis. While mTORC1 activity in hepatocytes is important in the regulation of ketogenesis and lipid metabolism, genetic deletion of rictor and associated loss of mTORC2 activity in liver has revealed that mTORC2 is a key regulator of hepatic glucose, lipid, and cholesterol metabolism. Figure from Huang et al. (283).

Selective hepatic insulin resistance as the underlying mechanism for the metabolic syndrome

High portal insulin levels prime the liver for rapid alterations in hepatic carbohydrate metabolism such as the stimulation of glycogen synthesis, the suppression of gluconeogenesis and glycogenolysis (295, 296). Insulin rapidly alters lipid homeostasis via the stimulation of lipogenesis and lipoprotein synthesis and the suppression of VLDL-TG secretion (14, 297). In the insulin resistant state, insulin fails to suppress gluconeogenesis and thus, hyperglycemia ensues while insulin retains its ability to enhance lipogenesis (298). Excessive hepatic lipogenesis can contribute to the development of NAFLD and atherogenic dyslipidemia (14, 15). Thus, the concept of selective hepatic insulin resistance, as described by Brown and Goldstein (299), could account for the pathogenesis of hyperglycemia and dyslipidemia associated with obesity, diabetes, and the metabolic syndrome. This concept, as illustrated in Figure 1.13, suggests that insulin-signal transduction bifurcates upstream of lipogenesis and gluconeogenesis, where regulation of the SREBP-1c driven lipogenic pathway remains intact while the regulation of the FoxO1-gluconeogeneic pathway becomes insulin resistant.

Dissecting the role of insulin-AKT signaling in the complex regulation of liver glucose and lipid metabolism is necessary for understanding the pathogenesis of hyperglycemia, atherogenic dyslipidemia, and NAFLD associated with obesity, diabetes, and the metabolic syndrome. Understanding the molecular mechanism underlying selective insulin resistance in liver requires a deeper understanding of how insulin and AKT regulate hepatic glucose and lipid metabolism which will be further investigated in Chapter V.

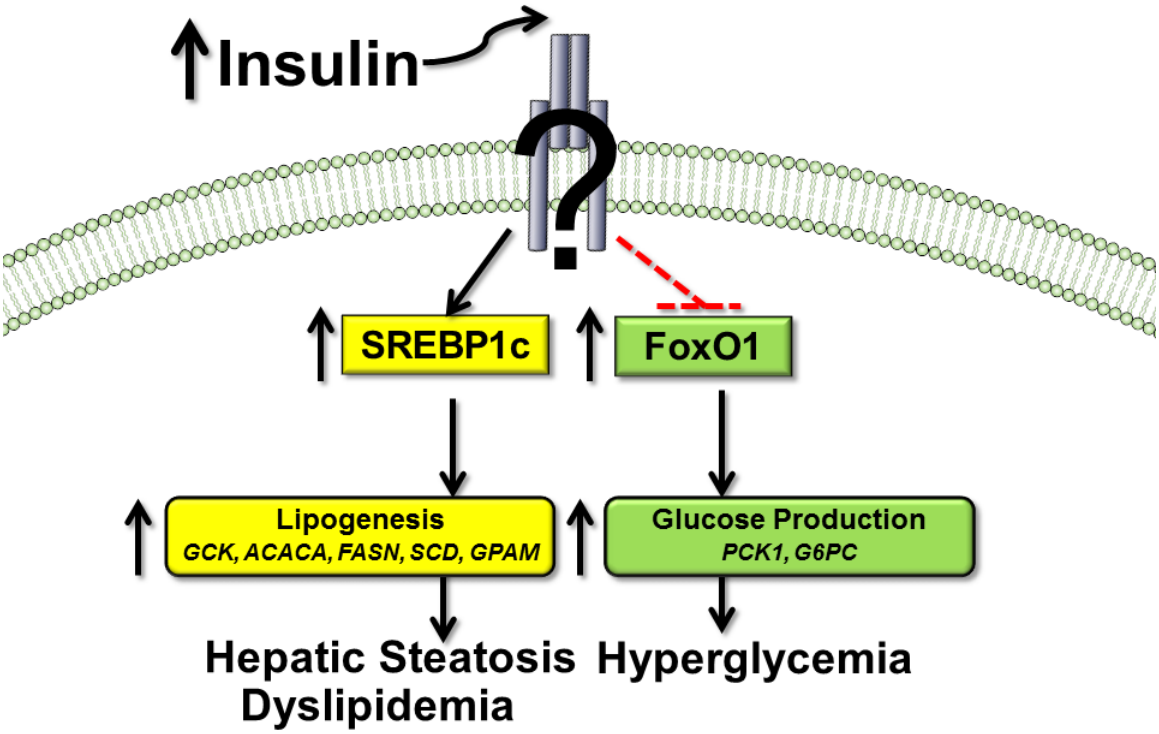

Figure 1.13. Selective hepatic insulin resistance. Selective hepatic insulin resistance has been hypothesized to generate hyperglycemia and dyslipidemia associated with obesity, diabetes, and the metabolic syndrome. It's characterized by inability of insulin to suppress the transcription factor Forkhead box protein O1 (FoxO1) leading to impaired suppression of hepatic glucose production (HGP). In parallel, insulin continues to stimulate the transcription factor sterol regulatory element binding protein (SREBP)-1c leading to excessive hepatic lipogensis which contributes to the development of NAFLD and atherogenic dyslipidemia. The molecular mechanism underlying selective insulin resistance in the liver remains elusive. Adapted from Brown and Goldstein (299).

Rationale and Hypothesis

Elevated plasma TG levels contribute to an atherogenic dyslipidemia that is associated with obesity, diabetes, and the metabolic syndrome. Numerous models of obesity are characterized by increased CNS NPY tone that contributes to excess food intake and obesity. We previously demonstrated that ICV administration of NPY in lean fasted rats also elevates hepatic production of VLDL-TG. *Thus, the overarching hypothesis is that elevated CNS NPY action contributes to dyslipidemia by activating central circuits that modulate liver lipid metabolism.*

This body of work sought to elucidate the molecular mechanisms by which CNS NPY signaling leads to rapid increases in hepatic VLDL-TG secretion, specifically focused on the molecular determinants in the hypothalamus (Chapter III) and on hepatic-specific mechanisms (Chapter IV and V). In Chapter III, we investigated whether the effects of NPY on feeding and/or obesity are dissociable from effects on hepatic VLDL-TG secretion. We first asked whether ICV NPY administration retains the effect to increase hepatic VLDL-TG secretion when given chronically (3 days, twice daily) but when food intake, body weight, and fat mass are matched exactly to control levels. Secondly, we sought to determine which of the various NPY receptor subtypes (Y1, Y2, Y4 and Y5) are involved in feeding versus VLDL-TG secretion. Thus, using these approaches, we sought to determine whether the effect on feeding versus lipids overlap or are dissociable, as this might have structure-function and/or therapeutic implications in obesity and the metabolic syndrome.

Based on the observation in Chapter III that CNS NPY rapidly increases hepatic VLDL-TG secretion while not altering adipocyte lipolysis (FFA and glycerol), we hypothesized that key regulatory steps involved in liver lipid metabolism might be robustly regulated by increased CNS NPY signaling. The liver-specific molecular mechanisms by which increased CNS NPY signaling rapidly regulates hepatic lipoprotein metabolism are not well understood. Nor is the lipid source that generates the TG that is loaded onto the nascent VLDL particle in response to increased CNS NPY action currently known. We, therefore, sought to identify the novel regulatory mechanisms in the liver engaged by NPY. Our study employed two approaches: first, we determined whether liver PL is a novel source of lipid for hepatic VLDL-TG secretion in the *fa/fa* ZF rat, a rodent model characterized by elevated NPY tone and dyslipidemia, independently of hyperphagia and obesity; and secondly, we determined whether CNS NPY signaling via the Y1 receptor elevates hepatic VLDL-TG secretion by modulating key regulatory enzymes involved in liver PL remodeling in lean fasted, metabolically normal rats and whether this is a GC dependent effect. We ultimately sought to elucidate the novel regulatory mechanisms in the liver in response to

increased CNS NPY action that leads to the modulation of hepatic lipoprotein metabolism in the absence of increased visceral adiposity, as this might yield novel insight and therapeutic implications for the dyslipidemia associated with obesity, diabetes, and the metabolic syndrome.

Previous studies (189, 191, 192, 202) show that under conditions characterized by increased hypothalamic NPY tone (i.e. fasting, obesity, and diabetes), NPY activates sympathetic outflow to the liver. This in turn induces hepatic insulin resistance to impair insulin's ability to suppress HGP and hepatic VLDL-TG secretion, contributing to the dyslipidemia and dysglycemia associated with obesity, diabetes, and the metabolic syndrome (13). *We hypothesized that CNS NPY may induce "selective hepatic insulin resistance" to promote hyperglycemia and hyperlipidemia.* As described by Brown and Goldstein (299), the concept of selective hepatic insulin resistance suggests that the insulin-signal transduction bifurcates upstream of lipogenesis and gluconeogenesis, where the regulation of one pathway (lipogenesis) remains intact while regulation of the other (gluconeogenesis) is impaired, a mechanism by which hyperglycemia and hypertriglyceridemia can ensue. In Chapter V, we generated a mouse model of impaired hepatic insulin action targeting the concept of selective hepatic insulin resistance independent of CNS NPY signaling. We have impaired the function of mTORC2 in liver by hepatocyte-specific gene deletion of *Rictor*, which is a key mTORC2 regulatory protein. We sought to determine whether hepatic rictor directed mTORC2 activity is required for the regulation of liver lipid metabolism.

The results, interpretations, and the caveats of the experimental studies in this dissertation work are summarized in Chapter VI and placed in the context of the proposed integrated model of how CNS NPY regulates lipoprotein metabolism independently of increased food intake and visceral adiposity. Additionally, Chapter VI includes supportive preliminary data and proposed future directions to further delineate the molecular mechanisms by which increased CNS NPY signaling regulates liver lipid metabolism, focusing specifically on the molecular determinants in the hypothalamus, on the neural-hepatic circuit, and on liver-specific mechanisms.

CHAPTER II

MATERIALS AND METHODS

Ethics statement for experimental mouse and rat studies (Chapters III-V)

All Study protocols were approved by the Institutional Animal Care and Use Committee of the Tennessee Valley Veterans Affairs (VA) Healthcare System and Vanderbilt University (Nashville, TN).

Experimental animals: Long-Evans and *fa/fa* ZF rats (Chapters III and IV)

Animal studies

Male Long Evans rats (HsdBlu:LE), weighing 250-274 g, were purchased from Harlan (Indianapolis, IN). Zucker fatty rats (Crl:ZUC-Lepr^{fa}), weighing 300 g, were purchased from Charles River laboratories (Wilmington, MA). Rats were maintained under temperature- and humidity-controlled conditions with a 12-hour light/dark cycle (lights on at 6AM), and were given free access to water and a standard rodent chow diet (5001; 3.02 kcal/g, 58% carbohydrate, 28.5% protein,13.5% fat; Lab diet, Richmond, IN).

Intracerebroventricular (ICV) cannulation

Cannulation of the third ventricle in the brain allows infusion of the hypothalamic structures lying adjacent to the third ventricle. Placement of third ventricle cannula into Long Evans rats were performed using proper sterile technique and under general anesthesia induced and maintained by inhalation of isoflurane. Buprenex (0.05 mg/kg body weight) was administered postoperatively to mitigate pain and distress. The superior and dorsal aspect of the head and neck were shaved and placed into a small animal stereotaxic apparatus (ASI instruments; Warren, MI).

The skin was prepared by successive scrubbing with betadine. A 1.5-cm mid-sagittal skin incision was made and cleaned with sterile swabs to expose the skull. The skull was leveled and properly aligned using lambda and bregma as reference points at the cranial plate junctions. Using a battery powered drill, a single, open burr hole was drilled into the skull, 2.2 mm posterior to bregma. The superior sagittal sinus was retracted laterally, and a 22-gauge stainless steel guide cannula (C313G; Plastics One, Roanoke, VA) was lowered 7.5 mm directly midline, ventral to the dura, and then fixed to the skull with anchor screws and dental acrylic. A removable obturator (C313DC-SPC; Plastics One) was inserted into the guide cannula to seal and to prevent infection. The skin was sutured with sterile 4-0 silk Ethicon sutures. Rats were treated with antibiotic (Ceftriaxone, 0.1 g/kg body weight, Intraperitoneal; IP) on the day of the surgery and 2 days post-operatively. Animals were allowed to recover for 5-7 days after surgery during which body weights were monitored. Surgical recovery was defined by steady weight gain and final body weight not less than 10% below pre-surgery body weight.

Correct placement of cannula was verified by an angiotensin II drinking test (300). If the cannula is placed correctly, angiotensin II activates the thirst center of the hypothalamus and direct administration to the third ventricle stimulates a measurable thirst response (301). For this test, rats were injected with a 1 μl of a 10 ng/μl angiotensin II solution via the ICV cannula and water consumption was measured over a 1-hour period. Animals that do not drink greater than 5 ml of water in 1-hour post-treatment were excluded from the study.

Carotid catheter surgery

Placement of carotid catheter into Long Evans rats were performed using proper sterile technique and under general anesthesia induced and maintained by inhalation of isoflurane. Buprenex (0.05 mg/kg body weight) was administered postoperatively to mitigate pain and distress. The skin on the interscapula and ventral surface of the neck was shaved and sterilized with betadine. A small longitudinal incision was made in the skin over the region where the

anterior jugular, acromeodeltoid, and cephalic veins join together. The connective tissues surrounding this junction were carefully removed. The common carotid artery was separated from the vagus nerve and muscle, and two thin threads of 6-0 silk sutures were passed under the artery. The cephalic thread was tied to prevent bleeding and then the artery was clamped. A small incision was made in the carotid artery just below the ligature, and a sterile MicroRenathane catheter (R-CAC-M37-R; Brain Tree Scientific, Braintree, MA) filled with heparinized saline (200 U/ml) was inserted into the artery lumen. The clamp was taken off and the catheter was threaded into the artery at a pre-determined distance. The catheter was fixed with the cephalic thread (previously used to prevent bleeding) and a second thread. The catheter was flushed with heparinized saline (200 U/ml) and the tubing was closed with a stainless steel plug. A blunt needle (16-gauge) was carefully inserted through the incision on the interscapula and pushed subcutaneously until the end comes out through the incision in the neck. The catheter was carefully seized and pulled slowly through the needle. The implanted catheter was securely sutured in place and all incisions in skin were sutured with sterile 4-0 silk Ethicon sutures. Rats were treated with antibiotic (Ceftriaxone, 0.1 g/kg body weight, IP) on the day of the surgery and 2 days post-operatively. Animals were allowed to recover for 5-7 days after surgery during which body weights were monitored.

NPY receptor agonist selectivity and dosing

The NPY EC_{50} values as measured *in vitro* are 2.6, 5.1, 814, and 4.9 nM for the Y1, Y2, Y4, and Y5 receptor subtypes, respectively (105). All peptide ligands used in our studies are selective compounds for their respective NPY receptor subtypes and bind with sub-nanomolar affinity (105). The Y1 selective peptide, [F7, P34]-NPY, has >3,000-fold selectivity for the Y1 receptor over that of either the Y2 or Y5 receptor (302). For Y2 receptor activation, we used hPYY (3-36), which has a 181-, >1,000-, and 5-fold greater affinity for the Y2 receptor than for Y1, Y4, and Y5 receptor subtypes, respectively (303). To activate the Y4 receptor, we used hPP

that has a 2.2-, >56-, and 1.4-fold greater affinity for the Y4 receptor than for Y1, Y2, and Y5 receptor subtypes, respectively (105, 109). We also used a Y5 agonist, [Ala^{31}, Aib^{32}]-NPY, which has >77-, 12-, and >77-fold selectivity for the Y5 receptor than for the Y1, Y2, and Y4 receptor subtypes, respectively (105, 109). The dose of agonist utilized for each receptor subtype was estimated based on *in vitro* receptor potencies relative to NPY (105, 109, 302, 303) for food intake and lipid studies. The dosages chosen for ICV treatment were: NPY (1 nmol); Y1 agonist, [F7, P34]-NPY (1 nmol); Y2 agonist, hPYY (3-36; 1 nmol); Y4 agonist, hPP (1 nmol); and Y5 agonist, [Ala^{31}, Aib^{32}]-NPY (2 nmol).

Intracerebroventricular infusions

Studies were performed 5-7 days after surgery when body weight curves returned to a pre-surgery trajectory. Recombinant NPY and a selective agonist for the Y2 receptor, human PYY (3-36, hPYY), were purchased from GenScript (Piscataway, NJ). A selective agonist for the Y1 receptor, [F7, P34]-NPY, and the Y5 receptor, [Ala^{31}, Aib^{32}]-NPY, were synthesized (302, 304). A selective agonist for Y4, human PP (hPP), was purchased from Tocris Bioscience (Ellisville, Missouri). All receptor agonists were dissolved in 0.9% normal saline and freshly prepared on the day of the study. All ICV compounds were administered in a 2 µl volume over 1 min.

Chronic NPY pair-feeding study

Recombinant NPY was administered ICV (1 nmol) twice daily (8AM and 5PM) over 3 days in rats matched for body weight. To control for the orexigenic effects of NPY, NPY-treated rats were pair-fed (PF) to the caloric intake of the ICV vehicle (saline; Veh)-treated control rats. Blood collected daily by tail prick was measured for plasma TG and cholesterol levels. At the end of the study (day 3), 4-hour fasted rats were given either ICV NPY (1 nmol) or Veh and at 120 min post injection, animals were euthanized followed by collection of trunk blood. Body weight

and body composition using an EchoMRI-700 nuclear magnetic resonance (NMR) spectrometer (Echo Medical Systems, Houston, TX) to determine lean and fat mass were measured on study day 3.

Food intake studies

We assessed food intake responses to agonists of each receptor subtype compared to vehicle control, 12-hour fasted, and NPY-treated animals. Rats with surgically implanted ICV cannulae and matched for body weight, were studied. We administered ICV compounds, NPY (1 nmol), [F7, P34]-NPY (1 nmol), hPYY (3-36; 1 nmol), hPP (1nmol), [Ala^{31}, Aib^{32}]-NPY (2 nmol) or Veh (saline) to *ad-libitum* chow-fed rats at 10AM (lights on at 6AM) and measured 2-hour food intake post injection.

Tyloxapol (lipid production) experiments

For lipid production studies, rats with ICV cannulae and carotid catheters were matched for body weight and fasted with free access to water from 6 to 10AM. We previously confirmed by agarose gel electrophoresis that 4-hour fasted rats on laboratory chow have nearly undetectable levels of chylomicrons in the plasma compared with fed rats (211). Indirect calorimetry in a separate group of rats confirmed that animals are in a postabsorptive state after a 4-hour fast (211). Altogether, these findings suggest that chylomicrons do not contribute to the observed changes in TGs (211). A baseline blood sample was drawn from the carotid catheter, then plasma TG clearance was blocked by an intravenous infusion of tyloxapol (300 mg/kg body weight), which at the dosage used, potently inhibits LPL activity (IC_{50} 12.5μM) (305-307). Thirty minutes after tyloxapol infusion, ICV compounds or Veh were injected at time 0 min. Also at 0 min and at 30 min intervals, 200 μl of blood was collected in a tube containing 2 μl 50 mM ethylenediaminetetraacetic acid (EDTA) (211). The TG secretion rate was determined as the

slope of the concentration of plasma TGs over time using linear regression analysis (calculated from time 0 to 120 min).

Notably, one caveat of our experimental design was the use of tyloxapol to measure TG production rates. Tyloxapol is a non-ionic detergent and has been reported to have non-specific physiologic effects related to lipoprotein metabolism (307). Millar et al. (307) reports that over a prolonged time period after tyloxapol injection in mice, results in decreased TG production rates which appears to be due to a decrease in TG production and not a lack of inhibition of plasma TG clearance. Consistent with these findings, tyloxapol is known to accumulate in lysosomes in liver which may affect TG trafficking and VLDL-TG secretion and thus, account for the reported hepatic TG accumulation in livers of tyloxapol injected mice after 24-hour treatment (307). Therefore, to avoid any non-specific effects from the use of tyloxapol during the measurement of TG production rates, all experiments which required detailed biochemical analysis were conducted in the absence of tyloxapol.

fa/fa ZF rat pair-feeding study

The leptin resistant *fa/fa* ZF rat is a genetic model of obesity and is characterized by high NPY tone and dyslipidemia (65, 66, 134, 135). To control for hyperphagia and positive energy balance in *ad-libitum* chow-fed ZF rats, the ZF rats were pair-fed to the caloric intake of the control lean Zucker rats (*fa/-*). Body weights were measured daily. At the end of the study (day 38), 4-hour fasted rats were euthanized followed by collection of trunk blood and liver tissues.

Experimental animals: Mice (Chapter V)

Generation of mice with hepatocyte-specific gene deletion of *Rictor*

Mice with alleles in which exon 3 of the *Rictor* gene is flanked by loxP sites, *Rictor*$^{flox/flox}$ mice (308) were crossed with *albumin-Cre* transgenic mice (*Alb-Cre*$^{+/-}$; strain, B6.Cg-Tg (*Alb-*

Cre) 21Mgn/J; The Jackson Laboratory, Bar Harbor, ME) to obtain heterozygous *Rictor*$^{flox/WT}$*Alb-Cre*$^{+/-}$ offspring (where "WT" and "-" indicate wild-type alleles). These heterozygous mice were then crossed to produce hepatocyte-specific *Rictor* knockout (HRicKO) mice with genotype *Rictor*$^{flox/flox}$*Alb-Cre*$^{+/+ \text{ or } +/-}$ and age-matched littermate control mice with the following genotypes: *Rictor*$^{flox/flox}$*Alb-Cre*$^{-/-}$, *Rictor*$^{flox/WT}$*Alb-Cre*$^{-/-}$, *Rictor*$^{WT/WT}$*Alb-Cre*$^{+/+}$, *Alb-Cre*$^{+/-}$ or *Alb-Cre*$^{-/-}$. The HRicKO mice were born at expected Mendelian ratios and did not display any apparent defects in fertility or maturation (data not shown). Age-matched male HRicKO and control mice were studied at 3-5 months of age (young) and when they were greater than 9 months of age (old). Genotyping was performed by polymerase chain reaction (PCR) methods using DNA obtained from tail clippings with primers specific for the rictor floxed and recombined alleles as previously described (308), as well as primers to detect the presence of *Alb-Cre*: *Alb-3'*; 5'-ATGAAATGCGAGGTAAGTATG G-3'; *Cre 102*; 5'-CGCCGCATAACCAGTGAAAC-3.' Both *Rictor*$^{flox/flox}$ and *Alb-Cre*$^{+/-}$ mice used for breeding were fully backcrossed to the C57BL6/J strain. The mice were maintained under temperature- and humidity-controlled conditions with a 12-hour light/dark cycle and were given free access to food and water.

Animals and dietary treatment

Eight-week old HRicKO and age-matched control mice were either maintained on standard chow (5001; Lab diet, Richmond, IN) or placed on a diet containing 45% kcal high-fat diet (HFD; D12451, Research diets, New Brunswick, NJ) for 10 weeks. We also studied the effects of a micronutrient matched low-fat diet (LFD) and HFD on the phenotype. Ten-week old mice were initially placed on a 10% kcal LFD (D01060501, Research diets) for 10 weeks and then switched to a micronutrient matched 45% kcal HFD (D01060502, Research diets) for an additional 23 weeks. Body composition (whole body, fat mass and lean mass) was measured using an NMR spectrometer (Bruker Optics). At the end of these dietary studies, 4-hour fasted

mice were euthanized followed by collection of trunk blood in EDTA-coated tubes and tissues harvested for analysis.

Body composition analysis (Chapters III and V)

Body composition was determined by NMR spectroscopy to measure whole body, fat mass and lean mass. These measurements were performed using the EchoMRI-700 NMR spectrometer (Echo Medical Systems) for rats and the Minispec mq7.5 (Bruker Optics) in the Mouse Metabolic Phenotyping Center at Vanderbilt University (Nashville, TN) for mice. Animals were weighed immediately prior to collecting body composition measurements performed at the same time of day throughout each study to minimize any fluctuations due to feeding status of the animals.

Indirect calorimetry

Energy expenditure (EE) and fat oxidation were assessed by indirect calorimetry in 16-17 week old control and HRicKO mice after 8-9 weeks of LFD. Mice were housed individually in oxymax cages (Columbus Instruments; Columbus, Ohio). VO2 and VCO2 (ml/hour) were calculated based on the input and output rates of O2 consumption and CO2 production, which were used to determine the respiratory quotient (RQ = VCO2/VO2) and heat (kcal/hour = (3.815+1.232xRQ) x (VO2)) using the provided software (ExpeData 1.6.1; Sable Systems, Las Vegas, NV). EE data (kcal/12-hour) were normalized to NMR measured lean mass, obtained the day mice were placed in the oxymax cages.

Glucose, insulin, and pyruvate tolerance tests

For glucose tolerance tests (GTT), 4-hour fasted mice were administered glucose, 1 g/kg body weight (from 50% dextrose), by IP injection. For insulin tolerance tests (ITT), 4-hour fasted mice were administered IP insulin, 0.8 U/kg body weight (Novolin Regular insulin). For pyruvate

tolerance test (PTT), mice were fasted overnight then administered 2 g/kg of body weight sodium pyruvate by IP injection. Blood glucose concentrations were measured by tail prick using a Freestyle handheld glucometer from Abbott labs (Abbott Park, IL) at 30 min before injection (baseline), also at 0, 5, 15, 30, 60, and 120 min after the injection. Total area under the blood glucose curve (AUC) was calculated for each GTT, ITT, and PTT.

In vivo insulin stimulation study

After 10 weeks of HFD feeding, 21 week old HRicKO and age-matched littermate control mice were fasted for 4-hour and then administered an IP injection of insulin (Novolin Regular insulin), 0.6 U/kg body weight, and subsequently euthanized 30 min post injection. Trunk blood samples were collected in EDTA-coated tubes and liver samples harvested for analysis.

Histology

Liver sections were embedded in optimal cutting temperature compound (Tissue-Tek) and snap frozen for cryosectioning. Sections (4 µM) were stained with Oil Red O (ORO) and hematoxylin and eosin (H&E). All histological sectioning and staining were performed by the Vanderbilt Translational Pathology Shared Resource Core (Nashville, TN). Images were taken at 20X magnification using a digital microscope (ScanScope CS; Aperio, Vista, CA).

LXR agonist study

A LXR agonist T0901317 (Cayman Chemical, Ann Arbor, MI) was dissolved in vehicle (10% ethanol/50% polyethylene glycol/0.9% normal saline) to 10 mg/ml before administration. After 23 weeks of HFD feeding, 45 week old HRicKO and age-matched control mice were treated IP daily (at 6PM) with either 50 mg/kg body weight T0901317 or vehicle. To measure plasma lipids and glucose on day 2 of treatment in *ad-libitum* fed mice, 100 µl of blood was

collected by submandibular bleed in EDTA-coated tubes. Blood glucose concentrations were measured using a glucometer. After 6 days of treatment, *ad-libitum* fed mice were euthanized and trunk blood samples collected in EDTA-coated tubes, and tissues harvested for analysis.

Molecular and biochemical techniques

Genotyping of mice

Genotyping of mice for the "floxed" *Rictor* allele and *Albumin-Cre* transgene was performed by PCR using DNA extracted from tail clippings (1-2 mm) by the Hot Shot method (309). Clippings were heated in an alkaline lysis reagent (100 µL, 25 mM NaOH, 0.2 mM EDTA, pH 12) in a thermomixer (95 °C; 25 min) with constant shaking (550 rpm), after which neutralization reagent (100 µl, 40 mM Tris –HCL, pH 5) was added. PCR was performed with 2 µL of DNA using 5' Hotmastermix 2.5 (annealing temperature 60 °C, 40 cycles) and the following PCR primers for the floxed and wildtype *Rictor* allele: *PiaT41*; 5'-ACTGAATATGTTCATGGTTGTG-3'; *PiaEx3*; 5'-GAAGTTATTCAGATGGCCCAGC-3' as well as primers to detect the presence of *Alb-Cre*: *Alb-3'*; 5'-ATGAAATGCGAGGTAAGTATG G-3'; *Cre 102*; 5'-CGCCGCATAACCAGTGAAAC-3'and internal control primers were used for all Cre PCR screening reactions: *MIR015*; 5'-CAAATGTTGCTTGTCTGGTG-3'; *MIR016*; 5'-GTCAGTCGAGTGCACAGTTT-3'(annealing temperature 60 °C, 40 cycles). The amplified DNA was separated by electrophoresis on an agarose gel (Alb-Cre, 1% agarose; Rictor, 2.3% agarose, 0.5 µg/ml ethidium bromide (EtBr), 1X Tris-acetate (TAE) composed of 40 mM Tris (pH 7.6), 20 mM acetic acid, and 1 mM EDTA) followed by ultraviolet (UV) light detection of bands stained with EtBr. Mice were genotyped based on the presence of expected PCR products for the *Rictor* allele; homozygous floxed mutant (554 bp), heterozygotes (554 bp and 466 bp) and wild type mice (466 bp). A single band (565 bp) indicated the presence of the *Albumin-Cre* transgene and the internal control was detected at 150 bp.

Lipoprotein fractionation

Plasma samples (150 µl) were size fractionated on a Superose 6 10/300 GL column (17-5172-01; GE Healthcare Biosciences, Little Chalfont, UK) utilizing the Bio-Rad BioLogic Duo-Flow HPLC unit and subsequently, 300 µl column fractions were collected in a 96-well plate. All lines were flushed with HPLC buffer (5 M NaCl, 0.5 M Na_2HPO_4, 0.5 M EDTA). The plasma samples were centrifuged for 5 min at 10,000 x *g* at 4 °C to pellet any remaining particulates. Using a Hamilton glass syringe (Model 1725 TLL Hamilton Glass Syringe with Slots; 60373-856; VWR, Radnor, PA) fitted with a 22-gauge needle, 150 µL of centrifuged plasma was slowly drawn up and loaded into the port of the AVR7-3 valve. Next, the fractionation was run at a rate of 0.5 ml/min and the pressure held constant (~70 psi for a new column). The plasma sample was size-fractionated on the Superose 6 10/300 GL column (volume roughly 24 ml). After the sample passes through the column, the buffer lines direct the sample to the Bio-Rad BioLogic Bio-Frac fraction collector, where it is collected in 300 µL fractions in a 96-well plate.

Plasma hormones, metabolites, and lipid measurements

For all studies, trunk blood was collected in EDTA-coated tubes and placed on ice. Samples were centrifuged at 2000 x *g* for 13 min at 4 °C, the plasma supernatants were transferred to a new tube and stored at -80 °C. Plasma samples were assayed for insulin, glucagon, and corticosterone concentrations using a double antibody radioimmunoassay (RIA) procedure. The Vanderbilt Diabetes Center Hormone Assay & Analytical Services Core (Nashville, TN) conducted these assays using the respective insulin and glucagon RIA kit from Millipore (Billerica, MA) and corticosterone ImmuChem Double Antibody RIA kit from MP Biomedicals (Solon, OH). Plasma lipids were assayed using an enzymatic colorimetric assay conducted in 96-well plate format and absorbance measured spectrophotometrically using the following reagent kits: Triglycerides and Total Cholesterol (Raichem, San Diego, CA), Non-Esterified Fatty Acids (Wako Diagnostics, Richmond, VA), and Glycerol (Sigma-Aldrich, St.

Louis, MO). For all lipid assays, samples and standards were run in triplicate. Blood glucose concentrations were measured from trunk blood obtained at study termination using a glucometer from Roche Diagnostics (Accu-chek advantage, Indianapolis, IN) for rats and a Freestyle handheld glucometer from Abbott labs for mice.

Liver, plasma, and fecal lipid fractionation by gas chromatography method

Of note for Chapter V: Feces were collected over a 48-hour period from 21 week old *ad-libitum* fed HRicKO and age-matched littermate control mice fed either LFD or HFD for 10 weeks. Lipids were extracted from liver, plasma, or feces using the method of Folch-Lees (310). The extracts were filtered, and lipids recovered in the chloroform phase. Individual lipid classes were separated by thin layer chromatography using Silica Gel 60 A plates developed in petroleum ether, ethyl ether, acetic acid (80:20:1) and visualized by rhodamine 6G. Phospholipids, diglycerides, triglycerides, and cholesteryl esters were scraped from the plates and methylated using BF_3/methanol as described by Morrison and Smith (311). The methylated fatty acids were extracted and analyzed by gas chromatography. Gas chromatographic analyses were carried out on an Agilent 7890A gas chromatograph equipped with flame ionization detectors and a capillary column (SP2380, 0.25 mm x 30 m, 0.25 μm film, Supelco, Bellefonte, PA). Helium was used as a carrier gas. The oven temperature was programmed from 160 °C to 230 °C at 4 °C/min. Fatty acid methyl esters were identified by comparing the retention times to those of known standards. Inclusion of lipid standards with odd chain fatty acids permitted quantification of the amount of lipid in the sample. Dipentadecanoyl phosphatidylcholine (C15:0), diheptadecanoin (C17:0), trieicosenoin (C20:1), and cholesteryl eicosenoate (C20:1) were used as standards. To quantify total cholesterol, internal standard (5-a-cholestane) was added to a portion of the lipid extract and then saponified at 80 °C in 1 N KOH in 90% methanol for 1-hour. The nonsaponifiable sterol was extracted into hexane, concentrated under nitrogen, and then solubilized in carbon disulfide to

inject onto the gas chromatograph. The lipid profiles were performed in the lipid sub-core of the Vanderbilt Diabetes Center Hormone Assay & Analytical Services Core (Nashville, TN).

Protein extraction and quantification

Total protein was extracted from frozen liver, muscle, and adipose tissues. Muscle and adipose tissues were pulverized with a tissue pulverizer prior to sonication. Tissues were sonicated in cold T-Per Tissue Protein Extraction Buffer (10 µl/mg tissue; Thermoscientific; Rockford, IL) containing 1:100 (v:v) of protease inhibitor cocktail and 1:100 (v:v) of phosphatase inhibitor cocktail (Sigma; St. Louis, MO) with a Sonicator at setting 8, for less than 5 sec (Virtis Virsonic 100 Ultrasonic Cell Disrupter; AN SP Industries Company; Gardiner, NY). Following sonication, all samples were clarified by centrifugation at 14,000 x *g* for 20 min at 4 °C. The protein extract (supernatant) was immediately transferred to a clean pre-chilled tube. Next, protein concentration of the protein extract was determined in duplicate using a Pierce BCA Protein Assay Kit (Thermoscientific) performed according to the manufacturer's instructions. Samples were diluted to 1 mg/ml with T-Per buffer containing protease and phosphatase inhibitor cocktail and stored at -80 °C until further analyses.

Nuclear-cytoplasmic protein fractionation and quantification

To prepare nuclear and cytoplasmic extracts of liver tissues, NE-PER Nuclear and Cytoplasmic Extraction Reagents (Thermoscientific) were used according to the manufacturer's protocol. Protease and phosphatase inhibitor cocktail was added to CER I and NER at 1:100 (v:v) immediately before use. Briefly, frozen liver tissues (60 mg) were added to 600 µl of CER I buffer and homogenized to disrupt the cell membrane and release cytoplasmic contents. Next, the homogenate was incubated on ice for 10 min followed by the addition of 33 µl of Cold Cer II buffer and then centrifuged at 14,000 x *g* for 5 min. The supernatant containing the cytoplasmic extract was immediately transferred to a clean pre-chilled tube. The pellet containing the intact

nuclei was lysed with addition of 300 µl of cold NER buffer and then vortexed for 15 sec at the highest setting every 10 min for a total of 40 min. The suspended pellet was centrifuged at 14,000 x *g* for 10 min to yield the supernatant containing nuclear extract which was transferred to a clean pre-chilled tube. Next, protein concentration of the extract was determined in duplicate using a Pierce BCA Protein Kit (Thermoscientific) performed according to the manufacturer's instructions. Samples were diluted to 1 mg/ml with the appropriate buffers containing protease and phosphatase inhibitor cocktail and stored at -80 °C until further analyses.

Western blot analysis

Protein samples (1 mg/ml) were mixed with 4X Sample Buffer and 20X Reducing Agent (Bio-Rad; Hercules, CA), heated to 85 °C for 10 min, and immediately loaded into a well on a gel (10.5 µg total protein per lane) along with a Kaleidoscope Precision Plus Protein Standard (Bio-Rad). Samples were subjected to denaturing electrophoresis on either a 7% or 4-12% Bis-Tris XT gel using the Bio-Rad XT Criterion System (Bio-Rad). Protein samples were transferred to 0.2 µm nitrocellulose membranes using the Criterion Blotter module, according to the manufacturer's instructions (Bio-Rad). Membranes were blocked in blocking buffer (5% BSA, 0.2% Tween 20) for 1-hour at room temperature and then incubated with primary antibodies (diluted 1:1000) in blocking buffer at 4 °C with gentle rocking overnight. Blots were washed (3 times for 10 min each) at room temperature in TBS-T (Tris Buffered Saline; 150 mM NaCl, 20 mM Tris pH 7.5 with 0.1% (v/v) Tween 20; Sigma Aldrich; St. Louis, MO). Then, blots were incubated with species-specific horseradish peroxidase (HRP)-conjugated secondary antibody (diluted 1:7500) in 50/50 blocking buffer and Starting Block T20 Blocking buffer (Thermoscientific) for 1-hour at room temperature and subsequently, washed in TBS-T (3 times for 10 min). Antibody detection was performed with Western Lightening Plus-ECL Enhanced Chemiluminescence Substrate Kit (Perkin Elmer) and HyBlot CL Autoradiography Film (Denville Scientific, Metuchen, NJ). Band

intensity from X-ray film detection was analyzed by densitometry using ImageJ software from the National Institutes of Health.

Primary antibodies used for immunoblotting are the following: ACC, phosphorylated (p) ACC (Ser79), ACL, AKT, AKT (pThr308), AKT (pSer473), FAS, FoxO1 (pSer256), GSK3β (pSer9), lipin-1 (pSer106), mTOR, Rictor, Raptor, S6K1 (pThr389), S6K1, β-Tubulin (all from Cell Signaling Technology), Actin, ARF-1, Calnexin, GAPDH, GR, GSK3β, HDAC-1, Insig2A, IRβ (Tyr1162/1163), lipin-1, MTP, PKCα (pSer657), PKCα, SCD-1, SGK (pSer422), SGK, PEPCK (all from Santa Cruz Biotechnology), and LXRα from Abcam; HSP70 was purchased from Enzo Life Sciences (Framingdale, NY). The antibody that detects the mature (68KDa) and the precursor (125KDa) form of SREBP-1c (312) was kindly provided by Alyssa Hasty (Vanderbilt University) and the antibody that detects apolipoprotein B-100/48 (313) was kindly provided by Larry Swift (Vanderbilt University). Secondary antibodies used at a 1:7500 dilution for immunodetection are the following: donkey anti-goat IgG HRP purchased from Santa Cruz Biotechnology; anti-rabbit IgG HRP and anti-mouse IgG HRP conjugate purchased from Promega (Madison, WI).

RNA isolation and quantitative real-time (RT)-PCR

Liver samples were homogenized and RNA isolated using TRIzol reagent (Invitrogen, Carlsbad, CA). Sample RNA concentrations were quantified on a Nanodrop 1000 spectrophotometer (Nanodrop Technologies; Wilmington, DE). RNA integrity was determined using a total of 2 μg of RNA by electrophoresis on a agarose gel (1% agarose, 0.5 μg/ml EtBr, 1X TAE) followed by UV light detection of 18S and 28S ribosomal RNA bands stained with EtBr. A cDNA template was synthesized from equal amounts of each sample of RNA (2 μg) using the High Capacity cDNA Reverse Transcription Kit (Applied Biosystems, Foster City, CA) and performed on the I-Cycler thermal cycler (Biorad). RT-PCR was conducted using standard curves in each assay (six-point serial dilution of cDNA synthesized from XpressRef^{TM} rat or mouse

universal total RNA; SuperArray Bioscience, Frederick, MD), IQ SYBR Green Supermix, and performed in triplicate using the I-Cycler thermal cycler (Biorad) with 1 cycle of 95 °C for 3 min followed by 40 cycles of 95 °C for 30 sec, optimal annealing temperature for 30 sec, and 72 °C for 30 sec. A standard curve was used to calibrate relative quantification of product in the exponential phase of the amplification curve in all experiments at 95-105% amplification efficiency. Quantification results for the RNA of interest were normalized to the housekeeping gene, ribosomal protein L13a (*RPL13A*) and for comparative analysis, RNA ratios of the treatment group were normalized to the control group. Real time primers were previously published or designed using Beacon Designer (Beacon Design Software; Palo Alto, CA) by the Vanderbilt Molecular Cell Biology Resource Cores (Nashville, TN). Primer sets used for RT-PCR are listed in Table 2.1.

Statistical analysis

Data are presented as mean ± standard error of the mean (SEM). Two-group comparisons were performed using Student's *t*-test (unpaired, two-tailed) and three-group (or more) comparisons by one-way analysis of variance (ANOVA) with Bonferroni's post-test analysis. In Chapter III, the main effect of treatment to increase plasma TGs over time was compared by two-way repeated measures ANOVA with Bonferroni's post-test analysis. In Chapter IV, the main effect of treatment on body weight over time was compared by two-way repeated measures ANOVA with Bonferroni's post-test analysis. In Chapter V, the main effects of HFD and genotype on food intake, body weight, fat mass, and lean mass over time were compared by two-way repeated measures ANOVA with Bonferroni's post-test analysis. All analyses were performed using GraphPad Prism, version 5.04, 2010 (GraphPad Software, San Diego, CA). Differences with $p<0.05$ were considered statistically significant and $p\geq0.05$ but <0.1 reported as a trend.

Table 2.1. Primer sequences used for quantitative RT-PCR analysis

Gene	Species	Forward (5' to 3')	Reverse (5' to 3')
ACACA (ACC-1)	mouse/rat	GGGACTTCATGAATTTGCTGATTCTCAGTT	GTCATTACCATCTTCATTACCTCAATCTC
ACLY (ACL)	mouse	GCCAGCGGGAGCACATC	CTTTGCAGGTGCCACTTCATC
ACOX1	mouse/rat	CTCTCTATGGGATCAGCCAGAA	CCACTCAAACAAGTTTTCATACACA
ARF1	mouse/rat	CGGAACCAGAAGTGAACCAGACC	CGTTTGCCACATGAGAGGAAAGC
CD36	rat	CAATGAGTAGGTCTCCAACCG	GTTGGCAAGAAGCAAGTGC
CPT1A	mouse/rat	GGAGACAGACACCATCCAACATA	AGGTGATGGACTTGTCAAACC
CYP7A1	mouse	CCAGGGAGATGCTCTGTGTTC	ACCCAGACAGCGCTCTTTGAT
DGAT1	rat	GGATGGTCCCTACTATCCAG	CCACCAGTCCCTGTAGAACT
DGAT2	mouse/rat	GGAACCGCAAAGGCTTTGTA	AATAGGTGGGAACCAGATCAGC
FASN (FAS)	mouse/rat	AGGATGTCAACAAGCCCAAG	ACAGAGGAGAAGGCCACAAA
FDPS	mouse	ATGGAGATGGGCGAGTTCTTC	CCGACCTTTCCCGTCACA
G6PC	mouse/rat	ATCCGGGGCATCTACAATG	TGGCAAAGGGTGTAGTGTCA
GPAM (GPAT)	mouse/rat	CATCCTCTTTTGCCACAACAT	ACAGAATGTCTTTGCGTCCA
HMGCR	mouse	CTTGTGGAATGCCTTGTGATTG	AGCCGAAGCAGCACATGAT
HMGCS1	mouse	GCCGTGAACTGGGTCGAA	GCATATATAGCAATGTCTCCTGCAA
INSIG1	mouse	TAGCCACCATCTTCTCCTCC	CCAACGAACACGGCAATA
INSIG2	mouse	CCCTCAATGAATGTACTGAAGGATT	TGTGAAGTGAAGCAGACCAATGT
LDLR	mouse	TCCATCGCAGCTGGGTCTGT	TACACTGTGTCACATTGACGC
LDLR	rat	CAGTGCGGCGTAGGATTG	GGATCACAGACCCGAAATGT
LPIN1	mouse/rat	TCACTACCCAGTACCAGGGC	TGAGTCCAATCCTTTCCCAG
NR1H3 (LXRα)	mouse/rat	ATCGCCTTGCTGAAGACCTCTG	GATGGGGTTGATGAACTCCACC
PPARA	rat	TGGAGTCCACGCATGTGAAG	CGCCAGCTTTAGCCGAATAG
PCK1 (PEPCK)	mouse/rat	CTGGCACCTCAGTGAAGACA	TCGATGCCTTCCCAGTAAAC
RICTOR	mouse	ATTCGAGGGCGGAATGACAG	CTCCCTCAAGTTATCAGAAGGTTC
RPL13A	mouse	AGATGCACTATCGGAAGAAGAAG	AGTCTTTATTGGGTTCACACCAG
RPL13A	rat	TACTCTGGAGGAGAAACGGAAG	GCCTGTTTCCTTAGCCTCAA
SCAP	mouse	ATTTGCTCACCGTGGAGATGTT	GAAGTCATCCAGGCCACTACTAATG
SCD (SCD-1)	mouse	CCCAGTCGTACACGTCATTTT	CATCATTCTCATGGTCCTGCT
SCD	rat	TGAAAGCTGAGAAGCTGGTG	CAGTGTGGGCAGGATGAAG
SREBF1 (SREBP1c)	mouse/rat	GGAGCCATGGATTGCACATT	CCTGTCTCACCCCCAGCATA
SREBF2 (SREBP2)	mouse	GCGTTCTGGAGACCATGGA	ACAAAGTTGCTCTGAAAACAAATCA
FDFT1 (SS)	mouse	CCAACTCAATGGGTCTGTTCCT	TGGCTTAGCAAAGTCTTCCAACT

CHAPTER III

CENTRAL NERVOUS SYSTEM NEUROPEPTIDE Y SIGNALING VIA THE Y1 RECEPTOR PARTIALLY DISSOCIATES FEEDING BEHAVIOR FROM LIPOPROTEIN METABOLISM IN LEAN RATS

Adapted from Rojas et al. *Am J Physiol Endocrinol Metab* 303 (12): E1479-E1488, 2012

Introduction

Despite the fact that clinicians have become increasingly adept at treating classical cardiovascular risk factors (i.e. hypertension, smoking, and cholesterol) (4), cardiovascular disease remains one of the leading causes of deaths worldwide (8), potentially due to the parallel diabetes and obesity epidemics (9). The dyslipidemia associated with diabetes and obesity consists of elevated VLDL-TG together with small-dense LDL-C and reduced HDL-C levels (14-16), and is an increasingly recognized component of cardiovascular risk, morbidity and mortality (16).

A current model of dyslipidemia associated with obesity and diabetes suggests that increased visceral fat mass and insulin resistance leads to elevated adipocyte lipolysis which increases FFA delivery to liver, where it is efficiently cleared, re-esterified to TG and loaded onto a nascent apoB particle, ultimately resulting in VLDL maturation and secretion (23, 24). This process is ordinarily suppressed by integrated hepatic insulin action (29, 30). With a rise in VLDL-TG in the circulation, CETP exchanges cholesterol esters from HDL and LDL particles with TGs from VLDL, ultimately lowering HDL-C levels and facilitating the accumulation of atherogenic, LDL-C particles (reviewed in (15, 31)).

In the context of integrated energy homeostasis, short term energy stores are provided by glucose and glycogen, while long term needs are met by adipose- and liver-derived lipids, a

process that is tightly regulated by the CNS. NPY expressing neurons are widely distributed in the CNS, concentrated in the mediobasal hypothalamus, important in the regulation of feeding and energy homeostasis, and increasingly recognized as having a role in lipid homeostasis (211). NPY is a potent orexigenic peptide, and when delivered by chronic infusion directly into the brain of rats and mice, has been observed to promote hyperphagia, obesity dyslipidemia, and the metabolic syndrome (131, 132), similar to that of the leptin deficient *ob/ob* mouse (62, 67, 133) and the genetically leptin resistant *fa/fa* ZF rat (65, 66). These genetic models of obesity are characterized by high NPY mRNA and peptide levels in the hypothalamus, secondary to the absence of negative feed-back regulation by leptin (134-137). Rodent models of DIO (made obese by feeding a highly palatable diet) and STZ-induced diabetes (insulin deficient), which are more typical of human diabetes, are also characterized by elevated CNS NPY tone (139, 140).

Positive energy balance and obesity pathogenesis are thought to result from defects in inhibitory feedback signaling to the CNS, including neuronal insulin and leptin resistance, and impaired nutrient sensing (74, 75). *We hypothesized that increases in NPY tone within these neural circuits may contribute to dyslipidemia in addition to obesity.* We previously demonstrated that ICV administration of NPY directly into the third ventricle of lean, fasted, wild-type rats increase hepatic VLDL-TG secretion independently of food intake (211). Peripherally administered NPY had no such effect, and taken together, these findings suggest that NPY-regulated neural circuits may be involved in the regulation of TG metabolism in the liver (211).

NPY is a 36 amino acid neuropeptide member of the NPY family that includes PYY and PP (93). NPY affects a wide variety of physiological functions via the activation of a population of distinct G-protein-coupled NPY receptor subtypes, Y1, Y2, Y4, and Y5 (93, 105). All NPY receptor subtypes are expressed in the hypothalamus (113, 114). The effects of NPY on feeding and energy homeostasis are thought to be largely mediated by hypothalamic Y1 and Y5 receptors (reviewed in (93)). Y2 receptors, having affinity for both NPY and PYY (105), act in an inhibitory manner on both orexigenic NPY as well as anorexigenic POMC neurons in the ARC

(116). The hypothalamic Y4 receptor is highly selective for PP over NPY or PYY (105) and is thought to mediate anorexigenic effects by decreasing hypothalamic NPY (314). Yet, the receptor subtype(s) involved in the central NPY regulation of lipoprotein metabolism are not well understood. Nor is the relative effect of a given receptor on feeding versus lipoprotein metabolism. In genetic models in which the NPY Y1, Y2, Y4, or Y5 receptor has been deleted on an *ob/ob* background (a rodent model of severe hypertriglyceridemia), the effect on TGs is not reported except for the Y2 receptor deletion having no effect (167, 170, 176, 177).

Our study employed two approaches: first, determining whether CNS NPY retains the effect on hepatic VLDL-TG secretion chronically (3 days; twice daily ICV administration) in the absence of increased food intake and fat mass; and second, determining whether different CNS NPY receptors mediate feeding versus VLDL-TG regulatory effects. We evaluated the effect of selective ICV NPY Y1, Y2, Y4, and Y5 receptor agonists on both feeding and hepatic VLDL-TG secretion in lean fasted rats in order to determine which receptor subtype(s) are involved in the central NPY regulation of lipoprotein metabolism versus feeding. We ultimately sought to determine whether the effects on feeding versus lipids overlap or are dissociable as this might yield novel structure-function insight and/or therapeutic implications in obesity and the metabolic syndrome.

Results

Chronic NPY treatment increases plasma TG levels independently of food intake, positive energy balance, and increased body adiposity

Previously, we demonstrated that ICV administration of NPY into the third ventricle of lean rats increases hepatic VLDL-TG secretion independently of feeding, as the animals were denied access to food just prior to and during experimental procedures (211). Because exogenous administration of NPY to a lean animal can drive the development of obesity and the metabolic

syndrome (131, 132), we sought to determine whether a more chronic NPY administration increases plasma TGs independently of its orexigenic effects to increase food intake and body adiposity. NPY was administered ICV (1 nmol) twice daily over 3 days in chow-fed rats. Importantly, to prevent an induction of food intake, we pair-fed NPY-treated rats to the caloric intake of Veh-treated controls. At the end of the study (day 3), 4-hour fasted rats were given either ICV NPY (1 nmol) or Veh, and trunk blood was collected at study termination (120 min post injection). Pair-feeding successfully matched the body composition of NPY-treated rats relative to Veh-treated animals, resulting in no differences in body weight, lean mass, and fat mass at study termination (Fig. 3.1A). However, we found that chronic NPY injections in pair-fed rats resulted in a ~50% increase in plasma TGs by treatment days 2 and 3 ($p<0.01$; $n=6$/group; Fig. 3.1B) with no observed alteration in total plasma cholesterol levels (p=ns; Table 3.1). The effect of chronic NPY treatment to increase plasma TG over time was dependent on the treatment ($F(1, 22) = 7.99$, $p<0.01$).

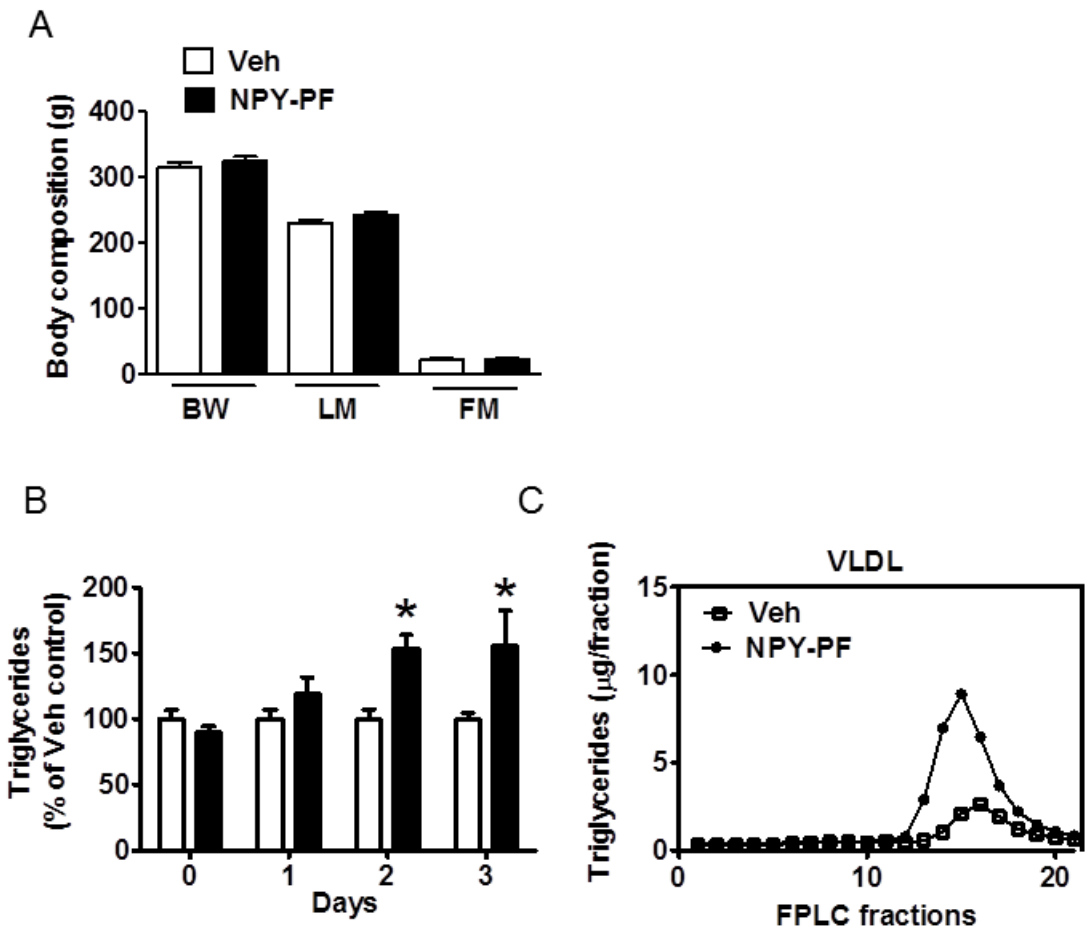

Figure 3.1. Chronic NPY treatment induces hypertriglyceridemia independently of positive energy balance. A: The effects of chronic ICV NPY treatment (3 days, twice daily; 1 nmol) in chow-fed rats pair-fed (NPY-PF; black bars) to the caloric intake of ICV vehicle (Veh; white bars) treated rats (*n*=6/group) on body weight (BW), lean mass (LM) and fat mass (FM) are illustrated. Data are presented as mean ± SEM and were analyzed by Student's t-test (unpaired, two-tailed), p=ns for NPY-PF vs. Veh comparisons. B: Daily plasma TG levels (% of Veh control) from blood collected by tail prick of NPY-PF (black bars) and Veh-treated (white bars) rats are shown. Data are presented as mean ± SEM and were analyzed by two-way repeated measures ANOVA with Bonferroni's post-test analysis; *p<0.01 for NPY-PF vs. Veh comparisons. The effect of chronic NPY treatment to increase plasma TG over time was dependent upon treatment ($F(1, 22) = 7.99$, $p<0.01$). C: The TG content of FPLC fractions of sized-fractionated individual plasma samples from NPY-PF (black circles) and Veh-treated (clear squares) rats as measured on study day 3 are illustrated for comparison of fractions 10-20, the size range corresponding to VLDL.

The changes in TGs observed with chronic NPY treatment in pair-fed rats ($p<0.05$; Table 3.1) were not due to elevated adipocyte lipolysis, as we did not observe any changes in FFA or glycerol at study termination ($p=ns$; Table 3.1), consistent with our previous findings (211). Although glucagon levels were significantly elevated in comparison to Veh treatment ($p<0.05$; Table 3.1), insulin levels only trended higher ($p=0.09$; Table 3.1). Individual plasma samples were sized-fractionated by FPLC and quantified for TG content. As previously observed with an acute injection of ICV NPY in lean fasted rats, chronic NPY treatment in pair-fed rats increased TG content in VLDL containing fractions (fractions 10-20; Fig. 3.1C).

Table 3.1. Effects of chronic NPY administration to pair-fed chow-fed rats at 120 min post ICV injection on glucoregulatory hormones and metabolites

	Veh	**NPY-PF**
TG (mg/dl)	80.5±5.0	156±32*
Cholesterol (mg/dl)	97.6±10.0	83.8±3.6
FFA (mmol/l)	0.31±0.03	0.23±0.02
Glycerol (mg/dl)	10.4±1.8	15.6±4.7
Insulin (ng/ml)	1.04±0.10	2.09±0.50
Glucagon (pg/ml)	63.1± 4.4	107±14*

Data are presented as mean ± SEM (n=6/group) and were analyzed by Student's t-test (unpaired, two-tailed). *$p<0.05$ for NPY-PF vs. vehicle (Veh) comparisons.

Selective activation of NPY receptor subtypes induces hyperphagia in lean *ad-libitum* chow-fed rats

We first sought to identify an ICV dosage of NPY that would lead to a physiologically relevant feeding response. Lean *ad-libitum* chow-fed rats were given either ICV NPY (1 nmol) or Veh, and the 2-hour feeding response post injection was compared to the 2-hour refeeding response of 12-hour fasted rats. As expected, both ICV NPY treatment and 12-hours of fasting potently induced hyperphagia in comparison to Veh treatment (Fig. 3.2). We found that 1 nmol NPY given ICV induced the same 2-hour feeding response as observed after a 12-hour fast

(p=*ns;* Fig. 3.2). All of the selective NPY receptor agonists, Y1 ([F7, P34]-NPY; 1 nmol), Y2 (hPYY 3-36; 1 nmol), Y4 (hPP; 1 nmol), and Y5 ([Ala^{31}, Aib^{32}]-NPY; 2 nmol) induced hyperphagia in *ad-libitum* chow-fed rats relative to Veh (Fig. 3.2). Therefore, all of the selective receptor agonists (Y1, Y2, Y4, and Y5) induced a 2-hour feeding response similar in magnitude to 12 hours of fasting (p=*ns;* Fig. 3.2). Of particular note, the Y2 receptor agonist, at a dose equivalent to NPY (1 nmol), stimulated feeding above all the other compounds except for the Y5 agonist (Fig. 3.2). Collectively, these data confirm that we used physiologically relevant doses (1-2 nmol) of each selective receptor agonist for our food intake and lipid studies.

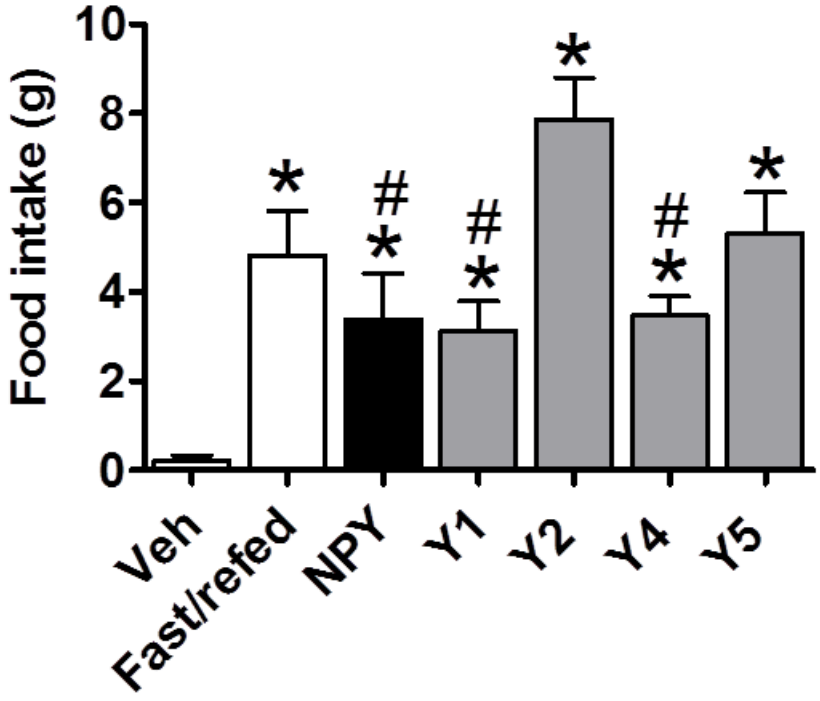

Figure 3.2. Effects of CNS administered NPY receptor subtype agonists on 2-hour food intake. Food intake was measured in lean *ad-libitum* chow-fed rats for 2-hours after receiving an ICV injection of Veh (*n*=13), NPY (1 nmol; *n*=4), or a selective NPY receptor subtype agonist for Y1 ([F7, P34]-NPY; 1 nmol), Y2 (hPYY 3-36; 1 nmol), Y4 (hPP; 1 nmol), or Y5 ([Ala^{31}, Aib^{32}]-NPY; 2 nmol) (*n*=4-6/group). These 2-hour food intake measurements are shown in comparison with a 2-hour refeeding response of a 12-hour fasted lean rat (Fast/refed; *n*=3). Data are presented as mean ± SEM and were analyzed by one-way ANOVA. Significant differences ($p<0.05$), as tested with Bonferroni's post-test, are indicated by *for comparisons relative to Veh and $^{\#}$for comparisons relative to Y2 receptor agonist.

A Y1 receptor agonist increases plasma TG levels to the greatest extent relative to other NPY receptor subtype agonists

In corroboration with our previous findings (211), NPY significantly increased the hepatic TG production rate (6.4±0.5 mg/dl/min for NPY (*n*=5) vs. 3.5±0.1 mg/dl/min for Veh (*n*=26), p<0.0001; Fig. 3.3A and E). We found that the Y1 receptor agonist, [F7, P34]-NPY (1 nmol), also increased hepatic TG production rate to a similar extent (6.7±0.4 mg/dl/min for Y1 (*n*=7) vs. Veh, p<0.0001; Fig. 3.3B and E). The Y2 receptor agonist, hPYY (3-36; 1 nmol), stimulated TG production by 1.5-fold (5.1±0.3 mg/dl/min for Y2 (*n*=7) vs. Veh, p<0.01; Fig. 3.3C and E) and was less potent than the Y1 receptor agonist (Y1 vs. Y2, p<0.01; Fig. 3.3E). Neither the Y4, hPP (1 nmol), nor Y5, [Ala^{31}, Aib^{32}]-NPY (2 nmol), receptor agonists increased the rate of hepatic TG production beyond that of Veh treatment (p=*ns*; Fig. 3.3D and E). The ability of NPY, and its Y1 and Y2 receptor agonists, to increase TG production over time was treatment dependent ($F(6, 50) = 11.75$, p<0.0001). Collectively, our results suggest that while Y1 and Y2 receptor agonists both regulate plasma TG levels and food intake, an NPY signal mediated through a Y1 receptor more potently increases hepatic TG production, while one mediated through the Y2 receptor has a greater effect on food intake (compare Fig. 3.2 and 3.3E).

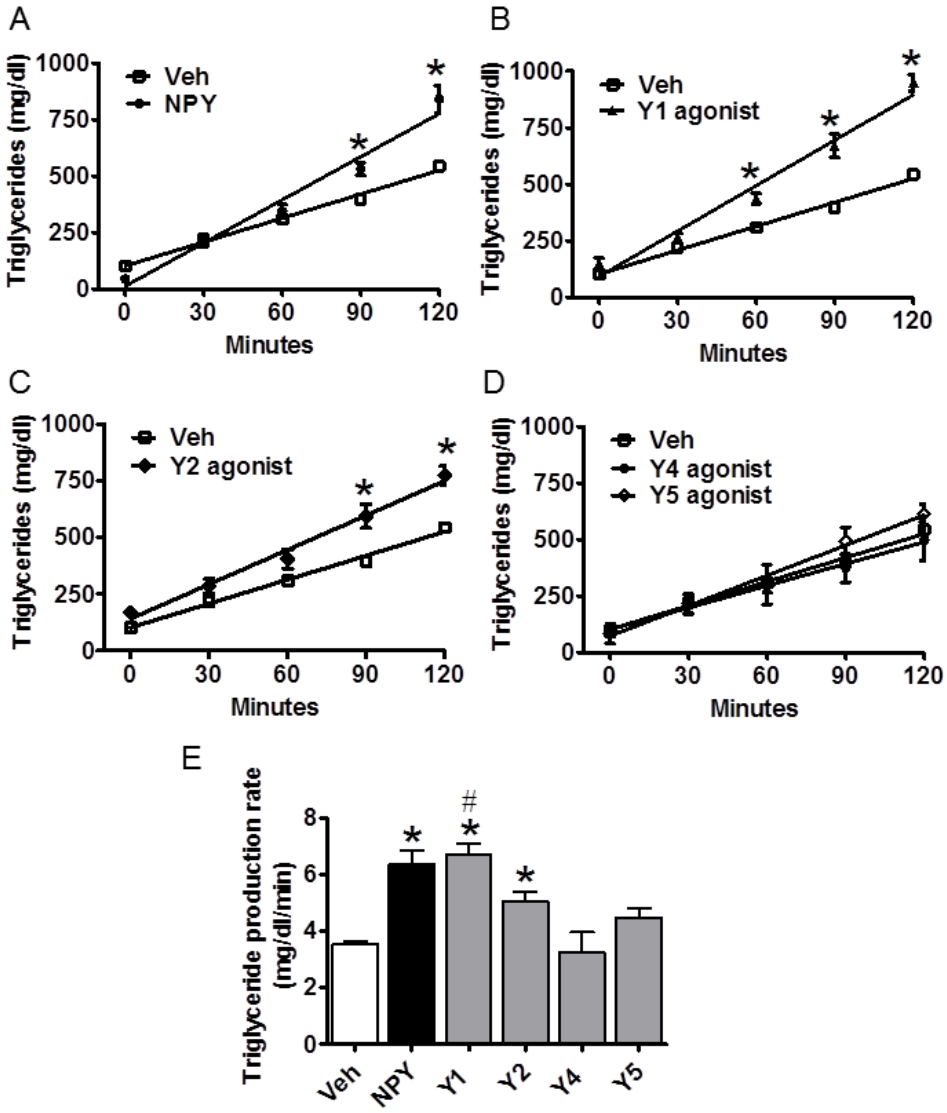

Figure 3.3. Effect of each CNS NPY receptor subtype (Y1, Y2, Y4, and Y5) on hepatic TG production. A-D: Plasma TG levels after an intra-arterial injection of tyloxapol (at time -30 min), and then at time 0 min, ICV injections of (A) NPY (1 nmol; black circles) or Veh (clear squares); or (B) Y1 receptor agonist ([F7, P34]-NPY, 1 nmol; black triangles) or Veh (clear squares); or (C) Y2 receptor agonist (hPYY 3-36, 1 nmol; black diamonds) or Veh (clear squares); or (D) Y4 receptor agonist (hPP, 1 nmol; black circles) or Y5 receptor agonist ([Ala^{31}, Aib^{32}]-NPY, 2 nmol; clear diamonds) or Veh (clear squares); were administered to lean 4-hour fasted rats (NPY, *n*=5; NPY receptor agonists, *n*=4-7/group; Veh, *n*=26). Data are presented as mean ± SEM and significant differences (*p<0.05) for treatment vs. Veh were determined by two-way repeated measures ANOVA (A-D). The ability of NPY, and its Y1 and Y2 receptor agonists, to increase TG production over time was treatment dependent ($F(6, 50) = 11.75$, $p<0.0001$). E: Depicts the TG production rates calculated from the change in plasma TG levels over time after ICV treatment of either NPY or NPY receptor agonists (Y1, Y2, Y4, and Y5) compared to Veh in lean 4-hour fasted rats. Data are presented as mean ± SEM and statistical significance, as determined by one-way ANOVA with Bonferroni's post-test analysis ($p<0.05$), is designated by either a *for comparisons relative to Veh or a $^{\#}$for the receptor agonist comparison of Y1 relative to Y2.

ICV administered Y1 receptor agonist enhances hepatic secretion of TGs in the form of VLDL-lipoprotein

Since Y1 and Y2 receptor agonists both increased hepatic TG production, we next confirmed that modulation of CNS NPY signaling via these receptor subtypes increase TGs in the VLDL fraction. In order to avoid any non-specific effects from the use of tyloxapol during the measurement of TG production rates, we performed these experiments in the absence of tyloxapol. NPY (1 nmol), Y1 receptor agonist (1 nmol), Y2 receptor agonist (1 nmol), or Veh were given ICV and, then trunk blood was collected at study termination (120 min post injection). Of note, each receptor subtype agonist was tested in a separate cohort of animals, and each cohort was matched to its own Veh control group. NPY increased plasma TGs by ~200% (NPY vs. Veh, $p<0.001$, *n*=6-13/group; Fig. 3.4A). Similarly, the Y1 receptor agonist recapitulated the NPY effect by doubling plasma TG levels (Y1 receptor agonist vs. Veh, $p<0.001$, *n*=6-13/group; Fig. 3.4A), whereas the Y2 receptor agonist had no effect on plasma TGs in the absence of tyloxapol (Y2 receptor agonist vs. Veh, p=*ns*, *n*=6-13/group; Fig. 3.4A). Pooled plasma samples were sized-fractionated by FPLC and TG content was quantified in each column fraction. NPY treatment increased TG content in column fractions (10-20) that corresponded in size to that of VLDL (Fig 3.4B); consistent with our previous findings (211). Similarly, the Y1 receptor agonist increased TG content in these fractions (Fig. 3.4B), whereas the Y2 receptor agonist had little effect (Fig. 3.4B). Neither treatment with NPY nor the agonists for Y1 or Y2 receptor subtypes altered total plasma cholesterol levels (data not shown).

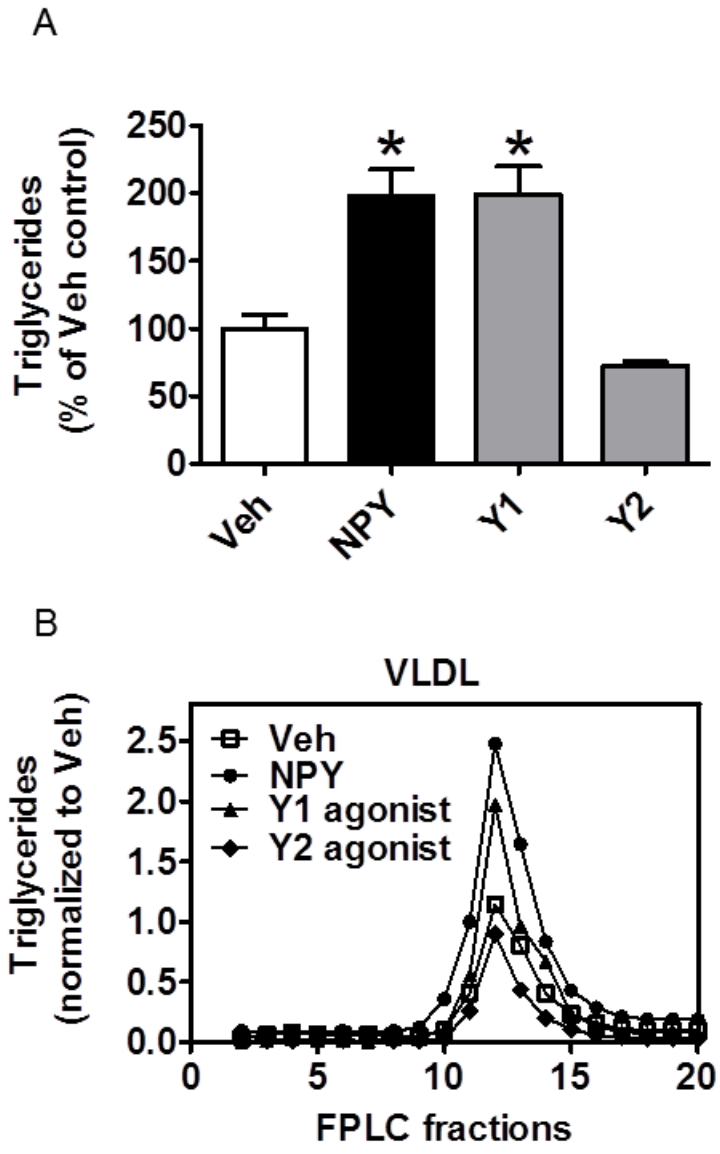

Figure 3.4. Effects of CNS NPY receptor subtypes, Y1 and Y2, on hepatic VLDL-TG secretion. A and B: NPY (1 nmol), Veh or receptor agonists for either Y1 ([F7, P34]-NPY, 1 nmol) or Y2 (hPYY 3-36, 1 nmol) were given ICV in the absence of tyloxapol to 4-hour fasted, lean rats (*n*=6-13/group), and trunk blood was collected at 120 min post injection. Each receptor subtype agonist was tested in a separate cohort of animals, and each cohort was matched to its own Veh control group, so plasma TG levels of each treatment group were normalized to their matched Veh controls. A: Plasma TG levels of each treatment group (% of Veh control) are shown. Data are presented as mean ± SEM and statistical significance ($p<0.05$), as determined by one-way ANOVA with Bonferroni's post-test analysis, is indicated by a *for all comparisons relative to Veh. B: The TG content of FPLC fractions after size fractionation of pooled plasma samples is illustrated. Column fractions 10-20, the size range corresponding to VLDL, are illustrated to allow comparisons between the different ICV treatment groups: Veh (clear squares), NPY (black circles), Y1 receptor agonist (black triangles), and Y2 receptor agonist (black diamonds).

Increased CNS NPY Y1 or Y2 receptor signaling did not alter markers of adipocyte lipolysis or glucoregulatory hormones

Current models suggest that increased adipocyte lipolysis during states of fasting or insulin resistance leads to increased substrate (FFA and glycerol) delivery to the liver for greater VLDL-TG secretion (23, 24, 315). Thus, we sought to determine whether CNS NPY signaling via the Y1 or Y2 receptor increases lipolysis. Extending our previous findings (211), as well as those of others (192), ICV NPY did not activate markers of lipolysis, FFA and glycerol, nor did ICV Y1 or Y2 receptor agonists (p=*ns*; Table 3.2).

ICV infusion of NPY influences glucose metabolism and sensitivity to insulin in fasted rats (189-192); therefore, we determined whether CNS NPY signaling via either the Y1 or Y2 receptor alters glucoregulatory hormones. The Y2 receptor agonist increased plasma glucose levels by 13% (p<0.05; Table 3.2); whereas neither NPY nor Y1 receptor agonist had any effect on glucose concentration (p=*ns*; Table 3.2). ICV administered NPY, Y1 and Y2 receptor agonists did not alter plasma insulin and glucagon levels (p=*ns*; Table 3.2).

Table 3.2. Effects of CNS NPY and agonists for Y1 and Y2 receptor subtypes at 120 min post ICV injection on glucoregulatory hormones and metabolites

	NPY		**Y1 agonist**		**Y2 agonist**	
	Veh	**NPY**	**Veh**	**Y1**	**Veh**	**Y2**
FFA (mmol/l)	0.33±0.03	0.39±0.05	0.26±0.04	0.25±0.02	0.30±0.04	0.37±0.02
Glycerol (mg/dl)	10.0±0.8	11.4±0.3	14.9±2.2	16.9±1.4	10.2±2.2	6.2±1.2
Insulin (ng/ml)	1.1±0.2	1.5±0.3	2.6±0.4	3.8±0.9	3.7±0.3	3.8±0.2
Glucagon (pg/ml)	79±7	76±4	77±10	76±6	76±11	86±12
Blood glucose (mg/dl)	137±5	145±6	150±5	159±6	135±4	152±4*

Data are presented as mean ± SEM (*n*=6-7/group) and were analyzed by Student's *t*-test (unpaired, two-tailed); *p<0.05 for ICV treatment vs. vehicle (Veh) comparisons.

CNS NPY signaling via the Y1 receptor modulates liver stearoyl-CoA desaturase-1 mRNA levels

Hypothalamic signaling via several hormones (especially leptin) and metabolites regulates hepatic stearoyl-CoA desaturase-1 gene expression (203, 215, 216, 316, 317); thus, liver expression of SCD-1 is a robust marker of known hypothalamic-liver regulatory pathways. First, we investigated whether increased CNS NPY signaling via the Y1 receptor modulated relevant liver regulatory targets. Lean, 4-hour fasted rats were given either ICV NPY (1 nmol), the Y1 receptor agonist (1 nmol), or Veh, and at either 60 or 120 min post injection, trunk blood and liver samples were collected. Of note, NPY and the Y1 receptor agonist were tested in a separate cohort of animals, and each cohort was matched to its own Veh control group. Similar to our findings at 120 min post ICV injection (Fig. 3.4A), we found at 60 min post ICV injection that treatment with either NPY or the Y1 receptor agonist doubles plasma TG levels with respect to Veh (NPY 256±60% vs. Veh 100±11%, $p<0.01$; Y1 receptor agonist 171±21% vs. Veh, $p<0.01$, n=5-11/group). We then quantified expression levels of key lipid metabolic markers involved in VLDL assembly and secretion. At both 60 and 120 min, neither NPY nor the Y1 receptor agonist altered levels of phosphorylated-acetyl-CoA carboxylase (ACC; Ser79), ACC, FAS, hepatic apoB-48 or MTP ($p=ns$, n=5-7/group; Fig. 3.5A and B) consistent with our previous findings (211). CNS NPY did induce SCD-1 mRNA levels relative to Veh by 4-fold ($p<0.05$, n=5/group; Fig. 3.5C), while the Y1 receptor agonist increased SCD-1 mRNA levels by 5-fold ($p<0.01$, n=5-6/group; Fig. 3.5D). Thus, signaling via the Y1 receptor recapitulates CNS NPY regulation of hepatic *SCD* gene expression, which is a known marker of hypothalamic-hepatic metabolic regulation, and whose gene product is involved in lipid metabolism.

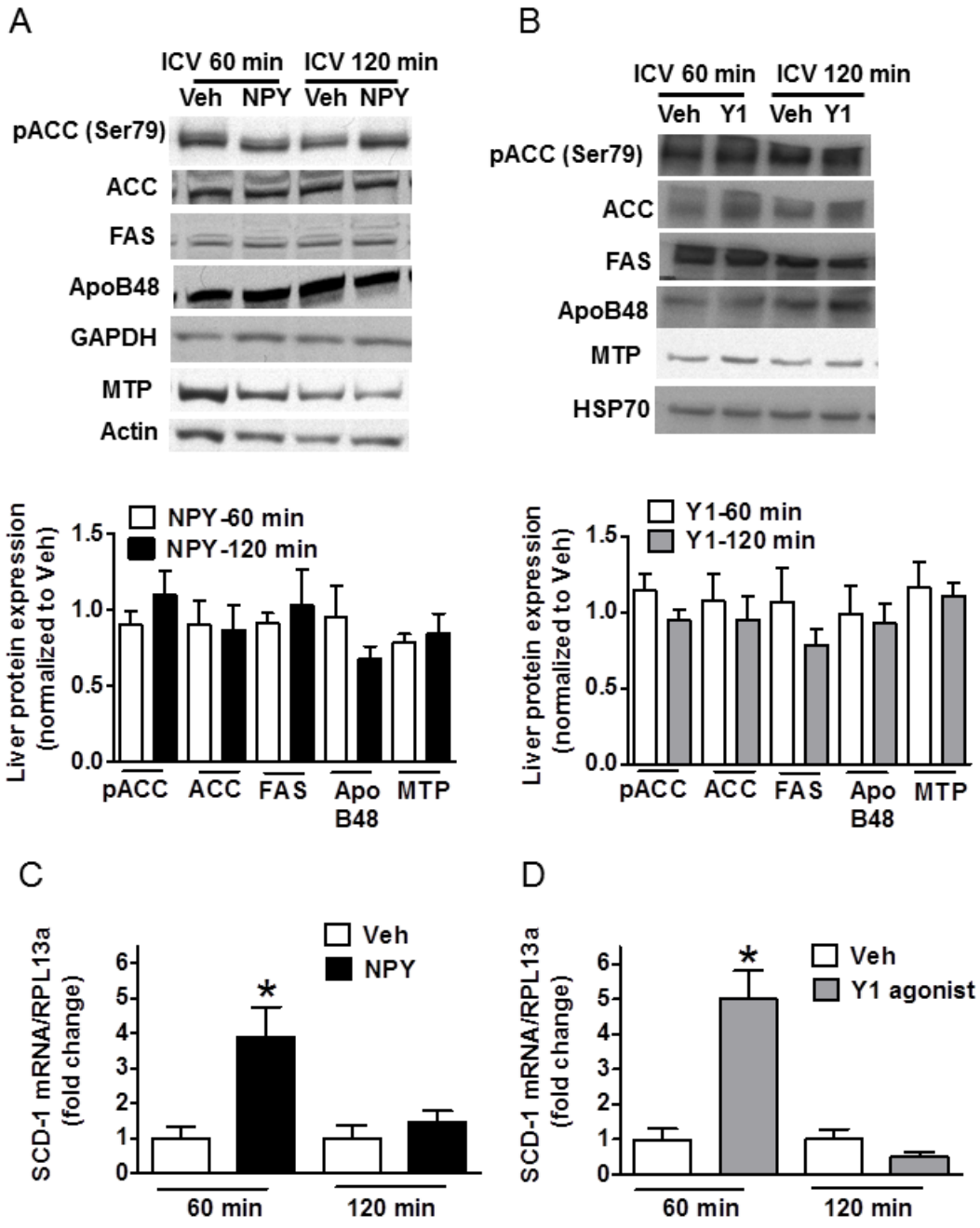

Figure 3.5. CNS NPY signaling via the Y1 receptor induces hepatic SCD-1 mRNA expression. A and B: Representative immunoblots of key lipid metabolic markers involved in VLDL assembly and secretion are shown. Protein extracts prepared from livers of 4-hour fasted lean rats (*n*=5-7/group) isolated 60 or 120 min after ICV injection of (A) NPY (1 nmol) or Veh, or (B) Y1 receptor agonist ([F7, P34]-NPY, 1 nmol) or Veh, were immunoblotted to detect levels of phosphorylated-ACC (Ser79), ACC, FAS, apoB-48, and MTP. Western blots were analyzed by densitometry (normalized to Veh control) for (A) ICV NPY treatment at 60 (white bars) and 120 min (black bars) post injection and (B) ICV Y1 receptor agonist treatment at 60 (white bars) and 120 min (gray bars) post injection. Densitometry results were corrected relative to those of the

protein loading control glyceraldehyde 3-phosphate dehydrogenase (GAPDH), actin, or heat shock protein 70 (HSP70). C and D: RNA were isolated from livers of 4-hour fasted rats that were obtained 60 or120 min after treatment with (C) ICV NPY (black bars) or Veh (white bars), or (D) ICV Y1 receptor agonist (gray bars) or Veh (white bars), and were assessed by quantitative RT-PCR for changes in SCD-1 mRNA levels. SCD-1 mRNA levels, normalized to the reference RNA RPL13a, are shown. For comparative analysis, RNA ratios were normalized to the Veh control. Data are presented as mean ± SEM and were analyzed by Student's *t*-test (unpaired, two-tailed); *indicates a significant difference ($p<0.05$) between ICV treatment and Veh.

Discussion

Atherogenic dyslipidemia characterized in part by elevated plasma TG levels is the major lipid abnormality associated with obesity, diabetes, and the metabolic syndrome (14-16). *While peripheral factors (visceral adiposity and insulin resistance) clearly contribute to this disorder (23, 24), we hypothesized that increased CNS NPY action contributes both to the pathogenesis of obesity and obesity dyslipidemia.* We sought to determine if the effects of NPY on feeding and/or weight gain are dissociable from the effects on hepatic VLDL-TG secretion. We employed two approaches: first, asking whether NPY retains the effect on hepatic VLDL-TG secretion chronically in the absence of increased food intake and weight gain; and second, whether different NPY receptors mediate effects on feeding versus hepatic VLDL-TG secretion. We found that chronic (3 days) ICV injections of NPY in animals pair-fed to Veh-treated controls in order to maintain identical body composition also led to hypertriglyceridemia, which suggests that hyperphagia and accumulation of excess adiposity are not required for this effect. Moreover, using selective NPY receptor agonists, we demonstrate, within the limits of our model, that central NPY signaling via the Y1 receptor predominantly regulates effects on hepatic lipoprotein production. The Y2 receptor agonist modestly stimulated VLDL-TG production albeit at a dose that had a profound effect on feeding. Neither the Y4 nor the Y5 agonist had an effect on plasma TGs. Conversely, all agonists stimulated feeding, with the NPY Y2 receptor agonist having a more robust effect on feeding than TG production. In contrast, at the same dose used for the NPY Y2 receptor agonist, the NPY Y1 receptor agonist had a greater effect on TG production than feeding. Thus, we postulate that NPY regulates feeding and lipoprotein metabolism partially via separate NPY receptor systems and/or mechanisms.

While our study, and others (124, 318), reveal that central administration of the NPY Y2 receptor agonist, PYY 3-36, stimulates feeding under some conditions, Batterham et al. (123) reported that this Y2 receptor agonist has an inhibitory effect on food intake when administered by direct intra-arcuate injection or via peripheral administration. Because the inhibitory Y2

receptor is found on both the ARC NPY and POMC neurons this adds an additional layer of complexity to the regulation of the NPY/POMC neural circuit by Y2 agonists. Both endogenous and exogenous Y2 agonist action in the ARC is context dependent as elegantly described in Ghamari-Langroudi et al. (116). An additional consideration is that ICV administration of the Y2 agonist may result in its dispersion to other hypothalamic and non-hypothalamic regions. Finally, the potential activation of the Y5 receptor by PYY 3-36 could also explain the increase in food intake.

A strength of our study was that we matched test compounds for potency on feeding behavior (similar to a 12-hour fast), with the exception of the Y2 receptor agonist. A weakness is that we utilized only a single dosage of each test compound. It is conceivable that, at significantly higher or lower doses, opposite and/or differential effects on feeding relative to VLDL-TG secretion may have been observed. Indeed a "U-shaped" curve, as well as exquisite dose-dependency of the effects of several neuropeptides has been noted (319, 320). Thus, this study does not reveal whether dose-response effects of NPY Y1 receptor signaling on feeding resemble or differ from those on VLDL-TG secretion.

We previously reported that the NPY Y5 receptor agonist, BWX-46, increased VLDL-TG secretion in lean fasted rats (211), a finding not replicated here using [Ala^{31}, Aib^{32}]-NPY (Fig. 3.3D and E). However, the NPY Y5 receptor agonist [Ala^{31}, Aib^{32}]-NPY (2 nmol ICV) employed in our current study has greater than 77-fold selectivity for the Y5 than for the Y1 receptor (105, 109), whereas BWX-46 (12 nmol ICV) employed in our previous study has less Y5 selectively and greater cross reactivity with the Y1 receptor (321). Thus, at the dose used in our previous study (211), it appears likely that BWX-46 activated both the NPY Y1 and Y5 receptor resulting in the observed increase in VLDL-TG production.

Elevated hypothalamic NPY tone with a concomitant reduction of POMC tone is associated with obesity and diabetes in rodent models (139, 140) and humans (98, 143, 144), likely due to defects in inhibitory feedback signals to the CNS i.e. insulin and leptin resistance

(74, 75). Because we show that Y1 receptor activation has a greater effect than activation of the Y2 receptor on lipoprotein metabolism, it informs of potential structure-function relationships of the NPY-regulated neural circuitry involved. There is reportedly a close physical localization and apparent functional relationship between NPY Y1 and Y2 receptors in neurons found within the ARC, the LHA, the DMN, and the PVN, whereas the VMN contains only Y1 receptor positive neurons (114). Furthermore, a study by Chee et al. (110) reports that NPY inhibits the excitatory (anorexigenic) outflow between the VMN and ARC POMC neural circuitry via the activation of the Y1 receptor subtype in the VMN. Moreover, studies in VMN-lesioned rats, which recapitulates a state of elevated NPY tone, have elevated plasma TGs (212), even as early as 10 days postoperatively, together with decreased plasma FFA and glucose levels (213). Finally, perfused livers from VMN-lesioned rats secrete more TGs than controls (213). Altogether, these data suggest that the VMN is a potential hypothalamic site in which NPY may regulate lipoprotein metabolism via selective activation of the Y1 receptor. Of course, our initial studies reported here, employing ICV injections cannot localize the effect. Future studies, thus will involve selective inhibition of the Y1 receptor in PVN compared to VMN with microinjection techniques in an obese, hypertriglyceridemic rodent model characterized by elevated NPY tone (i.e. *fa/fa* Zucker fatty rat). Collectively, these findings may lend plausibility that the brain is a potential therapeutic target to treat obesity dyslipidemia.

Our finding that the NPY Y1 receptor is most robustly coupled to lipoprotein metabolism is consistent with the conclusions from a genetic association study in severely obese human subjects matched for body mass index, in which those individuals with the CC haplotype (relative to the TT/CT polymorphism) of the un-translated region of the *NPY1R* gene had elevated fasting serum TGs and significantly lower HDL-C concentrations (221). It is not yet clear if this haplotype correlates with a relative gain of NPY Y1 receptor function, but we would hypothesize in the context of our findings that the CC haplotype is a relatively hyperfunctional allele and thus, would confer increased TGs in the setting of obesity.

Several studies have investigated the effect of global deletion of the NPY Y1, Y2, Y4, and Y5 receptors on the background of the *ob/ob* mouse, which is a leptin deficient, obese rodent model characterized by elevated CNS NPY tone and severe hypertriglyceridemia. Unfortunately, these studies only report on the effect of this genetic manipulation on energy homeostasis and not on whether deletion of the various NPY receptors attenuate hypertriglyceridemia, except for the Y2 receptor which was noted to have no effect (167, 170, 176, 177). Because all of the NPY receptor subtypes are expressed both centrally and peripherally (except for the brain specific Y5 receptor) (105), it would be interesting to determine whether brain specific deletion of the Y1 receptor in the obese *ob/ob* mouse would attenuate hypertriglyceridemia.

Current models suggest that increased adipocyte lipolysis during states of fasting or insulin resistance leads to increased substrate (FFA and glycerol) delivery to liver, which can increase hepatic VLDL-TG secretion (23, 24). The observation that increased NPY signaling via the Y1 receptor doubled VLDL-TGs, while plasma FFA and glycerol levels were unchanged, suggests that adipocyte lipolysis was not increased, and thus would not account for the NPY stimulated increase in hepatic VLDL-TG production. Moreover, we observed this same effect in rats given chronic NPY treatments under pair-fed conditions leading to the doubling of VLDL-TG secretion independent of changes in adipocyte lipolysis. Although CNS Y2 receptor signaling did not alter markers of adipocyte lipolysis, the Y2 receptor agonist surprisingly had no effect on plasma TGs in the absence of tyloxapol (Fig. 3.4A and B). Given that the Y2 receptor agonist did increase VLDL-TG secretion modestly in the presence of tyloxapol (Fig. 3.3C and E), suggests that Y2 receptor activation may also have an effect to enhance TG clearance perhaps through the modulation of adipose tissue LPL activity (322).

SCD-1 catalyzes the desaturation of palmitic and stearic acids to palmitoleic and oleic acids and its expression is known to be regulated by CNS leptin (316, 317), glucose (215) and melanocortin action (203) in the same hypothalamic feeding circuits engaged by NPY. Whereas leptin suppresses SCD-1 (and NPY tone (136)), we have observed a robust induction of hepatic

SCD-1 expression in response to CNS NPY treatment. This effect is recapitulated by Y1 receptor activation, providing further evidence that NPY signaling via the Y1 receptor is mechanistically involved in hepatic lipid metabolism.

Provision of oleic acid or modulation of SCD-1 activity changes VLDL production rate by increasing triglyceride loading in the late maturation phase (215, 316). Presently, we demonstrate that the elevation in hepatic VLDL-TG secretion by increased CNS NPY signaling via the Y1 receptor is associated with a rapid (within 60 min) induction of hepatic *SCD* gene expression, which would suggest that SCD-1 activation may contribute to changes in VLDL-TG secretion. This is supported by previous findings in which hypothalamic glucose (215) and glycine (216) metabolism reduced hepatic SCD-1 mRNA and inhibited hepatic VLDL-TG secretion. Although the definitive mechanistic link between hepatic SCD-1 and the alteration of VLDL-TG secretion by CNS NPY signaling remains to be determined, changes in the formation rate of hepatic oleic acid may be an important mediator (215).

Our results show that neither the NPY nor the Y1 agonist influenced the level of key *de novo* lipogenic enzymes, phospho-ACC (Ser79), ACC and FAS. Hepatic apoB is an essential component of liver-derived VLDL, if lipid is not loaded by MTP, apoB becomes a target for proteasomal degradation (230). In contrast to humans, the rat produces predominately apoB-48 instead of apoB-100 in the liver (227). Our results show that there were no significant changes in hepatic tissue levels of apoB-48 detectable by Western blot from increased CNS NPY and Y1 receptor signaling (Fig. 3.5A and B), although this method is not as sensitive as radiolabeling methods. Similarly, we found that MTP, which plays a pivotal role in VLDL maturation and secretion of triglyceride-rich lipoproteins (230, 323), was unaltered by NPY and Y1 receptor agonist treatment (Fig. 3.5A and B). Collectively, these data suggest that CNS NPY acts primarily via the Y1 receptor to increase plasma TGs and likely does so by altering the late maturation step of VLDL assembly and secretion.

In conclusion, we demonstrate, within the limits of our model, that the effects of NPY on feeding and/or weight gain are relatively dissociable from the effects on hepatic VLDL-TG secretion. Three days of twice daily ICV NPY injections, in animals pair-fed to Veh-treated controls to maintain identical caloric intake and body composition, led to hypertriglyceridemia. CNS NPY signaling via the Y1 receptor predominantly regulates effects on hepatic lipoprotein production, whereas the activation of the Y2 receptor has a greater effect on feeding. Altogether, these findings raise the possibility that NPY regulates feeding and lipoprotein metabolism partially via separate NPY receptor systems and/or mechanisms.

CHAPTER IV

CENTRAL NERVOUS SYSTEM NEUROPEPTIDE Y PROMOTES HEPATIC LIPIN-1 MEDIATED PHOSPHOLIPID REMODELING ELEVATING VLDL-TRIGLYCERIDE SECRETION

Manuscript in preparation

Introduction

Concomitant with the parallel obesity and diabetes epidemics (9), an increasing healthcare burden is due to the complications of hyperlipidemia such as CVD, cerebrovascular disease, and peripheral vascular disease. Elevated VLDL-TG production from liver contributes to atherogenic dyslipidemia consisting of small-dense LDL-C and reduced HDL-C levels (14-16) associated with obesity and diabetes. Hypertriglyceridemia is a key component of the metabolic syndrome (14-16), which is an increasingly recognized component of cardiovascular risk, morbidity and mortality (16).

A current model of dyslipidemia associated with obesity and diabetes suggests that increased visceral fat and relative insulin resistance in adipose leads to increased substrate (FFA) delivery to the liver concomitant with hepatic insulin resistance, leading to increased production of VLDL-TG (23, 24). *While peripheral factors clearly contribute to this disorder (23, 24), we hypothesized that regulation of lipid homeostasis is normally subject to CNS regulatory forces.* CNS NPY expressing neurons, concentrated in the mediobasal hypothalamus as well as numerous other brain regions, are an important regulator of feeding and energy homeostasis, and increasingly recognized as having a role in lipid homeostasis (211, 222).

Elevated hypothalamic NPY tone with a concomitant reduction of POMC tone is associated with obesity and diabetes in rodent models (139, 140) and humans (98, 143, 144). This

is thought to result from defects in inhibitory feedback signaling to the CNS, including neuronal insulin and leptin resistance, and impaired nutrient sensing, leading to impaired ability of these neuronal subsets to sense energy excess (74, 75). *We hypothesized that increases in NPY tone within these neural circuits may contribute to dyslipidemia independent of positive energy balance and increased visceral adiposity.* In Chapter III, we demonstrated that ICV NPY administration directly to the third ventricle of the brain can double hepatic VLDL-TG secretion in lean fasted rats (211, 222), and does so, in large part, via the CNS NPY Y1 receptor (222). Moreover, as shown in Chapter III, NPY rapidly increases VLDL-TG secretion from liver while plasma FFA and glycerol levels were unchanged, suggesting that adipocyte lipolysis was not increased, and thus would not account for the NPY-induced hypertriglyceridemia (211, 222). *We, therefore, hypothesized that key regulatory steps involved in liver lipid metabolism might be robustly regulated by increased CNS NPY signaling.*

VLDL is the chief carrier of TG in the postprandial state (236). The assembly and secretion of TG-rich VLDL represents a key component of hepatic TG homeostasis, which is a tightly regulated and complex two-step process (reviewed in (228)). In the first step, a small quantity of TG is assembled onto the structural protein, apoB-100 during its co-translational translocation through the rough ER lumen and this process is catalyzed by MTP to form an HDL-sized VLDL precursor lipoprotein (228). If lipid is not loaded by MTP, apoB becomes a target for proteasomal degradation (230).

The second step, which is less well-characterized, involves the fusion of a larger droplet of TG with the apoB-containing VLDL precursor to form the mature VLDL particle before exiting from the ER (228, 231). This process can be blocked by integrated hepatic insulin action leading to enhanced degradation of apoB and suppression of VLDL secretion (29, 30). VLDL maturation is dependent on the key regulatory enzymes ARF-1 and PLD (233), which can be effectively blocked by Brefeldin A (235).

Evidence suggest that TG utilized for VLDL assembly and secretion can originate from sources other than that arising from hepatic fatty acid synthesized *de novo* and from extracellular FFAs (224). It has been reported that up to 70% of secreted VLDL-TG by liver is attributable to the hydrolysis and re-esterification of pre-existing PL and cytosolic TG (224). Clearly, some of the TG which ends up as VLDL is derived from a pool of intracellular PL, a novel source of lipid given the current assumption that intracellular membrane PL merely plays a structural role in VLDL assembly (224).

Key regulatory enzymes involved in the transfer of PL fatty acids into TG, otherwise known as PL remodeling, involve PLD which is activated by ARF-1 leading to the production of PA from the phospholipid, PC. PA is then dephosphorylated by the key rate-limiting enzyme, PAP-1 producing the TG precursor, DAG. The resulting DAG serves as a substrate for the synthesis of TG and PLs, PC and PE that is required for lipidation of the nascent VLDL particle resulting in maturation and secretion as TG-rich VLDL particles by the liver (238).

Mammalian PAP-1 is encoded by the *Lpin* gene family consisting of *Lpin1*, *Lpin2*, and *Lpin*3. All lipin isoforms contain PAP-1 activity and are expressed in the liver (reviewed in (324)). The subcellular localization and compartmentalization of lipin-1 determines its dual molecular function as either a glycerolipid biosynthetic enzyme or a transcriptional co-activator (reviewed in (249)). Insulin stimulates the phosphorylation of lipin-1 at Ser106 which is dependent on PI3K activity and mTOR pathway (250) sequestering it into the cytosol, which affects its intrinsic PAP-1 activity (251). Dephosphorylation of lipin-1 occurs in response to fatty acids (i.e. oleic acid) leading to its translocation from the cytosol to the ER membrane where it performs its PAP-1 activity (252), generating the lipid substrates (TG, PC, and PE) required for VLDL assembly and secretion (238, 253). Conversely, lipin-1 in the nucleus acts as a transcriptional co-activator with PGC-1α and PPARα leading to the induction of genes involved in fatty acid oxidation, including *CPT1A* (248, 254).

Only lipin-1 but not lipin-2 or -3 expression and activity is upregulated by GCs (259), which act through the GR bound to functional GRE upstream of the *Lpin1* promoter region (260), an effect that is synergized by glucagon through cAMP formation and antagonized by insulin in mouse and rat hepatocytes (259). Thus, it is hypothesized that under conditions that lead to elevated activity of the HPA axis such as stress, starvation, and diabetes, resulting in an increase in circulating GC, the subsequent GC induced increase in lipin-1 activity augments the capacity for the liver to sequester excess FFA as TG for VLDL secretion when FFAs are not immediately required for β-oxidation (238, 259).

The activity of the HPA axis is reportedly increased in obesity and diabetes in humans (193-196) and in rodent models of genetic obesity (177, 197), DIO (198), and STZ-induced diabetes (199). These rodent models of obesity and diabetes are characterized by high NPY mRNA and peptide levels in the hypothalamus, secondary to the absence of negative feed-back regulation by insulin and leptin (134-137, 139, 140). Chronic ICV NPY infusion has been shown to activate the HPA axis in normal animals leading to elevated circulating GC, corticosterone (200, 201). Therefore, some of the hormonal and metabolic effects of chronic CNS NPY signaling in normal rats depends on circulating corticosterone, since adrenalectomy prevented these NPY-induced effects, including hyperphagia, obesity, hyperinsulinemia, and hypertriglyceridemia (201).

The hepatic-specific molecular mechanisms by which increased CNS NPY signaling rapidly regulates hepatic lipoprotein metabolism are not well understood. Nor is the lipid source that generates the TG that is loaded onto the nascent VLDL particle in response to increased CNS NPY action currently known. We, therefore, sought to identify the novel regulatory mechanisms in the liver engaged by NPY. Our study employed two approaches: first, we determined whether liver PL is a novel source of lipid for hepatic VLDL-TG secretion in the *fa/fa* ZF rat, a rodent model characterized by elevated NPY tone and dyslipidemia, independently of hyperphagia and obesity; secondly, we determined whether CNS NPY signaling via the Y1 receptor elevates

hepatic VLDL-TG secretion by modulating key regulatory enzymes involved in liver PL remodeling in lean fasted, metabolically normal rats and whether this is a GC dependent effect. We ultimately sought to elucidate the novel regulatory mechanisms in the liver in response to increased CNS NPY action that leads to the modulation of hepatic lipoprotein metabolism in the absence of increased visceral adiposity as this might yield novel insight and therapeutic implications for the dyslipidemia associated with obesity, diabetes, and the metabolic syndrome.

Results

Liver PL as a novel source of lipid for hepatic VLDL-TG secretion in the *fa/fa* Zucker fatty rat

The leptin resistant *fa/fa* ZF rat is a genetic model of obesity and is characterized by high NPY tone and dyslipidemia (65, 66, 134, 135). To control for hyperphagia and positive energy balance in *ad-libitum* chow-fed ZF rats, the food intake of the PF ZF rats were carefully matched to the caloric intake of the control lean Zucker rats (*fa/-*). *Ad-libitum* fed ZF rats rapidly developed obesity (Fig. 4.1A) whereas pair-feeding successfully matched the body weight of the ZF rats to that of control animals (Fig. 4.1A). At the end of the study (day 38), *ad-libitum* fed ZF rats developed severe hypertriglyceridemia and hypercholesterolemia (Fig. 4.1B and C). Intriguingly, pair-feeding normalized the plasma TG and not the cholesterol levels in the ZF rats to that of control levels (Fig. 4.1B and C). Although pair-feeding altered plasma TG concentrations in the ZF rat (Fig. 4.1B), it had no effect on liver TG content (Fig. 4.1D) whereas liver PL content was completely normalized to control levels (Fig. 4.1E). Remarkably, PL ($r=0.9$; $p<0.0001$; Fig. 4.1F) and not TG ($r=0.4$; p=ns; Fig. 4.1G) content in liver tightly correlated with plasma TG levels. These data collectively suggest that in a rodent model characterized by elevated NPY tone, liver PL stores may provide a novel source of lipid for hepatic VLDL-TG secretion.

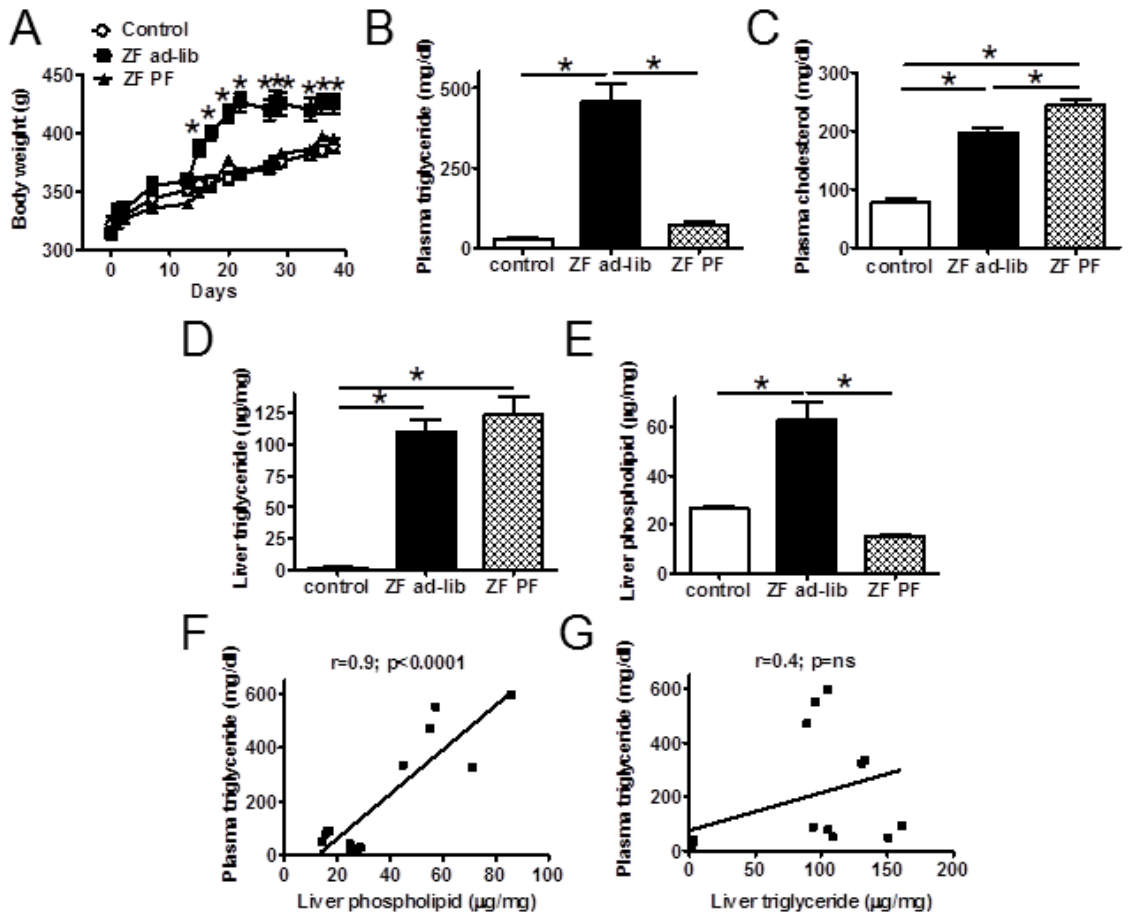

Figure 4.1. Liver PL as a novel source of lipid for hepatic VLDL-TG secretion in the *fa/fa* Zucker fatty rat. A: The food intake of the pair-fed (PF) chow-fed *fa/fa* Zucker fatty (ZF) rats (black triangles) was calorically matched to that of the lean ZF (*fa/-*) controls (white circles) and the effect on daily body weight (BW; *n*=5/group) are illustrated in comparison to the *ad-libitum* (ad-lib) fed ZF rats (black squares). Data are presented as mean ± SEM and were analyzed by two-way repeated measures ANOVA with Bonferroni's post-test analysis; *p<0.05 for control vs. ZF ad-lib comparisons. The main effect of genotype to increase BW over time was dependent on the treatment [BW: (F (2,12) =12.09, p=0.0013]. B-E: Plasma and livers were collected from 4-hour fasted ad-lib fed ZF (black bars), PF ZF (hatched bars), and lean control (white bars) rats to measure plasma triglyceride (TG; B) and cholesterol (C) as well as liver TG (D) and phospholipid (PL; E). Data are presented as mean ± SEM and were analyzed by one-way ANOVA with Bonferroni's post-test analysis; *p<0.05 for all comparisons. F. Correlational analysis of plasma TG versus liver PL levels in all groups. G. Correlational analysis of plasma TG versus liver TG levels in all groups.

TG loaded onto VLDL in response to CNS NPY signaling may be generated from liver FFA and/or intrahepatic PL and not TG stores in lean fasted rats

In Chapter III, we demonstrated that ICV administration of NPY or an NPY Y1 receptor agonist into the third ventricle of lean rats rapidly increases hepatic VLDL-TG secretion independent of feeding (211, 222). We found that NPY and the Y1 receptor agonist did not activate the markers of adipocyte lipolysis, in the form of FFA and glycerol to increase VLDL-TG production at 60 min post injection (Table 4.1), which is in corroboration with our findings at 120 min post injection (as shown in Chapter III (222)). *Thus, we sought to test the hypothesis that TG loaded onto VLDL particle in response to CNS NPY signaling is generated from intrahepatic PL and not TG stores.*

Table 4.1. Effects of the CNS NPY and agonist for Y1 receptor subtype at 60 min post ICV injection on glucoregulatory hormones and metabolites

	NPY		**Y1 agonist**	
	Veh	**NPY**	**Veh**	**Y1**
FFA (mmol/l)	0.32±0.03	0.32±0.03	0.27±0.05	0.21±0.05
Glycerol (mg/dl)	12.5±1.22	15.5±1.12	17.3±3.44	24.5±1.50
Insulin (ng/ml)	0.80±0.2	1.18±0.2	2.99±0.5	5.45±0.4*
Glucagon (pg/ml)	101±13	120±13	100±10	108±5.3
Blood glucose (mg/dl)	127±6.0	130±9.2	153±2.6	152±4.0

Data are presented as mean ± SEM (n=6-7/group) and were analyzed by Student's t-test (unpaired, two-tailed); *P<0.01 for the ICV treatment vs. vehicle (Veh) comparison.

We investigated the impact of ICV injection of NPY and the Y1 agonist on hepatic lipoprotein metabolism at an early (60 min) versus latter (120 min) time point. In this study, lean 4-hour fasted rats were given either ICV NPY (1 nmol), the Y1 receptor agonist ([F7, P34]-NPY; 1 nmol), or saline vehicle (Veh), and at either 60 or 120 min post injection, trunk blood and liver samples were collected at study termination. Of note, NPY and the Y1 receptor agonist were tested in a separate cohort of animals, and each cohort was matched to its own Veh control group. We found that at 60 min post ICV injection, both NPY and the Y1 receptor agonist increased

plasma TG content by 2-fold (Fig. 4.2A and B) with no change in plasma FFA content (Fig. 4.2A and B). Similarly, at 120 min, ICV NPY agonist increased plasma TG content by 2-fold (Fig. 4.2A). To determine whether changes in plasma TG observed are a result of changes in intrahepatic TG and/or PL stores, we measured hepatic lipid content. We found that at 60 min post injection, ICV NPY induced a small but not statistically significant reduction (24%) of hepatic TG content (Fig. 4.2C) concomitant with elevated hepatic FFA levels (Fig. 4.2C) and no alteration in PL content in liver (Fig. 4.2D). Remarkably, at a longer fasting time of 120 min post injection, liver PL levels dropped by 16% in ICV Veh-treated rats relative to 60 min post injection (Fig. 4.2D). Conversely, ICV NPY treatment at 120 min post injection prevented the fall in liver PL content (Fig. 4.2D) with no alteration in hepatic TG and FFA content (Fig. 4.2C). These findings suggest that the TG source for sustained VLDL-TG secretion by central NPY signaling may be derived either from liver FFA and/or intrahepatic PL and not TG stores.

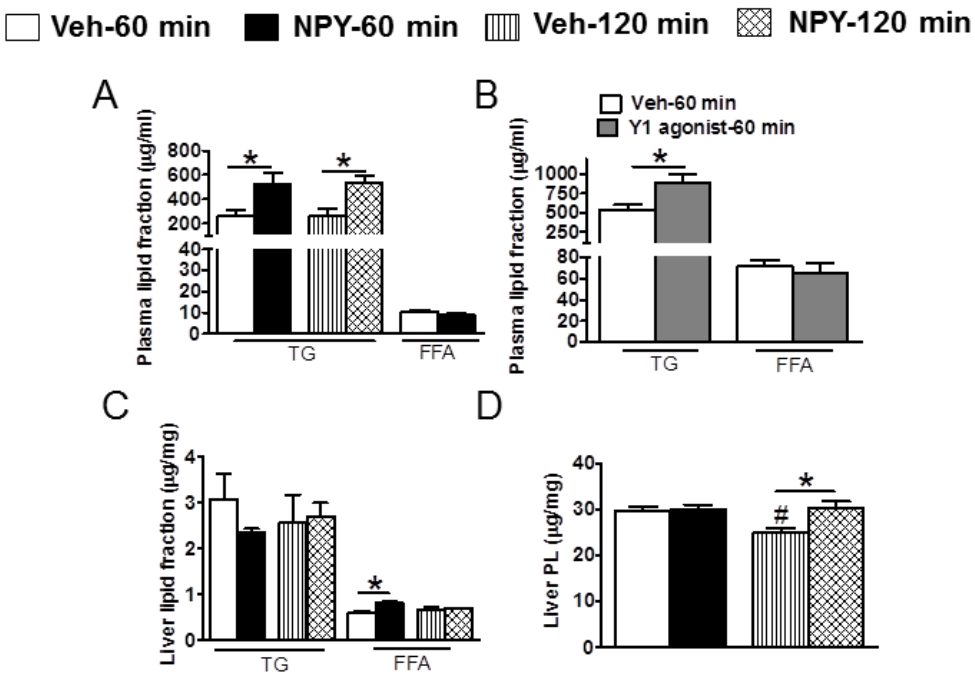

Figure 4.2. TG loaded onto VLDL in response to CNS NPY signaling may be generated from liver FFA and/or intrahepatic PL and not TG stores in lean fasted rats. Lean fasted rats (*n*=5-6/group) were given either ICV NPY (1 nmol; black bars) or the Y1 receptor agonist ([F7, P34]-NPY; 1 nmol; gray bars) or saline vehicle (Veh; white bars) at 60 min post injection. In comparison, lean fasted rats (*n*=5-6/group) were treated with either ICV NPY (hatched bars) or Veh (striped bars) at 120 min post injection. Trunk blood and liver samples were collected at study termination to measure the following: plasma TG and FFA content in ICV NPY- (A) and Y1 agonist- (B) treated rats as well as liver TG, FFA, and PL in ICV NPY-treated rats versus Veh controls (C and D). Data are presented as mean ± SEM and were analyzed by Student's *t*-test (unpaired, two-tailed); *indicates a significant difference ($p<0.05$) between ICV treatment and Veh; #indicates a significant difference ($p<0.05$) between ICV Veh treatment at 60 min versus 120 min.

CNS NPY signaling promotes an increase in oleic and linoleic acid content in liver PL and not TG pool

Because the monounsaturated fatty acid (MUFA), oleate (C18:1w9) derived either from dietary fat or synthesized *de novo* in liver has been shown to markedly regulate the final steps in the assembly of VLDL particles in hepatocytes (215), we next asked whether NPY administered ICV in lean fasted rats rapidly elevates levels of C18:1w9 content in both liver and plasma TG. Surprisingly, we found that ICV NPY increased both C18:1w9 and the dietary-derived

polyunsaturated fatty acid (PUFA), linoleic acid (C18:2w6) content in the liver early on (60 min; Fig. 4.3A). Furthermore, we found that C18:1w9 and C18:2w6 content was increased in liver PL and not TG at both 60 min and 120 min post injection by ICV NPY treatment (Fig. 4.3B and C).

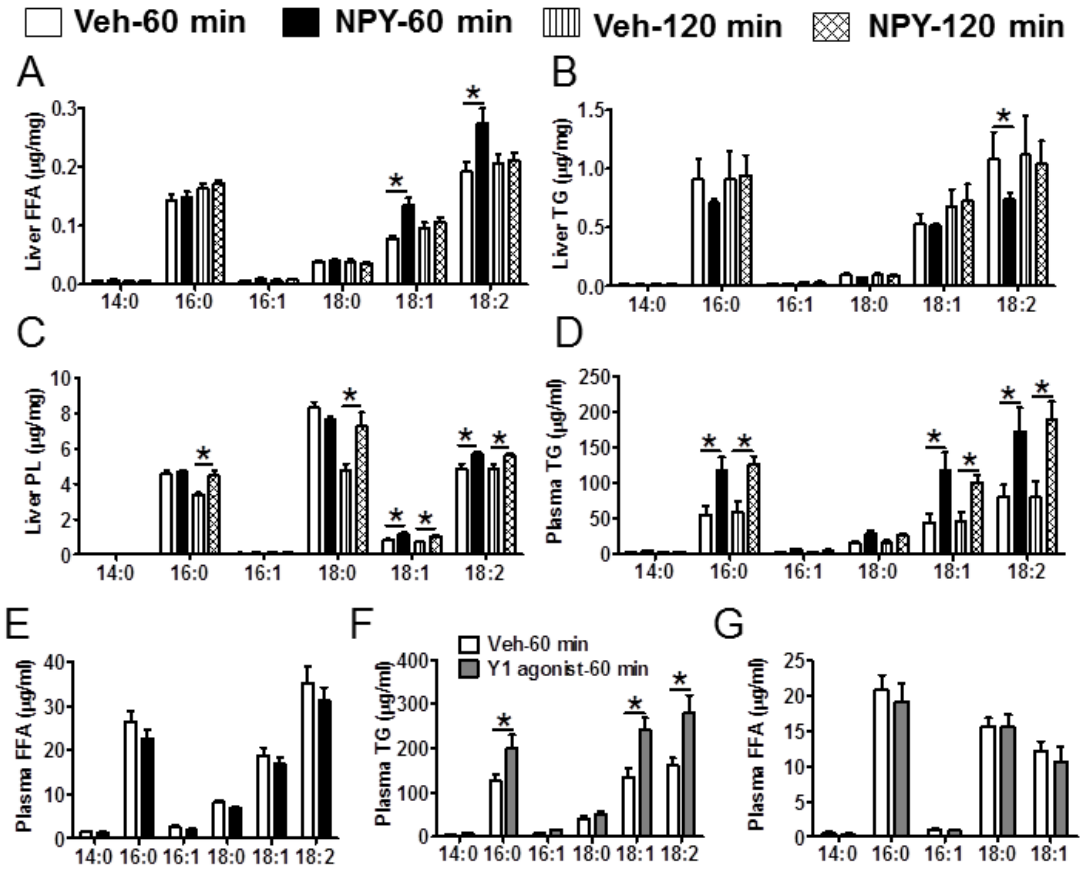

Figure 4.3. CNS NPY signaling promotes an increase in oleic and linoleic acid content in liver PL and not TG pool. Trunk blood and liver samples were collected at study termination in lean fasted rats (*n*=5-6/group) treated with either ICV NPY (1 nmol; black bars) or the Y1 receptor agonist ([F7, P34]-NPY; 1 nmol; gray bars) or vehicle (Veh; white bars) at 60 min post injection and from lean fasted rats (*n*=5-6/group) treated with either ICV NPY (hatched bars) or Veh (striped bars) at 120 min post injection to measure the following: In ICV NPY- vs. Veh-treated rats, liver FFA (A), TG (B), PL (C) in addition to plasma TG (D) and FFA (E); In ICV Y1 agonist- vs. Veh-treated rats, plasma TG (F) and FFA (G). Data are presented as mean ± SEM and were analyzed by Student's *t*-test (unpaired, two-tailed); *indicates a significant difference ($p<0.05$) between ICV treatment and Veh.

Because this data suggest that these unsaturated long chain fatty acids (LCFA) are being utilized for the synthesis of liver PL, which can generate TG for hepatic VLDL secretion, we next

determined whether this leads to a corresponding increase in C18:1w9 and C18:2w6 content in plasma TGs. Indeed, ICV NPY treatment increased C18:1w9 and C18:2w6 content in plasma TGs at both 60 min and 120 min post injection (Fig. 4.3D) and the ICV Y1 agonist recapitulated this effect at 60 min (Fig. 4.3F). Additionally, both NPY and the Y1 agonist treatment increased saturated LCFA, palmitic acid (C16:0) in plasma TG (Fig. 4.3D and F) which appears to be derived from liver PL and not TG (Fig. 4.3B and C). As expected, we observed with ICV NPY and Y1 agonist treatment no changes in FFA composition in plasma FFAs at 60 min post injection (Fig. 4.3E and G) indicating that adipocyte lipolysis is not increased and thus, does not contribute to the observed changes in plasma TGs. Furthermore, we found in the ICV NPY-treated group, that both C18:1w9 and C18:2w6 enriched in liver PL and not the TG and FFA pool correlated positively with plasma TG levels (C18:1w9, PL: r=0.6; p=0.0031; C18:2w6, PL: r=0.4; p=0.045; Fig. 4.4A and B). However, there was no observed correlation for C16:0 either enriched in liver PL, TG, or FFA with plasma TG (Fig. 4.4C). Altogether, this data suggest that increased CNS NPY signaling promotes an accumulation of oleic and linoleic acid early on (60 min) and that these FFAs are being utilized for the synthesis of liver PL and not TG which in turn, may generate the lipid source for NPY-induced hepatic VLDL-TG secretion.

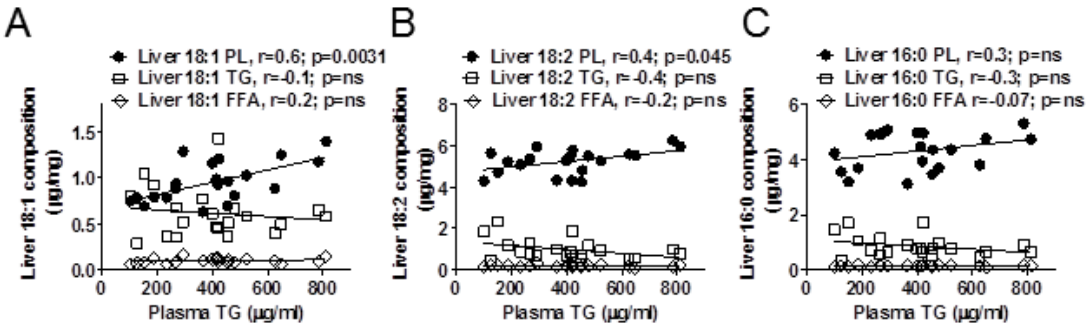

Figure 4.4. Oleic and linoleic enriched liver PL (and not TG and FFA) correlates with plasma TGs. Correlational analysis of liver PL, TG, or FFA enriched with oleic (18:1; A), linoleic (18:2; B), or palmitic acid (16:0; C) versus plasma TG levels in ICV NPY- vs. Veh-treated rats at 60 and 120 min post injection.

Effects of CNS NPY signaling via the Y1 receptor on key enzymes involved in liver lipid metabolism, VLDL-TG assembly and secretion

We next investigated the underlying cause for the accumulation of oleic and linoleic in the livers of lean fasted rats treated with either ICV NPY or Y1 agonist which may be due to impaired liver FFA oxidation, increased hepatic FFA uptake and/or increased hepatic *de novo* synthesis of oleic acid. Consistent with previous studies (127, 192), we found that both ICV NPY and the Y1 receptor agonist reduced the mRNA expression of CPT-1α by 40 to 50% at 60 min post injection (Fig. 4.5A and C). CPT-1α is the key rate limiting mitochondrial transmembrane enzyme that transports LCFAs, such as oleic and linoleic acid into the mitochondria for β-oxidation (325). The mRNA expression of other enzymes involved in oxidative metabolism, PPARα and ACOX1 were unaltered by ICV NPY treatment (Fig. 4.5A). Additionally, ICV NPY treatment did not alter mRNA expression of the key enzymes involved in hepatic uptake of LCFAs and apoB containing lipoproteins, Cluster of Differentiation 36 (CD36) (326) and LDL receptor (LDLR) (327), respectively (Fig. 4.5A).

Next, we examined the effect of ICV NPY and Y1 agonist treatment on the hepatic mRNA expression of enzymes involved in *DNL*, VLDL assembly and secretion at 60 min post injection. Remarkably, we found that ICV NPY significantly induced mRNA expression of the master transcriptional regulator of lipogenesis, SREBP-1c and the mRNA expression of its downstream target genes, ACC-1, FAS, and SCD-1 (328) by 3- to 4-fold (Fig. 4.5B). Conversely, mRNA expression of DGAT-1 and -2, enzymes involved in TG synthesis for cytoplasmic droplet or for VLDL formation (239) remained unchanged (Fig. 4.5B). Surprisingly, ICV Y1 agonist induced only SCD-1 mRNA expression (and not ACC-1 and FAS) independent of SREBP1c expression (Fig. 4.5C).

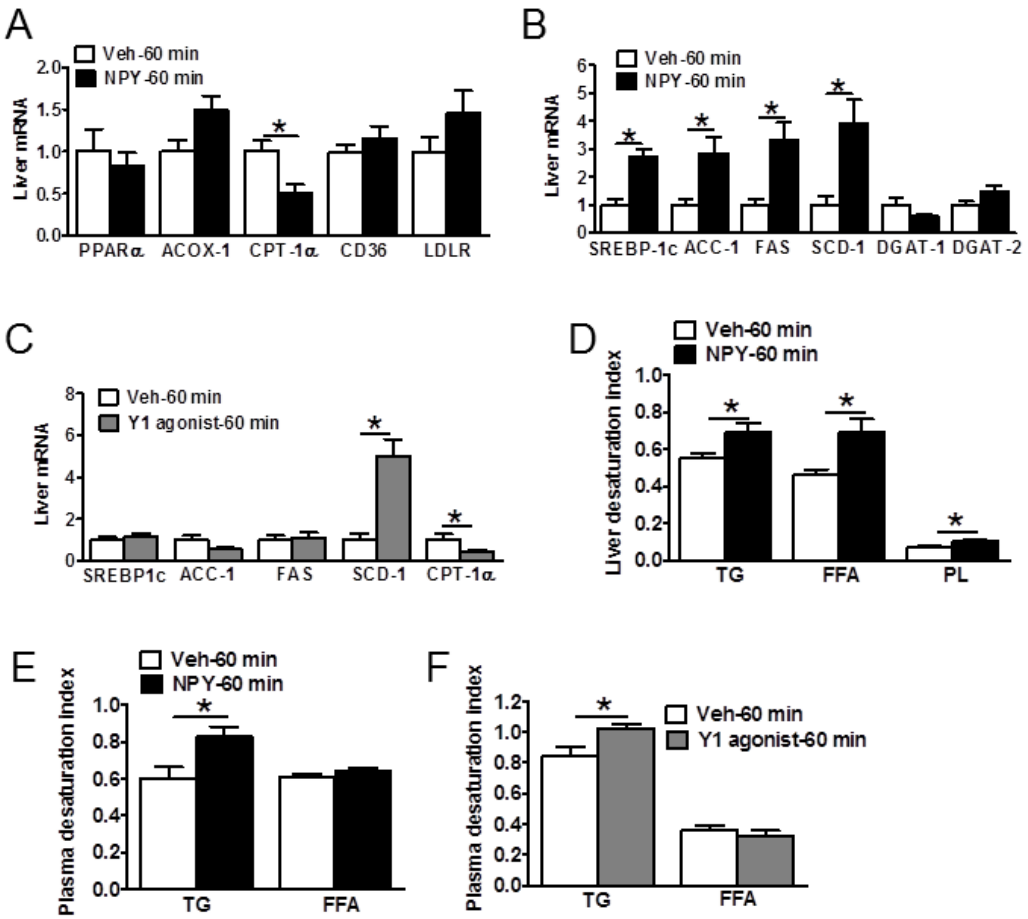

Figure 4.5. Effects of CNS NPY signaling via the Y1 receptor on key enzymes involved in liver lipid metabolism, VLDL-TG assembly and secretion. RNA was isolated from livers of 4-hour fasted rats that were obtained 60 min after treatment with ICV NPY (black bars), ICV Y1 receptor agonist (gray bars) or vehicle (Veh; white bars), and were assessed by quantitative RT-PCR. A and B: In ICV NPY- vs. Veh-treated rats (*n*=5-6/group), mRNA levels of enzymes involved in fatty acid oxidation (PPARα, ACOX-1, and CPT-1α) and hepatic uptake of LCFA and apoB containing lipoproteins (CD36 and LDLR), *de novo* lipogenesis (SREBP1c, ACC-1, FAS, and SCD-1) and TG synthesis for cytoplasmic droplet or for VLDL formation (DGAT-1 and -2). C: In ICV Y1 agonist- vs. Veh-treated rats (*n*=6-7/group), mRNA levels of enzymes involved in *de* novo lipogenesis (SREBP1c, ACC-1, FAS, and SCD-1) and fatty acid oxidation (CPT-1α). mRNA levels of genes were normalized to the reference RNA RPL13A. For comparative analysis, RNA ratios were normalized to the Veh control. D and E: Desaturation index (16:1+18:1/16:0+18:0) of (D) liver TG, FFA, and PL in addition to (E) plasma TG and FFA in fasted NPY- (black bars) vs. Veh-treated (white bars) rats at 60 min post ICV injection. F: Desaturation index (16:1+18:1/16:0+18:0) of plasma TG and FFA in fasted Y1 agonist- (gray bars) vs. Veh-treated (white bars) rats at 60 min post ICV injection. Data are presented as mean ± SEM and were analyzed by Student's *t*-test (unpaired, two-tailed); *indicates a significant difference ($p<0.05$) between ICV treatment and Veh.

CNS NPY signaling via the Y1 receptor modulates liver SCD-1 activity

SCD-1 is responsible for desaturating saturated fatty acids (SFA), palmitate (C16:0) and stearate (C18:0) to MUFA, palmitoleate (C16:1) and oleate (C18:1w9), which serve as major constituents for synthesis of liver TGs, CEs, and lipoproteins (329, 330). SCD-1 is also known to be a target of leptin (316, 317) and glucose action (215) in the same hypothalamic feeding circuits. Therefore, we assessed the impact of CNS NPY signaling via the Y1 receptor on liver SCD-1 activity. An excellent estimate of *in vivo* hepatic SCD-1 activity is the calculation of the desaturation index, which is the ratio of the SCD-1 product (C16:1+C18:1) to the precursor (C16:0+C18:0) (215, 330). Remarkably, we found that ICV NPY significantly induced the hepatic desaturation index in liver TG, FFA, and PL at 60 min post injection (Fig. 4.5D) resulting in an increase in the desaturation index in plasma TG (Fig. 4.5E) while not altering the adipose-derived plasma FFAs (Fig. 4.5E). Similarly, ICV Y1 agonist recapitulated the effect of NPY resulting in an increase in the desaturation index in plasma TG with no alteration in FFAs (Fig. 4.5F). Altogether, these data suggest that increased CNS NPY signaling via the Y1 receptor increases oleic acid content in liver by modulating hepatic SCD-1 activity and suppressing fatty acid oxidation.

CNS NPY signaling promotes hepatic PL remodeling via ARF-1 and lipin-1 to induce hypertriglyceridemia

The key regulatory enzymes involved in liver PL remodeling to generate the TG precursor for VLDL maturation are ARF-1 (233, 234) and lipin-1 (238). We found that ICV NPY and Y1 agonist promoted an increase in ARF-1 mRNA expression by 2-fold at 60 min post injection (Fig. 4.6A). By 120 min post injection, ARF-1 protein expression was increased 3-fold by ICV NPY treatment (Fig. 4.6C and D). Remarkably, lipin-1 mRNA expression was induced by ICV NPY treatment at 60 min post injection (Fig. 4.6B). Both ICV NPY and Y1 agonist increased lipin-1 mRNA and protein expression by 2- to 3-fold at 120 min (Fig. 4.6B, E and F).

Furthermore, lipin-1 mRNA levels positively correlated with plasma TGs for both ICV NPY and the Y1 agonist treatment relative to Veh (NPY: r=0.5; p=0.03; Y1: r=0.7; p=0.03; Fig. 4.6G). Collectively, these data suggest that increased CNS NPY signaling via the Y1 receptor may promote liver PL remodeling via ARF-1 and lipin-1 and thus, generates the TG precursor to rapidly increase hepatic VLDL-TG secretion.

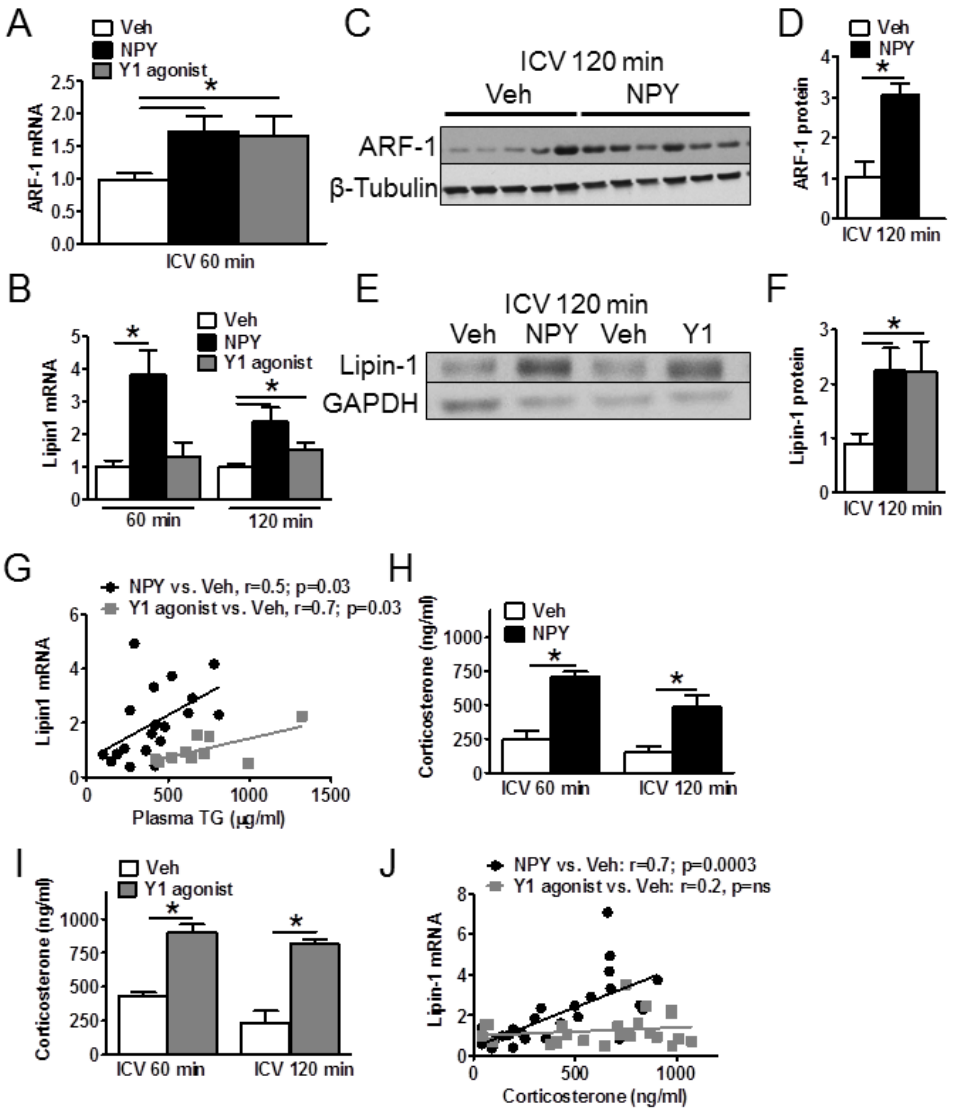

Figure 4.6. CNS NPY signaling promotes hepatic PL remodeling via ARF-1 and lipin-1 to induce hypertriglyceridemia. RNA from livers of 4-hour fasted lean rats (*n*=5-7/group) were obtained 60 or 120 min after treatment with ICV NPY (black bars), ICV Y1 receptor agonist (gray bars) or vehicle (Veh; white bars), and were assessed by quantitative RT-PCR. A and B: mRNA of key regulatory enzymes involved in PL remodeling, ARF-1 (A) and lipin-1 (B). C-F: Protein extracts prepared from livers of 4-hour fasted lean rats isolated 120 min after ICV

injection of NPY (black bars), Y1 receptor agonist (gray bars) or Veh (white bars) were immunoblotted to detect levels of ARF-1 (C and D) and lipin-1 (E and F). Images of Western blots were analyzed by densitometry and data shown are relative to levels of Veh controls after normalization to total β-Tubulin or GAPDH. G: Correlational analysis of lipin-1 mRNA and plasma TG levels in ICV NPY- (black circles) and Y1 agonist- (gray squares) treated rats at 60 and 120 min post injection. H and I: Plasma corticosterone levels in 4-hour fasted ICV NPY- (black bars; H) and Y1 receptor agonist- (gray bars; I) treated rats at 60 and 120 min post injection relative to Veh treatment (white bars). J: Correlational analysis of lipin-1 mRNA and plasma corticosterone levels in ICV NPY- (black circles) and Y1 agonist- (gray squares) treated rats at 60 and 120 min post injection. Data are presented as mean ± SEM and were analyzed by Student's *t*-test (unpaired, two-tailed); *indicates a significant difference ($p<0.05$) between ICV treatment and Veh.

Increased CNS NPY signaling via the Y1 receptor leads to elevated circulating corticosterone levels

Because ICV infusion of NPY influences glucose metabolism and sensitivity to insulin in fasted rats (189-191) in addition to regulating the activity of the HPA axis (200, 201), we next sought to determine whether NPY signaling via the Y1 receptor alters glucoregulatory hormones and circulating corticosterone levels early on (60 min). In corroboration with our previous findings at 120 min post ICV injection in Chapter III (222), there was no effect of ICV NPY on altering plasma insulin, glucagon and blood glucose levels at 60 min post injection (Table 4.1). Although ICV Y1 agonist did not alter plasma glucagon and blood glucose levels, plasma insulin levels were increased by 2-fold at 60 min post injection (Table 4.1). Remarkably, we found that plasma corticosterone levels were markedly elevated by both ICV NPY and Y1 agonist treatment at 60 and 120 min post injection (Fig. 4.6H and I) in lean fasted rats.

CNS NPY signaling promotes hepatic lipin-1 expression and subcellular localization via a GC dependent mechanism

Glucocorticoids act through GRα bound to the GRE site upstream of the *Lpin-1* promoter region to induce gene transcription (260). Because GCs have been shown previously to stimulate hepatic lipin-1 expression and activity (259), we next investigated whether CNS NPY signaling via the Y1 receptor is dependent on circulating corticosterone levels to induce *Lpin1* gene expression. Indeed, we found that lipin-1 mRNA expression positively correlates with corticosterone levels at both 60 and 120 min post ICV NPY injection relative to Veh ($r=0.7$, $p=0.0003$; Fig. 4.6J). Surprisingly we did not observe this correlation with the Y1 agonist treatment (Y1 vs. Veh: $r=0.2$, p=ns; Fig. 4.6J).

Because the association of lipin-1 with the ER governs the lipid substrate availability for VLDL assembly and secretion (238), we next examined lipin-1 protein expression in subcellular fractions of livers from lean fasted rats treated with either ICV NPY or Veh at 60 or 120 min post

injection. Of note, we found that the ER-membrane proteins were enriched in only the nuclear and not the cytoplasmic fraction; thus, we denoted this fraction as nuclear/ER (compare Fig. 4.7A and B). Interestingly, lipin-1 protein was significantly increased in the nuclear/ER fraction at 60 and 120 min post ICV NPY injection (Fig. 4.7A and C) whereas there was either a small reduction or no change in cytoplasmic lipin-1 protein levels relative to Veh treatment, respectively (Fig. 4.7B and C). Similarly, GRα protein expression showed a similar pattern as lipin-1, with highest expression in the nuclear/ER fraction (Fig. 4.7A, B, and D). Additionally, we show that nuclear/ER GRα protein expression positively correlates with both lipin-1 mRNA ($r=0.5$; $p=0.01$; Fig. 4.7E) and nuclear/ER protein expression ($r=0.5$, $p=0.04$; Fig. 4.7E). These data collectively suggest that increased CNS NPY signaling promotes hepatic lipin-1 expression and association with the ER where it performs its PAP-1 activity via a GC dependent mechanism in order to modulate hepatic VLDL-TG secretion.

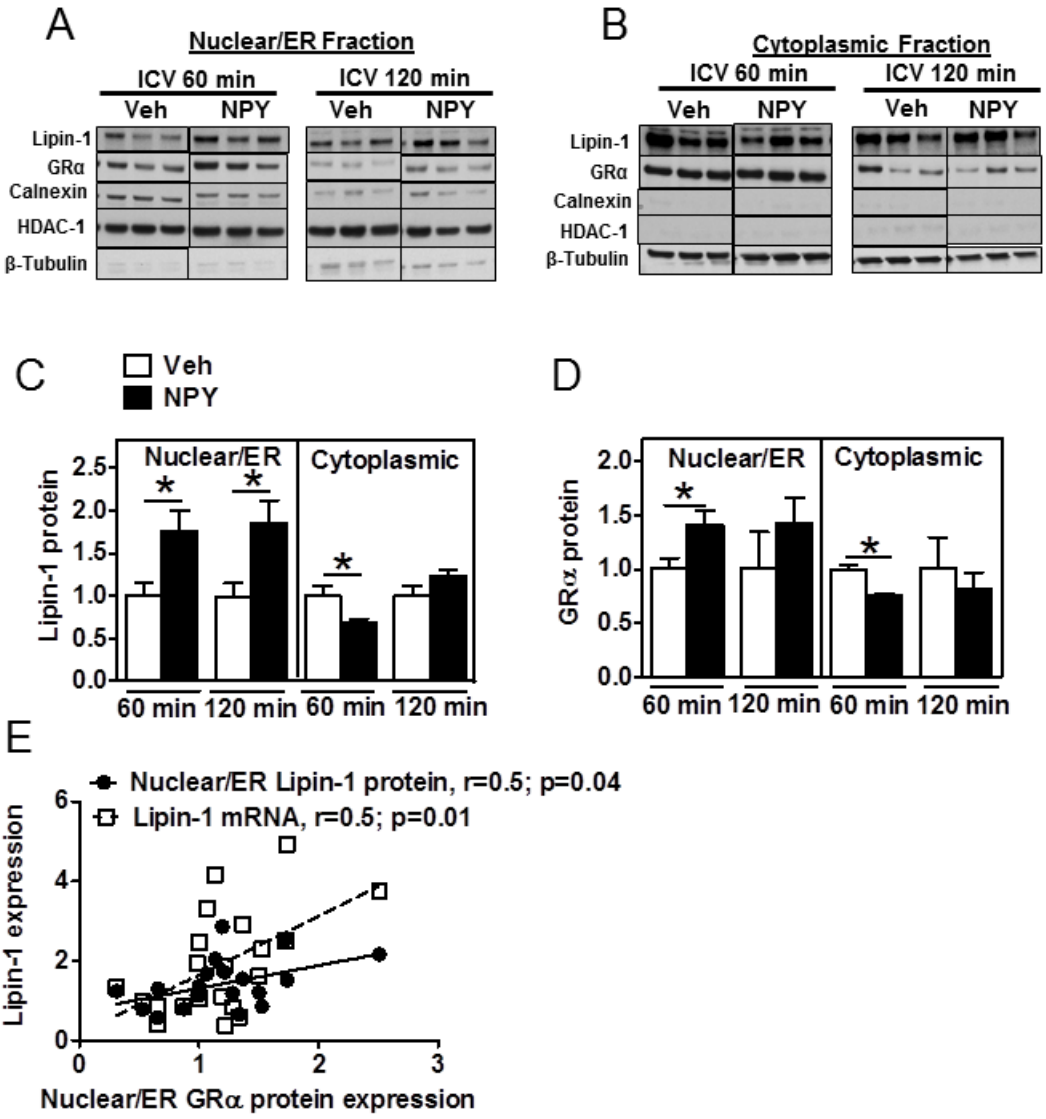

Figure 4.7. CNS NPY signaling promotes hepatic lipin-1 expression and subcellular localization via a GC dependent mechanism. A-D: Western blot analysis of nuclear/ER (A) and cytoplasmic (B) fractions from livers of 4-hour fasted lean rats (*n*=5-6/group) isolated 60 or 120 min after ICV injection of NPY (black bars) or vehicle (Veh; white bars) and were immunoblotted to detect levels of lipin-1 (A-C) and GRα (A, B, and D). Calnexin, Histone deacetylase 1 (HDAC1), and β-Tubulin were used as marker proteins of ER membrane, nuclear, and cytoplasmic fractions, respectively. Of note, ER-membrane proteins were found only in the nuclear fraction and thus, this fraction is denoted as nuclear/ER (A). Western blots were analyzed by densitometry and data shown are relative to levels of Veh controls after normalization to β-Tubulin or HDAC1. E: Correlational analysis of lipin-1 mRNA (white squares) or lipin-1 nuclear/ER membrane protein (black circles) expression versus nuclear/ER GRα protein expression in ICV NPY-treated rats at 60 and 120 min post injection. Data are presented as mean ± SEM and were analyzed by Student's *t*-test (unpaired, two-tailed); *indicates a significant difference ($p<0.05$) between ICV treatment and Veh.

Discussion

Hypertriglyceridemia and overproduction of VLDL-TG are key components of the metabolic syndrome (14-16) and atherogenic dyslipidemia, which is an increasingly recognized component of cardiovascular risk (16). *While hepatic VLDL-TG secretion can be regulated by peripheral factors (visceral adiposity and insulin resistance), we hypothesized that increased CNS NPY signaling contributes to the pathogenesis of obesity dyslipidemia independently of positive energy balance and increased fat mass.* The key observation of our previous studies in Chapter III (211, 222) is that increased CNS NPY signaling via the Y1 receptor doubled hepatic VLDL-TG production while not altering plasma FFA and glycerol levels. This data suggest that increased adipocyte lipolysis does not account for the NPY-induced hypertriglyceridemia. This is also corroborated by other studies (192). We, therefore, sought to determine the source of TG utilized for VLDL assembly and secretion in response to increased CNS NPY action, which must originate from sources other than that arising from extracellular FFAs. We postulated that liver PL might be the novel lipid source because our results show the following: 1) ICV NPY treatment in lean fasted rats doubled plasma TGs in the absence of significant changes in liver TG content at 60 and 120 min post injection; and 2) the obese, ZF rat model of severe hypertriglyceridemia indicated changes in hepatic PL content. Intriguingly, we found that ZF rats pair-fed to the lean ZF controls to maintain identical body composition, altered the plasma TG concentrations, which surprisingly had no effect on liver TG content. However liver PL content tightly correlated with plasma TG levels. Both of these observations suggest the possibility that the additional lipid loaded onto VLDL in response to CNS NPY signaling via the Y1 receptor is generated from PL stores and involves modulating the activities of key regulatory enzymes involved in PL remodeling. Our study ultimately sought to identify the novel regulatory mechanisms in the liver engaged by NPY.

Our study found that CNS NPY Y1 receptor is coupled to the suppression of liver CPT-1α transcript, which encodes the rate limiting mitochondrial transmembrane enzyme that

transports LCFAs, such as oleic and linoleic acid into the mitochondria for β-oxidation (325). Remarkably, our observation is consistent with the study by Zhang et al. (127) that found greater utilization of lipid as an oxidative fuel source in Y1 receptor null mice. This most likely involved increases in liver and muscle CPT-1 protein levels as well as increases in activity of enzymes involved in β-oxidation, suggesting that Y1-receptor-signaling controls mitochondrial capacity for FFA transport and oxidation. Similarly, a previous study showed that administration of ICV Y1 agonist in mice led to an increase in the respiratory exchange ratio, indicative of reduced lipid oxidation, suggesting involvement of the CNS Y1 receptor in the regulation of oxidative fuel selection (210).

The likelihood that central NPY signaling suppresses liver FFA oxidation via the inhibition of CPT-1α is further confirmed by Bruinstroop et al. (192), who reported that ICV NPY decreases CPT-1α mRNA expression via the SNS in lean fasted rats and this NPY effect was completely abolished by Sx. Because NPY is co-localized with NE in hepatic nerves, this raises the possibility that NPY released with NE on sympathetic nerve stimulation may activate Y1 receptors on hepatic blood vessels or on hepatocytes to modulate blood flow, and thereby, directly or indirectly modulate substrate availability in the form of extracellular FFAs for lipid oxidation (127). Clearly, the CNS NPY effect to suppress lipid oxidation via the SNS is in direct competition with the peripheral effects of fasting, which normally promote an increase in liver β-oxidation (192).

It is hypothesized that when oxidation is inhibited, this potentially augments the capacity of the liver to sequester excess FFA as TG for VLDL secretion (238, 259). Consistent with this hypothesis, we found that the suppression of CPT-1α expression with ICV NPY treatment coincided with a corresponding accumulation of the MUFA, oleate and the PUFA, linoleate in liver. However, only one study reported in lean 12-hour fasted mice that acute pharmacologic inhibition of hepatic CPT-1 with TDGA increased MUFAs with a corresponding decrease in SFAs and PUFAs in liver (331). Therefore, it would be interesting to determine whether the

changes in individual hepatic FFAs in response to an acute inhibition of liver CPT-1 in fasted rats recapitulates our findings in liver with ICV NPY treatment.

SCD-1 is the enzyme responsible for desaturating palmitic and stearic acids to palmitoleic and oleic acids, respectively, and is known to be a target of CNS leptin (316, 317), glucose (215) and melanocortin action (203) in the same hypothalamic feeding circuits engaged by NPY. Provision of oleic acid or modulation of SCD-1 activity changes VLDL production rate by increasing TG loading in the late maturation phase (215, 316). Indeed, we observed a robust induction of hepatic SCD-1 expression and activity (as measured by the desaturation index (215, 330)) in response to CNS NPY treatment and this effect was recapitulated by Y1 receptor activation (222). Therefore, changes in the formation rate of hepatic oleic acid (215) is most likely mechanistically linked to the modulation of hepatic SCD-1 activity and lipid oxidation (CPT-1α) by increased CNS NPY tone, which in turn may contribute to changes in hepatic VLDL-TG secretion.

The other possibility that may promote an accumulation of oleic and linoleic acid in the liver is the increased hepatic uptake of extracellular FFAs. However, we found that ICV NPY treatment did not alter adipocyte lipolysis in the form of plasma FFA and glycerol in lean fasted rats. Nor did ICV NPY treatment alter mRNA expression of CD36 (326) and LDLR (327), key enzymes involved in hepatic uptake of LCFA and apoB containing lipoproteins (i.e. chylomicron and VLDL remnants). Moreover, we previously confirmed that 4-hour fasted rats are in a post-absorptive state and thus, TG carrying chylomicrons derived from the gut do not contribute to the observed changes in plasma TGs (211, 222).

Entry of LCFAs into the liver are immediately activated by acyl-CoA synthetase to form a LCFA-acyl-CoA that if not immediately utilized for β-oxidation will enter the glycerolipid biosynthetic pathway for the generation of liver TG and PLs (237). Contrary to the normal effects of fasting, in which oleic and linoleic acid are preferentially oxidized (332-334), we found preferential incorporation of these LCFAs into liver PL and not into TGs in response to ICV NPY

treatment in lean fasted rats at 60 and 120 min post injection. In support of our findings, a study by Lin et al. (335) found that supplementation of Hep G2 cells with linoleic acid strongly increased cellular PL synthesis whereas supplementation with oleic acid had a lesser effect; this study indicates that unsaturated LCFAs can be selectively incorporated into the liver PL pool.

The key finding of our study is the observed corresponding increase of oleic and linoleic acid content in plasma TG in both ICV NPY- and Y1 agonist-treated rats at 60 and 120 min post injection. Moreover, FFAs enriched in liver PL (and not TG and FFA) positively correlated with plasma TGs. Therefore, this data suggest the possibility that these FFAs enriched in liver PL provided the TG precursor that was loaded onto the nascent VLDL particle and was secreted as VLDL-TG. This finding, that some of the TG which ends up as VLDL, is derived from a pool of intracellular PL in response to central NPY action is novel. We, therefore, postulate that increased CNS NPY tone may determine the rate of PL "turnover" or "availability" for TG synthesis and VLDL production by altering the activities of key regulatory enzymes involved in PL remodeling.

We herein report, for the first time to our knowledge that CNS NPY and the Y1 agonist robustly increased the mRNA and protein expression of key regulatory enzymes involved in liver PL remodeling, ARF-1 (which activates PLD) and lipin-1 in lean fasted rats. We postulate that NPY modulates ARF-1 to increase PLD activity. In turn, PLD catalyzes the production of PA, derived from the much larger PL pool, instead of the intracellular TG pool as this pathway is implicated by several studies to be involved in VLDL maturation (224, 233, 234). Indeed, overexpression of ARF-1 or PLD in cultured rat hepatocytes can increase VLDL secretion whereas hepatic overexpression of a dominant negative ARF-1 results in a suppressive effect (234). However, to demonstrate the involvement of ARF-1 and PLD in the CNS NPY response would require additional studies to determine whether selective hepatic ARF-1 or PLD inhibition using either a pharmacologic and/or genetic approach will block the effect of central NPY signaling on hepatic VLDL-TG production.

Our finding that CNS NPY increases liver oleic acid content in lean fasted rats early on (60 min post injection) increases the likelihood that oleic acid may promote lipin-1 translocation from the cytosol to the ER membrane to modulate VLDL assembly and secretion (238, 253). Consistent with this observation, we found that lipin-1 protein expression was robustly elevated in the ER membrane containing nuclear and not the cytoplasmic fraction in the livers of lean fasted rats treated with ICV NPY at 60 min and 120 min post injection. These data suggest the possibility that lipin-1 may be closely associated with the microsomal membrane where it performs its PAP-1 activity. In turn, we speculate that this resulted in the conversion of PL-derived PA into DAG which serves as a substrate for the synthesis of TG and PL that is then assembled onto the nascent VLDL particle leading to VLDL maturation and secretion (238). Indeed, overexpression of lipin-1 in cultured rat hepatocytes in the presence of oleic acid markedly increases TG synthesis and secretion whereas siRNA mediated knockdown of lipin-1 decreased VLDL assembly and secretion (238). In support our findings, we additionally show that lipin-1 mRNA expression positively correlates with plasma TGs in both ICV NPY- and Y1 agonist-treated rats, further implicating lipin-1 as a major mediator in central NPY modulation of hepatic lipoprotein metabolism.

Intriguingly, our finding that lipin-1 protein levels are simultaneously elevated in the nuclear fraction raises the possibility that nuclear localized lipin-1 may also be acting as a transcriptional coactivator with PGC-1α and PPARα to upregulate genes involved in β-oxidation (248, 254); this would oppose its function as a glycerolipid biosynthetic enzyme. However, our findings that the mRNA expression of oxidative genes, were either suppressed (CPT-1α) or not altered (PPARα and ACOX-1) with ICV NPY treatment lessens this possibility. Nevertheless, to demonstrate whether NPY-induced hypertriglyceridemia is dependent on liver lipin-1 will require additional studies, such as investigating whether adenoviral overexpression of a hepatic lipin-1 mutant with impaired PAP-1 activity in lean fasted rats will abolish NPY-induced hepatic VLDL-TG secretion.

Elevated CNS NPY tone and increased activity of the HPA axis is associated with obesity and diabetes in rodent models (139, 140, 177, 197-199) and humans (143, 144, 193-196). Chronic central NPY infusion has been shown to activate the HPA axis in normal animals leading to the elevation in the circulating GC, corticosterone (200, 201). Herein, our study shows that an acute ICV administration of NPY or the Y1 agonist in lean fasted rats robustly elevates circulating corticosterone levels at 60 and 120 min post injection. Of particular interest is that some of the hormonal and metabolic effects of central NPY infusion in rats are dependent on circulating corticosterone as these NPY-induced effects can be prevented by adrenalectomy, including hypertriglyceridemia (201).

Previous studies (238, 259) report that lipin-1 is responsible for the observed increase in VLDL secretion upon GC treatment in cultured rat hepatocytes (264-266). *We, therefore, hypothesize in the context of these findings, that central NPY regulation of liver lipin-1 to modulate hepatic lipoprotein metabolism may be dependent on liver GC action.* Both *in vitro* (259) and *in vivo* (248) studies in mouse and rat hepatocytes show that the synthetic GC, dexamethasone stimulates the expression and activity of liver lipin-1, but not lipin-2, and -3, by acting through the GR that is bound to functional GRE upstream of the *Lpin1* promoter region (260). In support of this hypothesis, GRα shows a similar pattern as lipin-1 with highest protein expression in the nuclear/ER fraction in the livers of ICV NPY-treated rats. Furthermore, we found that nuclear/ER GRα protein expression positively correlates with mRNA and nuclear/ER protein expression of lipin-1. This increases the likelihood that GRα is bound to the *Lpin1* promoter region (260) in response to an elevation in circulating corticosterone levels induced by CNS NPY. This NPY effect results in the GC mediated induction of lipin-1 expression and activity (259), and subsequent elevation in VLDL-TG secretion. However, further studies will be required to demonstrate this hypothesis and would involve investigating whether the CNS NPY effect on hepatic lipin-1 and VLDL-TG secretion can be blocked by either a highly selective liver-specific GR antagonist and/or by adrenalectomy in lean fasted rats.

It is of particular interest to our study that NE activation of adrenergic signaling in rat liver via the α_1-adrenergic receptor is coupled to the activation of the protein kinase C (PKC)/CREB pathway (336). In turn, CREB may induce *Lpin1* gene transcription by binding to CRE upstream of the *Lpin1* promoter as reported in previous studies (262, 263). Moreover, abundant evidence by Bruinstroop et al. (192), as well as other studies (189, 202), indicate that increased CNS NPY tone during fasting increases sympathetic outflow to the liver, ultimately inducing hepatic insulin resistance and elevating hepatic VLDL-TG secretion. *Therefore, in the context of our findings, it is hypothesized that pathological elevations in CNS NPY tone in obesity and diabetes contributes to the associated increase in both the activity of the HPA axis and sympathetic outflow to the liver.* Ultimately, this may result in increased GC and NE signaling in the liver and thus, these metabolites may synergize to upregulate hepatic lipin-1 expression and its PAP-1 activity. In turn, this may impair the ability of insulin to suppress lipin-1 leading to increased VLDL-TG secretion. Given the current limitations of our study, future studies to investigate this hypothesis will involve determining whether the CNS NPY effect on hepatic lipin-1 and VLDL-TG secretion can be blocked by Sx and whether the concomitant treatment of a highly selective liver specific GR antagonist will synergistically attenuate the NPY effect.

CHAPTER V

HEPATIC RICTOR/MTORC2 IS REQUIRED FOR HIGH-FAT DIET-INDUCED LIVER STEATOSIS AND DYSLIPIDEMIA

Adapted from Rojas et al. Submitted to *J. Lipid Res* 2012 (under revision)

Introduction

The availability of mice with genetic deletion of raptor (mTORC1) and rictor (mTORC2) in insulin responsive tissues (337-342) has provided new insights into mTOR function as a regulator of mammalian metabolism. mTORC1 activity in hepatocytes is important in the regulation of ketogenesis (343) and lipid metabolism (344-346). Conversely, genetic deletion of rictor and associated loss of mTORC2 activity in liver (347, 348) revealed that mTORC2 regulates hepatic glucose, lipid, and cholesterol metabolism. Key studies (347, 348) showed that hepatic mTORC2 deficiency impairs insulin-AKT signaling through FoxO1 and glucokinase, leading to dysregulation of glycolysis and gluconeogenesis while impairing the ability of AKT to stimulate hepatic lipogenesis and cholesterogenesis through SREBP-1c and SREBP-2. However, it is not clear on the details of the molecular mechanism of how defective hepatic mTORC2 activity impairs the induction and/or processing of SREBPs and liver lipid metabolism and whether this is partially independent of AKT and/or mTORC1 signaling. A better understanding of these molecular mechanisms is critical for the development of new approaches to treat disorders of liver lipid metabolism such as NAFLD (349, 350) and atherogenic dyslipidemia (14, 15) associated with obesity, diabetes, and the metabolic syndrome.

Insulin regulation of metabolic processes often involves PI3K signaling, that is coupled to PDK-1 and the Ser/Thr kinase AKT (281). AKT is activated via phosphorylation at Ser473 by rictor containing mTORC2 in addition to PDK1-directed phosphorylation at Thr308 (282, 283).

AKT2 is the major isoform of AKT expressed in liver and mediates many of the metabolic actions of insulin (284, 285). Hepatic overexpression of constitutively active AKT leads to the development of NAFLD, hypertriglyceridemia, and hypoglycemia (286). These effects are phenocopied by loss of hepatic PTEN, a negative regulator of PI3K-dependent protein kinase activity, including AKT (287). The loss of AKT2 effectively negates the effect of PTEN deficiency on fatty liver and improved systemic glucose tolerance (288), and similarly, reverses hepatic steatosis in obese, insulin resistant mouse models (285). These effects on glycemia are due, in part, to AKT directed phosphorylation and inhibition of the transcription factor FoxO1. Phosphorylation of FoxO1 by AKT leads to its nuclear exclusion resulting in the termination of transcription of its target genes involved the regulation of gluconeogenesis, PEPCK and G6PC thereby limiting HGP (289).

The liporegulatory effects of insulin-AKT signaling in the liver involve both SREBP-1c and SREBP-2, which regulate many genes involved in fatty acid, triglyceride, and cholesterol biosynthesis (276). The molecular mechanisms underlying AKT regulation of these two distinct SREBP isoforms remain unclear (351). It is known that insulin signaling increases transcription and proteolytic processing of SREBPs from an inactive precursor to an active nuclear transcriptional regulator (reviewed in (328, 351)). While insulin regulation of SREBP-1c (344, 346, 352-355) and SREBP-2 (345, 346, 356) involves mTORC1-dependent signaling, we sought to expand our understanding of mTORC1-independent mechanisms involved.

The precise mechanism by which insulin induces SREBP-1c transcription is likewise unclear, but may involve Liver X receptor-α (LXRα) and one of the nuclear SREBP isoforms, producing a feed forward stimulation (357). LXRα (NR1H3) is a nuclear hormone receptor with high hepatic expression that transcriptionally regulates SREBP-1c via an RXR/LXR DNA responsive element (LXRE) in the *SREBF1* (SREBP-1c) promoter (358), and is activated by oxysterol ligands, derivatives of cholesterol (359-361). Animals lacking LXRα have reduced basal expression of SREBP-1c and its downstream lipogenic target genes, *ACACA* (ACC), *FASN*

(FAS), and *SCD* (SCD-1) (360, 362), which also contain LXREs and can be directly regulated by LXRs (363-365). A high cholesterol diet causes both an inhibition of sterol responsive SREBP-2 and the activation of LXRα, resulting in increased SREBP-1c mRNA and nuclear protein expression concomitant with increased expression of SREBP-1c lipogenic target genes and lipogenesis (360, 362). Treatment with a synthetic LXR agonist replicates these effects (360, 366). Thus, LXRα is thought to couple the regulation of cholesterol and fatty acid metabolism in liver.

Because AKT is also regulated by other inputs (PDK-1), and is a major mediator of insulin's effect on metabolic processes, we sought to determine whether hepatic rictor directed mTORC2 activity is required for the regulation of liver lipid metabolism. We show here that hepatocyte-specific deletion of the *Rictor* gene, which encodes a key mTORC2 regulatory protein in mice (HRicKO), leads to protection from HFD-induced hepatic steatosis and dyslipidemia, but are glucose intolerant. Furthermore, we have uncovered a novel aspect of mTORC2/AKT signaling that leads to SREBP-2 activation of cholesterol biosynthesis, full LXRα activation, and concomitant activation of SREBP-1c. This rictor/mTORC2 dependent pathway facilitates the cooperative interaction of LXRα and insulin signaling to fully induce SREBP-1c mediated lipogenesis, which leads to hepatic steatosis and dyslipidemia in HFD-induced obesity.

Results

Loss of hepatic rictor reduced serine phosphorylation of mTORC2 target proteins

Alb-Cre mediated excision of floxed alleles for exon 3 within the *Rictor* gene in HRicKO mice led to a 90 to 96% reduction in rictor mRNA (Fig. 5.1A) and protein levels (Fig. 5.1B), respectively in liver. Expression of this mTORC2 specific component was not altered in other tissues examined (Fig. 5.1C and D). The expression of mTOR and an mTORC1 specific component raptor were not altered (Fig. 5.1B-D). Loss of hepatic rictor resulted in reduced

mTORC2 activity in liver as illustrated by reduced phosphorylation of mTORC2 target proteins, AKT-Ser473, PKCα-Ser657, and SGK-Ser422 in liver (Fig. 5.1B) but not in other tissues (Fig. 5.1C and D).

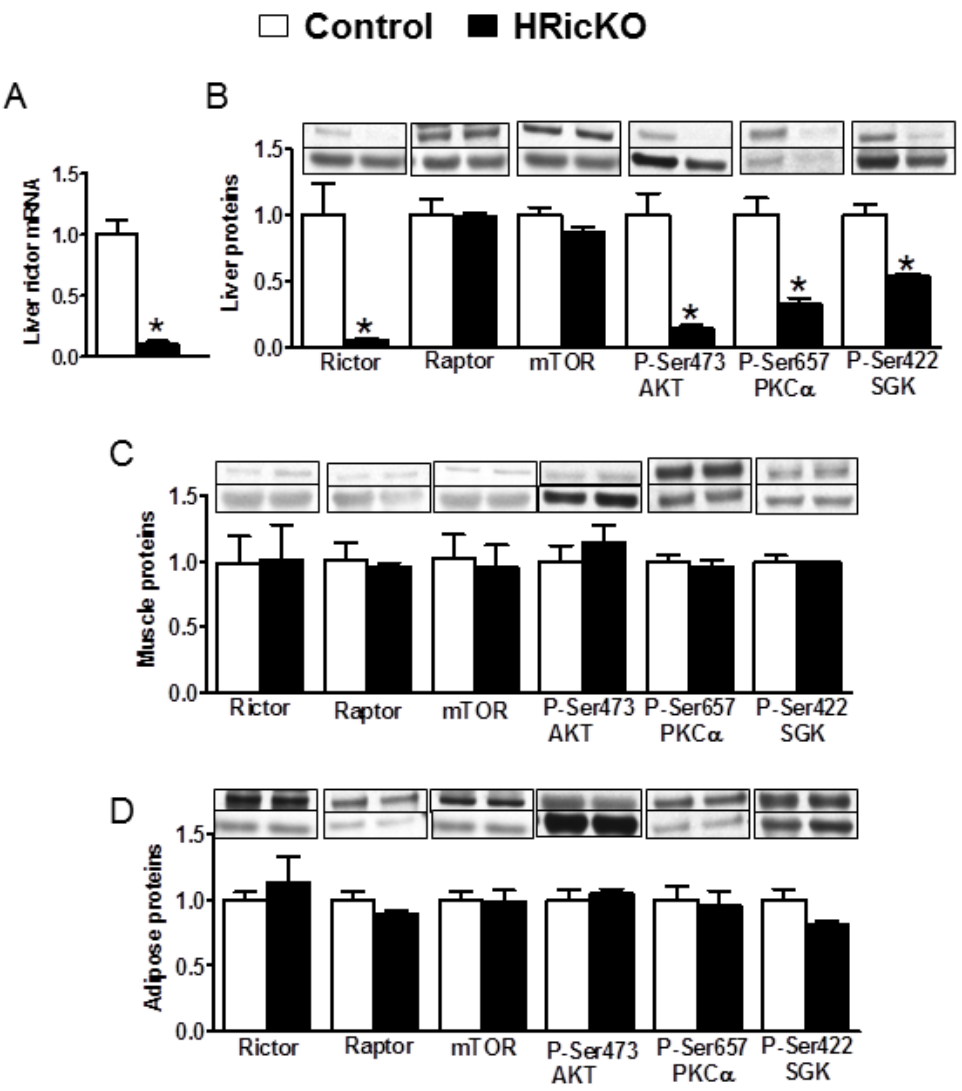

Figure 5.1. Loss of rictor expression and mTORC2 activity in liver of HRicKO mice. A: mRNA levels of rictor from livers of 12 week old chow-fed HRicKO (black bars; *n*=3) and control mice (white bars; *n*=6) normalized to levels of control mice. B-D: Protein extracts from 12 week old chow-fed HRicKO (black bars; *n*=3) and control mice (white bars; *n*=6) were prepared from liver (B), muscle (C), and adipose tissue (D) and immunoblotted for rictor, raptor, mTOR, and phosphorylated (p) Ser473 AKT, pSer657 PKCα, and pSer422 SGK. Images of Western blots were analyzed by densitometry and data shown are relative to levels of control mice after normalization to levels of total AKT, PKCα, SGK, or GAPDH. Data are expressed as mean ± SEM and were analyzed by Student's *t*-test (unpaired, two-tailed); *indicates a significant difference ($p<0.05$) from control mice.

Loss of hepatic rictor prevented the development of diet-induced obesity

Chow-fed HRicKO mice developed normally and at 12 weeks of age were comparable to littermate controls in body weight, fat mass, and lean mass (Fig. 5.2A). Indirect calorimetry revealed that LFD-fed HRicKO mice with similar fat and lean mass exhibited higher EE than their littermate controls throughout the day (Table 5.1). When normalized to lean mass, HRicKO mice exhibited significantly higher EE only during the dark (feeding) and not during the light (postprandial) cycle (Table 5.1). HRicKO mice exhibited lower RQ during the light period, indicating that HRicKO mice oxidize more fat than controls (Table 5.1). Therefore, we examined whether these phenotypical differences would confer resistance to HFD-induced obesity.

Table 5.1. Energy homeostasis analysis in HRicKO and control mice on low-fat diet

		Control	HRicKO
	FM (g)	2.26±0.10	2.53±0.16
	LM (g)	18.0±0.39	19.0±0.40
EE (kcal)	Light	3.5±0.1	3.9±0.1*
	Dark	4.4±0.1	4.9±0.2*
EE (kcal/g LM)	Light	0.196±0.005	0.204±0.005
	Dark	0.243±0.006	0.259±0.005*
RQ (VCO2/VO2)	Light	0.91±0.02	0.85±0.01*
	Dark	0.93±0.01	0.94±0.01

Energy expenditure (EE) and respiratory quotient (RQ) were measured over 24-hour by indirect calorimetry in individually housed control and HRicKO mice after 8-9 weeks on low-fat diet (n=10/group). Values for EE (kcal/12-h) were also normalized to NMR measured lean mass (LM), obtained the day mice were placed in the oxymax cages. Data are expressed as mean ± SEM and were analyzed by Student's t-test (unpaired, two-tailed); *indicates a significant difference ($p<0.05$) from control mice. Fat mass (FM).

On a HFD, HRicKO mice had no alteration in lean mass, but gained substantially less body weight (34%) and fat mass (57%) than HFD-fed controls despite having similar food intake (Fig. 5.2B-F). Liver (Fig. 5.2G) and epididymal fat pad weights (Fig. 5.2H) were reduced by 36% and 50%, respectively, whereas pancreas tissue weights were unaltered (Fig. 5.2I) in HFD-fed

HRicKO mice relative to HFD-fed controls. These results indicate that loss of hepatic rictor prevents HFD-induced obesity without altering food intake.

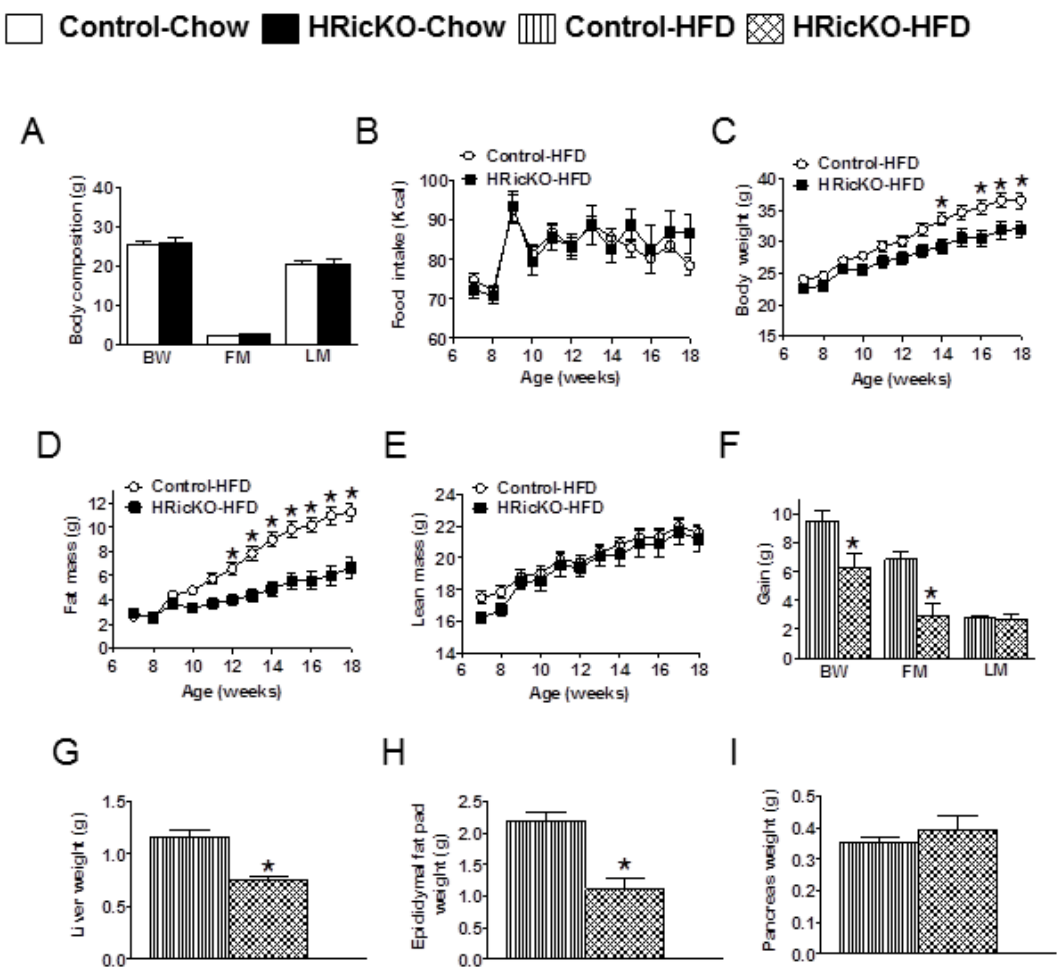

Figure 5.2. Loss of hepatic rictor prevented the development of diet-induced obesity. A: Body weight (BW), fat mass (FM), and lean mass (LM) were measured in 12 week old chow-fed HRicKO (black bars) and control mice (white bars). B-E: HRicKO (black squares, *n*=7) and control mice (white circles, *n*=9) were placed on a high-fat diet (HFD) at 8 weeks of age and food intake (Kcal) (B), BW (C), FM (D), and LM (E) were measured weekly for 10 weeks. Data are presented as mean ± SEM and were analyzed by two-way repeated measures ANOVA with Bonferroni's post-test analysis; *p<0.05 for control vs. HRicKO comparisons. The main effect of genotype to reduce BW and FM over time was dependent on HFD [BW: (F (1, 14) =5.77, p=0.0308); FM: (F (1, 14) =17.49, p=0.0009)]. (F) BW, FM, and LM gain were measured after 10 weeks of HFD feeding in HRicKO (hatched bars) and control mice (striped bars). G-I: Weights of liver (G), epididymal fat pad (H) and pancreas (I) were measured in 4-hour fasted HRicKO (hatched bars) and control mice (striped bars) on 10 weeks of HFD. Data are expressed as mean ± SEM and were analyzed by Student's *t*-test (unpaired, two-tailed); *indicates a significant difference (p<0.05) from control mice.

HFD-fed HRicKO mice are protected from the development of hepatic steatosis and dyslipidemia

HFD-fed HRicKO mice had a 23% and 57% reduction, respectively in fasting plasma TG and cholesterol levels (Fig. 5.3A and B). There were no differences in plasma TG and cholesterol in the chow-fed HRicKO mice (Fig. 5.3A and B). Feeding control mice a HFD led to a 2.5-fold increase in plasma cholesterol levels relative to chow-fed control mice (Fig. 5.3B) while HRicKO mice fed a HFD did not develop hypercholesterolemia (Fig. 5.3B). Both chow- and HFD-fed HRicKO mice had significantly higher fasting plasma FFA levels compared to the control mice (Fig. 5.3C).

Consistent with hypolipidemia, HFD-fed HRicKO mice have a 42% reduction in liver TG and cholesterol content relative to HFD-fed controls (Fig. 5.3D and E). HFD-fed control and HRicKO mice had significantly higher liver TG content relative to the chow-fed mice (Fig. 5.3D). While HFD-fed controls had significantly higher liver cholesterol content than chow fed controls, the HFD-fed HRicKO mice trended towards greater liver cholesterol content relative to chow-fed HRicKO mice ($p=0.051$, Fig. 5.3E). Liver FFA content was significantly higher in HRicKO mice on both chow and HFD relative to control mice (Fig. 5.3F). The decrease in hepatic TG content in HFD-fed HRicKO mice was corroborated by the absence of large, intracellular lipid droplets using H&E and ORO staining (Fig. 5.3G).

Intestinal lipid absorption contributes to whole-body energy and lipid homeostasis; therefore, it was imperative to determine if this was impaired in HRicKO mice by measuring fecal lipid content in animals on LFD and HFD. There was less TG content in feces (collected over a 48-hour period) from the HFD-fed HRicKO mice relative to HFD-fed controls (Fig. 5.3H). Cholesterol levels were similar between groups (Fig. 5.3I) as was fecal FFA content, which was similar in HRicKO relative to control mice on LFD and HFD (Fig. 5.3J). These results suggest that the protection from HFD-induced hepatic steatosis and dyslipidemia found in HRicKO mice did not result from reduced intestinal lipid absorption or increased excretion.

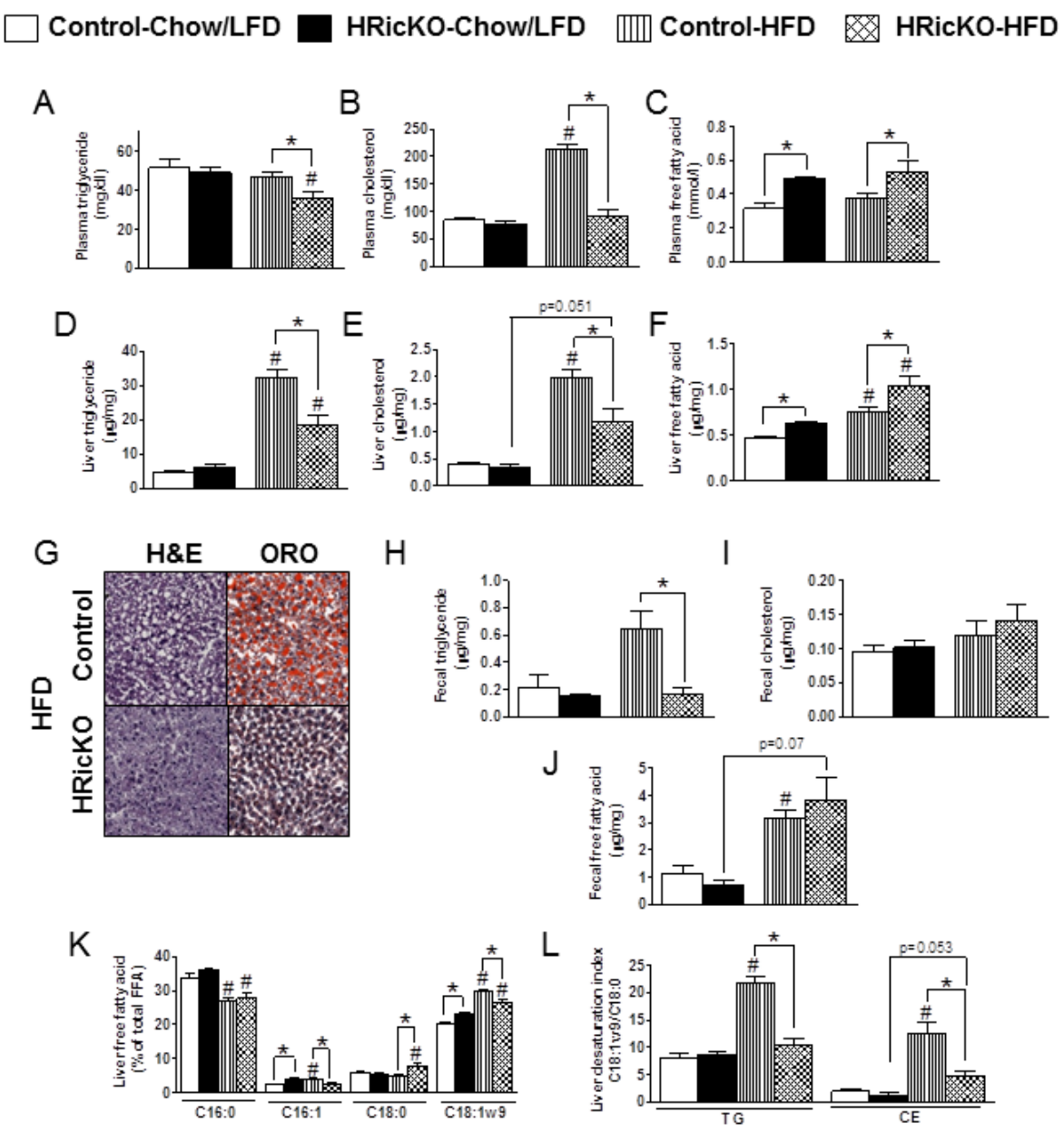

Figure 5.3. HFD-fed HRicKO mice are protected from the development of hepatic steatosis and dyslipidemia. A-F: Plasma and livers were collected from 4-hour fasted 12 week old chow-fed HRicKO (black bars) and control (white bars) mice (*n*=3-6/group) and from 4-hour fasted 18 week old HRicKO (hatched bars) and control (striped bars) mice on HFD for 10 weeks (*n*=7-9/group) to measure plasma triglyceride (TG; A), cholesterol (B), and free fatty acid (FFA; C) as well as liver TG (D), cholesterol (E) and FFA (F). G. Representative images of hematoxylin and eosin (H&E) and Oil Red O (ORO) staining from livers of 4-hour fasted HRicKO and control mice after 10 weeks of HFD; original magnification, 20X. H-J: Feces were collected from paired (2 mice/cage) *ad-libitum* fed 21 week old HRicKO (black bars) and control (white bars) mice on a low-fat diet (LFD; *n*=4/group) vs. 21 week old HRicKO (hatched bars) and control (striped bars) mice on HFD (*n*=6/group), after 10 weeks on diet, to measure fecal TG (H), cholesterol (I) and FFA (J) content. K and L: Liver FFA (% of total FFA; K) and liver desaturation index

(C18:1w9/C18:0; L) of TG and cholesteryl esters (CE) in 4-hour fasted chow-fed (*n*=3-6/group) HRicKO (black bars) and control mice (white bars) and HFD-fed (*n*=7-9/group) HRicKO (hatched bars) and control mice (striped bars). Data are expressed as mean ± SEM and were analyzed by Student's *t*-test (unpaired, two-tailed); *indicates a significant difference ($p<0.05$) from control mice. $^{\#}$indicates a significant difference ($p<0.05$) from chow-fed or LFD-fed mice of the same genotype.

HFD-fed HRicKO mice have reduced SCD-1 activity

SCD-1 is responsible for desaturating saturated FFA, palmitate (C16:0) and stearate (C18:0), to MUFA, palmitoleate (C16:1) and oleate (C18:1w9), which serve as major constituents for synthesis of liver TGs, CEs, and lipoproteins (329, 330). Interestingly, livers of the HFD-fed HRicKO mice have significantly reduced C16:1 and C18:1w9 and higher C18:0 levels relative to HFD-fed control mice (Fig. 5.3K). The SCD-1 desaturation index, which is a ratio of the SCD-1 product (C18:1w9) to the precursor (C18:0) is an excellent estimate of *in vivo* SCD-1 activity (215, 330) was found to be significantly reduced in liver TG and CE fractions in HFD-fed HRicKO mice relative to HFD-fed control mice (Fig. 5.3L). These data suggest that loss of hepatic rictor results in lower SCD-1 activity that in turn, reduces the synthesis of MUFA substrates necessary for TG and CE biosynthesis in liver.

HRicKO mice on HFD are hyperinsulinemic, glucose intolerant, and insulin resistant

On both chow and HFD (12-18 weeks of age), blood glucose levels were similar in fasted HRicKO mice relative to control mice (Fig. 5.4A). However, fasted plasma insulin levels were increased by ~2- and 3-fold respectively in HRicKO mice on chow and HFD compared to the control mice (Fig. 5.4B). Given that the HRicKO mice are hyperinsulinemic, we tested glucose tolerance. HRicKO mice on LFD developed mild glucose intolerance (Fig. 5.4C); whereas HFD feeding led to greater glucose intolerance in HRicKO mice compared to HFD-fed controls (Fig. 5.4D). Older (>9 months) HRicKO mice fed a HFD for 17 weeks were severely glucose intolerant (Fig. 5.4E). Insulin sensitivity was assessed by insulin tolerance test. After 10 weeks of diet, LFD-fed HRicKO mice remained insulin tolerant (Fig. 5.4F). Conversely, HFD-fed HRicKO mice developed mild insulin resistance (Fig. 5.4G). Collectively, these data indicate that loss of hepatic rictor potentiates hyperinsulinemia, glucose intolerance, and insulin resistance in DIO.

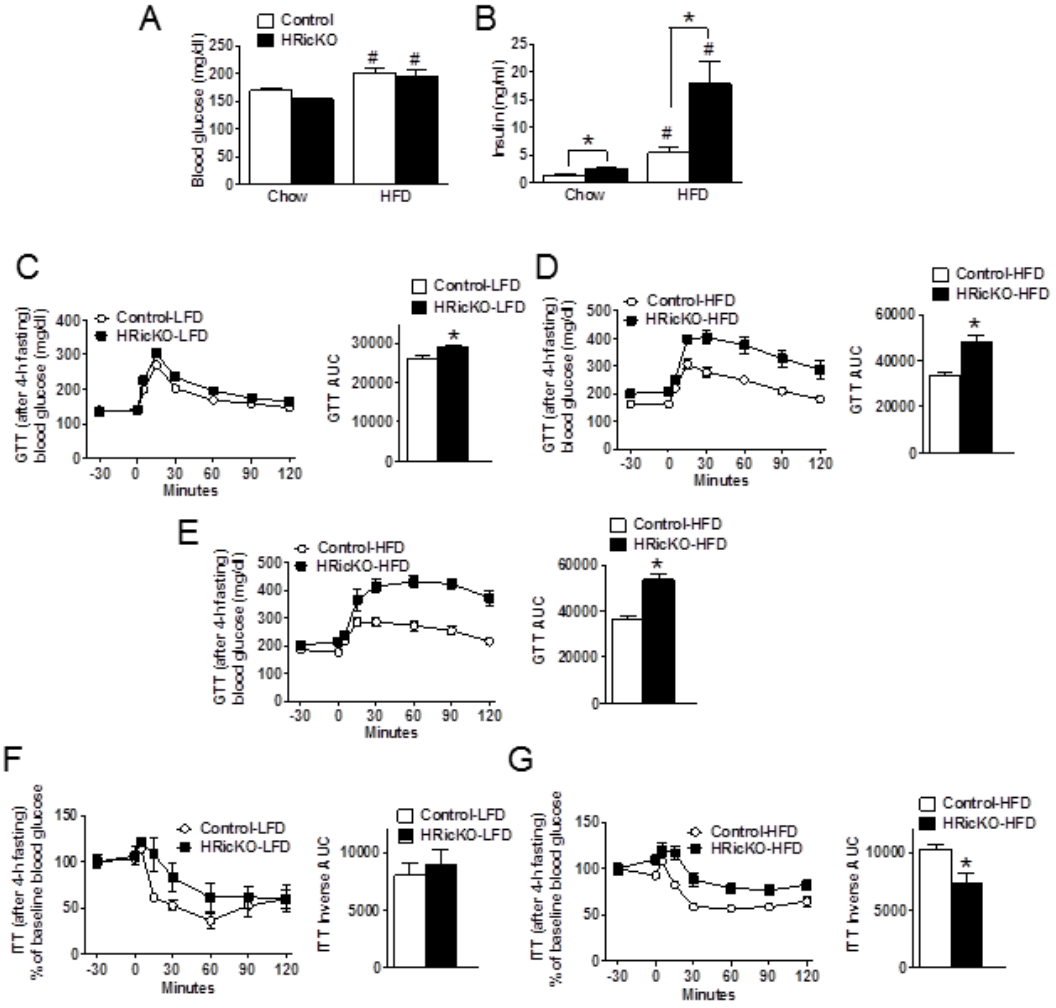

Figure 5.4. Hepatic mTORC2 deficiency potentiates glucose intolerance and insulin resistance in HFD-fed mice. A and B: Blood glucose (A) and plasma insulin (B) levels were measured in 4-hour fasted 12-18 week old HRicKO (black bars) and control (white bars) mice either on chow-diet (*n*=3-6/group) or HFD for 10 weeks (*n*=7-9/group). C and D: Glucose tolerance tests (GTT) were performed after intraperitoneal (IP) injection of glucose (1g/Kg BW) in 4-hour fasted 11-25 week old HRicKO (black squares) and control (white circles) mice either on a LFD (*n*=8-10/group; C) or HFD (*n*=10/group; D) for 4 weeks. E: Additional GTT on 38 week old HRicKO (black squares) and control (white circles) mice after 17 weeks of HFD (*n*=8-10/group). Blood glucose levels were measured at the indicated time points. Bar graphs to the right show the calculated area under the curve (AUC) of glucose levels. F and G: Insulin tolerance test (ITT) were performed after IP injection of insulin (0.8U/Kg BW) in 4-hour fasted 20-30 week old HRicKO (black squares) and control (white circles) mice either on a LFD (*n*=3-5/group; F) or HFD (*n*=9-10/group; G) for 10 weeks. Blood glucose levels were measured at the indicated time points. Results are expressed as % of baseline (100%; time = -30 min) blood glucose levels. Bar graphs to the right show the calculated inverse AUC of glucose levels. Data are expressed as mean ± SEM and were analyzed by Student's *t*-test (unpaired, two-tailed); *indicates a significant difference ($p<0.05$) from control mice. $^{\#}$indicates a significant difference ($p<0.05$) from chow-fed mice of the same genotype.

Proximal insulin signaling

To investigate the signaling events underlying altered glycemic and lipogenic control, we harvested livers from basal and insulin-treated HFD-fed HRicKO and control mice. While insulin-stimulated phosphorylation of AKT Ser473 was measurable in control mice (Fig. 5.5A and C), AKT Ser473 phosphorylation was not increased in HRicKO mice (Fig. 5.5A and C). Basal phosphorylation of AKT Thr308 was increased in HRicKO mice (Fig. 5.5A and D), but insulin stimulation failed to significantly increase the already elevated basal levels (Fig. 5.5A and D). The pattern of AKT Thr308 phosphorylation levels among the different groups corresponded to an identical pattern of insulin receptor-β (IRβ) Tyr1162/Tyr1163 phosphorylation with elevated basal and lack of a significant increase in insulin-induced levels of phosphorylation (Fig. 5.5A and B), which is potentially consistent with their hyperinsulinemia (Fig. 5.4B).

Hepatic mTORC2 deficiency leads to differential coupling of AKT to downstream substrates

We next determined whether impaired hepatic mTORC2 activity (as reflected by reduced AKT Ser473 phosphorylation) modifies AKT specificity for downstream substrates as observed in previous studies (282, 342, 367-369). Basal FoxO1 Ser253 phosphorylation levels were increased relative to controls (Fig. 5.5A and E), but failed to increase in response to insulin treatment in HRicKO mice, in contrast to controls (Fig. 5.5A and E). Conversely, basal and insulin-stimulated phosphorylation of the downstream AKT substrate, Ser9 of glycogen synthase kinase 3β (GSK3β), was intact in both control and HRicKO mice (Fig. 5.5A and F). We also assessed phosphorylation of Thr389 of S6K, which is a target of AKT-mTORC1 activity. Basal and insulin-stimulated phosphorylation of S6K at Thr389, were similar in control and HRicKO mice (Fig. 5.5A and G). Likewise, insulin and mTORC1-dependent phosphorylation of lipin-1 on Ser106 was intact in both control and HRicKO mice (Fig. 5.5A and H). Thus, hepatic mTORC2

deficiency in HRicKO mice fed a HFD leads to impaired transduction of the insulin-AKT signal to the glucoregulatory FoxO1 axis but intact transduction to GSK3β and mTORC1.

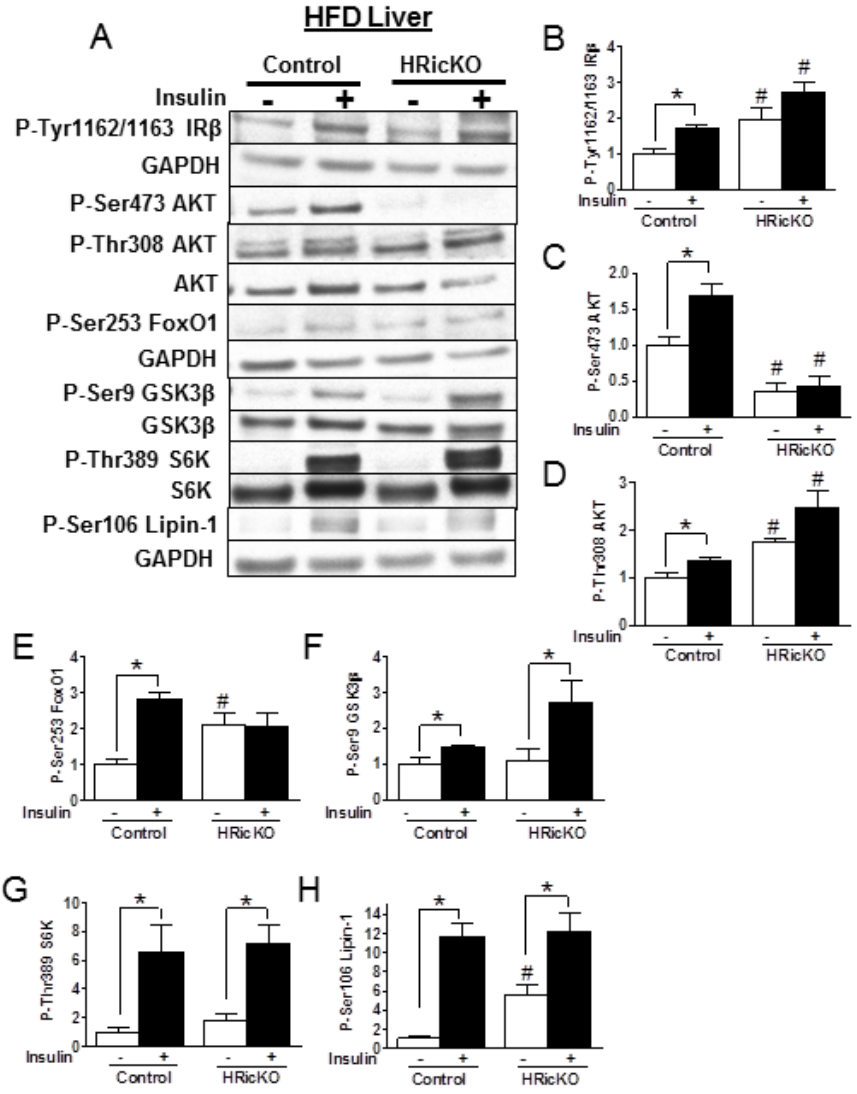

Figure 5.5. Hepatic mTORC2 deficiency in mice fed a HFD leads to impaired transduction of the insulin-AKT signal to the glucoregulatory FoxO1 axis but intact transduction to GSK3β and mTORC1. A-H*:* Representative Western blots (A) of liver extracts prepared from 4-hour fasted 18-21 week old non-insulin-treated (white bars) and insulin-treated (black bars) mice (*n*=6/group) on 10 weeks of HFD are shown and were immunoblotted with antibodies to levels of (B) pTyr1162/pTyr1163 IRβ, (C) pSer473 AKT, (D) pThr308 AKT, (E) pSer253 FoxO1, (F) pSer9 GSK3β, (G) pThr389 S6K, and (H) pSer106 lipin-1. Four-hour fasted mice were injected with insulin as described in materials and methods. Western blots were analyzed by densitometry and data shown are relative to levels of non-insulin-treated control mice after normalization to the corresponding levels of total protein for each phosphorylated protein or to the level of GAPDH. Data are expressed as mean ± SEM and were analyzed by Student's *t*-test (unpaired, two-tailed); *indicates a significant difference ($p<0.05$) from non-insulin-treated mice. $^{\#}$indicates a significant difference ($p<0.05$) from control mice of the same treatment.

Hepatic mTORC2 deficiency leads to gluconeogenic dysregulation on exposure to HFD

Consistent with reduced insulin-stimulated phosphorylation of FoxO1in livers of HFD-fed HRicKO mice (Fig. 5.5A and E), expression of the key enzymes involved in gluconeogenesis, PEPCK and G6PC were not reduced in response to insulin in HRicKO mice, unlike controls (Fig. 5.6A). HFD-fed HRicKO mice showed moderately higher blood glucose levels compared to controls during a pyruvate tolerance test (Fig. 5.6B). These data suggest HRicKO mice have a higher functional capacity for HGP (348).

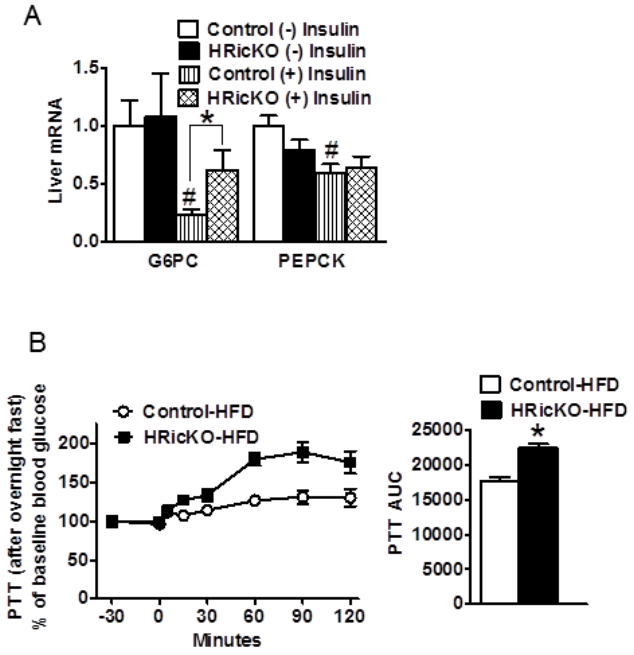

Figure 5.6. Loss of hepatic rictor leads to inability of insulin to suppress the gene expression of key enzymes involved in gluconeogenesis in HFD-fed mice. A**:** mRNA levels of key enzymes involved in gluconeogenesis, G6PC and PEPCK, from livers of non-insulin-treated HRicKO (black bars; *n*=6) and control mice (white bars; *n*=6) as well as insulin-treated livers of HRicKO (hatched bars; *n*=7) and control mice (striped bars; *n*=9) after 10 weeks of HFD feeding. Results are normalized to levels of non-insulin treated control mice. Four-hour fasted mice were injected with insulin as described in materials and methods. B: Pyruvate tolerance test (PTT) were performed after IP injection of pyruvate (2 g/Kg BW) in overnight fasted 16 week old HRicKO (black squares) and control (white circles) mice on HFD for 8 weeks and blood glucose levels were measured at the indicated time points. Results are expressed as % of baseline (100%; time -30 min) blood glucose levels. Bar graphs to the right show the calculated AUC of the blood glucose curve (*n*=8-10/group). Data are expressed as mean ± SEM and were analyzed by Student's *t*-test (unpaired, two-tailed); *indicates a significant difference ($p<0.05$) from control mice and $^{\#}$indicates a significant difference ($p<0.05$) from non-insulin-treated mice of the same genotype.

Hepatic mTORC2 deficiency in HFD-fed HRicKO mice leads to impaired regulation of insulin-stimulated *de novo* fatty acid and cholesterol biosynthesis in liver

To investigate the role of mTORC2 signaling in the regulation of SREBP-1c in HFD-fed mice, we examined SREBP-1c activation at the transcriptional and post-translational levels. The mRNA levels of key lipogenic transcription factors, LXRα and SREBP-1c, as well as the SREBP-1c target gene, SCD-1, were robustly up-regulated in HFD-fed control mice relative to chow-fed controls (Fig. 5.7A). In contrast, HFD-fed HRicKO mice had mRNA levels of SREBP-1c and SCD-1 similar to those of chow-fed HRicKO mice, whereas LXRα mRNA levels were above chow-fed levels but significantly lower than HFD-fed controls (Fig. 5.7A). Additionally, other SREBP-1c lipogenic targets, ATP citrate lyase (ACL), FAS, and DGAT-2, were all significantly lower by ~50 to 70% in livers of HFD-fed HRicKO mice compared to HFD-fed controls, whereas no significant changes were detected for mRNA levels of ACC-1 and GPAT (Fig. 5.7B).

SREBP proteins are synthesized as inactive, membrane bound precursor proteins that become associated with the SREBP cleavage activating protein (SCAP). Insulin-induced gene (Insig) proteins reside in the ER and bind to SCAP, and thus retain the SCAP/SREBP-1c complex in the ER, preventing SREBP-1c proteolytic processing to generate an active transcription factor (370). Insulin increases degradation of the Insig-2a transcript (344, 371), which is the major liver transcript observed in fasted animals (372). We found a significant reduction in Insig-2a transcript in livers of HFD-fed HRicKO mice (Fig. 5.7B), whereas no alterations in SCAP mRNA levels were observed compared to HFD-fed controls (Fig. 5.7B). However, consistent with reduced mRNA levels of SREBP-1c, both the precursor and the mature nuclear form of SREBP-1c were reduced by ~50% in livers of HFD-fed HRicKO mice (Fig. 5.7C and D). Also consistent, protein levels of the SREBP-1c target gene, SCD-1, were significantly reduced in HRicKO compared to control mice fed a HFD (Fig. 5.7E).

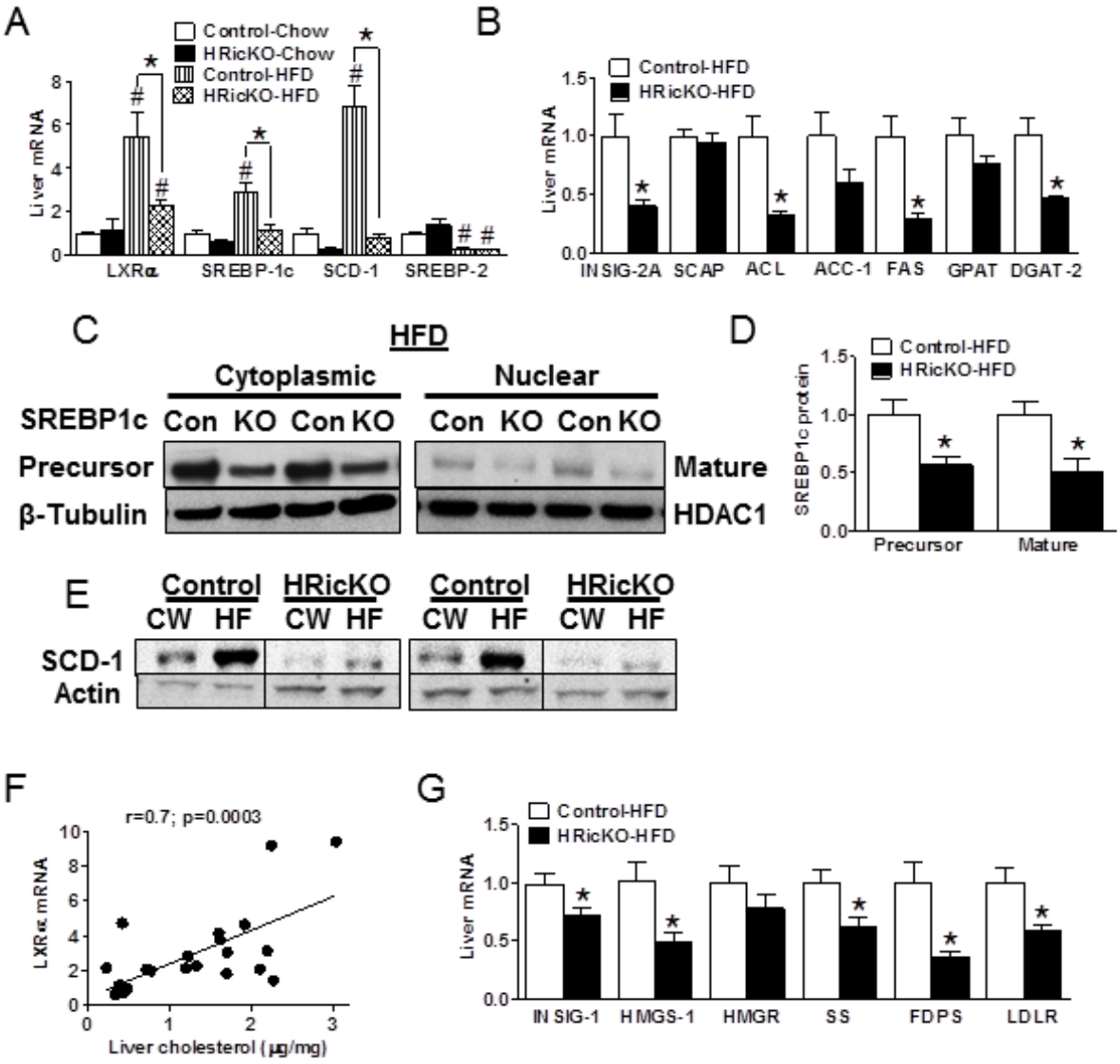

Figure 5.7. Hepatic mTORC2 deficiency in HFD-fed HRicKO mice leads to impaired regulation of insulin-stimulated *de novo* fatty acid and cholesterol biosynthesis in liver. A: mRNA levels of key transcription factors involved in lipid biosynthesis, LXRα, SREBP-1c, SREBP-2, and the SREBP-1c target lipogenic gene, SCD-1 from livers of 4-hour fasted 12 week old chow-fed HRicKO (black bars; *n*=3) and control (white bars; *n*=6) mice and from livers of 4-hour fasted 18 week old HRicKO (hatched bars; *n*=7) and control (striped bars; *n*=9) mice after 10 weeks of HFD feeding. Results are normalized to levels of chow-fed control mice. B: mRNA levels of enzymes involved in SREBP-1c processing (INSIG-2A and SCAP) and enzymes involved in fatty acid and triglyceride synthesis (ACL, ACC-1, FAS, GPAT, and DGAT-2) from livers of 4-hour fasted 18 week old HFD-fed HRicKO (black bars) and control (white bars) mice. Results are normalized to levels of control mice. C and D: SREBP-1c processing was analyzed by Western blot analysis of nuclear and cytoplasmic fractions from livers of 4-hour fasted 18 week old HRicKO (KO; black bars; *n*=7) and control (Con; white bars; *n*=9) mice after 10 weeks of HFD feeding. The precursor form was detected in cytoplasmic fractions and the mature form of SREBP-1c was detected in nuclear fractions. β-Tubulin and HDAC1 were used as marker proteins of cytoplasmic and nuclear fractions, respectively. Western blots were analyzed by

densitometry and data shown are relative to levels of control mice after normalization to β-Tubulin or HDAC1. E: Protein levels of SREBP-1c target gene, SCD-1, were analyzed in whole cell liver extracts from 12-18 week old HRicKO and control mice either on chow-diet (CW; *n*=3-6/group) or after 10 weeks of HFD (HF; *n*=7-9/group) relative to the normalization control, actin. F: Correlational analysis of LXRα mRNA expression versus liver cholesterol levels in HRicKO and control mice either on chow or HFD. G: mRNA levels of enzymes involved in SREBP-2 processing (INSIG-1) and cholesterol biosynthesis, HMGS-1, HMGR, SS, FDPS, and LDLR from livers of 4-hour fasted 18-week old HFD-fed HRicKO (black bars; *n*=7) and control (white bars; *n*=9) mice. Results are normalized to levels of control mice. Data are expressed as mean ± SEM and were analyzed by Student's *t*-test (unpaired, two-tailed); *indicates a significant difference ($p<0.05$) from control mice. $^{\#}$indicates a significant difference ($p<0.05$) from chow-fed mice of the same genotype.

The mechanism for reduced SREBP-1c expression might be transcriptional rather than translational or post-translational. We hypothesized that reduced LXRα action in combination with reduced nuclear SREBP-1c in livers of HFD-fed HRicKO mice may impair the ability of insulin to fully induce SREBP-1c in a feed forward manner, and thereby fail to induce lipogenesis (357). Interestingly, we found that LXRα mRNA levels positively correlated with liver cholesterol content in both chow and HFD-fed mice (r=0.7; p=0.0003; Fig. 5.7F). In addition, HFD-fed HRicKO mice have significantly reduced liver cholesterol levels compared to HFD-fed controls (Fig. 5.3E) and the oxidized form of cholesterol (oxysterol) is known to act as an activating ligand for LXRα (359-361). These correlations raised the possibility that in addition to reduced LXRα expression, there may also be a failure to activate existing LXRα protein. We, therefore, quantified markers of cholesterol biosynthesis, which ultimately generate LXRα agonists.

As expected (360, 362), feeding HFD, which contains 0.1% cholesterol (0.95mg/g), to HRicKO and control mice led to a robust reduction in mRNA levels of liver SREBP-2 relative to chow-fed mice (Fig. 5.7A). However, mRNA levels of many of the target genes of SREBP-2, including the cholesterogenic enzymes HMG-CoA synthase-1 (HMGS-1), squalene synthase (SS), farnesyl diphosphate synthase (FDPS) and the LDLR, but not HMG-CoA reductase (HMGR) were lower by ~40 to 60% in the HFD-fed HRicKO livers compared to HFD-fed controls (Fig. 5.7G). Surprisingly, we did not detect lower SREBP-2 mRNA levels in HFD-fed HRicKO mice, but found levels similar to those of HFD-fed control mice (Fig. 5.7A). Likewise unexpected, mRNA levels of the sterol responsive Insig-1, which regulates SREBP-2 processing (370), were also significantly reduced in livers of HFD-fed HRicKO mice (Fig. 5.7G). *Collectively, these data support a working model whereby hepatic rictor and mTORC2 activity is required to maintain elevated expression of SREBP-2 target genes, thereby increasing cholesterol levels in HFD-fed control mice. In HRicKO mice with reduced cholesterol, LXRα ligands*

(oxysterols) necessary for LXRα activation may be lacking, thereby blocking the cooperative interaction of insulin and LXRα activity to fully induce SREBP-1c mediated lipogenesis.

Activation of hepatic LXRα rescues glycemic and lipogenic, but not cholesterol biosynthetic defects in HFD-fed HRicKO mice

Given that our model centers upon a defect in LXRα activation, we sought to determine if treatment with a selective LXR agonist, T0901317 (366), would rescue the altered glucose and lipid metabolism observed in the HFD-fed HRicKO mice. HFD-fed control and HRicKO mice were treated daily with IP injections of T0901317 (50 mg/kg body weight) or vehicle, and then studied for effects on glucose and lipid metabolism in the *ad-libitum* fed state on day 2 and 6 of treatment. On day 2, the LXR agonist-treated group had reduced blood glucose levels in both control and HRicKO mice; although the effect was of greater magnitude in HRicKO mice given their initially higher glucose levels (Table 5.2). Plasma TG levels were increased by 4- and 8-fold in HRicKO and control mice, respectively, with LXR agonist treatment (Table 5.2). Markers of adipocyte lipolysis, FFA and glycerol, were elevated in both LXR agonist-treated control and HRicKO mice (Table 5.2). Elevated lipolysis may have supplied substrate for enhanced liver lipoprotein synthesis and the resulting hypertriglyceridemia (23, 24, 315). LXR agonist did not, however, increase plasma cholesterol levels in HRicKO mice to those of control levels by day 2 of treatment (Table 5.2).

On day 6 of LXR agonist treatment, blood glucose levels remained significantly reduced and elevated plasma insulin levels in HRicKO mice were normalized (Table 5.2). Elevated plasma TG found on day 2 of LXR agonist treatment was attenuated by day 6 (Table 5.2), consistent with previous findings (373), and is thought to be due to reduced lipolysis and increased lipoprotein lipase activity in liver (374). Elevated plasma cholesterol levels were significantly reduced in LXR agonist-treated control mice, whereas no changes in cholesterol levels were seen in the HRicKO mice (Table 5.2).

Table 5.2. Metabolic parameters measured on day 2 and 6 in *ad-libitum* high-fat diet-fed control and HRicKO mice treated intraperitoneal (IP) daily with either a selective LXR agonist T0901317 or vehicle

		Control		HRicKO	
		Vehicle	T0901317	Vehicle	T0901317
Glucose	Day 2	130±5	98±5*	241±29#	104±4*
mg/dl	Day 6	168±9	74±11*	160±12	106±4*,#
Triglyceride	Day 2	72.8±4.7	552±58*	48.7±2.9#	191±39*,#
mg/dl	Day 6	74.6±7.0	122±22*	68.0±3.3	73.1±8.4#
Free Fatty acid	Day 2	0.36±0.04	1.01±0.11*	0.33±0.03	0.70±0.02*,#
mmol/l	Day 6	0.27±0.04	0.57±0.13*	0.24±0.04	0.31±0.01#
Glycerol	Day 2	52.7±2.8	102±9*	53.9±2.5	73.9±6.5*,#
mg/dl	Day 6	54.9±3.6	59±14	56.0±6.0	64.9±7.5
Cholesterol	Day 2	238±10	230±16	127±19#	158±13#
mg/dl	Day 6	215±9	155±11*	139±16#	172±8
Insulin	Day 2	-	-	-	-
ng/ml	Day 6	3.6±0.7	2.8±1.9	15.3±3.9#	4.4±0.6*
Epid Fat pad	Day 2	-	-	-	-
weight (g)	Day 6	2.3± 0.2	1.6±0.1*	1.2±0.2#	1.1±0.1#

After 23 weeks of feeding a high-fat diet, HRicKO and control mice at 45 weeks of age were treated IP daily with either a selective LXR agonist T0901317 (50 mg/kg BW) or vehicle for a total of 6 days. On day 2 of treatment, blood was collected by submandibular bleed in *ad-libitum* fed LXR agonist-treated and vehicle-treated mice to measure plasma hormone and metabolite levels (n=5/group). On day 6 of treatment, blood and epididymal (epid) fat pads were collected from euthanized *ad-libitum* fed LXR agonist-treated (n=3-5/group) and vehicle-treated mice (n=5/group) to measure plasma hormone and metabolite levels, as well as, epid fat pad weights. Data are expressed as mean ± SEM and were analyzed by Student's t-test (unpaired, two-tailed); *indicates a significant difference ($p<0.05$) from vehicle-treated mice. #indicates a significant difference ($p<0.05$) from control mice of the same treatment.

Consistent with elevated adipocyte lipolysis, the epididymal fat pad weights were significantly reduced in LXR agonist-treated control mice, whereas the LXR agonist treatment did not further reduce fat pad weights in the HRicKO mice (Table 5.2). LXR agonist increased liver weights by 1.3- and 1.5-fold in control and HRicKO mice, respectively (Fig. 5.8A). These LXR-treated livers were engorged with medium- to large-sized intracellular lipid droplets relative to vehicle-treated mice (Fig. 5.8E), indicating enhanced lipogenesis. Consistent with this histology, LXR agonist treatment in control and HRicKO mice increased liver TG content by 5-

and 12-fold, respectively (Fig. 5.8B). In contrast, liver cholesterol content decreased by 47% and 67% in control and HRicKO mice, respectively (Fig. 5.8C). LXR agonist-treated control and HRicKO mice had elevated liver FFA content (Fig. 5.8D). Collectively, these data demonstrate that chronic LXRα activation ameliorates the dysglycemia while restoring hepatic steatosis and hypertriglyceridemia in HFD-fed HRicKO mice.

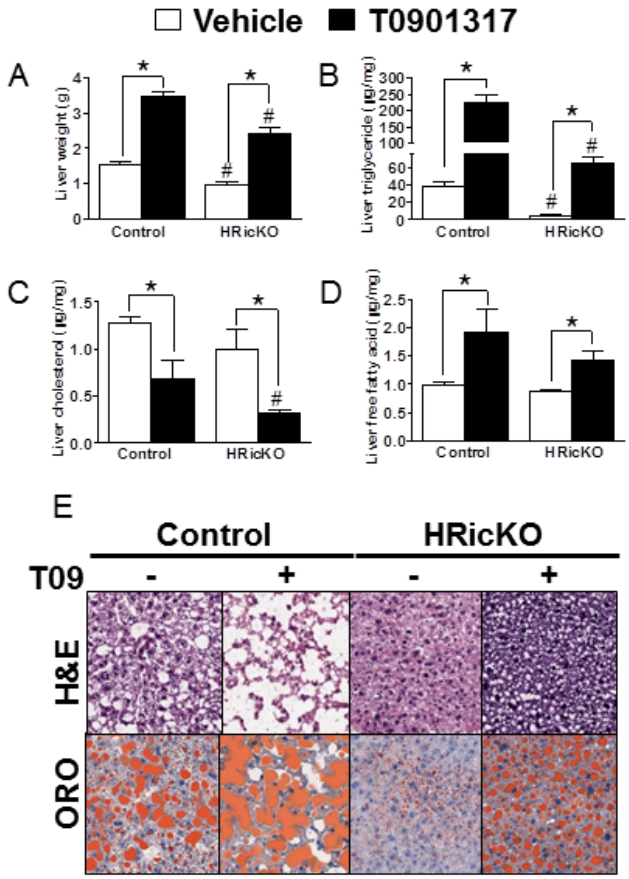

Figure 5.8. Activation of hepatic LXRα rescues glycemic and lipogenic, but not cholesterol biosynthetic defects in HFD-fed HRicKO mice. After 23 weeks of feeding a HFD, HRicKO and control mice at 45 weeks of age were treated intraperitoneal (IP) daily with either a selective LXR agonist (T0901317, 50 mg/kg BW) or vehicle for a total of 6 days. A-E: On day 6 of treatment, liver tissues were collected from euthanized *ad-libitum* fed HRicKO and control mice treated with ether LXR agonist (black bars; *n*=3-5/group) or vehicle (white bars; *n*=5/group) to measure the following: (A) liver weights and hepatic content of (B) TG, (C) cholesterol and (D) FFA. E: Representative images of H&E and ORO staining from livers of *ad-libitum* fed HRicKO and control mice treated with either the LXR agonist T0901317 (T09) or vehicle for 6 days; original magnification, 20X. Data are expressed as mean ± SEM and were analyzed by Student's *t*-test (unpaired, two-tailed); *indicates a significant difference ($p<0.05$) from vehicle-treated mice. $^{\#}$indicates a significant difference ($p<0.05$) from control mice of the same treatment.

Hepatic LXRα activation suppresses PEPCK while robustly stimulating SREBP-1c

We investigated whether the effects of LXRα activation on glucose and lipids correlated with changes in relevant gluco- and lipo-regulatory LXRα target genes. SREBP-1c mRNA levels were induced by ~2- and 3-fold in livers of LXR agonist-treated *ad-libitum* HFD-fed control and HRicKO mice, respectively (Fig. 5.9A). Hepatic SCD-1 mRNA levels, a gene target of LXRα and SREBP-1c, were robustly upregulated by 14- and 60-fold in control and HRicKO mice, respectively (Fig. 5.9B). ACL mRNA levels, a lipogenic gene target of SREBP-1c, was upregulated by 2-fold in livers of HRicKO mice (Fig. 5.9C).

LXR agonist treatment induced a significant increase in mature (transcriptionally active) and precursor forms of SREBP-1c protein in HRicKO livers (Fig. 5.10A-C). In contrast, in LXR agonist-treated control mice, the level of the mature form of SREBP-1c was significantly increased (Fig. 5.10A and C) with no alteration in the level of the precursor form relative to vehicle treatment (Fig. 5.10A and B). Interestingly, the LXR agonist induced Insig-2 expression (Fig. 5.10A and D), which is involved in inhibiting the cleavage of SREBP-1c. LXR agonist treatment induced protein levels of the lipogenic enzymes, ACC and SCD-1 in HRicKO livers similar to those of LXR-treated controls (Fig. 5.10A, E and G). Conversely, FAS and ACL were significantly induced only in LXR agonist-treated HRicKO livers (Fig. 5.10A, F and H).

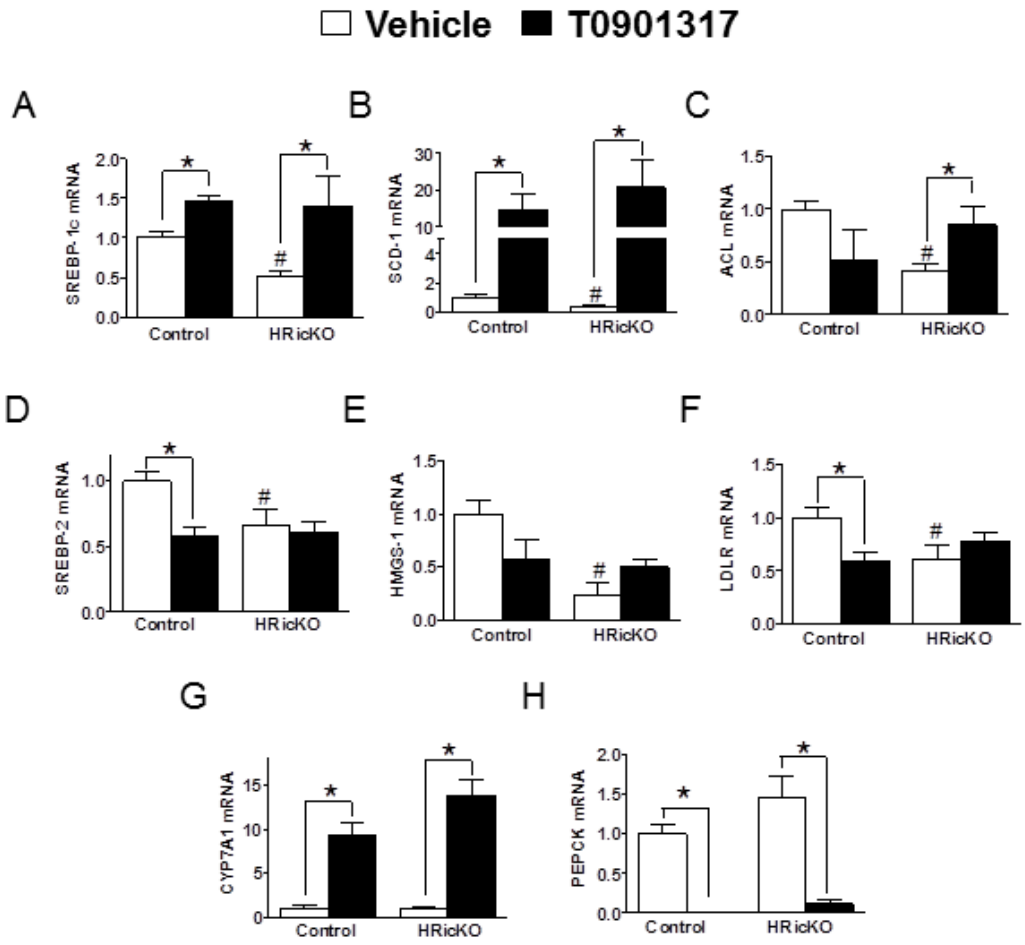

Figure 5.9. Analysis of mRNA levels of direct target genes of LXRα from livers of HRicKO mice treated with either LXR agonist or vehicle. A-H: mRNA levels of direct target genes of LXRα from livers of 45 week old HFD-fed HRicKO and control mice either treated daily IP with the LXR agonist T0901317 (black bars; *n*=3-5/group) or vehicle (white bars; *n*=5/group) for 6 days. The gene expression levels for (A) SREBP-1c, (B) SCD-1, (C) ACL, (D) SREBP-2, (E) HMGS-1, (F) LDLR, (G) CYP7A1, and (H) PEPCK were analyzed. Results were normalized to levels of vehicle-treated control mice. Data are expressed as mean ± SEM and were analyzed by Student's *t*-test (unpaired, two-tailed); *indicates a significant difference ($p<0.05$) from vehicle-treated mice and $^{\#}$indicates a significant difference ($p<0.05$) from control mice of the same treatment.

Remarkably, the transcript levels of genes associated with cholesterol biosynthesis, SREBP-2, HMGS-1, and LDLR were consistently reduced in vehicle-treated *ad-libitum* HFD-fed HRicKO mice relative to vehicle-treated controls (Fig. 5.9D-F). Treatment with LXR agonist reduced SREBP-2 and expression of its target genes in control mice, whereas LXR agonist

treatment did not further reduce expression of these genes in the HRicKO livers (Fig. 5.9D-F). Conversely, a direct target of LXRα, cholesterol 7a-hydroxylase-1 (CYP7A1), which is a rate limiting enzyme in the synthesis of bile acids from cholesterol (362), was upregulated by 9- and 13-fold in livers of LXR-treated control and HRicKO mice, respectively (Fig. 5.9G).

In contrast to increased expression of lipogenic genes, PEPCK expression in both control and HRicKO mice was dramatically downregulated at both mRNA (Fig. 5.9H) and protein levels (Fig. 5.10A and I), confirming results of previous work that showed T0901317 decreased hepatic gluconeogenesis in *db/db* mice (375, 376). Thus, chronic LXRα activation with a selective LXR agonist, T0901317, in HFD-fed HRicKO mice ameliorates hyperglycemia, likely via suppressing expression of the key gluconeogenic enzyme, PEPCK, while stimulating a SREBP-1c mediated lipogenic program in liver.

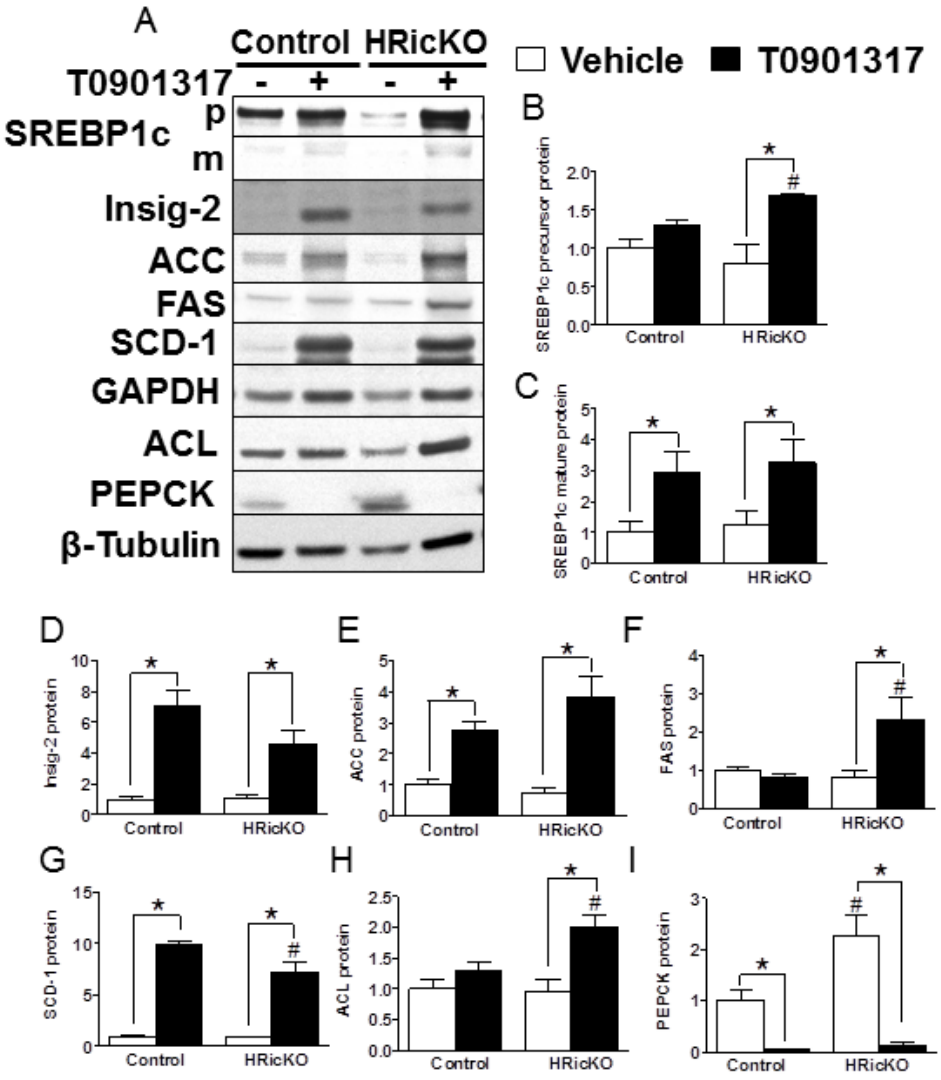

Figure 5.10. Hepatic LXRα activation suppresses PEPCK while robustly stimulating SREBP-1c. A-I: Western blot analysis of proteins (A) that are direct target genes of LXR in whole cell liver extracts from 45 week old HFD-fed HRicKO and control mice either treated IP daily for 6 days with the LXR agonist T0901317 (black bars; *n*=3-5/group) or vehicle (white bars; *n*=5/group): the precursor form (p in A and B) and mature form (m in A and C) of SREBP-1c, (D) Insig-2, (E) ACC, (F) FAS, (G) SCD-1, (H) ACL, and (I) PEPCK. Western blots were analyzed by densitometry and data shown are relative to levels of vehicle-treated control mice after normalization to GAPDH or β-Tubulin. Data are expressed as mean ± SEM and were analyzed by Student's *t*-test (unpaired, two-tailed); *indicates a significant difference ($p<0.05$) from vehicle-treated mice. #indicates a significant difference ($p<0.05$) from control mice of the same treatment.

Discussion

The gluco- and lipo-regulatory effects of hepatic AKT are largely due to the suppression of the FoxO1-gluconeogenic pathway and the regulation of the SREBPs, respectively. Because AKT is also regulated by other inputs (PDK-1), and is a major mediator of insulin's effect on metabolic processes, we sought to determine whether hepatic rictor directed mTORC2 activity is required for the regulation of liver lipid metabolism. *Specifically, we hypothesized that hepatic rictor directed mTORC2 activity is required to regulate SREBP-2 mediated cholesterogenesis in order to fully stimulate SREBP-1c mediated lipogenesis through oxysterol dependent activation of LXRα.* In the absence of hepatic mTORC2 regulatory protein, rictor, there is a dramatic decrease in mTORC2 mediated phosphorylation of AKT Ser473 in response to insulin. Although hepatocyte mTORC2 deficiency in chow-fed HRicKO mice confers little effect, we observed that HFD-feeding amplified hyperglycemia, insulin resistance, and hyperinsulinemia in HRicKO mice. Yet, paradoxically, these mice are lean on HFD and are protected from diet-induced hepatic steatosis and hyperlipidemia as previously reported (347, 348). Resistance to fat mass gain may be due to an increase in energy expenditure and fat oxidation, an effect independent of DIO, as this was observed in lean LFD-fed HRicKO mice (Table 5.1).

In agreement with prior observations, hepatic mTORC2 deficiency affects signaling through AKT and FoxO1 leading to impaired inhibition of the FoxO1-gluconeogenic pathway (347, 348). Defective regulation of FoxO1 and glucoregulatory genes would explain the glucose intolerance and compensatory hyperinsulinemia observed in the HFD-fed HRicKO mice. Yet, HRicKO mice failed to develop hepatic steatosis and dyslipidemia on exposure to HFD; they had lower triglyceride and cholesterol levels in both plasma and liver. We ruled out a contribution of impaired intestinal lipid absorption, since fecal lipid contents were not different among the mice. *The lack of impaired lipid absorption or increased excretion, therefore, suggested that defects in regulation of hepatic lipid biosynthesis were likely in the absence of mTORC2 signaling.* In support of this hypothesis, hepatic mTORC2 deficiency led to lower hepatic SCD-1 activity (215,

330), which in turn, contributes to the reduced availability of MUFAs that are necessary for TG and CE biosynthesis (329, 330).

In addition to reduced fatty acid desaturation, we also observed failure of a HFD to induce mRNA levels of SREBP-1c, SREBP-2 and their target genes involved in fatty acid, triglyceride, and cholesterol biosynthesis in HRicKO mice in corroboration with previous findings (347, 348). Interestingly, while hepatic FFA content was slightly elevated in both chow and HFD-fed HRicKO mice, a marker of adipocyte lipolysis in the form of plasma FFA was similarly elevated suggesting that the source of these excess FFA are derived from the periphery rather than from hepatic *DNL*. Additional support of the gene expression data is the concomitant finding of reduction in both the precursor and the mature form of the master transcriptional regulator of lipogenesis, SREBP-1c (347, 348).

Our data agree with previous observations that AKT2 is required for hepatic lipid accumulation in obese, insulin resistant mouse models (285). Indeed, in the study by Hagiwara et al. (348), the restoration of AKT2 signaling in rictor deficient hepatocytes rescued SREBP-1c and *DNL*. However, this study did not report whether restoration of AKT2 rescued SREBP-2 mediated cholesterol biosynthesis. Thus, we sought to extend this work in an effort to identify a molecular mechanism underlying the reduced activation of SREBP-1c and lipogenesis in HRicKO livers which may be coupled to cholesterol metabolism in liver and partially independent of AKT and mTORC1 signaling.

Recent cell culture and animal based studies suggest that activation of SREBP-1c and lipogenesis by AKT requires mTORC1 (344, 346, 352-355). One of the mechanism by which mTORC1 activates SREBP-1c is by the phosphorylation and nuclear exclusion of lipin-1, preventing lipin-1 mediated downregulation of nuclear SREBP-1c protein (346). Furthermore, loss of mTORC1 regulation of lipin-1 by hepatocyte specific deletion of raptor led to a resistance to hepatic steatosis and hypercholesterolemia in HFD-fed mice, and this phenotype was largely reversed by the adenoviral shRNA depletion of hepatic lipin-1 (346). Similarly, this defect was

reported by Yuan et al. (347) in hepatocyte specific rictor knockout mice concluding that lipogenesis requires mTORC2 to fully and independently activate both mTORC1 and AKT. However, this is contrary to our findings in which we observed intact mTORC1 mediated phosphorylation of lipin-1 in response to insulin in HRicKO livers, suggesting that the loss of mTORC1 regulation of SREBP-1c may not be the primary underlying mechanism, at least in our animals. Moreover, activation of mTORC1 either by hepatocyte-specific deletion of TSC1 or following a high carbohydrate meal in hepatic AKT2 knockout mice demonstrate that mTORC1 is insufficient to stimulate SREBP-1c mediated lipogenesis in the absence of AKT2 signaling (344, 377, 378). Thus, as also observed by Hagiwara et al. (348), intact mTORC1 activity in the context of genetically impaired mTORC2 leads to reduced SREBP-1c activation and defective lipogenesis, suggesting that activation of SREBP-1c may be partially independent of mTORC1.

An mTORC1 independent mechanism by which insulin-AKT2 signaling activates SREBP-1c is via the inhibition and degradation of Insig-2a transcript, while reciprocally augmenting Insig-1 gene expression (371). Thereby, this stimulates the ER-to-Golgi transport of the SCAP/SREBP-1c complex, ultimately stimulating SREBP-1c proteolytic processing to generate an active transcription factor (344, 371). Knockdown of Insig-2a expression mimics insulin-induced SREBP-1c proteolysis whereas exogenous expression of Insig-2a in hepatocytes blocks this effect (371). However, the observed reduction in both Insig-1 and Insig-2a transcripts in livers from HFD-fed HRicKO mice in our study did not translate to the expected greater levels of mature SREBP-1c. Thus, this implicates the possibility of increased degradation of mature SREBP-1c protein levels in HRicKO livers.

AKT prevents the degradation of mature SREBP-1c by the phosphorylation and inhibition of GSK3α/β preventing GSK3 mediated activation of the ubiquitin-proteasome pathway (379-381). Indeed, Hagiwara et al. (348) observed this defect in the livers of the hepatocyte specific rictor knockout mice concluding that constitutively active GSK3 and enhanced degradation of mature SREBP-1c may be the underlying mechanism for impaired

SREBP-1c activation. However, our observation that insulin-induced phosphorylation of GSK3β is intact in the HRicKO livers further suggest that GSK3 mediated degradation of SREBP-1c is not the underlying mechanism in our animals. Clearly, our data shows that hepatic rictor directed mTORC2 activity and subsequent AKT Ser473 phosphorylation is not required for the regulation of Insig-2a, GSK3β, and mTORC1, all mechanisms involved in the regulation of SREBP-1c. Thus, we sought to identify a novel, underlying defect in SREBP-1c activation in mTORC2 deficient hepatocytes that may occur partially independent of AKT.

A clue to a potential mechanism was revealed by the finding of significantly lower levels of plasma and liver cholesterol in HFD-fed HRicKO mice. SREBP-2 is a master regulator of liver cholesterol biosynthesis and its expression is significantly lower in livers of *ad-libitum* HFD-fed HRicKO mice. SREBP-2 positively regulates the expression of numerous genes involved in cholesterol biosynthesis, all of which were reduced in the livers of HRicKO mice. Unfortunately, commercially available antibodies were not of sufficient quality to detect SREBP-2 by Western blot analysis, so mRNA levels of target genes were assessed.

Connecting reduced SREBP mediated fatty acid and cholesterol biosynthesis is the knowledge that derivatives of cholesterol biosynthesis, oxysterols, serve as agonists for the nuclear transcription factor, LXRα, which in turn, positively regulates SREBP-1c expression (359-361). Consistent with the fact that oxysterols stimulate LXRα activity, is the observation in our mice that liver cholesterol content is strongly correlated with LXRα mRNA levels. *Thus, we hypothesized that reduced liver cholesterol content leads to reduced LXRα agonist levels (presumably oxysterol), which would lower LXRα transcriptional activity, and thus attenuate SREBP-1c expression and target gene activation.* Indeed, both LXRα and the nuclear form of SREBP-(1c and 2) bind regulatory sites (LXRE and SRE) on the *SREBF1* promoter to fully induce its transcription in response to insulin-AKT signaling in a feed forward fashion (357).

To test this hypothesis, we asked whether a selective LXRα agonist would rescue SREBP-1c expression, processing, transcriptional regulation, and lipogenesis. The selective

LXRα agonist, T0901317, has been shown both *in vitro* and *in vivo* to regulate LXR target genes (366, 373, 375, 382). Indeed, in our HRicKO mice, the LXR agonist rescued SREBP-1c expression, processing, and target gene expression. Functionally, LXR agonist treatment increased liver weight, liver triglyceride content, and potently enhanced steatosis in both control and HRicKO mice. Thus, the impaired induction of cholesterol biosynthesis resulting from *Rictor* gene deletion and reduced mTORC2 signaling appears to have resulted in attenuated LXRα transcriptional activity, and ultimately explaining the defects in SREBP-1c expression and function.

Interestingly, LXR agonist treatment paradoxically induced Insig-2 protein levels (an inhibitor of SREBP-1c processing) in both control and HRicKO mice. This observation can be reconciled by other published work, which suggests that concurrent induction of Insig-2 by LXRα may act to provide a readily available pool of SREBP-1c precursor that is primed for immediate cleavage by insulin-induced mechanisms (383). Of note, the marked decrease in liver cholesterol content in both LXR agonist-treated control and HRicKO mice was most likely due to the suppressive effects of the LXR agonist on SREBP-2 mediated cholesterol biosynthesis together with increased CYP7A1 directed cholesterol catabolism in liver, as reported by previous studies (362, 366).

Our data collectively supports a model (Fig. 5.11) where HFD-induced obesity, a state characterized by hyperinsulinemia and nutrient overload, requires hepatic rictor directed mTORC2 activity to stimulate SREBP-2 mediated cholesterol biosynthesis. Thus, cholesterol derived either from the diet or synthesized *de novo*, may provide the oxysterol agonists of LXRα necessary for activation. This ultimately enables the cooperative interaction of LXRα and insulin-AKT signaling to fully induce SREBP-1c mediated lipogenesis. As a result, HFD feeding in wild-type mice leads to the development of hepatic steatosis and dyslipidemia.

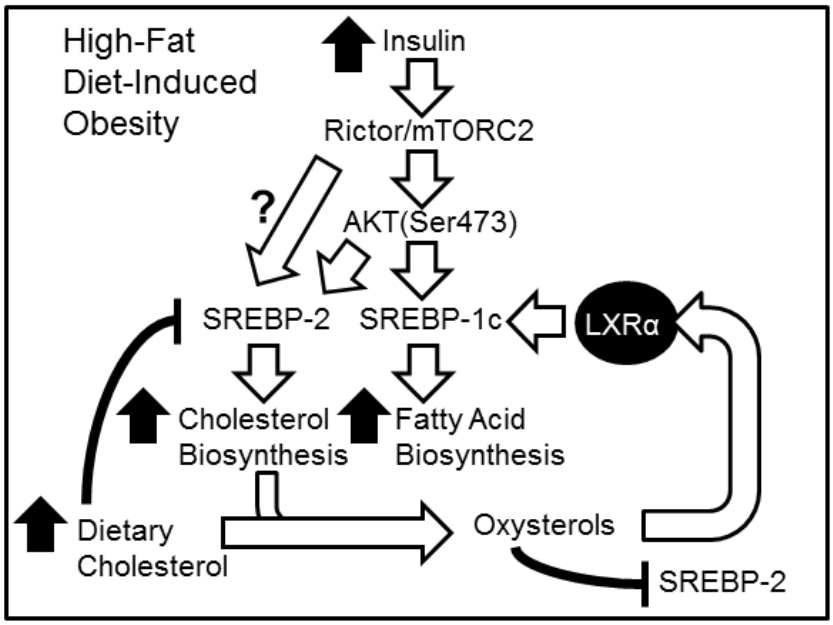

Figure 5.11. Model for the role of rictor directed mTORC2 activity in the regulation of hepatic lipid metabolism in high-fat diet-induced obesity.

Additionally, high-fat diet feeding in wild-type mice results in the accumulation of sterol metabolites, including cholesterol and oxysterols, and these metabolites tightly regulate cholesterol homeostasis in liver by binding to SCAP and/or Insig-1 to promote ER retention of SCAP/SREBP-2 complex as a negative feedback inhibition of SREBP-2 mediated cholesterol biosynthetic pathway (384). Concomitantly, oxysterol dependent activation of LXRα promotes the feed-forward induction of cholesterol catabolism in liver (362).

Our study did not definitively address whether hepatic rictor directed mTORC2 activity regulates SREBP-2 mediated cholesterol biosynthesis independently of AKT and/or other pathways. Other studies report that multiple molecular pathways are involved in the regulation of SREBP-2 and cholesterol metabolism, including mTORC1, PI3K/AKT, and MAP-kinase pathways in brain and liver (345, 346, 356, 385). Furthermore, hepatocyte specific deletion of AKT2 alone or in hepatic PTEN null mice leads to a robust reduction in SREBP-2 expression indicating that SREBP-2 regulation requires AKT2 (288). Therefore, to delineate the role of

rictor/mTORC2 in SREBP-2 regulation, future studies may involve investigating whether the overexpression of rictor in AKT2 null hepatocytes will restore SREBP-2 and cholesterol biosynthesis whereas expression of constitutively active AKT2 in rictor deficient hepatocytes may abolish this effect.

Another intriguing finding of our study is that hepatic rictor/mTORC2 mediated AKT Ser473 (and not Thr308) phosphorylation may be coupled to the regulation of SREBPs. To further investigate this observation, future studies would involve the genetic deletion of rictor in hepatocyte specific PTEN null mice to determine whether the attenuation of Ser473 in the presence of constitutively active Thr308 will phenocopy the loss of fatty liver observed in the double mutant PTEN/AKT2 null mice (288). The confirmation that Ser473 AKT is coupled to liver lipid metabolism may reveal novel therapeutic approaches to treat NAFLD and atherogenic dyslipidemia via the selective modulation of mTORC2 kinase activity.

In summary, we show loss of hepatic rictor and mTORC2 deficiency uncouples insulin regulation of glucose from lipid homeostasis on exposure to HFD leading to impaired suppression of the FoxO1-gluconeogenic pathway and failure to stimulate SREBP mediated fatty acid, triglyceride, and cholesterol biosynthesis. Our data suggest the intriguing possibility that selective modulation of mTORC2 kinase activity could lead to the suppression of the liporegulatory branch (LXRα, SREBP-1c and/or SREBP-2) while maintaining the glucoregulatory branch (FoxO1) resulting in the protection against the development of dysglycemia and hyperlipidemia associated with obesity, diabetes, and the metabolic syndrome.

CHAPTER VI

SUMMARY AND FUTURE DIRECTIONS

Overview

CVD remains one of the leading causes of death in the US and worldwide (6, 8). In an effort to curb this epidemic, clinicians have become increasingly adept at identifying and treating the classical cardiovascular risk factors, particularly hypercholesterolemia, hypertension, and smoking (4). For example, in the Heart Protection Study, the therapeutic effect of statin therapy to lower LDL-C levels in high risk patients produced a substantial 25% reduction in major CVD events and is a public health success (5). Yet, closer inspection reveals that 75% of the CVD risk remained despite statin therapy. *One hypothesis to explain this unaddressed risk is that the parallel obesity and diabetes epidemics (9) have generated additional novel factors for CVD beyond those in the Framingham model and beyond absolute LDL-C levels.*

An increasing healthcare burden is due to the complications of hyperlipidemia, such as CVD, cerebrovascular disease, and peripheral vascular disease. Elevated VLDL-TG secretion from liver contributes to atherogenic dyslipidemia consisting of small-dense LDL-C and reduced HDL-C levels (14-16) associated with obesity and diabetes. Hypertriglyceridemia and overproduction of VLDL-TG are key components of the metabolic syndrome (14-16) and atherogenic dyslipidemia, which is an increasingly recognized component of cardiovascular risk (16). Thus, a better understanding of the biology behind the regulation of lipoprotein metabolism, particularly in novel areas investigating the dyslipidemia associated with obesity and diabetes, may lead to fundamentally novel therapeutic treatments aimed at lowering some or all of the remaining CVD risk.

A current model of dyslipidemia in the context of obesity and diabetes, suggests that the VLDL-TG secretion rate is largely determined by the rate of substrate (FFA) delivery to the liver

and hepatic insulin sensitivity (23-25). Thus, a key component of the model is that as visceral fat mass expands, insulin resistance at the adipose and liver tissue develops. Adipocyte insulin resistance results in elevated adipocyte lipolysis, which is normally potently suppressed by insulin. Lipolysis leads to the release of FFA and glycerol into the portal circulation which are efficiently cleared by the liver and re-esterified to generate TG. This TG is loaded onto a nascent apoB particle, ultimately resulting in increased production of VLDL-TG (23-25), a process that is ordinarily suppressed by integrated hepatic insulin action (29, 30).

While peripheral factors clearly contribute to this disorder (23, 24), we hypothesized that regulation of lipid homeostasis is normally subject to additional CNS regulatory forces. CNS NPY expressing neurons, concentrated in the mediobasal hypothalamus as well as numerous other brain regions, are an important regulator of feeding and energy homeostasis, and increasingly recognized as having a role in lipid homeostasis (211, 222). Elevated hypothalamic NPY tone with a concomitant reduction of POMC tone is associated with obesity and diabetes in rodent models (139, 140) and humans (98, 143, 144), likely due to defects in inhibitory feedback signals to the CNS, i.e. insulin and leptin resistance (74, 75). We (211, 222) and others (191, 192) clearly show that CNS NPY signaling is also an important regulator of lipoprotein metabolism. We previously demonstrated that ICV administration of NPY directly into the third ventricle of lean, fasted, wild-type rats increases hepatic VLDL-TG secretion independently of increased food intake and visceral adiposity (211, 222). Peripherally administered NPY had no such effect and taken together, these findings suggest that NPY-regulated neural circuits may be involved in the regulation of TG metabolism in the liver (211, 222). *Thus, the overarching hypothesis is that elevated CNS NPY action contributes to dyslipidemia by activating central circuits that modulate liver lipid metabolism.*

This body of work is focused on identifying the mechanisms by which increased CNS NPY modulates hepatic lipoprotein metabolism, which involves the investigation of the molecular determinants in the hypothalamus (Chapter III) and hepatic-specific mechanisms

(Chapter IV). Numerous pharmacologic and genetic studies have investigated the role of CNS NPY receptor subtype(s), Y1, Y2, Y4, and Y5 in mediating the central NPY effect on feeding behavior and energy homeostasis (reviewed in (93, 386)). Yet, the receptor subtype(s) involved in the central NPY regulation of lipoprotein metabolism are not well understood. Nor is the relative effect of a given receptor on feeding versus lipoprotein metabolism. We designed the experiments in Chapter III to determine whether the effects of CNS NPY receptor subtype(s), Y1, Y2, Y4, and Y5 on feeding behavior versus VLDL-TG secretion overlap or are dissociable in lean rats. Ultimately, this work might provide insight into structure-function relationships within NPY-regulated neural circuits that not only control energy balance, but also lipoprotein metabolism.

The hepatic-specific molecular mechanisms by which increased CNS NPY signaling rapidly regulates hepatic lipoprotein metabolism are not well understood. Nor is the lipid source that generates the TG that is loaded onto the nascent VLDL particle in response to increased CNS NPY action currently known. In Chapter IV, we sought to identify the novel regulatory mechanisms in the liver engaged by NPY. Altogether, this work has overarching implications in further understanding how obesity-related CNS dysfunction contributes to the pathophysiology of the metabolic syndrome.

The role of CNS NPY receptor subtype(s) on feeding behavior versus lipoprotein metabolism

The studies in Chapter III were designed to determine if the effects of CNS NPY on feeding and/or weight gain are dissociable from the effects on hepatic VLDL-TG secretion. We employed two approaches: first, asking whether NPY retains the effect on hepatic VLDL-TG secretion chronically in the absence of increased food intake and weight gain; and second, whether different NPY receptor subtype(s), Y1, Y2, Y4, and Y5 mediate effects on feeding versus hepatic VLDL-TG secretion. First of all, results from these studies demonstrate that chronic ICV NPY injections in rats pair-fed to vehicle-treated controls develop

hypertriglyceridemia in the absence of increased food intake and body fat accumulation. Next, we found that an acute ICV injection of selective Y1, Y2, Y4, and Y5 receptor agonists all induced hyperphagia in lean *ad-libitum* fed rats with the Y2 receptor agonist having the most pronounced effect. Lastly, we found at equipotent doses for food intake, NPY Y1 receptor agonist robustly stimulated hepatic VLDL-TG secretion, while a Y2 receptor agonist had a modest effect on VLDL-TGs, and no effect was observed for Y4 and Y5 receptor agonists in lean fasted rats. As summarized in Table 6.1, our results collectively suggest that while Y1 and Y2 receptor agonists both regulate plasma TG levels and food intake, an NPY signal mediated through a Y1 receptor more potently increases hepatic TG production, while one mediated through the Y2 receptor has a greater effect on food intake. Altogether, these findings raise the possibility that NPY regulates feeding and lipoprotein metabolism partially via separate NPY receptor systems and/or mechanisms. Ultimately, these findings may lend plausibility that the brain is a potential therapeutic target to treat obesity dyslipidemia.

Table 6.1. Summary of the effects of NPY receptor subtype agonists on feeding behavior versus effects on hepatic VLDL-TG secretion in lean rats

NPY Receptor Subtype Agonist	*Ad-libitum* Food Intake	Hepatic VLDL-TG Secretion
Y1	↑	↑↑
Y2	↑↑	↑
Y4	↑	↔
Y5	↑	↔

However, there a number of caveats to our experimental design in Chapter III. One major caveat is whether a single ICV injection of NPY is producing a physiologic effect or if it is merely producing a non-specific pharmacologic effect. Moreover, we currently do not know the

local concentrations of NPY in the relevant brain regions. A single injection of ICV NPY could conceivably result in elevated concentrations and, therefore, produce non-specific or off-target signaling events in the CNS. Another caveat is the location of administration whereby ICV NPY injection could disperse to other non-hypothalamic regions. To address these caveats, we identified an ICV dosage of NPY that produced a physiologic response. Indeed, we show that ICV NPY treatment (1 nmol) produced a similar 2-hour feeding response in an *ad-libitum* fed lean rat as observed in the 12-hour fasted rat (characterized by high endogenous NPY tone). Furthermore, we matched the NPY receptor subtype agonists (Y1, Y2, Y4, and Y5) for potency on feeding behavior (similar to a 12-hour fast), with the exception of the Y2 receptor agonist. Thus, we generated approximately equipotent doses (1-2 nmol) for our food intake and lipid studies.

An additional caveat of our experimental design is that we utilized only a single dosage of each test compound. It is conceivable that, at significantly higher or lower doses, opposite and/or differential effects on feeding relative to VLDL-TG secretion may have been observed. Indeed a "U-shaped" curve, as well as exquisite dose-dependency of the effects of several neuropeptides has been noted (319, 320). For example, we previously reported that the NPY Y5 receptor agonist, BWX-46, increased VLDL-TG secretion in lean fasted rats (211), a finding not replicated in our current study using [Ala^{31}, Aib^{32}]-NPY (Fig. 3.3D and E). Given that BWX-46 in our previous study (211), was used at a higher dose (ICV 12 nmol) and has less Y5 selectively and greater cross reactivity with the Y1 receptor (321), it appears likely that BWX-46 activated both the NPY Y1 and Y5 receptor resulting in the observed increase in VLDL-TG production. Thus, future studies would involve running multiple doses to reveal whether dose-response effects of NPY Y1 receptor signaling on feeding resemble or differ from those on VLDL-TG secretion.

Structure-function relationships of the NPY-regulated neural circuitry involved in hepatic lipoprotein metabolism

An important finding of our studies in Chapter III is that the activation of the Y1 receptor has a greater effect than the Y2 receptor on hepatic lipoprotein metabolism, which informs us of potential structure-function relationships of the NPY-regulated neural circuitry involved. Intriguingly, there is reportedly a close physical localization and apparent functional relationship between NPY Y1 and Y2 receptor in the ARC, LHA, DMN, and PVN whereas the VMN contains only Y1 receptor positive neurons (114). *In the context of these findings, we hypothesize that the VMN is the potential hypothalamic site in which NPY may regulate lipoprotein metabolism via the selective activation of the Y1 receptor subtype.* In support of this hypothesis, VMN-lesioned rats, which recapitulates a state of elevated NPY tone, have elevated plasma TGs (212), even as early as 10 days postoperatively, together with decreased plasma FFA and glucose levels (213). In addition, perfused livers from VMN-lesioned rats secrete more TGs than controls (213). Thus, future studies to test this hypothesis will focus on delineating the hypothalamic site(s) involved in the CNS NPY effect on hepatic VLDL-TG secretion by utilizing microinjection techniques to localize the effect. For example, it would be interesting to determine whether microinjection of a selective Y1 receptor agonist in the VMN versus the PVN will recapitulate the NPY effect on hepatic VLDL-TG secretion in lean 4-hour fasted rats characterized by low endogenous CNS NPY tone. Conversely, it would be interesting to investigate whether microinjection of a selective Y1 receptor antagonist in the VMN versus the PVN in an obese, hypertriglyceridemic rodent model characterized by elevated NPY tone (i.e. *fa/fa* ZF rat) would attenuate dyslipidemia.

Given the limitations of our pharmacological approach, future studies would additionally involve genetic manipulation of the Y1 versus Y2 receptor subtype in the brain to determine whether NPY acts predominately via the Y1 receptor to modulate hepatic lipoprotein metabolism. Although previous studies report the effect of genetic deletion of NPY Y1, Y2, Y4, or Y5

receptor on an *ob/ob* background (a rodent model of severe hypertriglyceridemia) on energy homeostasis, the effect on plasma TGs is not reported except for the Y2 receptor deletion having no effect (167, 170, 176, 177). Therefore, future studies would involve investigating whether hypothalamic specific (i.e. VMN versus PVN) gene deletion of the Y1 versus Y2 receptor utilizing adenoviral or Cre-loxP methodology would attenuate hypertriglyceridemia in a mouse model characterized by elevated NPY tone and dyslipidemia (i.e. DIO or genetic obesity (*ob/ob* mouse)).

The role of CNS NPY Y1 receptor and downstream GIRK channels in mediating the NPY effect on hepatic VLDL-TG secretion

An important and unanswered question from our studies in Chapter III is the following: What are the neuronal signaling events and/or pathways downstream of the CNS NPY receptor subtype(s) that are involved in mediating the NPY effect on hepatic lipoprotein metabolism? Previous publications report that the inhibitory effect of NPY on ARC POMC neurons are mediated by the activation of the postsynaptic Y1 and Y2 receptor on the surface of POMC neurons (116, 387). NPY additionally suppresses POMC neuronal activity via the inhibition of the excitatory (anorexigenic) outflow between the VMN and ARC POMC neural circuitry by the activation of the Y1 receptor subtype and subsequent downstream GIRK channels in the VMN (110). Furthermore, neuronal GIRK channels have been implicated in the postsynaptic inhibition of VMN neurons, although the subunit composition(s) (GIRK1-4) remains unknown (388). *We hypothesize that the restoration of POMC tone by blocking the Y1 receptor or selective inhibition of downstream GIRK channel activity in the VMN will attenuate NPY-induced hypertriglyceridemia* (Figure 6.1).

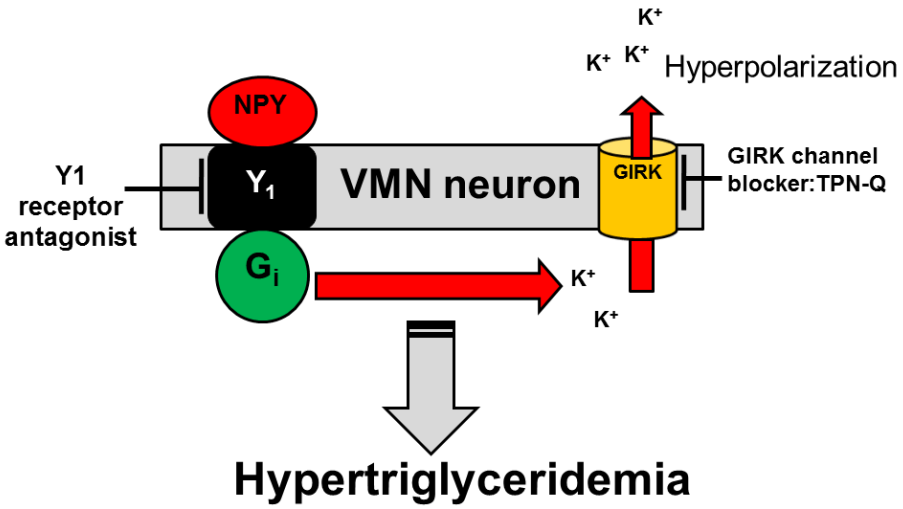

Figure 6.1. Proposed model suggesting that CNS NPY activates Y1 receptor and subsequent GIRK channels in the VMN to increase hepatic VLDL-TG secretion. It is hypothesized that blocking the Y1 receptor with a selective Y1 receptor antagonist or inhibition of the downstream GIRK channels with TPN-Q in the VMN will attenuate NPY-induced hypertriglyceridemia. Abbreviations: central nervous system (CNS); G-protein-coupled inwardly rectifying potassium channels (GIRK); neuropeptide Y (NPY); tertiapin-Q (TPN-Q); ventromedial nucleus (VMN).

In support of this hypothesis, preliminary data from our lab shows that selective inhibition of the GIRK1/4 channel with ICV injection of a high infinity inhibitor, tertiapin-Q (TPN-Q; 1 μg (389)) trends to attenuate NPY-induced hypertriglyceridemia in lean 4-hour fasted rats at 120 min post injection (Figure 6.2). Indeed, mice lacking GIRK1 and GIRK2 exhibit a lean phenotype whereas GIRK4 knockout mice exhibit a predisposition to late-onset obesity (388, 390). This implicates GIRK1/2 as potential candidates for the NPY effect which warrants further investigation. Future studies would test whether the microinjection of a selective GIRK1/2 channel blocker in the VMN of the obese ZF rat would attenuate hypertriglyceridemia in this dyslipidemic model.

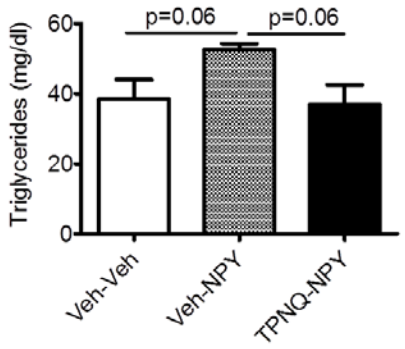

Figure 6.2. TPN-Q attenuates CNS NPY-induced hypertriglyceridemia. Fasted lean rats (*n*=6/group) were pretreated with either ICV vehicle (Veh) or the GIRK1/4 channel blocker, TPN-Q (1 μg) followed by ICV NPY (1 nmol) or Veh treatment. Abbreviations: central nervous system (CNS); G-protein-coupled inwardly rectifying potassium channels (GIRK); neuropeptide Y (NPY); tertiapin-Q (TPN-Q).

Liver phospholipid as the novel TG source for VLDL assembly and secretion in response to increased CNS NPY action

Although the current model of dyslipidemia associated with obesity and diabetes suggest that substrate (FFA) delivery to the liver contributes to the rate of VLDL-TG production (23-25), the key observation of our studies in Chapter III is that increased CNS NPY signaling via the Y1 receptor doubled hepatic VLDL-TG production while not altering plasma FFA and glycerol levels. Therefore, this data suggest that increased adipocyte lipolysis does not account for the NPY-induced hypertriglyceridemia. This is also corroborated by other studies (192). Despite these findings, to definitively proof the absence for a role of adipocyte lipolysis in NPY-induced hepatic VLDL-TG secretion will require tracer techniques. We, therefore, sought to determine the source of TG utilized for VLDL assembly and secretion in response to increased CNS NPY action, which must originate from sources other than that arising from extracellular FFAs. We postulated that liver PL might be the novel lipid source because our results show the following: 1) ICV NPY treatment in lean fasted rats doubled plasma TGs in the absence of significant changes in liver TG content; and 2) obese, ZF rats pair-fed to the lean ZF controls to maintain identical body composition altered the plasma TG concentrations with no effect on liver TG content.

However, the liver PL content of the pair-fed ZF rats tightly correlated with plasma TG levels. Both of these observations suggest the possibility that the additional lipid loaded onto VLDL in response to CNS NPY signaling via the Y1 receptor is generated from PL stores and involves modulating the activities of key regulatory enzymes involved in PL remodeling.

The observed accumulation of oleic and linoleic acid in the liver in response to ICV NPY treatment in lean fasted rats suggests that these LCFAs were not preferentially oxidized, which is contrary to the normal effects of fasting (332-334). Thus, an important finding in Chapter IV is that that these LCFAs were preferentially incorporated into liver PL and not the TG pool. Furthermore, we found a corresponding elevation of oleic and linoleic acid content in plasma TGs in response to ICV NPY treatment in lean fasted rats at 60 and 120 min post injection, an effect recapitulated by the Y1 agonist treatment. Therefore, this data suggest the possibility that these FFAs enriched in the liver PL pool provided the TG precursor that was loaded onto the nascent VLDL particle and was secreted as VLDL-TG. This finding, that some of the TG which ends up as VLDL, is derived from a pool of intracellular PL in response to central NPY action is novel. We, therefore, postulate that increased CNS NPY tone may determine the rate of PL "turnover" or "availability" for TG synthesis and VLDL production by altering the activities of key regulatory enzymes involved in PL remodeling.

We additionally hypothesized that the observed increase in the hepatic formation of oleic acid in response to CNS NPY is mechanistically linked to SCD-1 activity and the suppression of lipid oxidation (CPT-1α) in liver which in turn, may contribute to changes in VLDL-TG secretion. In support of this hypothesis, we demonstrated in Chapters III and IV that the elevation in hepatic VLDL-TG secretion by increased CNS NPY signaling via the Y1 receptor is associated with a rapid (within 60 min) induction of hepatic SCD-1 gene expression and activity, which would suggest that SCD-1 activation may contribute to changes in VLDL-TG secretion. Indeed, SCD-1 is a key enzyme responsible for desaturating palmitic and stearic acids to palmitoleic and oleic acids, respectively and is a known target of CNS leptin (316, 317), glucose (215) and

melanocortin action (203) in the same hypothalamic feeding circuits engaged by NPY. Furthermore, provision of oleic acid or modulation of SCD-1 activity changes VLDL production rate by increasing TG loading in the late maturation phase (215, 316). Future studies that would further delineate the role of liver SCD-1 and oleic acid formation in the NPY response would involve investigating whether ICV injection of NPY in mice lacking hepatic SCD-1 (391) may abolish the NPY effect on hepatic lipoprotein metabolism.

CNS NPY modulates key liporegulatory enzymes involved in PL remodeling elevating hepatic VLDL-TG secretion

We herein report, for the first time to our knowledge, that CNS NPY and the Y1 agonist robustly increased expression of key regulatory enzymes involved in liver PL remodeling, ARF-1 (which activates PLD) and lipin-1 in lean fasted rats. We postulate that NPY modulates ARF-1 to increase PLD activity. In turn, PLD catalyzes the production of PA, derived from the much larger PL pool, instead of the intracellular TG pool, as this pathway is implicated by several studies to be involved in VLDL maturation (224, 233, 234). For example, the overexpression of ARF-1 or PLD in cultured rat hepatocytes can increase VLDL secretion whereas hepatic overexpression of a dominant negative ARF-1 results in a suppressive effect (234). Notably, we only show changes in ARF-1 expression and not activity with ICV NPY treatment which is a major limitation of our study. Therefore, additional studies would be required to demonstrate the involvement of ARF-1 and PLD in the CNS NPY response and would involve the following experiments in lean fasted rats: 1) Determine whether selective hepatic PLD inhibition using either a pharmacologic and/or genetic approach would block the effect of central NPY signaling on hepatic VLDL-TG production; 2) Investigate whether the overexpression of a dominant negative ARF-1 would attenuate the effect of CNS NPY-induced hypertriglyceridemia.

A novel and important finding in Chapter IV is that lipin-1 protein expression was robustly elevated in the ER membrane containing nuclear and not the cytoplasmic fraction in the

livers of lean fasted rats treated with ICV NPY at 60 and 120 min post injection. This data suggest the possibility that the oleic acid generated from increased CNS NPY signaling promoted lipin-1 translocation from the cytosol to the ER membrane where it performs its PAP-1 activity. In turn, we speculate that this resulted in the conversion of PL-derived PA into DAG which serves as a substrate for the synthesis of TG and PL that is then assembled onto the nascent VLDL particle leading to VLDL maturation and secretion (238, 253). Indeed, previous studies report that the overexpression of lipin-1α or -1β isoform in cultured rat hepatocytes in the presence of oleic acid markedly increases glycerolipid synthesis and secretion of VLDL-TG whereas siRNA mediated knockdown of lipin-1 decreases VLDL assembly and secretion (238). Because the subcellular localization of lipin-1 determines its function as either an ER-localized glycerolipid biosynthetic enzyme or a nuclear-localized transcriptional coactivator of fatty acid oxidation genes, the following studies would be required to determine whether CNS NPY modulation of VLDL-TG secretion is dependent on the function of liver lipin-1 in lean fasted rats: 1) Determine whether the adenoviral overexpression of a lipin-1 mutant with impaired PAP-1 activity in liver abolishes the NPY effect on hepatic VLDL-TGs; 2) Test whether adenoviral overexpression of lipin-1 with a mutation in the transcriptional coactivator domain yet intact PAP-1 activity in liver results in hypertriglyceridemia in response to CNS NPY signaling.

Central NPY regulation of hepatic lipin-1 to modulate lipoprotein metabolism may be dependent on liver GC action

Previous studies (238, 259) report that lipin-1 is responsible for the increase in VLDL secretion in response to GC treatment in cultured rat hepatocytes (264-266). Coupled with this observation, some of the hormonal and metabolic effects of central NPY infusion in rats are dependent on circulating GC, corticosterone as these NPY-induced effects can be prevented by adrenalectomy, including hypertriglyceridemia (201). Furthermore, chronic central NPY infusion has been shown to activate the HPA axis in normal animals leading to the elevation in the

circulating GC, corticosterone (200, 201). *We, therefore, hypothesize, in the context of these findings, that central NPY regulation of hepatic lipin-1 to modulate lipoprotein metabolism may be dependent on liver GC action.* In support of this hypothesis, we also found that GRα protein levels were also increased in the nuclear/ER fraction showing a similar protein pattern as lipin-1 in the livers of ICV NPY-treated rats. This increases the likelihood that GRα is bound to the *Lpin1* promoter region (260) in response to elevations in circulating corticosterone levels induced by increased central NPY signaling. In turn, this may lead to the GC dependent induction of lipin-1 expression and activity (259) and subsequent elevation in VLDL-TG secretion. However, in the previously reported *in vitro* studies (264-266) investigating the modulation of VLDL-TG secretion by GCs, these studies focused on the chronic effects of GC action in cultured rat hepatocytes, which poses as a caveat to our acute experimental paradigm. Therefore, the counterargument for our study is that the potential acute effects of GCs on modulating VLDL-TG secretion may be mediated via non-genomic effects. Nevertheless, future studies to investigate this hypothesis would involve determining whether the CNS NPY effect on hepatic lipin-1 and VLDL-TG secretion can be blocked by either a highly selective liver-specific GR antagonist and/or by adrenalectomy in lean fasted rats.

The key autonomic nervous system signaling determinants involved in the neural-hepatic circuit that modulates hepatic VLDL-TG secretion in response to CNS NPY signaling

Although Chapter III and IV reveal important molecular mechanisms in the CNS NPY response at the level of the hypothalamus and the liver that leads to increased hepatic VLDL-TG secretion, a key and important remaining question is the following: What are the key autonomic nervous system signaling determinants involved in the neural-hepatic circuit that modulates hepatic VLDL-TG secretion in response to CNS NPY signaling? A recent study by Bruinstroop et al. (192) reveals that increased hypothalamic NPY signaling during fasting increases hepatic VLDL-TG secretion via sympathetic inputs to the liver. Intriguingly, this study (192) also reports

that ICV NPY decreases CPT-1α and induces ARF-1 mRNA expression via the SNS in lean fasted rats and this NPY effect was completely abolished by Sx, an observation consistent with our findings in Chapter IV.

Through our collaboration with Eveline Bruinstroop and Andries Kalsbeek, we sought to determine whether CNS NPY modulates key liporegulatory enzymes involved in PL remodeling via sympathetic inputs to the liver by conducting the following study in the absence of tyloxapol: Investigating whether CNS NPY infusion in fasted Wistar rats with selective liver Sx abolishes the NPY effect on key liporegulatory enzymes and thus, attenuates hepatic VLDL-TG secretion. So far, our preliminary data (Figure 6.3) from this study shows that ICV NPY treatment in hepatic sham-denervated control rats, robustly elevates SCD-1 mRNA and lipin-1 protein expression by ~2- to 3-fold, repectively. Remarkably, this NPY effect is completely abolished in the liver of Sx rats.

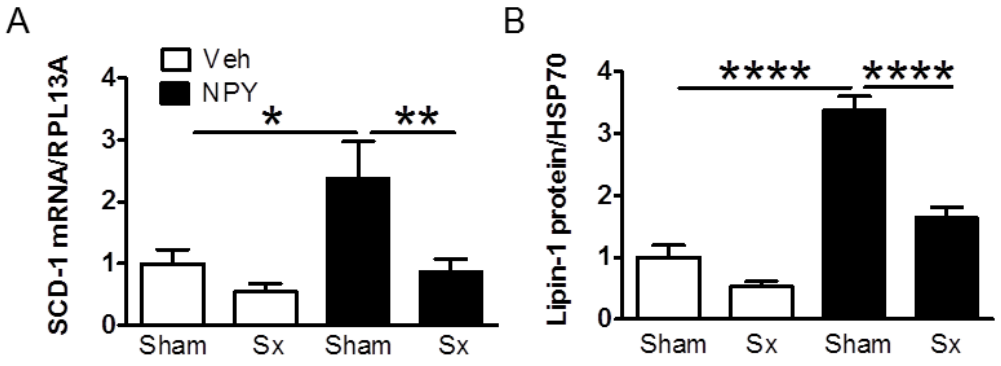

Figure 6.3. Hepatic Sx abolishes the stimulatory effect of ICV NPY on liver SCD-1 and lipin-1 expression compared to hepatic sham rats. To determine whether ICV NPY stimulates hepatic VLDL-TG secretion by modulating key liver liporegulatory enzymes via the sympathetic nervous system, male Wistar rats (*n*=7-8/group) were implanted with a third ventricle cannula and a jugular vein catheter. Subsequently, the animals received either a control sham-denervation (sham) or sympathetic denervation (Sx) of the liver. After recovery to pre-surgery body weight, rats were connected to a metal collar for adaptation the day before the surgery. The next morning at 8AM, food was removed. At 12PM, ICV NPY (Bachem; 1µg/µl; black bars) or vehicle (Veh; purified water; Milli-Q; white bars) was infused for 2-hours (bolus 5 µl/5 min, followed by 5 µl/hour). At study termination, animals were euthanized, trunk blood and liver tissues were collected. (A) Relative gene expression in the liver is shown for stearoyl-CoA desaturase-1 (SCD-1) RNA which was assessed by quantitative RT-PCR and normalized to the reference RNA ribosomal protein L13a (RPL13A). For comparative analysis, RNA ratios were normalized to the Veh control. (B) Protein extracts prepared from livers were immunoblotted to detect levels of lipin-1 and normalized to loading control, heat shock protein 70 (HSP70). Western blots were analyzed by densitometry (normalized to Veh control). Data are presented as mean ± SEM and were analyzed by one-way ANOVA with Bonferroni's post-test analysis; *$p<0.05$, ** $p<0.01$, **** $p<0.0001$.

In support of our preliminary data (Figure 6.3) and findings in Chapter IV, a previous study reports that NE activation of adrenergic signaling in rat liver via the α_1-adrenergic receptor is coupled to the activation of the PKC/CREB pathway (336). In turn, CREB may induce *Lpin1* gene transcription by binding to CRE upstream of the *Lpin1* promoter as reported in previous studies (262, 263). Therefore, this raises the possibility that pathological elevations in CNS NPY tone in obesity and diabetes contributes to the associated increase in both the activity of the HPA axis and sympathetic outflow to the liver. Ultimately, this may result in increased GC and NE signaling in the liver and thus, these metabolites may synergize to upregulate hepatic lipin-1

expression and its PAP-1 activity. This effect may impair the ability of insulin to suppress lipin-1 leading to increased hepatic VLDL-TG secretion.

Intriguingly, SCD-1, ARF-1, and CPT-1α all contain putative CRE sites in their promoters as determined by the CREB Target Gene Database by the Salk Institute (http://natural.salk.edu/CREB/). *Therefore, it is hypothesized that CREB may induce the expression and activity of ARF-1 and SCD-1 while simultaneously suppressing the expression and activity of CPT-1α in the livers of ICV NPY-treated rats.* Consistent with this hypothesis, a study by Vankoningsloo et al. (392) reports that treatment of 3T3-L1 adipocytes with antimycin A, which triggers CREB activation, resulted in the upregulation of SCD-1 and the downregulation of CPT-1α expression leading to TG accumulation in these cells. However, CREB has been also described in mouse liver to suppress lipogenesis while upregulating fatty acid oxidation by repressing PPARɣ and by inducing PGC-1α (393).

Finally, the important and remaining question is what accounts for the rapid changes in plasma TGs in response to increased CNS NPY signaling even earlier than 60 min post ICV injection as shown in Figure 3.3A-C? Clearly, this effect must be mediated by a rapid posttranslational event and not dependent on long-term transcriptional and translational changes. It is possible that the SNS in the form of increased liver NE signaling may mediate the short-term NPY effect on plasma TGs potentially by promoting the dephosphorylation of lipin-1 as reported previously (252). In turn, this leads to lipin-1 translocation and association with the ER to rapidly modulate VLDL-TG assembly and secretion through its PAP-1 activity. In parallel, increased liver GC signaling may be responsible for the long-term transcriptional and translational changes with increased CNS NPY signaling. Liver GC action may account for the observed upregulation in the expression of key liporegulatory enzymes, SCD-1, lipin-1, and ARF-1 at 60 and 120 min post ICV NPY injection. Clearly, future studies are warranted to determine whether the effect of CNS NPY on hepatic VLDL-TG secretion is dependent on either increased NE and/or GC action in liver.

Conclusions

An integrated model of how CNS NPY modulates hepatic lipoprotein metabolism

An integrated model (as shown in Figure 6.4) will be described next for how CNS NPY modulates hepatic lipoprotein metabolism based upon the individual findings presented in this dissertation (Chapter III and IV) and discussed in this Chapter. 1) The pathological elevation in CNS NPY signaling in obesity and diabetes results in the activation of the NPY Y1 receptor which contributes to the associated increase in both the activity of the HPA axis and sympathetic outflow to the liver. Ultimately, this may result in increased GC and NE signaling in the liver. 2) The adrenergic neurotransmitter, NE, binds to the α_1-adrenergic receptor which in turn leads to the activation of the PKC/CREB pathway (336). 3) In turn, CREB and GC may synergize to induce *Lpin1* gene expression and activity via the CRE (262, 263) and GRE (260) upstream of the *Lpin1* promoter. Because SCD-1, ARF-1, and CPT-1α all contain CRE sites in their promoter sequence, CREB may induce the expression and activity of ARF-1 and SCD-1 while simultaneously suppressing the expression and activity of CPT-1α. 4) Therefore, the corresponding suppression of fatty acid oxidation leads to the accumulation of oleic (C18:1w9) and linoleic (C18:2w6) acid which are channeled into the PL pool (and incidentally, oleic acid is a product of SCD-1 activity). 5) The oleic acid generated from SCD-1 promotes the translocation of lipin-1 to the ER where it performs its PAP-1 activity. 6) This results in the conversion of PA-derived from the PL pool into DAG which then can be converted by DGAT-1 to TG for VLDL maturation. 7) In parallel, PL remodeling by ARF-1 mediated activation of PLD generates additional PA substrate. 8) Thus, the lipin-1-derived DAG generates the TG substrate which is assembled onto an apoB carrying pre-VLDL precursor leading to the maturation and secretion of VLDL-TG by the liver.

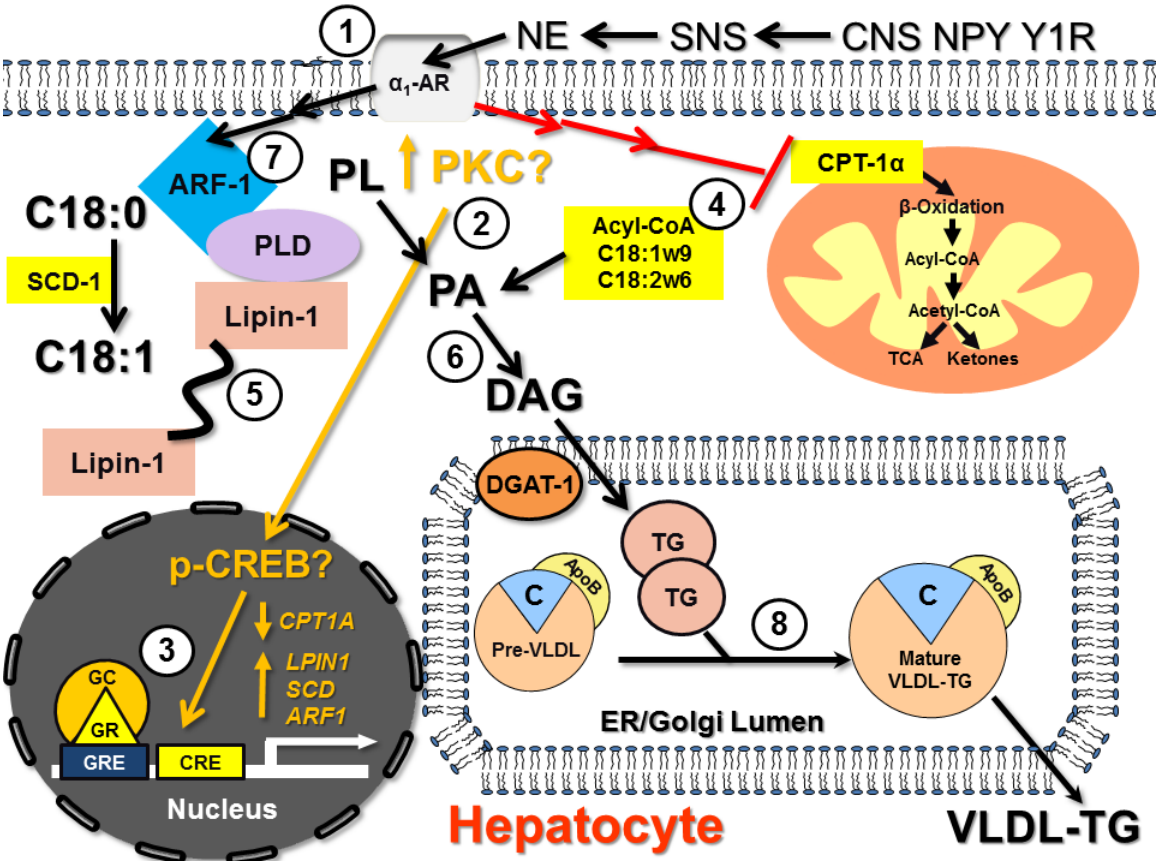

Figure 6.4. Proposed model in which CNS NPY via the Y1 receptor promotes hepatic lipin-1 mediated PL remodeling elevating VLDL-TG secretion via the SNS. Abbreviations: ADP-ribosylation factor (ARF-1); α_1-adrenergic receptor (α_1-AR); apolipoprotein B (apoB); carnitine palmitoyltransferase-1α (CPT-1α); cAMP-dependent regulatory elements (CRE); phosphorylated cAMP response element-binding protein (p-CREB); central nervous system (CNS); diacylglycerol (DAG); diacylglycerol acyltransferase-1 (DGAT-1); glucocorticoid (GC); glucocorticoid receptor (GR); glucocorticoid response element (GRE); neuropeptide Y (NPY); norepinephrine (NE); phosphatidic acid (PA); phospholipase D (PLD); phospholipid (PL); protein kinase C (PKC); stearoyl-CoA desaturase-1 (SCD-1); sympathetic nervous system (SNS); triglyceride (TG); very low-density lipoprotein-triglyceride (VLDL-TG).

The studies in this dissertation raise a very intriguing and important question: Why is lipoprotein metabolism additionally regulated by neuronal inputs and does this effect confer an evolutionary advantage? Clearly, NPY tone is elevated during states of energy deficiency, such fasting and starvation leading to food seeking behavior and energy conservation. However, in the absence of a reliable food supply in which starvation ensues, the mobilization of liver lipids in the form of VLDL-TG by increased CNS NPY signaling may provide a reliable energy source for the

peripheral tissues and thus, confers a survival advantage. In the context of human evolution, the NPY effect may have evolved during the time when humans were living under conditions of chronic caloric deprivation (i.e. hunters and gatherers) to confer a selective survival advantage by optimizing lipid metabolism as a reliable fuel source. Intriguingly, it is also speculated that increased CNS NPY signaling during fasting may promote the hepatic esterification of intracellular pro-inflammatory long chain fatty acyl-CoAs (i.e. palmitoyl-CoA, stearoyl-CoA) into the neutral TG form. Subsequently, the assembly of TG onto the nascent VLDL lipoprotein particle then can be exported as a neutral (non-toxic) lipid form to the peripheral tissues which may confer a protective effect against insulin resistance. Indeed, it is well-documented that the accumulation of long chain fatty acyl-CoAs and/or metabolites (i.e. DAG, ceramides) has been implicated in the pathogenesis of central and peripheral insulin resistance triggered by the activation of intracellular inflammatory signals (74, 394).

Today, in the 21st-century, humans in the US and worldwide are adapted to the current "Western lifestyle" characterized by the exposure and consumption of a surplus food supply in the form of calorically dense foods coupled with a sedentary life. Therefore, it is postulated that this evolutionary advantage of NPY may become dysfunctional in the current environment. Indeed, obesity is associated with elevated NPY tone and a reduction in POMC tone due to the manifestation of CNS insulin and leptin resistance. Consequently, this results in impaired CNS sensing of nutrient status in obese subjects leading to the perception of energy deprivation despite the presence of an excess in nutrients and enlarged, energy storage depot. *We, therefore, hypothesize, that the CNS NPY response to fasting may be required for optimal lipid metabolism but becomes dysfunctional in obesity and diabetes, contributing to the pathophysiology of the metabolic syndrome in the form of atherogenic dyslipidemia.*

In conclusion, this body of work has extended previous studies in our laboratory and others that implicates CNS NPY as an important regulator of hepatic lipoprotein metabolism beyond its effects on feeding and energy homeostasis. Most importantly, our studies demonstrate, within the

limits of our model, that the effects of NPY on feeding and/or weight gain are dissociable from the effect on hepatic VLDL-TG secretion. Therefore, the clinical implications of our studies are that while NPY and NPY receptors are recognized as therapeutic targets for the treatment of obesity, they are also an important target for treating dyslipidemia associated with obesity and diabetes independently of effects on feeding and increased visceral adiposity. However, it is clearly evident that more work is required to delineate the molecular mechanisms and/or pathways activated in the CNS and in the liver in response to elevated CNS NPY signaling that leads to the modulation of hepatic lipoprotein metabolism. Further elucidation of these mechanisms involved in the CNS NPY effect on hepatic VLDL-TG secretion will provide further insight into the pathophysiology of the metabolic syndrome potentially revealing novel and effective therapeutic interventions for the treatment of atherogenic dyslipidemia associated with obesity, diabetes, and the metabolic syndrome.

REFERENCES

1. **O'Donnell CJ, Elosua R** 2008 [Cardiovascular risk factors. Insights from Framingham Heart Study]. Revista espanola de cardiologia 61:299-310
2. **Jones DS, Podolsky SH, Greene JA** 2012 The burden of disease and the changing task of medicine. N Engl J Med 366:2333-2338
3. **Dawber TR, Meadors GF, Moore FE, Jr.** 1951 Epidemiological approaches to heart disease: the Framingham Study. American journal of public health and the nation's health 41:279-281
4. **Gregg EW, Cheng YJ, Cadwell BL, Imperatore G, Williams DE, Flegal KM, Narayan KM, Williamson DF** 2005 Secular trends in cardiovascular disease risk factors according to body mass index in US adults. JAMA 293:1868-1874
5. 2002 MRC/BHF Heart Protection Study of cholesterol lowering with simvastatin in 20,536 high-risk individuals: a randomised placebo-controlled trial. Lancet 360:7-22
6. **Roger VL, Go AS, Lloyd-Jones DM, Benjamin EJ, Berry JD, Borden WB, Bravata DM, Dai S, Ford ES, Fox CS, Fullerton HJ, Gillespie C, Hailpern SM, Heit JA, Howard VJ, Kissela BM, Kittner SJ, Lackland DT, Lichtman JH, Lisabeth LD, Makuc DM, Marcus GM, Marelli A, Matchar DB, Moy CS, Mozaffarian D, Mussolino ME, Nichol G, Paynter NP, Soliman EZ, Sorlie PD, Sotoodehnia N, Turan TN, Virani SS, Wong ND, Woo D, Turner MB** 2012 Heart disease and stroke statistics--2012 update: a report from the American Heart Association. Circulation 125:e2-e220
7. **Jemal A, Ward E, Hao Y, Thun M** 2005 Trends in the leading causes of death in the United States, 1970-2002. JAMA 294:1255-1259
8. **Gersh BJ, Sliwa K, Mayosi BM, Yusuf S** 2010 Novel therapeutic concepts: the epidemic of cardiovascular disease in the developing world: global implications. European heart journal 31:642-648
9. **Mokdad AH, Bowman BA, Ford ES, Vinicor F, Marks JS, Koplan JP** 2001 The continuing epidemics of obesity and diabetes in the United States. JAMA 286:1195-1200
10. **CDC** 2012 Overweight and obesity fact sheet. In: http://www.cdc.gov/obesity/data/facts.html
11. **Willett WC, Dietz WH, Colditz GA** 1999 Guidelines for healthy weight. N Engl J Med 341:427-434
12. **Heidenreich PA, Trogdon JG, Khavjou OA, Butler J, Dracup K, Ezekowitz MD, Finkelstein EA, Hong Y, Johnston SC, Khera A, Lloyd-Jones DM, Nelson SA, Nichol G, Orenstein D, Wilson PW, Woo YJ** 2011 Forecasting the future of cardiovascular disease in the United States: a policy statement from the American Heart Association. Circulation 123:933-944
13. **Eckel RH, Grundy SM, Zimmet PZ** 2005 The metabolic syndrome. Lancet 365:1415-1428
14. **Ginsberg HN, Zhang YL, Hernandez-Ono A** 2006 Metabolic syndrome: focus on dyslipidemia. Obesity (Silver Spring) 14 Suppl 1:41S-49S
15. **Ginsberg HN** 2000 Insulin resistance and cardiovascular disease. J Clin Invest 106:453-458
16. **Isomaa B, Almgren P, Tuomi T, Forsen B, Lahti K, Nissen M, Taskinen MR, Groop L** 2001 Cardiovascular morbidity and mortality associated with the metabolic syndrome. Diabetes Care 24:683-689
17. **Hajer GR, van Haeften TW, Visseren FL** 2008 Adipose tissue dysfunction in obesity, diabetes, and vascular diseases. European heart journal 29:2959-2971
18. **Kershaw EE, Flier JS** 2004 Adipose tissue as an endocrine organ. J Clin Endocrinol Metab 89:2548-2556

19. **Roth J, Qiang X, Marban SL, Redelt H, Lowell BC** 2004 The obesity pandemic: where have we been and where are we going? Obes Res 12 Suppl 2:88S-101S
20. **Gutierrez DA, Puglisi MJ, Hasty AH** 2009 Impact of increased adipose tissue mass on inflammation, insulin resistance, and dyslipidemia. Current diabetes reports 9:26-32
21. **Jovinge S, Hamsten A, Tornvall P, Proudler A, Bavenholm P, Ericsson CG, Godsland I, de Faire U, Nilsson J** 1998 Evidence for a role of tumor necrosis factor alpha in disturbances of triglyceride and glucose metabolism predisposing to coronary heart disease. Metabolism 47:113-118
22. **Qin B, Anderson RA, Adeli K** 2008 Tumor necrosis factor-alpha directly stimulates the overproduction of hepatic apolipoprotein B100-containing VLDL via impairment of hepatic insulin signaling. American journal of physiology Gastrointestinal and liver physiology 294:G1120-1129
23. **Riches FM, Watts GF, Naoumova RP, Kelly JM, Croft KD, Thompson GR** 1998 Hepatic secretion of very-low-density lipoprotein apolipoprotein B-100 studied with a stable isotope technique in men with visceral obesity. Int J Obes Relat Metab Disord 22:414-423
24. **Kissebah AH, Alfarsi S, Adams PW, Wynn V** 1976 Role of insulin resistance in adipose tissue and liver in the pathogenesis of endogenous hypertriglyceridaemia in man. Diabetologia 12:563-571
25. **Laws A, Hoen HM, Selby JV, Saad MF, Haffner SM, Howard BV** 1997 Differences in insulin suppression of free fatty acid levels by gender and glucose tolerance status. Relation to plasma triglyceride and apolipoprotein B concentrations. Insulin Resistance Atherosclerosis Study (IRAS) Investigators. Arteriosclerosis, thrombosis, and vascular biology 17:64-71
26. **Tschritter O, Fritsche A, Thamer C, Haap M, Shirkavand F, Rahe S, Staiger H, Maerker E, Haring H, Stumvoll M** 2003 Plasma adiponectin concentrations predict insulin sensitivity of both glucose and lipid metabolism. Diabetes 52:239-243
27. **Bajaj M, Suraamornkul S, Piper P, Hardies LJ, Glass L, Cersosimo E, Pratipanawatr T, Miyazaki Y, DeFronzo RA** 2004 Decreased plasma adiponectin concentrations are closely related to hepatic fat content and hepatic insulin resistance in pioglitazone-treated type 2 diabetic patients. J Clin Endocrinol Metab 89:200-206
28. **Banerji MA, Faridi N, Atluri R, Chaiken RL, Lebovitz HE** 1999 Body composition, visceral fat, leptin, and insulin resistance in Asian Indian men. J Clin Endocrinol Metab 84:137-144
29. **Sparks JD, Sparks CE** 1990 Insulin modulation of hepatic synthesis and secretion of apolipoprotein B by rat hepatocytes. J Biol Chem 265:8854-8862
30. **Brown AM, Gibbons GF** 2001 Insulin inhibits the maturation phase of VLDL assembly via a phosphoinositide 3-kinase-mediated event. Arteriosclerosis, thrombosis, and vascular biology 21:1656-1661
31. **Adiels M, Olofsson SO, Taskinen MR, Boren J** 2008 Overproduction of very low-density lipoproteins is the hallmark of the dyslipidemia in the metabolic syndrome. Arteriosclerosis, thrombosis, and vascular biology 28:1225-1236
32. **Miller M, Stone NJ, Ballantyne C, Bittner V, Criqui MH, Ginsberg HN, Goldberg AC, Howard WJ, Jacobson MS, Kris-Etherton PM, Lennie TA, Levi M, Mazzone T, Pennathur S** 2011 Triglycerides and cardiovascular disease: a scientific statement from the American Heart Association. Circulation 123:2292-2333
33. **Hokanson JE** 2002 Hypertriglyceridemia and risk of coronary heart disease. Curr Cardiol Rep 4:488-493
34. **Hokanson JE, Austin MA** 1996 Plasma triglyceride level is a risk factor for cardiovascular disease independent of high-density lipoprotein cholesterol level: a meta-

analysis of population-based prospective studies. Journal of cardiovascular risk 3:213-219

35. **Abdel-Maksoud MF, Hokanson JE** 2002 The complex role of triglycerides in cardiovascular disease. Seminars in vascular medicine 2:325-333
36. **Despres JP, Lamarche B, Mauriege P, Cantin B, Dagenais GR, Moorjani S, Lupien PJ** 1996 Hyperinsulinemia as an independent risk factor for ischemic heart disease. N Engl J Med 334:952-957
37. **Robins SJ, Rubins HB, Faas FH, Schaefer EJ, Elam MB, Anderson JW, Collins D** 2003 Insulin resistance and cardiovascular events with low HDL cholesterol: the Veterans Affairs HDL Intervention Trial (VA-HIT). Diabetes Care 26:1513-1517
38. **Sims EA** 1976 Experimental obesity, dietary-induced thermogenesis, and their clinical implications. Clinics in endocrinology and metabolism 5:377-395
39. **Seeley RJ, Matson CA, Chavez M, Woods SC, Dallman MF, Schwartz MW** 1996 Behavioral, endocrine, and hypothalamic responses to involuntary overfeeding. Am J Physiol 271:R819-823
40. **Woods SC, Seeley RJ, Rushing PA, D'Alessio D, Tso P** 2003 A controlled high-fat diet induces an obese syndrome in rats. J Nutr 133:1081-1087
41. **Hagan S, Niswender KD** 2012 Neuroendocrine regulation of food intake. Pediatric blood & cancer 58:149-153
42. **Ryan KK, Woods SC, Seeley RJ** 2012 Central nervous system mechanisms linking the consumption of palatable high-fat diets to the defense of greater adiposity. Cell Metab 15:137-149
43. **Kennedy GC** 1953 The role of depot fat in the hypothalamic control of food intake in the rat. Proc R Soc Lond B Biol Sci 140:578-596
44. **K.D. Niswender, D.J. Clegg, C.D. Morrison, G.J. Morton and S.C. Benoit** 2004 The Human Obesity Epidemic - A Physiological Perspective. Curr Med Chem – Immun, Endoc & Metab Agents 4:91-104
45. **Schwartz MW, Woods SC, Porte D, Jr., Seeley RJ, Baskin DG** 2000 Central nervous system control of food intake. Nature 404:661-671
46. **Niswender KD, Baskin DG, Schwartz MW** 2004 Insulin and its evolving partnership with leptin in the hypothalamic control of energy homeostasis. Trends Endocrinol Metab 15:362-369
47. **Grill HJ, Kaplan JM** 2002 The neuroanatomical axis for control of energy balance. Front Neuroendocrinol 23:2-40
48. **Morton GJ, Cummings DE, Baskin DG, Barsh GS, Schwartz MW** 2006 Central nervous system control of food intake and body weight. Nature 443:289-295
49. **Woods SC, Porte D, Jr.** 1977 Relationship between plasma and cerebrospinal fluid insulin levels of dogs. Am J Physiol 233:E331-334
50. **Bernstein IL, Lotter EC, Kulkosky PJ, Porte D, Jr., Woods SC** 1975 Effect of force-feeding upon basal insulin levels of rats. Proc Soc Exp Biol Med 150:546-548
51. **Bagdade JD, Bierman EL, Porte D, Jr.** 1967 The significance of basal insulin levels in the evaluation of the insulin response to glucose in diabetic and nondiabetic subjects. J Clin Invest 46:1549-1557
52. **Polonsky KS, Given BD, Van Cauter E** 1988 Twenty-four-hour profiles and pulsatile patterns of insulin secretion in normal and obese subjects. J Clin Invest 81:442-448
53. **Baura GD, Foster DM, Porte D, Jr., Kahn SE, Bergman RN, Cobelli C, Schwartz MW** 1993 Saturable transport of insulin from plasma into the central nervous system of dogs in vivo. A mechanism for regulated insulin delivery to the brain. J Clin Invest 92:1824-1830
54. **Schwartz MW, Bergman RN, Kahn SE, Taborsky GJ, Jr., Fisher LD, Sipols AJ, Woods SC, Steil GM, Porte D, Jr.** 1991 Evidence for entry of plasma insulin into

cerebrospinal fluid through an intermediate compartment in dogs. Quantitative aspects and implications for transport. J Clin Invest 88:1272-1281
55. **Schwartz MW, Figlewicz DP, Baskin DG, Woods SC, Porte D, Jr.** 1992 Insulin in the brain: a hormonal regulator of energy balance. Endocr Rev 13:387-414
56. **Woods SC, Lotter EC, McKay LD, Porte D, Jr.** 1979 Chronic intracerebroventricular infusion of insulin reduces food intake and body weight of baboons. Nature 282:503-505
57. **Air EL, Benoit SC, Blake Smith KA, Clegg DJ, Woods SC** 2002 Acute third ventricular administration of insulin decreases food intake in two paradigms. Pharmacol Biochem Behav 72:423-429
58. **Bruning JC, Gautam D, Burks DJ, Gillette J, Schubert M, Orban PC, Klein R, Krone W, Muller-Wieland D, Kahn CR** 2000 Role of brain insulin receptor in control of body weight and reproduction. Science 289:2122-2125
59. **Masaki T, Chiba S, Noguchi H, Yasuda T, Tobe K, Suzuki R, Kadowaki T, Yoshimatsu H** 2004 Obesity in insulin receptor substrate-2-deficient mice: disrupted control of arcuate nucleus neuropeptides. Obes Res 12:878-885
60. **Lin X, Taguchi A, Park S, Kushner JA, Li F, Li Y, White MF** 2004 Dysregulation of insulin receptor substrate 2 in β cells and brain causes obesity and diabetes. The Journal of Clinical Investigation 114:908-916
61. **Niswender KD, Morrison CD, Clegg DJ, Olson R, Baskin DG, Myers MG, Jr., Seeley RJ, Schwartz MW** 2003 Insulin activation of phosphatidylinositol 3-kinase in the hypothalamic arcuate nucleus: a key mediator of insulin-induced anorexia. Diabetes 52:227-231
62. **Zhang Y, Proenca R, Maffei M, Barone M, Leopold L, Friedman JM** 1994 Positional cloning of the mouse obese gene and its human homologue. Nature 372:425-432
63. **Considine RV, Sinha MK, Heiman ML, Kriauciunas A, Stephens TW, Nyce MR, Ohannesian JP, Marco CC, McKee LJ, Bauer TL, et al.** 1996 Serum immunoreactive-leptin concentrations in normal-weight and obese humans. N Engl J Med 334:292-295
64. **Hummel KP, Dickie MM, Coleman DL** 1966 Diabetes, a new mutation in the mouse. Science 153:1127-1128
65. **Phillips MS, Liu Q, Hammond HA, Dugan V, Hey PJ, Caskey CJ, Hess JF** 1996 Leptin receptor missense mutation in the fatty Zucker rat. Nature genetics 13:18-19
66. **Cleary MP, Vasselli JR, Greenwood MR** 1980 Development of obesity in Zucker obese (fafa) rat in absence of hyperphagia. Am J Physiol 238:E284-292
67. **Kennedy AJ, Ellacott KL, King VL, Hasty AH** 2010 Mouse models of the metabolic syndrome. Disease models & mechanisms 3:156-166
68. **Campfield LA, Smith FJ, Guisez Y, Devos R, Burn P** 1995 Recombinant mouse OB protein: evidence for a peripheral signal linking adiposity and central neural networks. Science 269:546-549
69. **Montague CT, Farooqi IS, Whitehead JP, Soos MA, Rau H, Wareham NJ, Sewter CP, Digby JE, Mohammed SN, Hurst JA, Cheetham CH, Earley AR, Barnett AH, Prins JB, O'Rahilly S** 1997 Congenital leptin deficiency is associated with severe early-onset obesity in humans. Nature 387:903-908
70. **Farooqi IS, Jebb SA, Langmack G, Lawrence E, Cheetham CH, Prentice AM, Hughes IA, McCamish MA, O'Rahilly S** 1999 Effects of recombinant leptin therapy in a child with congenital leptin deficiency. N Engl J Med 341:879-884
71. **Hinney A, Vogel CI, Hebebrand J** 2010 From monogenic to polygenic obesity: recent advances. European child & adolescent psychiatry 19:297-310
72. **Bray GA, Paeratakul S, Popkin BM** 2004 Dietary fat and obesity: a review of animal, clinical and epidemiological studies. Physiol Behav 83:549-555
73. **Brand-Miller JC, Holt SH, Pawlak DB, McMillan J** 2002 Glycemic index and obesity. Am J Clin Nutr 76:281S-285S

74. **Posey K, Clegg DJ, Printz RL, Byun J, Morton GJ, Vivekanandan-Giri A, Pennathur S, Baskin DG, Heinecke JW, Woods SC, Schwartz MW, Niswender KD** 2008 Hypothalamic proinflammatory lipid accumulation, inflammation, and insulin resistance in rats fed a high-fat diet. Am J Physiol Endocrinol Metab
75. **Picardi PK, Calegari VC, Prada Pde O, Moraes JC, Araujo E, Marcondes MC, Ueno M, Carvalheira JB, Velloso LA, Saad MJ** 2008 Reduction of hypothalamic protein tyrosine phosphatase improves insulin and leptin resistance in diet-induced obese rats. Endocrinology 149:3870-3880
76. **Cone RD, Cowley MA, Butler AA, Fan W, Marks DL, Low MJ** 2001 The arcuate nucleus as a conduit for diverse signals relevant to energy homeostasis. Int J Obes Relat Metab Disord 25 Suppl 5:S63-67
77. **Shen DD, Artru AA, Adkison KK** 2004 Principles and applicability of CSF sampling for the assessment of CNS drug delivery and pharmacodynamics. Adv Drug Deliv Rev 56:1825-1857
78. **Cummings DE, Schwartz MW** 2003 Genetics and pathophysiology of human obesity. Annu Rev Med 54:453-471
79. **Schwartz MW, Seeley RJ, Campfield LA, Burn P, Baskin DG** 1996 Identification of targets of leptin action in rat hypothalamus. J Clin Invest 98:1101-1106
80. **Schwartz MW, Sipols AJ, Marks JL, Sanacora G, White JD, Scheurink A, Kahn SE, Baskin DG, Woods SC, Figlewicz DP, et al.** 1992 Inhibition of hypothalamic neuropeptide Y gene expression by insulin. Endocrinology 130:3608-3616
81. **Mercer JG, Hoggard N, Williams LM, Lawrence CB, Hannah LT, Trayhurn P** 1996 Localization of leptin receptor mRNA and the long form splice variant (Ob-Rb) in mouse hypothalamus and adjacent brain regions by in situ hybridization. FEBS letters 387:113-116
82. **Elmquist JK, Bjorbaek C, Ahima RS, Flier JS, Saper CB** 1998 Distributions of leptin receptor mRNA isoforms in the rat brain. The Journal of comparative neurology 395:535-547
83. **Werther GA, Hogg A, Oldfield BJ, McKinley MJ, Figdor R, Mendelsohn FA** 1989 Localization and Characterization of Insulin-Like Growth Factor-I Receptors in Rat Brain and Pituitary Gland Using in vitro Autoradiography and Computerized Densitometry* A Distinct Distribution from Insulin Receptors. Journal of neuroendocrinology 1:369-377
84. **Uyama N, Geerts A, Reynaert H** 2004 Neural connections between the hypothalamus and the liver. The anatomical record Part A, Discoveries in molecular, cellular, and evolutionary biology 280:808-820
85. **Pritchard LE, Turnbull AV, White A** 2002 Pro-opiomelanocortin processing in the hypothalamus: impact on melanocortin signalling and obesity. The Journal of endocrinology 172:411-421
86. **Fan W, Boston BA, Kesterson RA, Hruby VJ, Cone RD** 1997 Role of melanocortinergic neurons in feeding and the agouti obesity syndrome. Nature 385:165-168
87. **Chen AS, Metzger JM, Trumbauer ME, Guan XM, Yu H, Frazier EG, Marsh DJ, Forrest MJ, Gopal-Truter S, Fisher J, Camacho RE, Strack AM, Mellin TN, MacIntyre DE, Chen HY, Van der Ploeg LH** 2000 Role of the melanocortin-4 receptor in metabolic rate and food intake in mice. Transgenic research 9:145-154
88. **Huszar D, Lynch CA, Fairchild-Huntress V, Dunmore JH, Fang Q, Berkemeier LR, Gu W, Kesterson RA, Boston BA, Cone RD, Smith FJ, Campfield LA, Burn P, Lee F** 1997 Targeted disruption of the melanocortin-4 receptor results in obesity in mice. Cell 88:131-141

89. **Farooqi IS, Yeo GS, Keogh JM, Aminian S, Jebb SA, Butler G, Cheetham T, O'Rahilly S** 2000 Dominant and recessive inheritance of morbid obesity associated with melanocortin 4 receptor deficiency. J Clin Invest 106:271-279
90. **Morton GJ, Schwartz MW** 2001 The NPY/AgRP neuron and energy homeostasis. Int J Obes Relat Metab Disord 25 Suppl 5:S56-62
91. **Ollmann MM, Wilson BD, Yang YK, Kerns JA, Chen Y, Gantz I, Barsh GS** 1997 Antagonism of central melanocortin receptors in vitro and in vivo by agouti-related protein. Science 278:135-138
92. **Tatemoto K, Carlquist M, Mutt V** 1982 Neuropeptide Y--a novel brain peptide with structural similarities to peptide YY and pancreatic polypeptide. Nature 296:659-660
93. **Kamiji MM, Inui A** 2007 Neuropeptide y receptor selective ligands in the treatment of obesity. Endocr Rev 28:664-684
94. **Cabrele C, Beck-Sickinger AG** 2000 Molecular characterization of the ligand-receptor interaction of the neuropeptide Y family. Journal of peptide science : an official publication of the European Peptide Society 6:97-122
95. **Larhammar D** 1996 Evolution of neuropeptide Y, peptide YY and pancreatic polypeptide. Regulatory peptides 62:1-11
96. **Allen YS, Adrian TE, Allen JM, Tatemoto K, Crow TJ, Bloom SR, Polak JM** 1983 Neuropeptide Y distribution in the rat brain. Science 221:877-879
97. **Caberlotto L, Fuxe K, Hurd YL** 2000 Characterization of NPY mRNA-expressing cells in the human brain: co-localization with Y2 but not Y1 mRNA in the cerebral cortex, hippocampus, amygdala, and striatum. J Chem Neuroanat 20:327-337
98. **Saderi N, Salgado-Delgado R, Avendano-Pradel R, Basualdo Mdel C, Ferri GL, Chavez-Macias L, Roblera JE, Escobar C, Buijs RM** 2012 NPY and VGF immunoreactivity increased in the arcuate nucleus, but decreased in the nucleus of the Tractus Solitarius, of type-II diabetic patients. PLoS One 7:e40070
99. **Pedrazzini T, Pralong F, Grouzmann E** 2003 Neuropeptide Y: the universal soldier. Cellular and molecular life sciences : CMLS 60:350-377
100. **Sousa DM, Herzog H, Lamghari M** 2009 NPY signalling pathway in bone homeostasis: Y1 receptor as a potential drug target. Current drug targets 10:9-19
101. **Kojima S, Ueno N, Asakawa A, Sagiyama K, Naruo T, Mizuno S, Inui A** 2007 A role for pancreatic polypeptide in feeding and body weight regulation. Peptides 28:459-463
102. **Karra E, Chandarana K, Batterham RL** 2009 The role of peptide YY in appetite regulation and obesity. J Physiol 587:19-25
103. **Minor RK, Chang JW, de Cabo R** 2009 Hungry for life: How the arcuate nucleus and neuropeptide Y may play a critical role in mediating the benefits of calorie restriction. Molecular and cellular endocrinology 299:79-88
104. **Silva AP, Cavadas C, Grouzmann E** 2002 Neuropeptide Y and its receptors as potential therapeutic drug targets. Clinica chimica acta; international journal of clinical chemistry 326:3-25
105. **Lindner D, Stichel J, Beck-Sickinger AG** 2008 Molecular recognition of the NPY hormone family by their receptors. Nutrition 24:907-917
106. **Larhammar D, Blomqvist AG, Yee F, Jazin E, Yoo H, Wahlested C** 1992 Cloning and functional expression of a human neuropeptide Y/peptide YY receptor of the Y1 type. J Biol Chem 267:10935-10938
107. **Herzog H, Hort YJ, Ball HJ, Hayes G, Shine J, Selbie LA** 1992 Cloned human neuropeptide Y receptor couples to two different second messenger systems. Proc Natl Acad Sci U S A 89:5794-5798
108. **Gerald C, Walker MW, Vaysse PJ, He C, Branchek TA, Weinshank RL** 1995 Expression cloning and pharmacological characterization of a human hippocampal neuropeptide Y/peptide YY Y2 receptor subtype. J Biol Chem 270:26758-26761

109. **Merten N, Lindner D, Rabe N, Rompler H, Morl K, Schoneberg T, Beck-Sickinger AG** 2007 Receptor subtype-specific docking of Asp6.59 with C-terminal arginine residues in Y receptor ligands. J Biol Chem 282:7543-7551
110. **Chee MJ, Myers MG, Jr., Price CJ, Colmers WF** 2010 Neuropeptide Y suppresses anorexigenic output from the ventromedial nucleus of the hypothalamus. J Neurosci 30:3380-3390
111. **Klenke U, Constantin S, Wray S** 2010 Neuropeptide Y directly inhibits neuronal activity in a subpopulation of gonadotropin-releasing hormone-1 neurons via Y1 receptors. Endocrinology 151:2736-2746
112. **Zhang L, Bijker MS, Herzog H** 2011 The neuropeptide Y system: pathophysiological and therapeutic implications in obesity and cancer. Pharmacology & therapeutics 131:91-113
113. **Fetissov SO, Kopp J, Hokfelt T** 2004 Distribution of NPY receptors in the hypothalamus. Neuropeptides 38:175-188
114. **Stanic D, Mulder J, Watanabe M, Hokfelt T** 2011 Characterization of NPY Y2 receptor protein expression in the mouse brain. II. Coexistence with NPY, the Y1 receptor, and other neurotransmitter-related molecules. The Journal of comparative neurology 519:1219-1257
115. **King PJ, Williams G, Doods H, Widdowson PS** 2000 Effect of a selective neuropeptide Y Y(2) receptor antagonist, BIIE0246 on neuropeptide Y release. European journal of pharmacology 396:R1-3
116. **Ghamari-Langroudi M, Colmers WF, Cone RD** 2005 PYY3-36 inhibits the action potential firing activity of POMC neurons of arcuate nucleus through postsynaptic Y2 receptors. Cell Metab 2:191-199
117. **Hirsch D, Zukowska Z** 2012 NPY and Stress 30 Years Later: The Peripheral View. Cellular and molecular neurobiology
118. **Wolak ML, DeJoseph MR, Cator AD, Mokashi AS, Brownfield MS, Urban JH** 2003 Comparative distribution of neuropeptide Y Y1 and Y5 receptors in the rat brain by using immunohistochemistry. The Journal of comparative neurology 464:285-311
119. **Mullins D, Kirby D, Hwa J, Guzzi M, Rivier J, Parker E** 2001 Identification of potent and selective neuropeptide Y Y(1) receptor agonists with orexigenic activity in vivo. Molecular pharmacology 60:534-540
120. **Haynes AC, Arch JR, Wilson S, McClue S, Buckingham RE** 1998 Characterisation of the neuropeptide Y receptor that mediates feeding in the rat: a role for the Y5 receptor? Regulatory peptides 75-76:355-361
121. **McCrea K, Wisialowski T, Cabrele C, Church B, Beck-Sickinger A, Kraegen E, Herzog H** 2000 2-36[K4,RYYSA(19-23)]PP a novel Y5-receptor preferring ligand with strong stimulatory effect on food intake. Regulatory peptides 87:47-58
122. **Parker EM, Balasubramaniam A, Guzzi M, Mullins DE, Salisbury BG, Sheriff S, Witten MB, Hwa JJ** 2000 [D-Trp(34)] neuropeptide Y is a potent and selective neuropeptide Y Y(5) receptor agonist with dramatic effects on food intake. Peptides 21:393-399
123. **Batterham RL, Cowley MA, Small CJ, Herzog H, Cohen MA, Dakin CL, Wren AM, Brynes AE, Low MJ, Ghatei MA, Cone RD, Bloom SR** 2002 Gut hormone PYY(3-36) physiologically inhibits food intake. Nature 418:650-654
124. **Tschop M, Castaneda TR, Joost HG, Thone-Reineke C, Ortmann S, Klaus S, Hagan MM, Chandler PC, Oswald KD, Benoit SC, Seeley RJ, Kinzig KP, Moran TH, Beck-sickinger AG, Koglin N, Rodgers RJ, Blundell JE, Ishii Y, Beattie AH, Holch P, Allison DB, Raun K, Madsen K, Wulff BS, Stidsen CE, Birringer M, Kreuzer OJ, Schindler M, Arndt K, Rudolf K, Mark M, Deng XY, Whitcomb DC, Halem H, Taylor J, Dong J, Datta R, Culler M, Craney S, Flora D, Smiley D, Heiman ML**

2004 Physiology: does gut hormone PYY3-36 decrease food intake in rodents? Nature 430:1 p following 165; discussion 162 p following 165
125. **Shi YC, Baldock PA** 2012 Central and peripheral mechanisms of the NPY system in the regulation of bone and adipose tissue. Bone 50:430-436
126. **Chambers AP, Woods SC** 2012 The role of neuropeptide Y in energy homeostasis. Handbook of experimental pharmacology:23-45
127. **Zhang L, Macia L, Turner N, Enriquez RF, Riepler SJ, Nguyen AD, Lin S, Lee NJ, Shi YC, Yulyaningsih E, Slack K, Baldock PA, Herzog H, Sainsbury A** 2010 Peripheral neuropeptide Y Y1 receptors regulate lipid oxidation and fat accretion. Int J Obes (Lond) 34:357-373
128. **Clark JT, Kalra PS, Crowley WR, Kalra SP** 1984 Neuropeptide Y and human pancreatic polypeptide stimulate feeding behavior in rats. Endocrinology 115:427-429
129. **Levine AS, Morley JE** 1984 Neuropeptide Y: a potent inducer of consummatory behavior in rats. Peptides 5:1025-1029
130. **Stanley BG, Leibowitz SF** 1984 Neuropeptide Y: stimulation of feeding and drinking by injection into the paraventricular nucleus. Life Sci 35:2635-2642
131. **Vettor R, Zarjevski N, Cusin I, Rohner-Jeanrenaud F, Jeanrenaud B** 1994 Induction and reversibility of an obesity syndrome by intracerebroventricular neuropeptide Y administration to normal rats. Diabetologia 37:1202-1208
132. **Raposinho PD, Pierroz DD, Broqua P, White RB, Pedrazzini T, Aubert ML** 2001 Chronic administration of neuropeptide Y into the lateral ventricle of C57BL/6J male mice produces an obesity syndrome including hyperphagia, hyperleptinemia, insulin resistance, and hypogonadism. Molecular and cellular endocrinology 185:195-204
133. **Halaas JL, Gajiwala KS, Maffei M, Cohen SL, Chait BT, Rabinowitz D, Lallone RL, Burley SK, Friedman JM** 1995 Weight-reducing effects of the plasma protein encoded by the obese gene. Science 269:543-546
134. **Beck B, Burlet A, Bazin R, Nicolas JP, Burlet C** 1993 Elevated neuropeptide Y in the arcuate nucleus of young obese Zucker rats may contribute to the development of their overeating. J Nutr 123:1168-1172
135. **Sanacora G, Kershaw M, Finkelstein JA, White JD** 1990 Increased hypothalamic content of preproneuropeptide Y messenger ribonucleic acid in genetically obese Zucker rats and its regulation by food deprivation. Endocrinology 127:730-737
136. **Schwartz MW, Baskin DG, Bukowski TR, Kuijper JL, Foster D, Lasser G, Prunkard DE, Porte D, Jr., Woods SC, Seeley RJ, Weigle DS** 1996 Specificity of leptin action on elevated blood glucose levels and hypothalamic neuropeptide Y gene expression in ob/ob mice. Diabetes 45:531-535
137. **Jang M, Romsos DR** 1998 Neuropeptide Y and corticotropin-releasing hormone concentrations within specific hypothalamic regions of lean but not ob/ob mice respond to food-deprivation and refeeding. J Nutr 128:2520-2525
138. **Stephens TW, Basinski M, Bristow PK, Bue-Valleskey JM, Burgett SG, Craft L, Hale J, Hoffmann J, Hsiung HM, Kriauciunas A, et al.** 1995 The role of neuropeptide Y in the antiobesity action of the obese gene product. Nature 377:530-532
139. **Sipols AJ, Baskin DG, Schwartz MW** 1995 Effect of intracerebroventricular insulin infusion on diabetic hyperphagia and hypothalamic neuropeptide gene expression. Diabetes 44:147-151
140. **Wilding JP, Gilbey SG, Mannan M, Aslam N, Ghatei MA, Bloom SR** 1992 Increased neuropeptide Y content in individual hypothalamic nuclei, but not neuropeptide Y mRNA, in diet-induced obesity in rats. The Journal of endocrinology 132:299-304
141. **Patel HR, Qi Y, Hawkins EJ, Hileman SM, Elmquist JK, Imai Y, Ahima RS** 2006 Neuropeptide Y deficiency attenuates responses to fasting and high-fat diet in obesity-prone mice. Diabetes 55:3091-3098

142. **Erickson JC, Hollopeter G, Palmiter RD** 1996 Attenuation of the obesity syndrome of ob/ob mice by the loss of neuropeptide Y. Science 274:1704-1707
143. **Baranowska B, Wolinska-Witort E, Martynska L, Chmielowska M, Mazurczak-Pluta T, Boguradzka A, Baranowska-Bik A** 2005 Sibutramine therapy in obese women--effects on plasma neuropeptide Y (NPY), insulin, leptin and beta-endorphin concentrations. Neuro endocrinology letters 26:675-679
144. **Baranowska B, Wolinska-Witort E, Wasilewska-Dziubinska E, Roguski K, Martynska L, Chmielowska M** 2003 The role of neuropeptides in the disturbed control of appetite and hormone secretion in eating disorders. Neuro endocrinology letters 24:431-434
145. **Bray MS, Boerwinkle E, Hanis CL** 1999 Linkage analysis of candidate obesity genes among the Mexican-American population of Starr County, Texas. Genetic epidemiology 16:397-411
146. **Roche C, Boutin P, Dina C, Gyapay G, Basdevant A, Hager J, Guy-Grand B, Clement K, Froguel P** 1997 Genetic studies of neuropeptide Y and neuropeptide Y receptors Y1 and Y5 regions in morbid obesity. Diabetologia 40:671-675
147. **Norman RA, Thompson DB, Foroud T, Garvey WT, Bennett PH, Bogardus C, Ravussin E** 1997 Genomewide search for genes influencing percent body fat in Pima Indians: suggestive linkage at chromosome 11q21-q22. Pima Diabetes Gene Group. American journal of human genetics 60:166-173
148. **Norman RA, Tataranni PA, Pratley R, Thompson DB, Hanson RL, Prochazka M, Baier L, Ehm MG, Sakul H, Foroud T, Garvey WT, Burns D, Knowler WC, Bennett PH, Bogardus C, Ravussin E** 1998 Autosomal genomic scan for loci linked to obesity and energy metabolism in Pima Indians. American journal of human genetics 62:659-668
149. **Goldstone AP, Unmehopa UA, Bloom SR, Swaab DF** 2002 Hypothalamic NPY and agouti-related protein are increased in human illness but not in Prader-Willi syndrome and other obese subjects. J Clin Endocrinol Metab 87:927-937
150. **Parker RM, Herzog H** 1999 Regional distribution of Y-receptor subtype mRNAs in rat brain. The European journal of neuroscience 11:1431-1448
151. **Leibowitz SF, Hammer NJ, Chang K** 1981 Hypothalamic paraventricular nucleus lesions produce overeating and obesity in the rat. Physiol Behav 27:1031-1040
152. **Inoue S, Satoh S, Tanaka K, Takamura Y, Murase T** 1993 Determinants of fasting hypertriglyceridemia in ventromedial hypothalamic obesity in rats. Am J Physiol 265:R786-791
153. **Billington CJ, Briggs JE, Harker S, Grace M, Levine AS** 1994 Neuropeptide Y in hypothalamic paraventricular nucleus: a center coordinating energy metabolism. Am J Physiol 266:R1765-1770
154. **Stanley BG, Kyrkouli SE, Lampert S, Leibowitz SF** 1986 Neuropeptide Y chronically injected into the hypothalamus: a powerful neurochemical inducer of hyperphagia and obesity. Peptides 7:1189-1192
155. **Stanley BG, Magdalin W, Seirafi A, Thomas WJ, Leibowitz SF** 1993 The perifornical area: the major focus of (a) patchily distributed hypothalamic neuropeptide Y-sensitive feeding system(s). Brain Res 604:304-317
156. **Daniels AJ, Chance WT, Grizzle MK, Heyer D, Matthews JE** 2001 Food intake inhibition and reduction in body weight gain in rats treated with GI264879A, a non-selective NPY-Y1 receptor antagonist. Peptides 22:483-491
157. **Kanatani A, Ishihara A, Asahi S, Tanaka T, Ozaki S, Ihara M** 1996 Potent neuropeptide Y Y1 receptor antagonist, 1229U91: blockade of neuropeptide Y-induced and physiological food intake. Endocrinology 137:3177-3182

158. **Wieland HA, Engel W, Eberlein W, Rudolf K, Doods HN** 1998 Subtype selectivity of the novel nonpeptide neuropeptide Y Y1 receptor antagonist BIBO 3304 and its effect on feeding in rodents. British journal of pharmacology 125:549-555
159. **Daniels AJ, Grizzle MK, Wiard RP, Matthews JE, Heyer D** 2002 Food intake inhibition and reduction in body weight gain in lean and obese rodents treated with GW438014A, a potent and selective NPY-Y5 receptor antagonist. Regulatory peptides 106:47-54
160. **Kask A, Vasar E, Heidmets LT, Allikmets L, Wikberg JE** 2001 Neuropeptide Y Y(5) receptor antagonist CGP71683A: the effects on food intake and anxiety-related behavior in the rat. European journal of pharmacology 414:215-224
161. **Polidori C, Ciccocioppo R, Regoli D, Massi M** 2000 Neuropeptide Y receptor(s) mediating feeding in the rat: characterization with antagonists. Peptides 21:29-35
162. **Yokosuka M, Dube MG, Kalra PS, Kalra SP** 2001 The mPVN mediates blockade of NPY-induced feeding by a Y5 receptor antagonist: a c-FOS analysis. Peptides 22:507-514
163. **Lopez-Valpuesta FJ, Nyce JW, Griffin-Biggs TA, Ice JC, Myers RD** 1996 Antisense to NPY-Y1 demonstrates that Y1 receptors in the hypothalamus underlie NPY hypothermia and feeding in rats. Proceedings Biological sciences / The Royal Society 263:881-886
164. **Flynn MC, Turrin NP, Plata-Salaman CR, Ffrench-Mullen JM** 1999 Feeding response to neuropeptide Y-related compounds in rats treated with Y5 receptor antisense or sense phosphothio-oligodeoxynucleotide. Physiol Behav 66:881-884
165. **Schaffhauser AO, Stricker-Krongrad A, Brunner L, Cumin F, Gerald C, Whitebread S, Criscione L, Hofbauer KG** 1997 Inhibition of food intake by neuropeptide Y Y5 receptor antisense oligodeoxynucleotides. Diabetes 46:1792-1798
166. **Tang-Christensen M, Kristensen P, Stidsen CE, Brand CL, Larsen PJ** 1998 Central administration of Y5 receptor antisense decreases spontaneous food intake and attenuates feeding in response to exogenous neuropeptide Y. The Journal of endocrinology 159:307-312
167. **Marsh DJ, Hollopeter G, Kafer KE, Palmiter RD** 1998 Role of the Y5 neuropeptide Y receptor in feeding and obesity. Nat Med 4:718-721
168. **Kushi A, Sasai H, Koizumi H, Takeda N, Yokoyama M, Nakamura M** 1998 Obesity and mild hyperinsulinemia found in neuropeptide Y-Y1 receptor-deficient mice. Proc Natl Acad Sci U S A 95:15659-15664
169. **Pedrazzini T, Seydoux J, Kunstner P, Aubert JF, Grouzmann E, Beermann F, Brunner HR** 1998 Cardiovascular response, feeding behavior and locomotor activity in mice lacking the NPY Y1 receptor. Nat Med 4:722-726
170. **Pralong FP, Gonzales C, Voirol MJ, Palmiter RD, Brunner HR, Gaillard RC, Seydoux J, Pedrazzini T** 2002 The neuropeptide Y Y1 receptor regulates leptin-mediated control of energy homeostasis and reproductive functions. The FASEB journal : official publication of the Federation of American Societies for Experimental Biology 16:712-714
171. **Ishihara A, Kanatani A, Mashiko S, Tanaka T, Hidaka M, Gomori A, Iwaasa H, Murai N, Egashira S, Murai T, Mitobe Y, Matsushita H, Okamoto O, Sato N, Jitsuoka M, Fukuroda T, Ohe T, Guan X, MacNeil DJ, Van der Ploeg LH, Nishikibe M, Ishii Y, Ihara M, Fukami T** 2006 A neuropeptide Y Y5 antagonist selectively ameliorates body weight gain and associated parameters in diet-induced obese mice. Proc Natl Acad Sci U S A 103:7154-7158
172. **Erondu N, Wadden T, Gantz I, Musser B, Nguyen AM, Bays H, Bray G, O'Neil PM, Basdevant A, Kaufman KD, Heymsfield SB, Amatruda JM** 2007 Effect of NPY5R

antagonist MK-0557 on weight regain after very-low-calorie diet-induced weight loss. Obesity (Silver Spring) 15:895-905

173. **Asakawa A, Inui A, Ueno N, Fujimiya M, Fujino MA, Kasuga M** 1999 Mouse pancreatic polypeptide modulates food intake, while not influencing anxiety in mice. Peptides 20:1445-1448
174. **Balasubramaniam A, Mullins DE, Lin S, Zhai W, Tao Z, Dhawan VC, Guzzi M, Knittel JJ, Slack K, Herzog H, Parker EM** 2006 Neuropeptide Y (NPY) Y4 receptor selective agonists based on NPY(32-36): development of an anorectic Y4 receptor selective agonist with picomolar affinity. Journal of medicinal chemistry 49:2661-2665
175. **Naveilhan P, Hassani H, Canals JM, Ekstrand AJ, Larefalk A, Chhajlani V, Arenas E, Gedda K, Svensson L, Thoren P, Ernfors P** 1999 Normal feeding behavior, body weight and leptin response require the neuropeptide Y Y2 receptor. Nat Med 5:1188-1193
176. **Sainsbury A, Schwarzer C, Couzens M, Jenkins A, Oakes SR, Ormandy CJ, Herzog H** 2002 Y4 receptor knockout rescues fertility in ob/ob mice. Genes & development 16:1077-1088
177. **Sainsbury A, Schwarzer C, Couzens M, Herzog H** 2002 Y2 receptor deletion attenuates the type 2 diabetic syndrome of ob/ob mice. Diabetes 51:3420-3427
178. **Pittner RA, Moore CX, Bhavsar SP, Gedulin BR, Smith PA, Jodka CM, Parkes DG, Paterniti JR, Srivastava VP, Young AA** 2004 Effects of PYY[3-36] in rodent models of diabetes and obesity. Int J Obes Relat Metab Disord 28:963-971
179. **Chelikani PK, Haver AC, Reeve JR, Jr., Keire DA, Reidelberger RD** 2006 Daily, intermittent intravenous infusion of peptide YY(3-36) reduces daily food intake and adiposity in rats. Am J Physiol Regul Integr Comp Physiol 290:R298-305
180. **Asakawa A, Inui A, Yuzuriha H, Ueno N, Katsuura G, Fujimiya M, Fujino MA, Niijima A, Meguid MM, Kasuga M** 2003 Characterization of the effects of pancreatic polypeptide in the regulation of energy balance. Gastroenterology 124:1325-1336
181. **Batterham RL, Le Roux CW, Cohen MA, Park AJ, Ellis SM, Patterson M, Frost GS, Ghatei MA, Bloom SR** 2003 Pancreatic polypeptide reduces appetite and food intake in humans. J Clin Endocrinol Metab 88:3989-3992
182. **Jesudason DR, Monteiro MP, McGowan BM, Neary NM, Park AJ, Philippou E, Small CJ, Frost GS, Ghatei MA, Bloom SR** 2007 Low-dose pancreatic polypeptide inhibits food intake in man. Br J Nutr 97:426-429
183. **Batterham RL, Cohen MA, Ellis SM, Le Roux CW, Withers DJ, Frost GS, Ghatei MA, Bloom SR** 2003 Inhibition of food intake in obese subjects by peptide YY3-36. N Engl J Med 349:941-948
184. **Berntson GG, Zipf WB, O'Dorisio TM, Hoffman JA, Chance RE** 1993 Pancreatic polypeptide infusions reduce food intake in Prader-Willi syndrome. Peptides 14:497-503
185. **Lin S, Shi YC, Yulyaningsih E, Aljanova A, Zhang L, Macia L, Nguyen AD, Lin EJ, During MJ, Herzog H, Sainsbury A** 2009 Critical role of arcuate Y4 receptors and the melanocortin system in pancreatic polypeptide-induced reduction in food intake in mice. PLoS One 4:e8488
186. **Obici S, Zhang BB, Karkanias G, Rossetti L** 2002 Hypothalamic insulin signaling is required for inhibition of glucose production. Nat Med 8:1376-1382
187. **Obici S, Feng Z, Karkanias G, Baskin DG, Rossetti L** 2002 Decreasing hypothalamic insulin receptors causes hyperphagia and insulin resistance in rats. Nat Neurosci 5:566-572
188. **German J, Kim F, Schwartz GJ, Havel PJ, Rhodes CJ, Schwartz MW, Morton GJ** 2009 Hypothalamic leptin signaling regulates hepatic insulin sensitivity via a neurocircuit involving the vagus nerve. Endocrinology 150:4502-4511

189. **van den Hoek AM, van Heijningen C, Schroder-van der Elst JP, Ouwens DM, Havekes LM, Romijn JA, Kalsbeek A, Pijl H** 2008 Intracerebroventricular administration of neuropeptide Y induces hepatic insulin resistance via sympathetic innervation. Diabetes 57:2304-2310
190. **Marks JL, Waite K** 1997 Intracerebroventricular neuropeptide Y acutely influences glucose metabolism and insulin sensitivity in the rat. Journal of neuroendocrinology 9:99-103
191. **van den Hoek AM, Voshol PJ, Karnekamp BN, Buijs RM, Romijn JA, Havekes LM, Pijl H** 2004 Intracerebroventricular neuropeptide Y infusion precludes inhibition of glucose and VLDL production by insulin. Diabetes 53:2529-2534
192. **Bruinstroop E, Pei L, Ackermans MT, Foppen E, Borgers AJ, Kwakkel J, Alkemade A, Fliers E, Kalsbeek A** 2012 Hypothalamic Neuropeptide Y (NPY) Controls Hepatic VLDL-Triglyceride Secretion in Rats via the Sympathetic Nervous System. Diabetes 61:1043-1050
193. **Rosmond R, Dallman MF, Bjorntorp P** 1998 Stress-related cortisol secretion in men: relationships with abdominal obesity and endocrine, metabolic and hemodynamic abnormalities. J Clin Endocrinol Metab 83:1853-1859
194. **Cameron OG, Kronfol Z, Greden JF, Carroll BJ** 1984 Hypothalamic-pituitary-adrenocortical activity in patients with diabetes mellitus. Archives of general psychiatry 41:1090-1095
195. **Roy M, Collier B, Roy A** 1990 Hypothalamic-pituitary-adrenal axis dysregulation among diabetic outpatients. Psychiatry research 31:31-37
196. **Andrew R, Phillips DI, Walker BR** 1998 Obesity and gender influence cortisol secretion and metabolism in man. J Clin Endocrinol Metab 83:1806-1809
197. **Duclos M, Timofeeva E, Michel C, Richard D** 2005 Corticosterone-dependent metabolic and neuroendocrine abnormalities in obese Zucker rats in relation to feeding. Am J Physiol Endocrinol Metab 288:E254-266
198. **Tannenbaum BM, Brindley DN, Tannenbaum GS, Dallman MF, McArthur MD, Meaney MJ** 1997 High-fat feeding alters both basal and stress-induced hypothalamic-pituitary-adrenal activity in the rat. Am J Physiol 273:E1168-1177
199. **Chan O, Inouye K, Vranic M, Matthews SG** 2002 Hyperactivation of the hypothalamo-pituitary-adrenocortical axis in streptozotocin-diabetes is associated with reduced stress responsiveness and decreased pituitary and adrenal sensitivity. Endocrinology 143:1761-1768
200. **Sainsbury A, Rohner-Jeanrenaud F, Cusin I, Zakrzewska KE, Halban PA, Gaillard RC, Jeanrenaud B** 1997 Chronic central neuropeptide Y infusion in normal rats: status of the hypothalamo-pituitary-adrenal axis, and vagal mediation of hyperinsulinaemia. Diabetologia 40:1269-1277
201. **Sainsbury A, Cusin I, Rohner-Jeanrenaud F, Jeanrenaud B** 1997 Adrenalectomy prevents the obesity syndrome produced by chronic central neuropeptide Y infusion in normal rats. Diabetes 46:209-214
202. **Yi CX, Foppen E, Abplanalp W, Gao Y, Alkemade A, la Fleur SE, Serlie MJ, Fliers E, Buijs RM, Tschop MH, Kalsbeek A** 2012 Glucocorticoid signaling in the arcuate nucleus modulates hepatic insulin sensitivity. Diabetes 61:339-345
203. **Wiedmer P, Chaudhary N, Rath M, Yi CX, Ananthakrishnan G, Nogueiras R, Wirth EK, Kirchner H, Schweizer U, Jonas W, Veyrat-Durebex C, Rohner-Jeanrenaud F, Schurmann A, Joost HG, Tschop MH, Perez-Tilve D** 2012 The HPA axis modulates the CNS melanocortin control of liver triacylglyceride metabolism. Physiol Behav 105:791-799
204. **Moltz JH, McDonald JK** 1985 Neuropeptide Y: direct and indirect action on insulin secretion in the rat. Peptides 6:1155-1159

205. **Dunbar JC, Ergene E, Barraco RA** 1992 Neuropeptide-Y stimulation of insulin secretion is mediated via the nucleus tractus solitarius. Hormone and metabolic research = Hormon- und Stoffwechselforschung = Hormones et metabolisme 24:103-105
206. **Gao J, Ghibaudi L, Hwa JJ** 2004 Selective activation of central NPY Y1 vs. Y5 receptor elicits hyperinsulinemia via distinct mechanisms. Am J Physiol Endocrinol Metab 287:E706-711
207. **Zarjevski N, Cusin I, Vettor R, Rohner-Jeanrenaud F, Jeanrenaud B** 1993 Chronic intracerebroventricular neuropeptide-Y administration to normal rats mimics hormonal and metabolic changes of obesity. Endocrinology 133:1753-1758
208. **Currie PJ, Coscina DV** 1995 Dissociated feeding and hypothermic effects of neuropeptide Y in the paraventricular and perifornical hypothalamus. Peptides 16:599-604
209. **Billington CJ, Briggs JE, Grace M, Levine AS** 1991 Effects of intracerebroventricular injection of neuropeptide Y on energy metabolism. Am J Physiol 260:R321-327
210. **Henry M, Ghibaudi L, Gao J, Hwa JJ** 2005 Energy metabolic profile of mice after chronic activation of central NPY Y1, Y2, or Y5 receptors. Obes Res 13:36-47
211. **Stafford JM, Yu F, Printz R, Hasty AH, Swift LL, Niswender KD** 2008 Central nervous system neuropeptide Y signaling modulates VLDL triglyceride secretion. Diabetes 57:1482-1490
212. **Bernardis LL, Schnatz JD** 1971 Localization in the ventromdedial hypothalamic nuclei of an area affecting plasma triglyceride and cholesterol levels. Journal of neuro-visceral relations 32:90-103
213. **Karakash C, Hustvedt BE, Lovo A, Le Marchand Y, Jeanrenaud B** 1977 Consequences of ventromedial hypothalamic lesions on metabolism of perfused rat liver. Am J Physiol 232:E286-293
214. **Baran K, Preston E, Wilks D, Cooney GJ, Kraegen EW, Sainsbury A** 2002 Chronic central melanocortin-4 receptor antagonism and central neuropeptide-Y infusion in rats produce increased adiposity by divergent pathways. Diabetes 51:152-158
215. **Lam TK, Gutierrez-Juarez R, Pocai A, Bhanot S, Tso P, Schwartz GJ, Rossetti L** 2007 Brain glucose metabolism controls the hepatic secretion of triglyceride-rich lipoproteins. Nat Med 13:171-180
216. **Yue JT, Mighiu PI, Naples M, Adeli K, Lam TK** 2012 Glycine Normalizes Hepatic Triglyceride-Rich VLDL Secretion by Triggering the CNS in High-Fat Fed Rats. Circ Res
217. **Singhal NS, Lazar MA, Ahima RS** 2007 Central resistin induces hepatic insulin resistance via neuropeptide Y. J Neurosci 27:12924-12932
218. **Karvonen MK, Pesonen U, Koulu M, Niskanen L, Laakso M, Rissanen A, Dekker JM, Hart LM, Valve R, Uusitupa MI** 1998 Association of a leucine(7)-to-proline(7) polymorphism in the signal peptide of neuropeptide Y with high serum cholesterol and LDL cholesterol levels. Nat Med 4:1434-1437
219. **Mitchell GC, Wang Q, Ramamoorthy P, Whim MD** 2008 A common single nucleotide polymorphism alters the synthesis and secretion of neuropeptide Y. J Neurosci 28:14428-14434
220. **Mashiko S, Ishihara A, Iwaasa H, Sano H, Oda Z, Ito J, Yumoto M, Okawa M, Suzuki J, Fukuroda T, Jitsuoka M, Morin NR, MacNeil DJ, Van der Ploeg LH, Ihara M, Fukami T, Kanatani A** 2003 Characterization of neuropeptide Y (NPY) Y5 receptor-mediated obesity in mice: chronic intracerebroventricular infusion of D-Trp(34)NPY. Endocrinology 144:1793-1801
221. **Blumenthal JB, Andersen RE, Mitchell BD, Seibert MJ, Yang H, Herzog H, Beamer BA, Franckowiak SC, Walston JD** 2002 Novel neuropeptide Y1 and Y5 receptor gene

variants: associations with serum triglyceride and high-density lipoprotein cholesterol levels. Clinical genetics 62:196-202
222. **Rojas JM, Stafford JM, Saadat S, Printz RL, Beck-Sickinger AG, Niswender KD** 2012 Central nervous system neuropeptide Y signaling via the Y1 receptor partially dissociates feeding behavior from lipoprotein metabolism in lean rats. Am J Physiol Endocrinol Metab 303:E1479-E1488
223. **Ginsberg HN** 1998 Lipoprotein physiology. Endocrinology and metabolism clinics of North America 27:503-519
224. **Wiggins D, Gibbons GF** 1996 Origin of hepatic very-low-density lipoprotein triacylglycerol: the contribution of cellular phospholipid. Biochem J 320 (Pt 2):673-679
225. **Sundaram M, Yao Z** 2010 Recent progress in understanding protein and lipid factors affecting hepatic VLDL assembly and secretion. Nutrition & metabolism 7:35
226. **Glickman RM, Rogers M, Glickman JN** 1986 Apolipoprotein B synthesis by human liver and intestine in vitro. Proc Natl Acad Sci U S A 83:5296-5300
227. **Cartwright IJ, Higgins JA** 1992 Quantification of apolipoprotein B-48 and B-100 in rat liver endoplasmic reticulum and Golgi fractions. Biochem J 285 (Pt 1):153-159
228. **Gibbons GF, Wiggins D, Brown AM, Hebbachi AM** 2004 Synthesis and function of hepatic very-low-density lipoprotein. Biochem Soc Trans 32:59-64
229. **Wetterau JR, Aggerbeck LP, Bouma ME, Eisenberg C, Munck A, Hermier M, Schmitz J, Gay G, Rader DJ, Gregg RE** 1992 Absence of microsomal triglyceride transfer protein in individuals with abetalipoproteinemia. Science 258:999-1001
230. **Fisher EA, Ginsberg HN** 2002 Complexity in the secretory pathway: the assembly and secretion of apolipoprotein B-containing lipoproteins. J Biol Chem 277:17377-17380
231. **Olofsson SO, Asp L, Boren J** 1999 The assembly and secretion of apolipoprotein B-containing lipoproteins. Current opinion in lipidology 10:341-346
232. **Valyi-Nagy K, Harris C, Swift LL** 2002 The assembly of hepatic very low density lipoproteins: evidence of a role for the Golgi apparatus. Lipids 37:879-884
233. **Asp L, Claesson C, Boren J, Olofsson SO** 2000 ADP-ribosylation factor 1 and its activation of phospholipase D are important for the assembly of very low density lipoproteins. J Biol Chem 275:26285-26292
234. **Asp L, Magnusson B, Rutberg M, Li L, Boren J, Olofsson SO** 2005 Role of ADP ribosylation factor 1 in the assembly and secretion of ApoB-100-containing lipoproteins. Arteriosclerosis, thrombosis, and vascular biology 25:566-570
235. **Rustaeus S, Lindberg K, Boren J, Olofsson SO** 1995 Brefeldin A reversibly inhibits the assembly of apoB containing lipoproteins in McA-RH7777 cells. J Biol Chem 270:28879-28886
236. **Diraison F, Beylot M** 1998 Role of human liver lipogenesis and reesterification in triglycerides secretion and in FFA reesterification. Am J Physiol 274:E321-327
237. **Prentki M, Madiraju SR** 2008 Glycerolipid metabolism and signaling in health and disease. Endocr Rev 29:647-676
238. **Bou Khalil M, Sundaram M, Zhang HY, Links PH, Raven JF, Manmontri B, Sariahmetoglu M, Tran K, Reue K, Brindley DN, Yao Z** 2009 The level and compartmentalization of phosphatidate phosphatase-1 (lipin-1) control the assembly and secretion of hepatic VLDL. Journal of lipid research 50:47-58
239. **Yamazaki T, Sasaki E, Kakinuma C, Yano T, Miura S, Ezaki O** 2005 Increased very low density lipoprotein secretion and gonadal fat mass in mice overexpressing liver DGAT1. J Biol Chem 280:21506-21514
240. **Han GS, Wu WI, Carman GM** 2006 The Saccharomyces cerevisiae Lipin homolog is a Mg2+-dependent phosphatidate phosphatase enzyme. J Biol Chem 281:9210-9218
241. **Langner CA, Birkenmeier EH, Ben-Zeev O, Schotz MC, Sweet HO, Davisson MT, Gordon JI** 1989 The fatty liver dystrophy (fld) mutation. A new mutant mouse with a

developmental abnormality in triglyceride metabolism and associated tissue-specific defects in lipoprotein lipase and hepatic lipase activities. J Biol Chem 264:7994-8003
242. **Langner CA, Birkenmeier EH, Roth KA, Bronson RT, Gordon JI** 1991 Characterization of the peripheral neuropathy in neonatal and adult mice that are homozygous for the fatty liver dystrophy (fld) mutation. J Biol Chem 266:11955-11964
243. **Peterfy M, Phan J, Xu P, Reue K** 2001 Lipodystrophy in the fld mouse results from mutation of a new gene encoding a nuclear protein, lipin. Nature genetics 27:121-124
244. **Zeharia A, Shaag A, Houtkooper RH, Hindi T, de Lonlay P, Erez G, Hubert L, Saada A, de Keyzer Y, Eshel G, Vaz FM, Pines O, Elpeleg O** 2008 Mutations in LPIN1 cause recurrent acute myoglobinuria in childhood. American journal of human genetics 83:489-494
245. **Csaki LS, Reue K** 2010 Lipins: multifunctional lipid metabolism proteins. Annual review of nutrition 30:257-272
246. **Peterfy M, Phan J, Reue K** 2005 Alternatively spliced lipin isoforms exhibit distinct expression pattern, subcellular localization, and role in adipogenesis. J Biol Chem 280:32883-32889
247. **Donkor J, Sariahmetoglu M, Dewald J, Brindley DN, Reue K** 2007 Three mammalian lipins act as phosphatidate phosphatases with distinct tissue expression patterns. J Biol Chem 282:3450-3457
248. **Finck BN, Gropler MC, Chen Z, Leone TC, Croce MA, Harris TE, Lawrence JC, Jr., Kelly DP** 2006 Lipin 1 is an inducible amplifier of the hepatic PGC-1alpha/PPARalpha regulatory pathway. Cell Metab 4:199-210
249. **Bou Khalil M, Blais A, Figeys D, Yao Z** 2010 Lipin - The bridge between hepatic glycerolipid biosynthesis and lipoprotein metabolism. Biochim Biophys Acta 1801:1249-1259
250. **Huffman TA, Mothe-Satney I, Lawrence JC, Jr.** 2002 Insulin-stimulated phosphorylation of lipin mediated by the mammalian target of rapamycin. Proc Natl Acad Sci U S A 99:1047-1052
251. **Eaton JM, Mullins GR, Brindley DN, Harris TE** 2013 Phosphorylation of lipin 1 and charge on the phosphatidic acid head group control its phosphatidic acid phosphatase activity and membrane association. J Biol Chem
252. **Harris TE, Huffman TA, Chi A, Shabanowitz J, Hunt DF, Kumar A, Lawrence JC, Jr.** 2007 Insulin controls subcellular localization and multisite phosphorylation of the phosphatidic acid phosphatase, lipin 1. J Biol Chem 282:277-286
253. **Cascales C, Mangiapane EH, Brindley DN** 1984 Oleic acid promotes the activation and translocation of phosphatidate phosphohydrolase from the cytosol to particulate fractions of isolated rat hepatocytes. Biochem J 219:911-916
254. **Barroso E, Rodriguez-Calvo R, Serrano-Marco L, Astudillo AM, Balsinde J, Palomer X, Vazquez-Carrera M** 2011 The PPARbeta/delta activator GW501516 prevents the down-regulation of AMPK caused by a high-fat diet in liver and amplifies the PGC-1alpha-Lipin 1-PPARalpha pathway leading to increased fatty acid oxidation. Endocrinology 152:1848-1859
255. **Chen Z, Gropler MC, Norris J, Lawrence JC, Jr., Harris TE, Finck BN** 2008 Alterations in hepatic metabolism in fld mice reveal a role for lipin 1 in regulating VLDL-triacylglyceride secretion. Arteriosclerosis, thrombosis, and vascular biology 28:1738-1744
256. **Gropler MC, Harris TE, Hall AM, Wolins NE, Gross RW, Han X, Chen Z, Finck BN** 2009 Lipin 2 is a liver-enriched phosphatidate phosphohydrolase enzyme that is dynamically regulated by fasting and obesity in mice. J Biol Chem 284:6763-6772

257. **Croce MA, Eagon JC, LaRiviere LL, Korenblat KM, Klein S, Finck BN** 2007 Hepatic lipin 1beta expression is diminished in insulin-resistant obese subjects and is reactivated by marked weight loss. Diabetes 56:2395-2399
258. **Klein S, Mittendorfer B, Eagon JC, Patterson B, Grant L, Feirt N, Seki E, Brenner D, Korenblat K, McCrea J** 2006 Gastric bypass surgery improves metabolic and hepatic abnormalities associated with nonalcoholic fatty liver disease. Gastroenterology 130:1564-1572
259. **Manmontri B, Sariahmetoglu M, Donkor J, Bou Khalil M, Sundaram M, Yao Z, Reue K, Lehner R, Brindley DN** 2008 Glucocorticoids and cyclic AMP selectively increase hepatic lipin-1 expression, and insulin acts antagonistically. Journal of lipid research 49:1056-1067
260. **Zhang P, O'Loughlin L, Brindley DN, Reue K** 2008 Regulation of lipin-1 gene expression by glucocorticoids during adipogenesis. Journal of lipid research 49:1519-1528
261. **Pittner RA, Fears R, Brindley DN** 1986 Effects of insulin, glucagon, dexamethasone, cyclic GMP and spermine on the stability of phosphatidate phosphohydrolase activity in cultured rat hepatocytes. Biochem J 240:253-257
262. **Chanda D, Kim YH, Kim DK, Lee MW, Lee SY, Park TS, Koo SH, Lee CH, Choi HS** 2012 Activation of Cannabinoid Receptor Type 1 (Cb1r) Disrupts Hepatic Insulin Receptor Signaling via Cyclic AMP-response Element-binding Protein H (Crebh)-mediated Induction of Lipin1 Gene. J Biol Chem 287:38041-38049
263. **Ryu D, Oh KJ, Jo HY, Hedrick S, Kim YN, Hwang YJ, Park TS, Han JS, Choi CS, Montminy M, Koo SH** 2009 TORC2 regulates hepatic insulin signaling via a mammalian phosphatidic acid phosphatase, LIPIN1. Cell Metab 9:240-251
264. **Martin-Sanz P, Vance JE, Brindley DN** 1990 Stimulation of apolipoprotein secretion in very-low-density and high-density lipoproteins from cultured rat hepatocytes by dexamethasone. Biochem J 271:575-583
265. **Mangiapane EH, Brindley DN** 1986 Effects of dexamethasone and insulin on the synthesis of triacylglycerols and phosphatidylcholine and the secretion of very-low-density lipoproteins and lysophosphatidylcholine by monolayer cultures of rat hepatocytes. Biochem J 233:151-160
266. **Wang CN, McLeod RS, Yao Z, Brindley DN** 1995 Effects of dexamethasone on the synthesis, degradation, and secretion of apolipoprotein B in cultured rat hepatocytes. Arteriosclerosis, thrombosis, and vascular biology 15:1481-1491
267. **Mangiapane EH, Lloyd-Davies KA, Brindley DN** 1973 A study of some enzymes of glycerolipid biosynthesis in rat liver after subtotal hepatectomy. Biochem J 134:103-112
268. **Sturton RG, Butterwith SC, Burditt SL, Brindley DN** 1981 Effects of starvation, corticotropin injection and ethanol feeding on the activity and amount of phosphatidate phosphohydrolase in rat liver. FEBS letters 126:297-300
269. **Whiting PH, Bowley M, Sturton RG, Pritchard PH, Brindley DN, Hawthorne JN** 1977 The effect of chronic diabetes, induced by streptozotocin, on the activities of some enzymes of glycerolipid synthesis in rat liver. Biochem J 168:147-153
270. **Sturton RG, Pritchard PH, Han LY, Brindley DN** 1978 The involvement of phosphatidate phosphohydrolase and phospholipase A activities in the control of hepatic glycerolipid synthesis. Effects of acute feeding with glucose, fructose, sorbitol, glycerol and ethanol. Biochem J 174:667-670
271. **Brindley DN, Cooling J, Glenny HP, Burditt SL, McKechnie IS** 1981 Effects of chronic modification of dietary fat and carbohydrate on the insulin, corticosterone and metabolic responses of rats fed acutely with glucose, fructose or ethanol. Biochem J 200:275-283

272. **Hu M, Wang F, Li X, Rogers CQ, Liang X, Finck BN, Mitra MS, Zhang R, Mitchell DA, You M** 2012 Regulation of hepatic lipin-1 by ethanol: role of AMP-activated protein kinase/sterol regulatory element-binding protein 1 signaling in mice. Hepatology 55:437-446
273. **Herzig S, Long F, Jhala US, Hedrick S, Quinn R, Bauer A, Rudolph D, Schutz G, Yoon C, Puigserver P, Spiegelman B, Montminy M** 2001 CREB regulates hepatic gluconeogenesis through the coactivator PGC-1. Nature 413:179-183
274. **Yoon JC, Puigserver P, Chen G, Donovan J, Wu Z, Rhee J, Adelmant G, Stafford J, Kahn CR, Granner DK, Newgard CB, Spiegelman BM** 2001 Control of hepatic gluconeogenesis through the transcriptional coactivator PGC-1. Nature 413:131-138
275. **Vega RB, Huss JM, Kelly DP** 2000 The coactivator PGC-1 cooperates with peroxisome proliferator-activated receptor alpha in transcriptional control of nuclear genes encoding mitochondrial fatty acid oxidation enzymes. Mol Cell Biol 20:1868-1876
276. **Horton JD, Bashmakov Y, Shimomura I, Shimano H** 1998 Regulation of sterol regulatory element binding proteins in livers of fasted and refed mice. Proc Natl Acad Sci U S A 95:5987-5992
277. **Ishimoto K, Nakamura H, Tachibana K, Yamasaki D, Ota A, Hirano K, Tanaka T, Hamakubo T, Sakai J, Kodama T, Doi T** 2009 Sterol-mediated regulation of human lipin 1 gene expression in hepatoblastoma cells. J Biol Chem 284:22195-22205
278. **Lu B, Lu Y, Moser AH, Shigenaga JK, Grunfeld C, Feingold KR** 2008 LPS and proinflammatory cytokines decrease lipin-1 in mouse adipose tissue and 3T3-L1 adipocytes. Am J Physiol Endocrinol Metab 295:E1502-1509
279. **Tsuchiya Y, Takahashi N, Yoshizaki T, Tanno S, Ohhira M, Motomura W, Takakusaki K, Kohgo Y, Okumura T** 2009 A Jak2 inhibitor, AG490, reverses lipin-1 suppression by TNF-alpha in 3T3-L1 adipocytes. Biochem Biophys Res Commun 382:348-352
280. **Grimsey N, Han GS, O'Hara L, Rochford JJ, Carman GM, Siniossoglou S** 2008 Temporal and spatial regulation of the phosphatidate phosphatases lipin 1 and 2. J Biol Chem 283:29166-29174
281. **Whiteman EL, Cho H, Birnbaum MJ** 2002 Role of Akt/protein kinase B in metabolism. Trends Endocrinol Metab 13:444-451
282. **Sarbassov DD, Guertin DA, Ali SM, Sabatini DM** 2005 Phosphorylation and regulation of Akt/PKB by the rictor-mTOR complex. Science 307:1098-1101
283. **Huang J, Manning BD** 2009 A complex interplay between Akt, TSC2 and the two mTOR complexes. Biochem Soc Trans 37:217-222
284. **Cho H, Mu J, Kim JK, Thorvaldsen JL, Chu Q, Crenshaw EB, 3rd, Kaestner KH, Bartolomei MS, Shulman GI, Birnbaum MJ** 2001 Insulin resistance and a diabetes mellitus-like syndrome in mice lacking the protein kinase Akt2 (PKB beta). Science 292:1728-1731
285. **Leavens KF, Easton RM, Shulman GI, Previs SF, Birnbaum MJ** 2009 Akt2 is required for hepatic lipid accumulation in models of insulin resistance. Cell Metab 10:405-418
286. **Ono H, Shimano H, Katagiri H, Yahagi N, Sakoda H, Onishi Y, Anai M, Ogihara T, Fujishiro M, Viana AY, Fukushima Y, Abe M, Shojima N, Kikuchi M, Yamada N, Oka Y, Asano T** 2003 Hepatic Akt activation induces marked hypoglycemia, hepatomegaly, and hypertriglyceridemia with sterol regulatory element binding protein involvement. Diabetes 52:2905-2913
287. **Stiles B, Wang Y, Stahl A, Bassilian S, Lee WP, Kim YJ, Sherwin R, Devaskar S, Lesche R, Magnuson MA, Wu H** 2004 Liver-specific deletion of negative regulator Pten results in fatty liver and insulin hypersensitivity [corrected]. Proc Natl Acad Sci U S A 101:2082-2087

288. **He L, Hou X, Kanel G, Zeng N, Galicia V, Wang Y, Yang J, Wu H, Birnbaum MJ, Stiles BL** 2010 The critical role of AKT2 in hepatic steatosis induced by PTEN loss. The American journal of pathology 176:2302-2308
289. **Nakae J, Oki M, Cao Y** 2008 The FoxO transcription factors and metabolic regulation. FEBS letters 582:54-67
290. **Wullschleger S, Loewith R, Hall MN** 2006 TOR signaling in growth and metabolism. Cell 124:471-484
291. **Vander Haar E, Lee SI, Bandhakavi S, Griffin TJ, Kim DH** 2007 Insulin signalling to mTOR mediated by the Akt/PKB substrate PRAS40. Nature cell biology 9:316-323
292. **Laplante M, Sabatini DM** 2009 mTOR signaling at a glance. Journal of cell science 122:3589-3594
293. **Garcia-Martinez JM, Alessi DR** 2008 mTOR complex 2 (mTORC2) controls hydrophobic motif phosphorylation and activation of serum- and glucocorticoid-induced protein kinase 1 (SGK1). Biochem J 416:375-385
294. **Facchinetti V, Ouyang W, Wei H, Soto N, Lazorchak A, Gould C, Lowry C, Newton AC, Mao Y, Miao RQ, Sessa WC, Qin J, Zhang P, Su B, Jacinto E** 2008 The mammalian target of rapamycin complex 2 controls folding and stability of Akt and protein kinase C. The EMBO journal 27:1932-1943
295. **Petersen KF, Laurent D, Rothman DL, Cline GW, Shulman GI** 1998 Mechanism by which glucose and insulin inhibit net hepatic glycogenolysis in humans. J Clin Invest 101:1203-1209
296. **Saltiel AR** 2001 New perspectives into the molecular pathogenesis and treatment of type 2 diabetes. Cell 104:517-529
297. **Sparks JD, Sparks CE** 1994 Insulin regulation of triacylglycerol-rich lipoprotein synthesis and secretion. Biochim Biophys Acta 1215:9-32
298. **Shimomura I, Matsuda M, Hammer RE, Bashmakov Y, Brown MS, Goldstein JL** 2000 Decreased IRS-2 and increased SREBP-1c lead to mixed insulin resistance and sensitivity in livers of lipodystrophic and ob/ob mice. Molecular cell 6:77-86
299. **Brown MS, Goldstein JL** 2008 Selective versus total insulin resistance: a pathogenic paradox. Cell Metab 7:95-96
300. **Drazen DL, Wortman MD, Schwartz MW, Clegg DJ, van Dijk G, Woods SC, Seeley RJ** 2003 Adrenalectomy alters the sensitivity of the central nervous system melanocortin system. Diabetes 52:2928-2934
301. **Wright JW, Morseth SL, Abhold RH, Harding JW** 1985 Pressor action and dipsogenicity induced by angiotensin II and III in rats. Am J Physiol 249:R514-521
302. **Soll RM, Dinger MC, Lundell I, Larhammer D, Beck-Sickinger AG** 2001 Novel analogues of neuropeptide Y with a preference for the Y1-receptor. Eur J Biochem 268:2828-2837
303. **Wyss P, Stricker-Krongrad A, Brunner L, Miller J, Crossthwaite A, Whitebread S, Criscione L** 1998 The pharmacology of neuropeptide Y (NPY) receptor-mediated feeding in rats characterizes better Y5 than Y1, but not Y2 or Y4 subtypes. Regulatory peptides 75-76:363-371
304. **Cabrele C, Langer M, Bader R, Wieland HA, Doods HN, Zerbe O, Beck-Sickinger AG** 2000 The first selective agonist for the neuropeptide YY5 receptor increases food intake in rats. J Biol Chem 275:36043-36048
305. **Schotz MC, Scanu A, Page IH** 1957 Effect of triton on lipoprotein lipase of rat plasma. Am J Physiol 188:399-402
306. **Otway S, Robinson DS** 1967 The use of a non-ionic detergent (Triton WR 1339) to determine rates of triglyceride entry into the circulation of the rat under different physiological conditions. J Physiol 190:321-332

307. **Millar JS, Cromley DA, McCoy MG, Rader DJ, Billheimer JT** 2005 Determining hepatic triglyceride production in mice: comparison of poloxamer 407 with Triton WR-1339. Journal of lipid research 46:2023-2028
308. **Shiota C, Woo JT, Lindner J, Shelton KD, Magnuson MA** 2006 Multiallelic disruption of the rictor gene in mice reveals that mTOR complex 2 is essential for fetal growth and viability. Developmental cell 11:583-589
309. **Truett GE, Heeger P, Mynatt RL, Truett AA, Walker JA, Warman ML** 2000 Preparation of PCR-quality mouse genomic DNA with hot sodium hydroxide and tris (HotSHOT). BioTechniques 29:52, 54
310. **Folch J, Lees M, Sloane Stanley GH** 1957 A simple method for the isolation and purification of total lipides from animal tissues. J Biol Chem 226:497-509
311. **Morrison WR, Smith LM** 1964 Preparation of Fatty Acid Methyl Esters and Dimethylacetals from Lipids with Boron Fluoride--Methanol. Journal of lipid research 5:600-608
312. **Matsuzaka T, Shimano H, Yahagi N, Amemiya-Kudo M, Okazaki H, Tamura Y, Iizuka Y, Ohashi K, Tomita S, Sekiya M, Hasty A, Nakagawa Y, Sone H, Toyoshima H, Ishibashi S, Osuga J, Yamada N** 2004 Insulin-independent induction of sterol regulatory element-binding protein-1c expression in the livers of streptozotocin-treated mice. Diabetes 53:560-569
313. **Swift LL** 1996 Role of the Golgi apparatus in the phosphorylation of apolipoprotein B. J Biol Chem 271:31491-31495
314. **Balasubramaniam A, Joshi R, Su C, Friend LA, James JH** 2007 Neuropeptide Y (NPY) Y2 receptor-selective agonist inhibits food intake and promotes fat metabolism in mice: combined anorectic effects of Y2 and Y4 receptor-selective agonists. Peptides 28:235-240
315. **Barrows BR, Parks EJ** 2006 Contributions of different fatty acid sources to very low-density lipoprotein-triacylglycerol in the fasted and fed states. J Clin Endocrinol Metab 91:1446-1452
316. **Cohen P, Miyazaki M, Socci ND, Hagge-Greenberg A, Liedtke W, Soukas AA, Sharma R, Hudgins LC, Ntambi JM, Friedman JM** 2002 Role for stearoyl-CoA desaturase-1 in leptin-mediated weight loss. Science 297:240-243
317. **Warne JP, Alemi F, Reed AS, Varonin JM, Chan H, Piper ML, Mullin ME, Myers MG, Jr., Corvera CU, Xu AW** 2011 Impairment of Central Leptin-Mediated PI3K Signaling Manifested as Hepatic Steatosis Independent of Hyperphagia and Obesity. Cell Metab 14:791-803
318. **Iyengar S, Li DL, Simmons RM** 1999 Characterization of neuropeptide Y-induced feeding in mice: do Y1-Y6 receptor subtypes mediate feeding? The Journal of pharmacology and experimental therapeutics 289:1031-1040
319. **Rioux KP, Le T, Swain MG** 2001 Decreased orexigenic response to neuropeptide Y in rats with obstructive cholestasis. American journal of physiology Gastrointestinal and liver physiology 280:G449-456
320. **Raposinho PD, Broqua P, Pierroz DD, Hayward A, Dumont Y, Quirion R, Junien JL, Aubert ML** 1999 Evidence that the inhibition of luteinizing hormone secretion exerted by central administration of neuropeptide Y (NPY) in the rat is predominantly mediated by the NPY-Y5 receptor subtype. Endocrinology 140:4046-4055
321. **Balasubramaniam A, Sheriff S, Zhai W, Chance WT** 2002 Bis(31/31')[[Cys(31), Nva(34)]NPY(27-36)-NH(2)]: a neuropeptide Y (NPY) Y(5) receptor selective agonist with a latent stimulatory effect on food intake in rats. Peptides 23:1485-1490
322. **Kuo LE, Kitlinska JB, Tilan JU, Li L, Baker SB, Johnson MD, Lee EW, Burnett MS, Fricke ST, Kvetnansky R, Herzog H, Zukowska Z** 2007 Neuropeptide Y acts

directly in the periphery on fat tissue and mediates stress-induced obesity and metabolic syndrome. Nat Med 13:803-811
323. **Bartels ED, Lauritsen M, Nielsen LB** 2002 Hepatic expression of microsomal triglyceride transfer protein and in vivo secretion of triglyceride-rich lipoproteins are increased in obese diabetic mice. Diabetes 51:1233-1239
324. **Reue K** 2009 The lipin family: mutations and metabolism. Current opinion in lipidology 20:165-170
325. **Bonnefont JP, Djouadi F, Prip-Buus C, Gobin S, Munnich A, Bastin J** 2004 Carnitine palmitoyltransferases 1 and 2: biochemical, molecular and medical aspects. Molecular aspects of medicine 25:495-520
326. **Koonen DP, Jacobs RL, Febbraio M, Young ME, Soltys CL, Ong H, Vance DE, Dyck JR** 2007 Increased hepatic CD36 expression contributes to dyslipidemia associated with diet-induced obesity. Diabetes 56:2863-2871
327. **Go GW, Mani A** 2012 Low-density lipoprotein receptor (LDLR) family orchestrates cholesterol homeostasis. The Yale journal of biology and medicine 85:19-28
328. **Horton JD, Goldstein JL, Brown MS** 2002 SREBPs: activators of the complete program of cholesterol and fatty acid synthesis in the liver. J Clin Invest 109:1125-1131
329. **Miyazaki M, Kim YC, Gray-Keller MP, Attie AD, Ntambi JM** 2000 The biosynthesis of hepatic cholesterol esters and triglycerides is impaired in mice with a disruption of the gene for stearoyl-CoA desaturase 1. J Biol Chem 275:30132-30138
330. **Attie AD, Krauss RM, Gray-Keller MP, Brownlie A, Miyazaki M, Kastelein JJ, Lusis AJ, Stalenhoef AF, Stoehr JP, Hayden MR, Ntambi JM** 2002 Relationship between stearoyl-CoA desaturase activity and plasma triglycerides in human and mouse hypertriglyceridemia. Journal of lipid research 43:1899-1907
331. **Grefhorst A, Hoekstra J, Derks TG, Ouwens DM, Baller JF, Havinga R, Havekes LM, Romijn JA, Kuipers F** 2005 Acute hepatic steatosis in mice by blocking beta-oxidation does not reduce insulin sensitivity of very-low-density lipoprotein production. American journal of physiology Gastrointestinal and liver physiology 289:G592-598
332. **Leyton J, Drury PJ, Crawford MA** 1987 Differential oxidation of saturated and unsaturated fatty acids in vivo in the rat. Br J Nutr 57:383-393
333. **Cunnane SC, Ryan MA, Nadeau CR, Bazinet RP, Musa-Veloso K, McCloy U** 2003 Why is carbon from some polyunsaturates extensively recycled into lipid synthesis? Lipids 38:477-484
334. **Lynn WS, Brown RH** 1959 Oxidation and activation of unsaturated fatty acids. Archives of biochemistry and biophysics 81:353-362
335. **Lin Y, Schuurbiers E, Van der Veen S, De Deckere EA** 2001 Conjugated linoleic acid isomers have differential effects on triglyceride secretion in Hep G2 cells. Biochim Biophys Acta 1533:38-46
336. **Thonberg H, Fredriksson JM, Nedergaard J, Cannon B** 2002 A novel pathway for adrenergic stimulation of cAMP-response-element-binding protein (CREB) phosphorylation: mediation via alpha1-adrenoceptors and protein kinase C activation. Biochem J 364:73-79
337. **Bentzinger CF, Romanino K, Cloetta D, Lin S, Mascarenhas JB, Oliveri F, Xia J, Casanova E, Costa CF, Brink M, Zorzato F, Hall MN, Ruegg MA** 2008 Skeletal muscle-specific ablation of raptor, but not of rictor, causes metabolic changes and results in muscle dystrophy. Cell Metab 8:411-424
338. **Kumar A, Harris TE, Keller SR, Choi KM, Magnuson MA, Lawrence JC, Jr.** 2008 Muscle-specific deletion of rictor impairs insulin-stimulated glucose transport and enhances Basal glycogen synthase activity. Mol Cell Biol 28:61-70

339. **Cybulski N, Polak P, Auwerx J, Ruegg MA, Hall MN** 2009 mTOR complex 2 in adipose tissue negatively controls whole-body growth. Proc Natl Acad Sci U S A 106:9902-9907
340. **Kumar A, Lawrence JC, Jr., Jung DY, Ko HJ, Keller SR, Kim JK, Magnuson MA, Harris TE** 2010 Fat cell-specific ablation of rictor in mice impairs insulin-regulated fat cell and whole-body glucose and lipid metabolism. Diabetes 59:1397-1406
341. **Polak P, Cybulski N, Feige JN, Auwerx J, Ruegg MA, Hall MN** 2008 Adipose-specific knockout of raptor results in lean mice with enhanced mitochondrial respiration. Cell Metab 8:399-410
342. **Gu Y, Lindner J, Kumar A, Yuan W, Magnuson MA** 2011 Rictor/mTORC2 is essential for maintaining a balance between beta-cell proliferation and cell size. Diabetes 60:827-837
343. **Sengupta S, Peterson TR, Laplante M, Oh S, Sabatini DM** 2010 mTORC1 controls fasting-induced ketogenesis and its modulation by ageing. Nature 468:1100-1104
344. **Yecies JL, Zhang HH, Menon S, Liu S, Yecies D, Lipovsky AI, Gorgun C, Kwiatkowski DJ, Hotamisligil GS, Lee CH, Manning BD** 2011 Akt stimulates hepatic SREBP1c and lipogenesis through parallel mTORC1-dependent and independent pathways. Cell Metab 14:21-32
345. **Wang BT, Ducker GS, Barczak AJ, Barbeau R, Erle DJ, Shokat KM** 2011 The mammalian target of rapamycin regulates cholesterol biosynthetic gene expression and exhibits a rapamycin-resistant transcriptional profile. Proc Natl Acad Sci U S A 108:15201-15206
346. **Peterson TR, Sengupta SS, Harris TE, Carmack AE, Kang SA, Balderas E, Guertin DA, Madden KL, Carpenter AE, Finck BN, Sabatini DM** 2011 mTOR Complex 1 Regulates Lipin 1 Localization to Control the SREBP Pathway. Cell 146:408-420
347. **Yuan M, Pino E, Wu L, Kacergis M, Soukas AA** 2012 Identification of Akt-Independent Regulation of Hepatic Lipogenesis by Mammalian Target of Rapamycin (mTOR) Complex 2. J Biol Chem
348. **Hagiwara A, Cornu M, Cybulski N, Polak P, Betz C, Trapani F, Terracciano L, Heim MH, Ruegg MA, Hall MN** 2012 Hepatic mTORC2 activates glycolysis and lipogenesis through Akt, glucokinase, and SREBP1c. Cell Metab 15:725-738
349. **Postic C, Girard J** 2008 Contribution of de novo fatty acid synthesis to hepatic steatosis and insulin resistance: lessons from genetically engineered mice. J Clin Invest 118:829-838
350. **Petersen KF, Dufour S, Befroy D, Lehrke M, Hendler RE, Shulman GI** 2005 Reversal of nonalcoholic hepatic steatosis, hepatic insulin resistance, and hyperglycemia by moderate weight reduction in patients with type 2 diabetes. Diabetes 54:603-608
351. **Krycer JR, Sharpe LJ, Luu W, Brown AJ** 2010 The Akt-SREBP nexus: cell signaling meets lipid metabolism. Trends Endocrinol Metab 21:268-276
352. **Li S, Brown MS, Goldstein JL** 2010 Bifurcation of insulin signaling pathway in rat liver: mTORC1 required for stimulation of lipogenesis, but not inhibition of gluconeogenesis. Proc Natl Acad Sci U S A 107:3441-3446
353. **Porstmann T, Santos CR, Griffiths B, Cully M, Wu M, Leevers S, Griffiths JR, Chung YL, Schulze A** 2008 SREBP activity is regulated by mTORC1 and contributes to Akt-dependent cell growth. Cell Metab 8:224-236
354. **Duvel K, Yecies JL, Menon S, Raman P, Lipovsky AI, Souza AL, Triantafellow E, Ma Q, Gorski R, Cleaver S, Vander Heiden MG, MacKeigan JP, Finan PM, Clish CB, Murphy LO, Manning BD** 2010 Activation of a metabolic gene regulatory network downstream of mTOR complex 1. Molecular cell 39:171-183

355. **Owen JL, Zhang Y, Bae SH, Farooqi MS, Liang G, Hammer RE, Goldstein JL, Brown MS** 2012 Insulin stimulation of SREBP-1c processing in transgenic rat hepatocytes requires p70 S6-kinase. Proc Natl Acad Sci U S A
356. **Suzuki R, Lee K, Jing E, Biddinger SB, McDonald JG, Montine TJ, Craft S, Kahn CR** 2010 Diabetes and insulin in regulation of brain cholesterol metabolism. Cell Metab 12:567-579
357. **Chen G, Liang G, Ou J, Goldstein JL, Brown MS** 2004 Central role for liver X receptor in insulin-mediated activation of Srebp-1c transcription and stimulation of fatty acid synthesis in liver. Proc Natl Acad Sci U S A 101:11245-11250
358. **Yoshikawa T, Shimano H, Amemiya-Kudo M, Yahagi N, Hasty AH, Matsuzaka T, Okazaki H, Tamura Y, Iizuka Y, Ohashi K, Osuga J, Harada K, Gotoda T, Kimura S, Ishibashi S, Yamada N** 2001 Identification of liver X receptor-retinoid X receptor as an activator of the sterol regulatory element-binding protein 1c gene promoter. Mol Cell Biol 21:2991-3000
359. **Janowski BA, Grogan MJ, Jones SA, Wisely GB, Kliewer SA, Corey EJ, Mangelsdorf DJ** 1999 Structural requirements of ligands for the oxysterol liver X receptors LXRalpha and LXRbeta. Proc Natl Acad Sci U S A 96:266-271
360. **Repa JJ, Liang G, Ou J, Bashmakov Y, Lobaccaro JM, Shimomura I, Shan B, Brown MS, Goldstein JL, Mangelsdorf DJ** 2000 Regulation of mouse sterol regulatory element-binding protein-1c gene (SREBP-1c) by oxysterol receptors, LXRalpha and LXRbeta. Genes & development 14:2819-2830
361. **DeBose-Boyd RA, Ou J, Goldstein JL, Brown MS** 2001 Expression of sterol regulatory element-binding protein 1c (SREBP-1c) mRNA in rat hepatoma cells requires endogenous LXR ligands. Proc Natl Acad Sci U S A 98:1477-1482
362. **Peet DJ, Turley SD, Ma W, Janowski BA, Lobaccaro JM, Hammer RE, Mangelsdorf DJ** 1998 Cholesterol and bile acid metabolism are impaired in mice lacking the nuclear oxysterol receptor LXR alpha. Cell 93:693-704
363. **Joseph SB, Laffitte BA, Patel PH, Watson MA, Matsukuma KE, Walczak R, Collins JL, Osborne TF, Tontonoz P** 2002 Direct and indirect mechanisms for regulation of fatty acid synthase gene expression by liver X receptors. J Biol Chem 277:11019-11025
364. **Chu K, Miyazaki M, Man WC, Ntambi JM** 2006 Stearoyl-coenzyme A desaturase 1 deficiency protects against hypertriglyceridemia and increases plasma high-density lipoprotein cholesterol induced by liver X receptor activation. Mol Cell Biol 26:6786-6798
365. **Talukdar S, Hillgartner FB** 2006 The mechanism mediating the activation of acetyl-coenzyme A carboxylase-alpha gene transcription by the liver X receptor agonist T0-901317. Journal of lipid research 47:2451-2461
366. **Schultz JR, Tu H, Luk A, Repa JJ, Medina JC, Li L, Schwendner S, Wang S, Thoolen M, Mangelsdorf DJ, Lustig KD, Shan B** 2000 Role of LXRs in control of lipogenesis. Genes & development 14:2831-2838
367. **Guertin DA, Stevens DM, Thoreen CC, Burds AA, Kalaany NY, Moffat J, Brown M, Fitzgerald KJ, Sabatini DM** 2006 Ablation in mice of the mTORC components raptor, rictor, or mLST8 reveals that mTORC2 is required for signaling to Akt-FOXO and PKCalpha, but not S6K1. Developmental cell 11:859-871
368. **Jacinto E, Facchinetti V, Liu D, Soto N, Wei S, Jung SY, Huang Q, Qin J, Su B** 2006 SIN1/MIP1 maintains rictor-mTOR complex integrity and regulates Akt phosphorylation and substrate specificity. Cell 127:125-137
369. **Polak P, Hall MN** 2006 mTORC2 Caught in a SINful Akt. Developmental cell 11:433-434

370. **McPherson R, Gauthier A** 2004 Molecular regulation of SREBP function: the Insig-SCAP connection and isoform-specific modulation of lipid synthesis. Biochemistry and cell biology = Biochimie et biologie cellulaire 82:201-211
371. **Yellaturu CR, Deng X, Park EA, Raghow R, Elam MB** 2009 Insulin enhances the biogenesis of nuclear sterol regulatory element-binding protein (SREBP)-1c by posttranscriptional down-regulation of Insig-2A and its dissociation from SREBP cleavage-activating protein (SCAP).SREBP-1c complex. J Biol Chem 284:31726-31734
372. **Haas JT, Miao J, Chanda D, Wang Y, Zhao E, Haas ME, Hirschey M, Vaitheesvaran B, Farese RV, Jr., Kurland IJ, Graham M, Crooke R, Foufelle F, Biddinger SB** 2012 Hepatic Insulin Signaling Is Required for Obesity-Dependent Expression of SREBP-1c mRNA but Not for Feeding-Dependent Expression. Cell Metab 15:873-884
373. **Zhang Y, Breevoort SR, Angdisen J, Fu M, Schmidt DR, Holmstrom SR, Kliewer SA, Mangelsdorf DJ, Schulman IG** 2012 Liver LXRalpha expression is crucial for whole body cholesterol homeostasis and reverse cholesterol transport in mice. J Clin Invest 122:1688-1699
374. **Zhang Y, Repa JJ, Gauthier K, Mangelsdorf DJ** 2001 Regulation of lipoprotein lipase by the oxysterol receptors, LXRalpha and LXRbeta. J Biol Chem 276:43018-43024
375. **Chisholm JW, Hong J, Mills SA, Lawn RM** 2003 The LXR ligand T0901317 induces severe lipogenesis in the db/db diabetic mouse. Journal of lipid research 44:2039-2048
376. **Liu Y, Yan C, Wang Y, Nakagawa Y, Nerio N, Anghel A, Lutfy K, Friedman TC** 2006 Liver X receptor agonist T0901317 inhibition of glucocorticoid receptor expression in hepatocytes may contribute to the amelioration of diabetic syndrome in db/db mice. Endocrinology 147:5061-5068
377. **Wan M, Leavens KF, Saleh D, Easton RM, Guertin DA, Peterson TR, Kaestner KH, Sabatini DM, Birnbaum MJ** 2011 Postprandial hepatic lipid metabolism requires signaling through Akt2 independent of the transcription factors FoxA2, FoxO1, and SREBP1c. Cell Metab 14:516-527
378. **Kenerson HL, Yeh MM, Yeung RS** 2011 Tuberous sclerosis complex-1 deficiency attenuates diet-induced hepatic lipid accumulation. PLoS One 6:e18075
379. **Sundqvist A, Bengoechea-Alonso MT, Ye X, Lukiyanchuk V, Jin J, Harper JW, Ericsson J** 2005 Control of lipid metabolism by phosphorylation-dependent degradation of the SREBP family of transcription factors by SCF(Fbw7). Cell Metab 1:379-391
380. **Kim KH, Song MJ, Yoo EJ, Choe SS, Park SD, Kim JB** 2004 Regulatory role of glycogen synthase kinase 3 for transcriptional activity of ADD1/SREBP1c. J Biol Chem 279:51999-52006
381. **Bengoechea-Alonso MT, Ericsson J** 2009 A phosphorylation cascade controls the degradation of active SREBP1. J Biol Chem 284:5885-5895
382. **Biddinger SB, Hernandez-Ono A, Rask-Madsen C, Haas JT, Aleman JO, Suzuki R, Scapa EF, Agarwal C, Carey MC, Stephanopoulos G, Cohen DE, King GL, Ginsberg HN, Kahn CR** 2008 Hepatic insulin resistance is sufficient to produce dyslipidemia and susceptibility to atherosclerosis. Cell Metab 7:125-134
383. **Hegarty BD, Bobard A, Hainault I, Ferre P, Bossard P, Foufelle F** 2005 Distinct roles of insulin and liver X receptor in the induction and cleavage of sterol regulatory element-binding protein-1c. Proc Natl Acad Sci U S A 102:791-796
384. **Shao W, Espenshade PJ** 2012 Expanding Roles for SREBP in Metabolism. Cell Metab 16:414-419
385. **Du X, Kristiana I, Wong J, Brown AJ** 2006 Involvement of Akt in ER-to-Golgi transport of SCAP/SREBP: a link between a key cell proliferative pathway and membrane synthesis. Molecular biology of the cell 17:2735-2745

386. **Lin S, Boey D, Herzog H** 2004 NPY and Y receptors: lessons from transgenic and knockout models. Neuropeptides 38:189-200
387. **Roseberry AG, Liu H, Jackson AC, Cai X, Friedman JM** 2004 Neuropeptide Y-mediated inhibition of proopiomelanocortin neurons in the arcuate nucleus shows enhanced desensitization in ob/ob mice. Neuron 41:711-722
388. **Perry CA, Pravetoni M, Teske JA, Aguado C, Erickson DJ, Medrano JF, Lujan R, Kotz CM, Wickman K** 2008 Predisposition to late-onset obesity in GIRK4 knockout mice. Proc Natl Acad Sci U S A 105:8148-8153
389. **Jin W, Lu Z** 1998 A novel high-affinity inhibitor for inward-rectifier K+ channels. Biochemistry 37:13291-13299
390. **Pravetoni M, Wickman K** 2008 Behavioral characterization of mice lacking GIRK/Kir3 channel subunits. Genes, brain, and behavior 7:523-531
391. **Miyazaki M, Flowers MT, Sampath H, Chu K, Otzelberger C, Liu X, Ntambi JM** 2007 Hepatic stearoyl-CoA desaturase-1 deficiency protects mice from carbohydrate-induced adiposity and hepatic steatosis. Cell Metab 6:484-496
392. **Vankoningsloo S, De Pauw A, Houbion A, Tejerina S, Demazy C, de Longueville F, Bertholet V, Renard P, Remacle J, Holvoet P, Raes M, Arnould T** 2006 CREB activation induced by mitochondrial dysfunction triggers triglyceride accumulation in 3T3-L1 preadipocytes. Journal of cell science 119:1266-1282
393. **Herzig S, Hedrick S, Morantte I, Koo SH, Galimi F, Montminy M** 2003 CREB controls hepatic lipid metabolism through nuclear hormone receptor PPAR-gamma. Nature 426:190-193
394. **Shulman GI** 2000 Cellular mechanisms of insulin resistance. J Clin Invest 106:171-176